Charles University

Faculty of Science

Program: Developmental and Cell Biology

Molecular events associated with resistance to tyrosine kinase inhibitors in leukemia cells

Molekulární změny spojené s rezistencí leukemických buněk na tyrozin kinázové inhibitory

Ph.D. thesis

Mgr. Tereza Hrdinová

Supervisor: doc. MUDr. Daniel Vyoral, CSc.

Specialist: Mgr. Ondřej Toman, Ph.D.

Prague, 2022

Prohlášení:

Prohlašuji, že jsem závěrečnou práci zpracovala samostatně a že jsem uvedla všechny použité informační zdroje a literaturu. Tato práce ani její podstatná část nebyla předložena k získání jiného nebo stejného akademického titulu.

V Praze, 22.2.2022

Tereza Hrdinová

Poděkování

Ráda bych poděkovala svým školitelům doc. MUDr. Danielovi Vyoralovi, CSc. a Mgr. Ondřejovi Tomanovi, Ph.D**.** za odborné vedení, cenné rady a ochotnou pomoc při práci v laboratoři na Oddělení proteomiky Ústavu hematologie a krevní transfuze.

Dále bych chtěla poděkovat všem kolegům z našeho oddělení za vytvoření příjemného místa pro práci, za veškerou pomoc a podporu. Také bych ráda poděkovala všem spolupracovníkům, kteří se podíleli na publikacích, které jsou součástí této disertační práce.

V nesposlední řadě bych chtěla poděkovat rodině a blízkým lidem za podporu během celého studia.

Table of contents

Abstract

Chronic myeloid leukemia (CML) is a myeloproliferative stem cell disease characterized by the expression of BCR-ABL oncoprotein with constitutive tyrosine kinase activity. Although the development of tyrosine kinase inhibitors (TKI) such as imatinib dramatically improved the treatment of CML, a certain subset of patients develops resistance to TKI drugs. The most common cause of TKI resistance are point mutations in the *BCR-ABL1* gene, followed by other mutation-independent mechanisms. Survival and proliferation of CML cells in the presence of TKI drugs are accompanied by adaptive changes in their metabolism. Drug resistance can be maintained by extrinsic signals, among which exosomes, small vesicles released by (drug-resistant) cells, have been shown to play an important role.

The aim of this thesis was to characterize two CML cell lines sensitive and resistant to imatinib, as well as the exosomes derived from imatinib-resistant CML cells by proteomic approaches. Identification of metabolic vulnerabilities in drug-resistant cells enables their targeting by clinically available drugs, thus offering potential therapeutic targets for their selective elimination. Analysis of exosomes derived from imatinib-resistant cells can identify specific membrane surface proteins exploitable as clinically relevant diagnostic markers associated with imatinib resistance.

Two imatinib resistant CML cell lines were established for this study. In imatinib-resistant CML-T1^{IR} cells, upregulation of Na^+/H^+ exchanger regulatory factor 1 (NHERF1) was found, which could influence cytosolic pH, Ca^{2+} concentration, or the WNT signaling pathway,. Testing selective toxicity of several compounds revealed that modulators of calcium homeostasis, calcium channel blockers, and calcium signaling inhibitors were selectively toxic to CML-T1^{IR} cells. In a model of imatinib-resistant K562^{IR} cells, upregulation of signal transducer and activator of transcription 3 (STAT3) was detected. STAT3 and the insulin-like growth factor 1 receptor/insulin receptor substrate 1 (IGF1R/IRS-1) signaling pathway were suggested as potential therapeutic targets in imatinib-resistant K562^{IR} cells. This work also shows that exosomes from donor K562^{IR} cells can be internalized by recipient imatinib-sensitive K562 cells and increase their survival in imatinib. Proteomic analysis of the exosomes from K562^{IR} cells revealed strong enrichment of three membrane proteins IFITM3, CD146, and CD36. The flow cytometry confirmed their enrichment also on the cell surface of the donor K562^{IR} cells. The results suggest that proteomic analysis is a powerful tool in designing potential therapeutic targets and clinically valuable diagnostic markers in TKI resistant CML cells.

Abstrakt

Chronická myeloidní leukémie (CML) je myeloproliferativní onemocnění hematopoézy charakterizované expresí konstitutivně aktivní tyrozin kinázy BCR-ABL. Ačkoli vývoj tyrozin kinázových inhibitorů (TKI) jako je imatinib zásadním způsobem zefektivnil léčbu CML, u určité skupiny pacientů vzniká rezistence na TKI léky. Nejčastější příčinou rezistence jsou bodové mutace v genu *BCR ABL1*, méně pak i další na mutaci nezávislé mechanismy. Růst rezistentních CML buněk v přítomnosti TKI léků je důsledkem adaptivních změn v jejich metabolismu. Rezistence může být udržována vnějšími signály, mezi nimiž sehrávají důležitou roli exozomy, malé membránové vezikuly uvolňované (rezistentními) buňkami.

Cílem této práce bylo proteomicky charakterizovat dvě buněčné linie CML (senzitivní a rezistentní na imatinib) a také exozomy, produkované rezistentními buňkami. Identifikace metabolických drah esenciálních pro růst rezistentních buněk v prostředí imatinibu umožňuje zacílit jejich metabolismus klinicky dostupnými léky, což nabízí potenciál pro jejich využití v (personalizované) léčbě. Proteomickou analýzou exozomů z rezistentních buněk lze identifikovat specifické povrchové membránové proteiny využitelné jako klinicky relevantní diagnostické markery rezistence na imatinib.

Pro tyto účely byly vyvinuty a analyzovány dvě buněčné linie CML, senzitivní a rezistentní na imatinib. U buněk CML-T1^{IR} rezistentních na imatinib byla zjištěna zvýšená exprese regulačního faktoru 1 Na^+/H^+ výměníku (NHERF1), který může ovlivňovat pH cytosolu, vnitrobuněčnou redistribuci Ca^{2+} nebo WNT signální dráhu. Testování selektivní toxicity odhalilo, že modulátory Ca^{2+} homeostázy, blokátory kalciových kanálů a inhibitory intracelulární Ca^{2+} dependentní signalizace byly více toxické pro CML-T1^{IR} buňky rezistentní na imatinib. Na dalším modelu buněk rezistentních na imatinib (K562^{IR}) byla prokázána silně zvýšená exprese transkripčního faktoru STAT3. Signalizace zprostředkovaná STAT3, signální dráha růstového faktoru IGF1 a adptorového proteinu IRS-1 byly navrženy jako potenciální terapeutické cíle. Bylo také prokázáno, že exosomy produkované imatinib rezistentními K562^{IR} buňkami jsou internalizovány buňkami K562 citlivými na imatinib a navodit jejich následné přežívání v imatinibu. Proteomická analýza odhalila silné nabohacení tří membránových proteinů IFITM3, CD146 a CD36 v exozomech produkovaných K562^{IR} buňkami. Průtoková cytometrie potvrdila nabohacení těchto proteinů i na povrchu rezistentních K562^{IR} buněk. Tyto výsledky naznačují, že proteomická analýza je efektivním nástrojem pro navrhování potenciálních terapeutických cílů a klinicky cenných diagnostických markerů v buňkách CML rezistentních na TKI.

Abbreviations

2-DE	two-dimensional gel electrophoresis
ABC /B1/G2	ATP-binding cassette transporter B1/G2
ABL1/ ABL	ABL proto-oncogene 1 / ABL proto-oncogene 1 protein
ACN	acetonitrile
AGC	automatic gain control
ALIX	ALG-2-interacting protein X
ALL	acute lymphocytic leukemia
AKT	thymomas of AKR mice
AML	acute myeloid leukemia
ATP	adenosine triphosphate
BAD	BCL2 associated agonist of cell death
BAX	BCL2 Associated X
BCL-2	B-cell lymphoma-2
BCL-xL	B-cell lymphoma-extra large
BCR / BCR	breakpoint cluster region / breakpoint cluster region protein
BCR-ABL1 / BCR-ABL	breakpoint cluster region-ABL proto-oncogene 1 / protein
BM	bone marrow
BMSC	bone marrow mesenchymal stromal cells
CAI	carboxyamidotriazole
CBL	Casitas B-cell lymphoma proto-oncogene
CD	cluster of differentiation
CFSE	carboxyfluorescein succinimidyl ester

c-KIT	KIT proto-oncogene, Receptor Tyrosine Kinase
c-MYC	Myc proto-oncogene protein
CML	chronic myeloid leukemia
CML-AP	chronic myeloid leukemia-accelerated phase
CML-BP	chronic myeloid leukemia-blast phase
CML-CP	chronic myeloid leukemia-chronic phase
CRKL	Crk-like protein
Cs A/H	cyclosporine A/H
CYP3A4	cytochrome P450 Family 3 Subfamily A Member 4
DAMPs	damage-associated molecular patterns
DCB	3′,4′-dichlorobenzamil hydrochloride
ddPCR	droplet digital PCR
DSBs	double strand breaks
DTT	dithiothreitol
DYRK2	dual specificity tyrosine-phosphorylation-regulated kinase 2
EGFR	epidermal growth factor receptor
ER	endoplasmic reticulum
ERK1/2	extracellular signal-regulated kinase 1/2
ESCRT	endosomal sorting complex required for transport
FA	formic acid
FACS	fluorescent-activated cell sorting
FasL	Fas ligand
FDR	false discovery rate
FOXO1	forkhead box O1 transcription factor

FPR1	formyl peptide receptor
Fura-2/AM	Fura-2-acetoxymethylester
FZD	Frizzled receptor
GAPDH	glyceraldehyde-3-phosphate dehydrogenase
GEF	guanine nucleotide exchange factor
GRB2	growth factor receptor-bound protein 2
GTPase	GTP-binding protein
GUSB	β-glucuronidase
HCK	hematopoietic cell kinase
HLA	human leukocyte antigen
HRR	homologous recombinational repair
HSC	hematopoietic stem cell
HSP 70/90	heat shock protein 70
EC_{50}	half-maximal effective concentration
ICAM-1	intercellular adhesion molecule-1
IFITM 1/2/3	interferon-induced transmembrane protein 1/2/3
IGF1	insulin-like growth factor 1
IGF1R	insulin-like growth factor 1 receptor
IL-	interleukin
ILV	intraluminal vesicles
IPG	immobilized pH gradient
IFN /α/ γ	interferon /alpha/gamma
IR	imatinib-resistant
IRS-1	insulin receptor substrate 1

JAK	Janus kinase
JNK	c-Jun N-terminal kinase
kD	kilo Dalton
LC-MS/MS	liquid chromatography coupled with tandem mass specrtometry
LFQ	label-free quantification
LSC	leukemia stem cell
MALDI	matrix-assisted laser desorption/ionization
MAPK	mitogen-activated protein kinase
MDR	multidrug resistance
MDR1	multidrug resistance protein 1
MEK	MAP kinase kinase
MEKK	mitogen-activated protein kinase kinase kinase
MFI	mean fluorescence intensity
MRP2	multidrug resistance-associated protein 2
MSC	mesenchymal stromal cells
mTOR	mammalian target of rapamycin
MTT	3-[4,5-dimethylthiazol-2-yl]-2,5 diphenyl tetrazolium bromide
MVB	multivesicular endosome (body)
MWCO	Molecular weight cut-off
NFAT	nuclear factor of activated T cells
NCX	sodium-calcium exchanger (Na^+/Ca^{2+} exchanger)
NGS	next generation sequencing
NHE3	sodium-hydrogen exchanger 3 (Na^+/H^+ exchanger 3)
NHERF1	Na^+/H^+ exchanger regulatory factor

NHEJ	non-homologous end joining
NO	nitric oxide
OCT1	organic cation transporter 1
PAGE	polyacrylamide gel electrophoresis
PBS	phosphate buffered saline
PBST	phosphate buffered saline with 0.1% Tween-20
PDGFR	platelet-derived growth factor receptor
PDZ	PSD-95/drosophila discs large/ZO-1
Ph chromosome	Philadelphia chromosome
PKC	protein kinase C
PI3K	phosphoinositide 3-kinase
PBS	phosphate-buffered saline
PPP	picropodophyllin
RAF	rapidly accelerated fibrosarcoma
RAS	rat sarcoma virus
RPMI	Roswell Park Memorial Institute medium
RT	room temperature
RT-PCR	real-time polymerase chain reaction
ROS	reactive oxygen species
SAPK	stress-activated protein kinase
SD	standard deviation
SDS	Sodium dodecyl-sulfate
SERCA	sarco/endoplasmic reticulum Ca^{2+} ATPase
SH2/SH3	Src homology domain 2/3

SH2-CD	SH2-catalytic domain linker
SHC	SHC-transforming protein
SOCE	store operated calcium entry
SRC	proto-oncogene tyrosine-protein kinase Src
STAT 1/3/5	signal transducer and activator of transcription 1/3/5
TFA	trifluoroacetic acid
TGF-β1	transforming growth factor beta 1
TNF	tumor necrosis factor
TOF	time of flight
TKI	tyrosine kinase inhibitor
TRAIL	tumor necrosis factor-related apoptosis-inducing ligand
TRPC 4/5	transient receptor potential calcium channel 4/5
VPS	vacuolar protein sorting-associated protein
WB	Western blot
WNT	Wingless-related integration site

1. Introduction

1.1. Chronic myeloid leukemia (CML)

Chronic myeloid leukemia is a myeloproliferative stem cell disease. In 1960, Peter Nowell and David Hungerford discovered an abnormal "minute chromosome" in patients with chronic granulocytic leukemia (Nowell 1962). This chromosome later became called the "Philadelphia (Ph) chromosome". In 1973, Janet Rowley found that the Ph chromosome is a result of reciprocal translocation between chromosomes 9 and 22 (Rowley, 1973). This translocation was detected in Ph-positive patients only and it was the first discovery of chromosomal abnormality as being firmly associated with cancer (Bartram et al., 1983). Another work revealed that ABL proto-oncogene 1 (*ABL1*) localizes in the region of chromosome 9 translocated to chromosome 22 (Heisterkamp et al., 1983). Chromosomal breakpoints are located into small region on chromosome 22 later named "breakpoint cluster region" (*BCR*) (Groffen et al., 1984). The most common breakpoints in CML pathology are fusions of exons 13 or 14 of BCR with ABL1 exon 2 (called b2a2 or b3a2) (Jain et al., 2016). Fusion of *BCR* gene with *ABL1* gene results in chimeric *BCR-ABL1* mRNA, which is present in patients with CML (Shtivelman et al., 1985; Stam et al., 1985). Later, it has been shown that *BCR-ABL1* fusion transcript results in production of P210 BCR-ABL, which is able to transform hematopoietic cells (Ben-Neriah et al., 1986b; Daley and Baltimore, 1988). This was proven by murine bone marrow transfection with a retrovirus encoding P210 BCR-ABL protein which resulted in the development of CML-like myeloproliferative syndrome in mice (Daley et al., 1990). In addition to major isoform P210 BCR-ABL, which is a hallmark of CML, P190 BCR-ABL isoform is present in a minority of CML patients and is associated with inferior response to imatinib (Adnan-Awad et al., 2021).

1.1.1. Structure and functions of Bcr and Abl proteins

The ***BCR* gene** encodes a 160 kilo Dalton (kDa) BCR protein (Maru and Witte, 1991). The N-terminus of the BCR protein contains a coiled-coil oligomerization domain, followed by a serine/threonine kinase domain, which overlaps with at least two Src homology 2 binding domains (SH2-binding domains) (Maru and Witte, 1991; Pendergast et al., 1991). The coiled-coil oligomerization domain is crucial for BCR-ABL tetramerization and for the enzymatic activation of BCR-ABL tyrosine kinase activity (McWhirter et al., 1993). One of the two SH2-binding domains of the BCR protein binds the ABL protein tyrosine kinase, while the other

SH2-binding domain binds to an adaptor protein, the growth factor receptor-bound protein 2 (GRB2) (Pendergast et al., 1991, 1993). In the central part of the BCR protein, guanine nucleotide exchange factor (GEF) and pleckstrin homology (PH) domains are located (Ron et al., 1991; Chuang et al., 1995). Finally, GTPase-activating protein (GAP) domain resides at the C-terminus of the Bcr protein (Diekmann et al., 1991) (Figure 1).

The ***ABL1* gene** is a proto-oncogene and the human homolog of Abelson Murine Leukemia Viral Oncogene Homolog 1 (Abelson and Rabstein, 1970). The *ABL1* gene encodes the 145 kDa ABL protein. The ABL protein has two isoforms 1a and 1b, which differ at their N-termini due to alternative splicing (Ben-Neriah et al., 1986a; Shtivelman et al., 1986). The form 1b is myristoylated on the N-terminus and is thus directed to the plasma membrane (Sefton et al., 1982; Ben-Neriah et al., 1986a; Jackson and Baltimore, 1989). Myristoyl modification of the N--terminus is important for autoinhibition of ABL kinase (Pluk et al., 2002; Nagar et al., 2003). The N-terminus is followed by SH3, SH2, and tyrosine kinase domains (Wang et al., 1984; McWhirter and Wang, 1991). The SH3 domain is rich in the amino acid proline and binds adaptor protein Crk-like proto-oncogene (CRKL) (Senechal et al., 1996). The C-terminal half of ABL contains binding elements for SH3 domains, nuclear localization and export signals, DNA binding domain, and actin binding domain (McWhirter and Wang, 1991; Kipreos and Wang, 1992; Miao and Wang, 1996; Taagepera et al., 1998) (Figure 1).

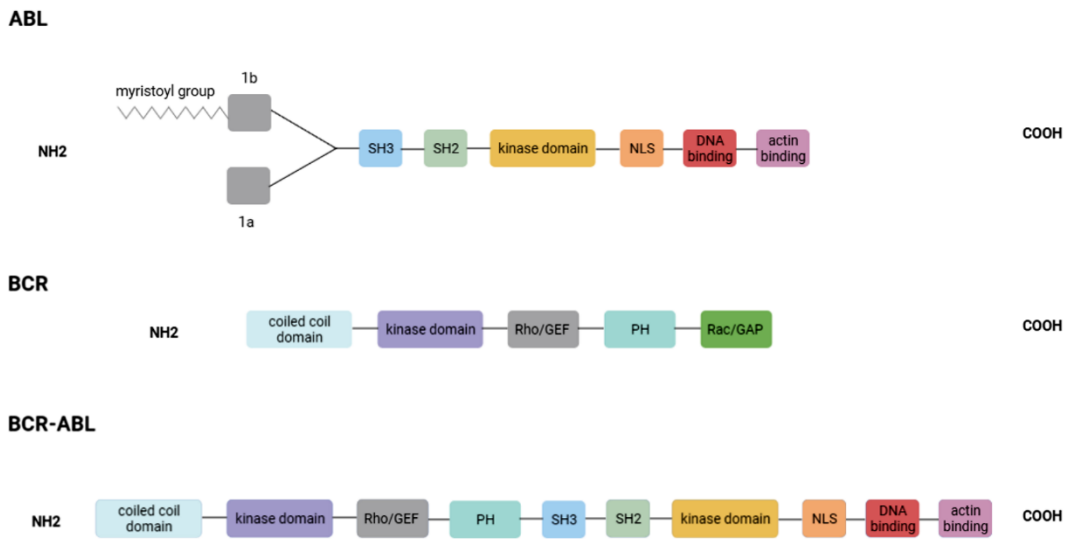

Figure 1. Schematic representation of ABL, BCR, and BCR-ABL protein domains. Created in BioRender.com

1.1.2. Constitutive activation of the BCR-ABL tyrosine kinase

When the ABL protein kinase is not fused with the BCR part, its activity is tightly regulated. ABL overexpression did not result in transformation of hematopoietic cells or fibroblasts (Van Etten et al., 1989).

Deregulation of ABL kinase activity by the fusion with N-terminal BCR sequences has been intensively studied. BCR-ABL exists in an inactive state consisting of monomeric and unphosphorylated form (Smith et al., 2003). The N-terminal coiled-coil domain of BCR causes association of two monomers of BCR-ABL into antiparallel dimers which further associate to form tetramer (McWhirter et al., 1993; Tauchi et al., 1996; Smith et al., 2003). Oligomer formation is followed by intramolecular autophosphorylation at Tyr1294 in the activation loop of BCR-ABL kinase. This phosphorylation may also lead to secondary phosphorylation events (Smith et al., 2003). For example, phosphorylation of Tyr1127 in the region between SH2 and kinase domains (SH2-CD linker) results in disruption of autoinhibitory interaction due to displacement of SH3 domain from the SH2-CD linker (Brasher and Van Etten, 2000; Smith et al., 2003). BCR-ABL oligomerization through coiled-coil domain and phosphorylation at two regulatory sites (Tyr1294 and Tyr1127) are crucial for catalytic activity of BCR-ABL kinase (McWhirter et al., 1993; Tauchi et al., 1996; Smith et al., 2003). Other phosphorylation site contributing to leukemogenesis is Tyr177 (Million and Van Etten, 2000). Tyr177 phosphorylation is important for the induction of CML-like disease in mice (Million and Van Etten, 2000).

1.2. Characteristics of CML

CML is a malignant blood disease characterized by uncontrolled growth of myeloid cells at different stages of maturation and by inhibition of erythropoiesis, thrombopoiesis, and lymphopoiesis in the bone marrow (BM) by the pathological clone. There are three phases of the disease: chronic (CML-CP), accelerated (CML-AP), and blast phase or blast crisis (CML-BP). CML is frequently diagnosed incidentally by a routine complete blood count test performed for unrelated reasons because patients with CML-CP may remain asymptomatic (Quintás-Cardama and Cortes, 2006). Symptoms are related to expansion of CML cells and include leukocytosis, malaise, splenomegaly, fatigue, and weight loss (Gomez et al., 1981; Quintás-Cardama and Cortes, 2006). Upon CML diagnosis, bone marrow aspiration is performed for cytogenetics and for morphology to determine the disease phase. A molecular diagnostic technique - the

quantitative real-time polymerase chain reaction (RT-PCR), performed from peripheral blood samples, is also used at the diagnosis of CML to identify the type of *BCR-ABL1* transcripts, and later to monitor response to the therapy by tyrosine kinase inhibitors (TKI) (reviewed in chapter 1.4.1) (Frazer et al., 2007; Hochhaus et al., 2020). Untreated patients progress to CML-BP after a median of 3 to 5 years. CML-AP is diagnosed with 10-19% of blasts in the peripheral blood or in the bone marrow, following with more than 20% of blasts are present in CML-BP. The symptoms of CML in AP and BP include fatigue, hepatomegaly, bone pain, anemia, bleeding, and recurrent infections (Gomez et al., 1981; Frazer et al., 2007). Prognosis varies among CML-CP and advanced phases (CML-AP, CML-BP) but also among patients within the same phase of the disease (Quintás-Cardama and Cortes, 2006). Early treatment with TKI upon diagnosis is crucial because patients treated with TKI (imatinib) within four years of diagnosis have a better prognosis and lower incidence of mutations in the *BCR-ABL1* gene (Frazer et al., 2007).

The incidence of CML is 1-2 cases per 100 000 adults per year, and it increases with age. CML accounts for approximately 15% of new cases of leukemia in adults (Hoffmann et al., 2015).

1.3. CML specific signaling

BCR-ABL$^+$ cells exhibit altered adhesion to stromal cells and extracellular matrix, which positively supports their proliferation. BCR-ABL kinase also activates and dysregulates downstream signaling pathways including rat sarcoma virus/mitogen-activated protein kinase (RAS/MAPK), phosphoinositide 3-kinase/thymomas of AKR mice kinase (PI3K/AKT), and Janus kinase/signal transducer and activator of transcription (JAK/STAT) leading to increased leukemia cells survival, proliferation, inhibition of apoptosis, and acquisition of self-renewal capacity (Figure 2).

1.3.1. Altered cellular adhesion

Adhesion to stromal cells negatively regulates proliferation of cells. CML progenitor cells escape from this regulation by reduced adhesion to stromal cells and extracellular matrix (Gordon et al., 1987). This disturbed adherence may also explain the pathological presence of immature cells in the blood (Gordon et al., 1987). Lack of adherent molecules on the surface of CML progenitor cells, such as P-selectin and intercellular adhesion molecule-1 (ICAM-1) or structural and functional abnormalities of beta-integrins are mostly responsible for reduced adhesion of CML

progenitor cells to stromal cells (Verfaillie et al., 1997; Pelletier et al., 2004). However, there is no correlation between the data from CML primary cells obtained from patients and the data obtained from cell lines where enhanced integrin function was described (Krämer et al., 1999). Moreover, adhesion to fibronectin stimulates proliferation of cells transfected with *BCR-ABL1* (Krämer et al., 1999).

Alterations in cellular adhesion of BCR-ABL$^+$ cells are mainly due to contribution of the CRKL protein (Uemura et al., 1999). CRKL is one of the major tyrosine phosphoproteins in primary leukemic neutrophils from patients with CML (Nichols et al., 1994). This phosphoprotein is involved in regulation of cellular motility and integrin-mediated adhesion by its association with focal adhesion sites (contacts between the cell and extracellular matrix) (Uemura et al., 1999). These contacts are provided by proteins such as paxillin, Casitas B-cell lymphoma (CBL) proto-oncogene, human enhancer of filamentation (HEF1), and Crk-associated substrate p130 (CAS) which binds to focal adhesion kinase (FAK) (Polte and Hanks, 1995; Salgia et al., 1995a, 1995b, 1996a, 1996b; Sattler et al., 1997).

BCR-ABL also influences the cytoskeleton by direct association with actin filaments and affects main cell adhesion regulators called small GTPases, such as RHO, RAC, and CDC42 (McWhirter and Wang, 1991; Renshaw et al., 1996; Skorski et al., 1998; Harnois et al., 2003). P210 BCR-ABL forms complex with RAC1, RAC2, RHOA, and CDC42. GEF domain of BCR-ABL may directly activate these GTPases (Harnois et al., 2003).
BCR-ABL increases expression of adhesion molecules such as a5b1 type of integrins, integrin a6 and CD44; it also stimulates very late activation antigen -4 and -5 (VLA-4 and VLA-5) integrin function (Bazzoni et al., 1996; Krämer et al., 1999; Deininger et al., 2000; Krause et al., 2006). Inversely, it was found that ABL kinase activity and localization are regulated by integrins (Lewis et al., 1996). BCR-ABL kinase probably interferes with integrin signal transduction in CML (Lewis et al., 1996).

1.3.2. RAS/MAPK signaling pathway

BCR-ABL protein kinase binds directly to proteins activating the small GTPase RAS, which is a critical regulator of cell growth and differentiation (Puil et al., 1994). Autophosphorylation of Tyr177 in BCR-ABL creates a binding site for GRB2 protein (Pendergast et al., 1993), which associates with Son of Sevenless (SOS) protein stimulating the conversion of inactive RAS-GDP to the active form RAS-GTP (Pendergast et al., 1993; Puil et al., 1994). RAS is also activated by SHC-transforming protein 1 (SHC) and CRKL protein, which are substrates of BCR-ABL (Puil

et al., 1994; Senechal et al., 1996). RAS protein is required for BCR-ABL-induced transformation (Sawyers et al., 1995). *BCR-ABL1* gene mutations which abolished binding to GRB2 or CRKL protein resulted in decreased fibroblast transforming activity (Pendergast et al., 1993; Senechal et al., 1996). GRB2 recruits the adapter protein GRB2-associated-binding protein 2 (GAB2), which is then phosphorylated by BCR-ABL kinase and activates PI3K/AKT and RAS/MAPK signaling pathways (Sattler et al. 2002). BCR-ABL activates different types of mitogen-activated protein kinases including rapidly accelerated fibrosarcoma kinase/mitogen-activated protein kinase/ERK kinase/extracellular signal-regulated kinase 1/2 (RAF/MEK/ERK1/2), stress-activated protein kinases/c-Jun N-terminal kinases (SAPK/JNK) and inhibits p38 kinase (Raitano et al., 1995; Cortez et al., 1997; Wong et al., 2003).

BCR-ABL kinase activates RAF/MEK/ERK signaling pathway important for cell proliferation by direct regulation of RAF activity (Skorski et al., 1995b; Cortez et al., 1997). Activation of transcription factor c-Jun by BCR-ABL is mediated through SAPK/JNK signaling pathway and it was shown that c-Jun is required for BCR-ABL transforming activity (Raitano et al., 1995). In contrast, p38 MAPK pathway is inhibited by BCR-ABL kinase in embryonic stem cell-derived hematopoietic progenitors (Wong et al., 2003).

1.3.3. PI3K/AKT kinase signaling pathway

PI3K signaling pathway mediates proliferation of BCR-ABL$^+$ cell lines and primary CML-BP cells (Skorski et al., 1995a). BCR-ABL activates PI3K pathway by forming a complex consisting of tyrosine phosphorylated CBL proto-oncogene, GRB2, and p85α subunit of PI3K (Jain et al., 1997). Activated PI3K stimulates AKT kinase in BCR-ABL$^+$ cells, which further influences downstream targets leading to downregulation of cyclin-dependent kinase inhibitor and thus accelerating the entry of the cells into the S phase of the cell cycle (Jonuleit et al., 2000; Komatsu et al., 2003). Inhibition of the regulatory p85 or catalytic p110 subunits of PI3K has negative effect on proliferation of BCR-ABL$^+$ cell lines and primary CML-BP cells (Skorski et al., 1995a). Activated AKT kinase also shows an antiapoptotic function by phosphorylating the BCL2-associated agonist of cell death (BAD) protein (del Peso et al., 1997). In BCR-ABL expressing cells, BAD is constitutively phosphorylated. (Neshat et al., 2000). Conversely, other work suggests that BCR-ABL resistance to apoptosis is independent of PI3K activity because PI3K inhibition does not interfere with BCR-ABL-mediated resistance to apoptosis (Amarante-Mendes et al., 1997). BCR-ABL can also block apoptosis by preventing the accumulation of

cytochrome c in the cytoplasm and inhibiting the activation of caspase 3 (Amarante-Mendes et al., 1998).

1.3.4. JAK/STAT signaling pathway

Phosphorylation of STATs was reported in BCR-ABL$^+$ cell lines (Carlesso et al., 1996; Ilaria and Van Etten, 1996). STAT5, and to lesser degree STAT1 and STAT3 were constitutively activated by BCR-ABL kinase (Ilaria and Van Etten, 1996). JAKs (normally activating STATs) were not consistently phosphorylated in BCR-ABL expressing cells and two dominant JAK negative mutants did not block activation of STAT5 suggesting BCR-ABL activates STAT family members directly (Carlesso et al., 1996; Ilaria and Van Etten, 1996). STAT5 activation contributes to malignant transformation of K562 cells (de Groot et al., 1999). Activated STAT5 is important for BCR-ABL$^+$ cell viability and growth (Nosaka et al., 1999; Sillaber et al., 2000). Transcription of B-cell lymphoma-extra large (*BCL-xL*) gene can also be stimulated by STAT5, which points out to its antiapoptotic activity (Gesbert and Griffin, 2000; Horita et al., 2000).

It was shown that BCR-ABL forms complex with other proteins: JAK2, heat shock protein (HSP) 90, tyrosine protein kinase Lyn (LYN), AKT, STAT3, glycogen synthase kinase-3-beta (GSK3β), and ERK (Samanta et al., 2010). Destabilization of this complex by JAK2/ABL kinase inhibitor ON044580 induces apoptosis of imatinib-sensitive and imatinib-resistant BCR-ABL$^+$ cells (Samanta et al., 2010).

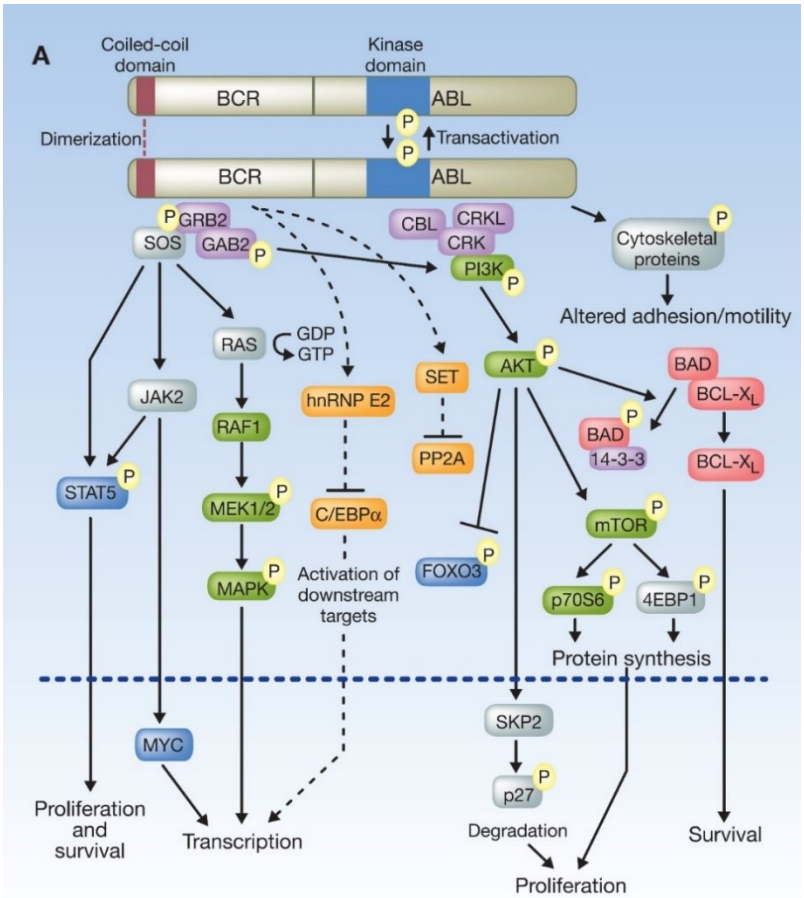

Figure 2. BCR-ABL kinase activated signaling. BCR-ABL activates multiple downstream signaling pathways including JAK/STAT, RAF/MEK/ERK, and PI3K/AKT, which contribute to the growth and survival of BCR-ABL$^+$ cells. (Modified from O'Hare et al., 2011).

1.4. CML therapy

Besides radiotherapy of the spleen, which reverses the splenomegaly, early treatments of CML consisted of busulfan, an alkylating agent, hydroxyurea, an inhibitor of ribonucleotide reductase, and interferon (IFN)-α (Kennedy, 1972; Morstyn et al., 1981; Hukku et al., 1983; Talpaz et al., 1986; Yoffe et al., 1987). IFN-α was the first drug, which increased hematological remission and induced partial or complete cytogenetic response, leading to longer survival of low-risk patients (Bonifazi et al., 2001; Kantarjian et al., 2003). Later, hematopoietic stem cell transplantation (HSCT) successfully eliminated Ph$^+$ cells in cases, when the donor cells were taken from identical twin or from human leukocyte antigen (HLA)-matched siblings (Fefer et al., 1979; McGlave et al., 1982). Although HSCT is the only curative CML treatment, this procedure is not suitable for all patients and carries a risk of transplantation-related mortality (Silver et al., 1999). CML was a lethal disorder until the introduction of HSCT. Later, the introduction of the first TKI targeting BCR-ABL, imatinib, has revolutionized therapy of CML. Targeted therapy using imatinib and other TKI dramatically improved survival and quality of life of patients with CML.

1.4.1. TKI treatment

1.4.1.1. Imatinib

Introduction of the compound CPG57148 of the 2-phenyl-aminopyrimidine class, called also STI-571, later imatinib mesylate (brand name Gleevec) represented a breakthrough in the treatment of CML (Buchdunger et al., 1996; Druker et al., 1996; Deininger et al., 1997). The evidence that BCR-ABL kinase is found exclusively in CML cells and represents the molecule responsible for disease progression provided an ideal target for pharmacologic inhibition. In the case of imatinib, an initial lead compound was identified by testing large libraries of compounds for inhibition of the protein kinase C (PKC) α (Capdeville et al., 2002). The activity of 2-phenyl-aminopyrimidine molecules was further optimized for inhibition of ABL and platelet-derived growth factor receptor (PDGFR) (Buchdunger et al., 1996). Imatinib selectively inhibited growth of BCR-ABL$^+$ cells (Druker et al., 1996). Studies showed important implications for BCR-ABL inhibition by imatinib (Schindler et al., 2000). Crystal structures of the catalytic domain of ABL showed that imatinib preferentially binds to and inhibits unphosphorylated ABL form (Schindler et al., 2000). Imatinib binds to the ATP binding site of the kinase domain and traps the kinase domain in an inactive conformation (Schindler et al., 2000; Nagar et al., 2002) (Figure 3). Inactive conformation of the ABL activation loop captured by imatinib mimics binding of peptide substrate (Nagar et al., 2002). The inactive conformation of the ABL activation loop is distinct from the inactive form of SRC kinases, which are closely related to the ABL kinase in sequence (Nagar et al., 2002). The major inactivating switch within the ABL kinase domain consists of a conformational change at the base of activation loop, a mechanism that differs from inactivation of the SRC kinase or the hematopoietic cell kinase (HCK). This conformation change flips the positions of aspartate (Asp) and phenylalanine (Phe) side chains in the conserved Asp-Phe-Gly (DFG) motif, which is incompatible with Mg^{2+} binding and catalysis ("DFG-out" or "DFG-flipped"). This phenomenon explains why imatinib does not inhibit the SRC kinase, where the kinase domain is in a closed position when the aspartate residue of the DFG motif is oriented toward the active site ("DFG-in" conformation) (Nagar et al., 2002). Imatinib makes six hydrogen bonds (M318, T315, E286, D381, H361, I360) and numerous van der Waals interactions with the BCR-ABL kinase (Nagar et al., 2002). In addition to BCR-ABL, imatinib was also found to inhibit kinase activity of PDGFR and the receptor tyrosine kinase c-KIT (Buchdunger et al., 1996, 2000; Carroll et al., 1997).

Imatinib was subjected to dose-escalating phase I study in 1998 and orally administrated to patients with CML-CP in whom treatment by IFN-α had failed (Druker et al., 2001). The results

from this study showed that imatinib has minimal adverse effects and is well tolerated (Druker et al., 2001). The study provided evidence for the important role of BCR-ABL tyrosine kinase activity in CML and established a proof of concept for the development of drugs targeting specific molecular abnormalities in cancer cells (Druker et al., 2001). Phase II study was performed with 400 mg of daily imatinib oral administration to patients with late chronic phase in whom previous IFN-α therapy had failed (Kantarjian et al., 2002). It was shown that imatinib induced major cytogenetic and hematologic responses in CML-CP patients (Kantarjian et al., 2002). In the phase III study, the combination of recombinant IFN-α and low dose cytarabine was compared with imatinib treatment of newly diagnosed CML-CP patients (O'Brien et al., 2003). The results showed that imatinib was better in comparison with IFN-α combined with a low dose of established cytostatic drug cytarabine, as a first line therapy in newly diagnosed CML-CP patients in terms of tolerability, cytogenetic and hematologic responses, and likelihood of progression to CML-BP (O'Brien et al., 2003).

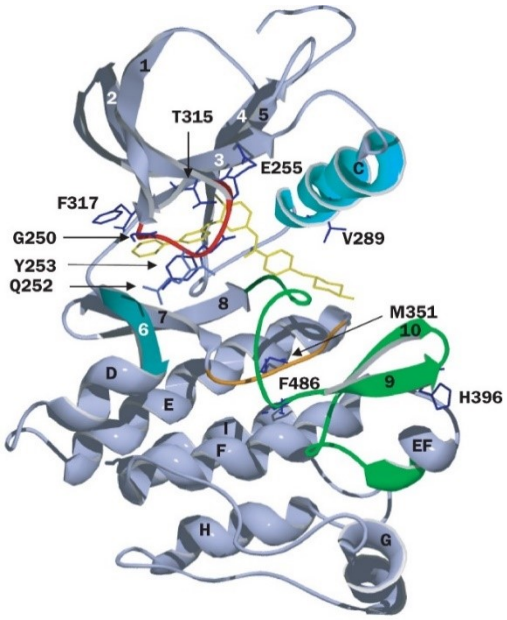

Figure 3. ABL kinase with imatinib (yellow). The positions of mutations are highlighted, activation loop (green), phosphate binding loop (red), and catalytic loop (orange), region interacting with phosphate binding loop (cyan). α helices are lettered and β strands are numbered according to the nomenclature used for insulin receptor tyrosine kinase. (Modified from (Gambacorti-Passerini et al., 2003a).

1.4.1.2. Nilotinib and dasatinib

Although imatinib streamlined the CML therapy, cases of drug resistance in CML patients began to emerge. It was revealed that loss of response to imatinib in CML patients was mainly due to occurrence of point mutations in imatinib binding sites in the tyrosine kinase domain of the BCR-ABL oncoprotein (reviewed in chapter 1.6.1). Therefore, a demand for more potent inhibition of

BCR-ABL kinase activity which overcomes imatinib resistance led to development of novel next generation inhibitors (Cilloni and Saglio, 2012). These inhibitors include nilotinib and dasatinib (Lombardo et al., 2004; Weisberg et al., 2005; Cilloni and Saglio, 2012).

Nilotinib (AMN107)

Nilotinib (brand name Tasigna) was introduced as a novel highly selective and potent inhibitor of the BCR-ABL kinase (Weisberg et al., 2005). Nilotinib binds to an inactive BCR-ABL conformation similarly to imatinib (Weisberg et al., 2005). Greater affinity of nilotinib results from a better topological fit to the BCR-ABL (Weisberg et al., 2005). Nilotinib is a more potent BCR-ABL inhibitor than imatinib in killing wild-type BCR-ABL expressing cells (Golemovic et al., 2005; Weisberg et al., 2005). Nilotinib inhibited wild-type BCR-ABL kinase in CML derived and transfected cells, and also prolonged the survival of mice injected with BCR-ABL transformed hematopoietic cell lines or with primary bone marrow cells (Golemovic et al., 2005; Weisberg et al., 2005). A key advantage of nilotinib over imatinib is the ability to inhibit some BCR-ABL forms with imatinib-resistant mutations (O'Hare et al., 2005; Weisberg et al., 2005). In addition, nilotinib was shown to prolong survival of mice with imatinib-resistant CML (Weisberg et al., 2005). However, *BCR-ABL1* harboring T315I mutation remains insensitive to nilotinib binding due to loss of a hydroxyl side chain and creation of a steric clash as it was described for imatinib (Schindler et al., 2000; O'Hare et al., 2005). Nilotinib also inhibits the c-KIT and PDGFR kinases (Weisberg et al., 2005). In dose escalating phase I study, patients with imatinib-resistant CML or acute lymphoblastic leukemia (ALL) received nilotinib orally at different doses once daily or twice daily. It was revealed that 600 mg twice daily is the maximum tolerated dose and 400 mg twice daily was selected to phase II trials (Kantarjian et al., 2006). Dose 400 mg twice daily was administrated to patients in CML-CP after imatinib failure or intolerance (Kantarjian et al., 2007a). Nilotinib safety, hematologic and cytogenetic responses, and overall survival of patients were evaluated (Kantarjian et al., 2007a). Nilotinib was effective in patients with imatinib resistant-mutations (except T315I) and in patients who developed mutation-independent mechanisms of resistance. The conclusion from this study is that nilotinib is safe and highly active in patients with CML-CP after imatinib failure or intolerance (Kantarjian et al., 2007a). The phase III study concluded that nilotinib was superior to imatinib in newly diagnosed patients with CML-CP (Saglio et al., 2010).

Dasatinib

Dasatinib (BMS-354825, brand name Sprycel) is based on the pyrido-[2,3-d]pyrimidine series of compounds. It is a potent dual biochemical inhibitor of SRC kinases and the BCR-ABL kinase

(Lombardo et al., 2004). A three dimensional structure of ABL interaction with dasatinib revealed that dasatinib binds to the ABL kinase when activation loop of ABL is in an active conformation (Lombardo et al., 2004). Oral administration of dasatinib in a xenograft mouse model of CML with subcutaneously implanted K562 cells resulted in tumor regression (Lombardo et al., 2004). Similar results were obtained with severe combined immunodeficiency (SCID) mice injected intravenously with Ba/F3 cells expressing *BCR-ABL1* with different mutations (Shah et al., 2004). Dasatinib treatment prolonged the survival of mice (Shah et al., 2004). However, mice harboring *BCR-ABL1* T315I mutation did not respond to dasatinib significantly (Shah et al., 2004). Dasatinib also inhibited growth of bone marrow progenitor cells isolated from CML patients responsive or nonresponsive to imatinib therapy. The results suggest that dasatinib is highly selective for leukemic cells compared to normal hematopoietic cells (Shah et al., 2004). In phase I study in 2006, patients with CML or Ph^+ ALL who were intolerant or resistant to imatinib were treated with different doses of dasatinib once or twice daily and tolerability and safety of dasatinib were evaluated (Talpaz et al., 2006). Hematologic and cytogenetic responses were observed in all patients except those with T315I mutation, which confer cross-resistance to all three TKI (Schindler et al., 2000; Shah et al., 2004; O'Hare et al., 2005; Talpaz et al., 2006). Phase II studies included four single arm studies START-A, START-B, START-L, START-C and one randomized study (Hochhaus et al., 2007, 2008; Kantarjian et al., 2007b; Cortes et al., 2008; Apperley et al., 2009). In phase II randomized study, dasatinib was compared to high doses of imatinib after therapy failure with usual imatinib doses. It was shown that dasatinib is safe and effective in patients with CML-CP resistant to imatinib. Cytogenetic and molecular response rates as well as progression-free survival of patients also improved compared to imatinib (Kantarjian et al., 2007b). Phase III study revealed that one 100 mg dasatinib daily dose is the best risk/benefit profile in comparison with 70 mg twice daily dose (Shah et al., 2008).

1.4.1.3. Bosutinib and Ponatinib

Bosutinib

Similarly to dasatinib, bosutinib (formerly SKI-606, 4-anilino-3-quinolinecarbonitrile) is a dual SRC/ABL kinase inhibitor, which inhibits SRC and BCR-ABL kinases in nanomolar concentrations (Boschelli et al., 2001; Golas et al., 2003). Bosutinib binds both active and inactive conformations of the BCR-ABL kinase domain (Puttini et al., 2006; Levinson and Boxer, 2012). Experiments using CML cell lines KU812, K562, and MEG-01 revealed that

bosutinib inhibits their proliferation and survival (Golas et al., 2003). Bosutinib was shown to have higher antiproliferative effect than imatinib encountering inhibition of imatinib-resistant *BCR-ABL1* kinase domain mutations (except the cross-resistant T315I) (Puttini et al., 2006). Oral bosutinib treatment of K562 mice xenograft models *in vivo* resulted in regression of the tumors (Golas et al., 2003). Similarly, bosutinib was active against xenograft mouse models injected with Ba/F3 cells expressing point mutations in *BCR-ABL1* except T315I (Puttini et al., 2006).

In the clinical studies, bosutinib was administered to imatinib-intolerant and imatinib-resistant CML patients as well as to patients after nilotinib or dasatinib failure to determine optimal dose (phase I) and to evaluate efficacy and safety of dosing (phase II) (Cortes et al., 2011; Khoury et al., 2012). From dose escalation phase I, 500 mg daily dose was chosen for the phase II study (Cortes et al., 2011; Khoury et al., 2012). Bosutinib is effective and tolerable in patients with chronic phase of imatinib-resistant or imatinib-intolerant CML (Cortes et al., 2011). Bosutinib was also studied as frontline therapy in newly diagnosed CML-CP patients in two phases III clinical trials. The first trial (BELA, Bosutinib Efficacy and Safety in Newly Diagnosed Chronic Myeloid Leukemia) compared 500 mg bosutinib once daily to 400 mg imatinib (Cortes et al., 2012b). However, bosutinib did not show superior rates of cytogenetic response so the primary endpoint of this study was not met (Cortes et al., 2012b; Brümmendorf et al., 2015). In the follow-up phase III study (BFORE, Bosutinib Trial in First-Line Chronic myelogenous Leukemia Treatment), a lower dose of bosutinib (400 mg daily) was compared to imatinib in newly diagnosed patients (Cortes et al., 2018). In this lower dose study, bosutinib provided higher rates of cytogenetic responses in a shorter time compared to imatinib (Cortes et al., 2018). In addition, bosutinib showed an effective balance between efficacy and toxicity (Cortes et al., 2018).

Ponatinib

Ponatinib was designed to overcome the cross-resistant gatekeeper T315I mutation, which confers resistance to imatinib, nilotinib, dasatinib, and bosutinib (Schindler et al., 2000; O'Hare et al., 2005, 2009). The crystallographic analysis of ponatinib in complex with ABL kinase with T315I mutation showed that ponatinib binds to ABL in the DFG-out (inactive) mode (O'Hare et al., 2009). Ponatinib inhibits growth of Ba/F3 cells expressing wild-type *BCR-ABL1* and *BCR-ABL1* kinase domain mutants and also inhibits proliferation of primary CML cells harboring wild-type *BCR-ABL* or *BCR-ABL1* T315I mutation (O'Hare et al., 2009). Ponatinib also inhibits SRC, vascular endothelial growth factor (VEGFR), fibroblast growth factor receptor (FGFR), and PDGFR kinases (O'Hare et al., 2009).

In phase I clinical trial, ponatinib was administered to patients with Ph^+ leukemias who were resistant to TKI including patients with *BCR-ABL1* T315I mutation to determine tolerated or recommended oral daily dose (Cortes et al., 2012a). In phase II trial in patients with CML or Ph^+ ALL, ponatinib was administered once daily at an initial dose of 45 mg (Cortes et al., 2013). However, additional follow-up from these ponatinib trials revealed higher frequency of serious adverse events, which led to abrupt withdrawal from the market in October 2013 (Gainor and Chabner, 2015). In addition, phase III trial comparing ponatinib and imatinib as the first-line treatment in CML was closed due to high rates of reported myocardial infarction, stroke, and peripheral vascular disease (Gainor and Chabner, 2015; Lipton et al., 2016). In January 2014, the marketing of ponatinib was resumed with new safety measures. Ponatinib is currently used in the second line therapy for T315I mutations (Pophali and Patnaik, 2016). Several studies evaluating efficacy/risk profile of lower doses of ponatinib in TKI resistant patients are currently underway.

1.4.2. Other therapeutic options for CML

Despite the success in clinical use of imatinib as well as other TKI, CML therapy remains associated with limited rates of molecular response and development of TKI resistant mutations. To overcome these obstacles, novel approaches to avoid complications associated with point mutations in the *BCR-ABL1* kinase emerge. For example, non-ATP competitive BCR-ABL inhibitors with distinct mechanisms of action are developed and undergoing preclinical and early clinical trials.

Non-ATP competitive and substrate competitive inhibitors

GNF-2 is a novel compound (4,6-disubstituted pyrimidine class) developed by cytotoxicity screen (Adrián et al., 2006). GNF-2 selectively inhibits proliferation and induces apoptosis of Ba/F3 cells expressing wild-type *BCR-ABL* as well as *BCR-ABL1* harboring E255V mutation (Adrián et al., 2006). GNF-2 also inhibits STAT5 phosphorylation but has no activity against other kinases (Adrián et al., 2006). GNF-2 binds to the myristoyl pocket located in the C lobe of the BCR-ABLkinase (Adrián et al., 2006).

Asciminib (ABL001) binds to the myristoyl pocket of BCR-ABL and induces an inactive BCR-ABL conformation (Wylie et al., 2017). Such distinct binding retains the activity against *BCR-ABL1* mutations insensitive to other TKI. It also offers a great possibility for dual targeting of the BCR-ABL kinase by combination with TKI (Wylie et al., 2017). Preclinical experiments have led to asciminib testing in clinical trials, which are still underway. Recent data from phase I clinical study showed asciminib activity in TKI resistant or intolerant patients (Hughes et al.,

2019). The first data from asciminib treatment in clinical practice revealed that asciminib is a safe and effective CML drug (Garcia-Gutiérrez et al., 2021).

ON12380 is a small molecule inhibitor, which competes with natural substrates of the BCR-ABL kinase, such as CRKL protein, and works synergistically with imatinib in inhibition of the wild-type BCR-ABL kinase (Gumireddy et al., 2005). ON12380 induced apoptosis of all imatinib-resistant mutants *in vitro* and caused regression of leukemia induced by intravenous injection of murine myeloid cells 32Dcl3 expressing T315I mutation (Gumireddy et al., 2005).

Vaccines for CML

It was shown that vaccines developed against antigens expressed in CML cells evoked immune responses. One such antigen is proteinase 3, expressed in myeloid cells, samples from acute myeloid leukemia (AML) and in CML patients (Dengler et al., 1995). CML cells were shown to present PR1 nanopeptide derived from proteinase 3 via HLA-A2.1 on their surface and cytotoxic T lymphocytes preferentially lysed these CML cells *in vitro* (Molldrem et al., 1996). PR1 vaccine was evaluated for safety, immunogenicity and clinical activity in phase I/II study in patients with AML, CML, or myelodysplastic syndrome (MDS) (Qazilbash et al., 2017).

Other vaccines are developed against junctional region of the *BCR-ABL1* b3a2 molecule, which represents a leukemia-specific antigen recognizable by cytotoxic T lymphocytes (Yotnda et al., 1998). In CML cell lines and primary cells, BCR-ABL protein can be processed by the proteasome and breakpoint peptides are presented by HLA class I antigen on the cell surface (Clark et al., 2001). Specific cytotoxic T lymphocytes were found in some patients which indicates that spontaneous immunization occurs *in vivo* (Yotnda et al., 1998). However, BCR-ABL antigen presentation and cytotoxic T lymphocyte response do not work optimally *in vivo*, otherwise CML would never receive medical attention (Clark et al., 2001). Preliminary data suggest that vaccination of patients with a peptide vaccine derived from b3a2 *BCR-ABL*1 sequence (CMLVAX100) improved patients´ cytogenetic responses and seven patients achieved complete cytogenetic response post-vaccination (Bocchia et al., 2005).

Vaccines are also developed from patients´ malignant cells containing HSP70 (Li et al., 2005) and from peptides of the Wilm´s tumor (WT-1) transcription factor, which is overexpressed in CML, AML, or ALL leukemia cells (Inoue et al., 1997). Another vaccine is derived from CML cell line K562 expressing several CML-associated antigens and engineered to produce granulocyte-macrophage colony-stimulating factor (GM-SCF) (Smith et al., 2010). These

vaccines in combination with imatinib induced immunogenic and clinical responses in patients (Li et al., 2005; Narita et al., 2010; Smith et al., 2010).

1.4.3. Treatment free remission and leukemic stem cells

The life expectancy of CML patients treated with TKI is approaching the life expectancy of the general population today (Bower et al., 2016). However, treatment of CML by TKI is expensive and complicated by adverse events and toxicities (Faden et al., 2009; Efficace et al., 2011; Yamamoto et al., 2019; Lyman and Henk, 2020). Therefore, clinicians and scientists explore the possibility of discontinuing TKI treatment in patients who achieved a deep molecular remission (Mahon et al., 2010; Ross et al., 2013; Yamamoto et al., 2019). Treatment withdrawal can be a risk because there is a population of leukemia stem cells (LSC) persisting in patients after TKI treatment (Bocchia et al., 2018). LSCs do not rely on BCR-ABL activity and targeting of BCR-ABL does not eliminate them from the patient´s body (Corbin et al., 2011). Regarding the impressive results obtained from the current CML treatment strategies, there are only few approaches that can optimize treatment of CML. One such is targeting the mutated BCR-ABL kinase including the gatekeeper T315I mutation insensitive to all inhibitors except ponatinib (Schindler et al., 2000; Shah et al., 2004; O'Hare et al., 2005, 2009; Puttini et al., 2006). Another approach investigates possible metabolic targets for eradication of leukemic stem cells.

1.5. Mechanisms and biological pathways exploited by LSC

LSC are defined as the source of malignant proliferation inducing leukemia when transplanted into immunodeficient mice (Bonnet and Dick, 1997). LCS are of $CD34^{+}CD38^{-}$ origin and sit at the peak of a hierarchy similar to the hierarchy in normal hematopoiesis (Bonnet and Dick, 1997). Different subgroups of LSC exist and expression of certain markers distinguishes CML LSC from their normal hematopoietic counterpart (Giustacchini et al., 2017). For example, CD36 is expressed on the surface of primitive CML cells and CML-BP cells, which have been observed to be less sensitive to imatinib and in more quiescent state (Ye et al., 2016; Landberg et al., 2018). LSC show increased expression of proteins involved in self-renewal and drug resistance. One of them is β-catenin. β-catenin activation in CML granulocyte-macrophage progenitors from patients in CML-AP or CML-BP enhances self-renewal of these cells (Jamieson et al., 2004). β -catenin is essential for the survival of murine LSC despite BCR-ABL inhibition by imatinib (Hu et al., 2009). Another protein involved in LSC expansion is the Smoothened (Smo) protein from the Hedgehog signaling pathway (Dierks et al., 2008; Zhao et al., 2009). Proteomic and

transcriptomic analysis of LSC from CML patients showed that a set of transcripts, which are aberrantly expressed in these cells, is regulated by p53 and the Myc proto-oncogene protein (c-MYC) (Abraham et al., 2016). Simultaneous activation of p53 and inhibition of c-MYC caused reduction of LSC viability, enhancement of apoptosis, and induction of cell differentiation (Abraham et al., 2016). Additionally, the Krüppel-like factor 4 (KLF4) transcription factor maintains low levels of the dual-specificity tyrosine-(Y)-phosphorylation-regulated kinase 2 (DYRK2), which is a key regulator of c-MYC and p53. DYRK2 may thus represent a single target to eliminate LSC (Park et al., 2019).

Recently, it was shown that LSC, which reside with HSC in the BM, rely more on upregulated oxidative phosphorylation via mitochondrial respiration for their survival. This fact can be exploited for their selective elimination. For example, combined treatment with imatinib and tigecycline, an antibiotic inhibiting mitochondrial protein translation, selectively eradicated LSC both *in vitro* and *in vivo* in immunocompromised mice transplanted with $CD34^+$ human CML cells (Kuntz et al., 2017). Other LSC specific metabolic features involve utilization of gonadal adipose tissue as a niche, which protects LSC from chemotherapy as it was shown in subpopulation of LSC in mouse CML-BP (Ye et al., 2016). This subpopulation of LSC exhibited upregulation of inflammatory cytokines and factors which promoted lipolysis by adipocytes. Free fatty acids generated by lipolysis drive fatty acid oxidation in LSC expressing the fatty acid transporter CD36 (Ye et al., 2016).

Targeting LSC is ineffective in CML because quiescent fraction of LSC is insensitive to TKI drug imatinib (Graham et al., 2002). This is supported by single-cell analysis of CML stem cells from patients treated by TKI, which identified LSC population enriched for quiescent and TKI resistant cells (Giustacchini et al., 2017). Another study suggests that LSC do not require BCR-ABL kinase activity for survival and thus inhibiting the BCR-ABL kinase does not eliminate LSC (Corbin et al., 2011).

Imatinib treatment is known to induce autophagy in numerous malignant hematopoietic cells including the BCR-ABL^+ cell lines, CML-BP cells, primary CML cells, cells carrying partially imatinib-resistant *BCR-ABL1* mutation (M351T), and CML stem cells. Inhibition of autophagy by pharmacological inhibitors or knockdown of autophagy genes, autophagy-related 5 homolog (ATG5) and autophagy-related 7 homolog (ATG7), potentiates imatinib-induced cell death in CML cell lines, primary CML cells, and CML stem cells (Bellodi et al., 2009).

1.6. Resistance to TKI

Approximately 20% of patients develop imatinib resistance (Quintás-Cardama et al., 2009). Targeted TKI therapy dramatically improved CML treatment and life quality of patients with CML. However, complications in the form of primary and secondary, BCR-ABL dependent or BCR-ABL independent mechanisms of resistance evolve. Resistance to imatinib can be classified as primary, in patients who exhibit lack of TKI efficiency from the start of therapy, and secondary (acquired), in patients who respond to imatinib treatment at the beginning and develop resistance later. Secondary resistance is precisely characterized by loss of major cytogenetic response and complete hematologic response. Resistance to imatinib can also be divided into other three categories: hematologic - lack of peripheral blood counts normalization, cytogenetic - persistence of the Ph chromosome, and molecular - persistence of *BCR-ABL1* mRNA. Consequences of acquired resistance are indeed a clinical failure of therapy.

1.6.1. BCR-ABL dependent mechanisms of resistance

BCR-ABL1 gene mutations

Point mutations in the kinase domain of the *BCR-ABL1* gene are the most common mechanism of resistance to imatinib (and other TKI drugs) in CML therapy (Gorre et al., 2001; Hochhaus et al., 2002; Shah et al., 2002). The frequency of mutations in the *BCR-ABL1* kinase ranges from 40% to 90% of the resistance cases, depending on the methodology of detection, the definition of resistance, and CML phase (Gorre et al., 2001; Shah et al., 2002). Regarding the resistance to imatinib, mutations in *BCR-ABL1* can be divided into two groups, those that alter amino acids residues involved in contact with imatinib and those that prevent BCR-ABL from achieving the inactive conformation required for binding of imatinib (Shah et al., 2002). Mutations sterically hinder drug occupancy of the active site (C – catalytic domain, residues 350 to 363), alter the deformability of the highly conserved phosphate binding P-loop (P-loop, residues 244 to 255), and/or influence the conformation of the activation loop (A-loop, residues 381 to 402) surrounding the active site (Shah et al., 2002). The mutations that are frequently found in clinical samples are located to the P-loop region (Branford et al., 2002, 2003; Jabbour et al., 2006). Some studies suggest that P-loop mutations are associated with poor clinical outcome (Branford et al., 2003). However, another study did not confirm association of P-loop mutations with poor outcome (Jabbour et al., 2006). This can be explained by patient selection and therapy approaches using novel TKI (Jabbour et al., 2006).

Crystallization studies of ABL kinase with imatinib showed that the amino acids Y253 and T315 are critical for imatinib binding (Schindler et al., 2000; Corbin et al., 2002). T315 creates an important hydrogen bond with imatinib (Nagar et al., 2002). Gorre *et al* (Gorre et al., 2001) were the first who detected *BCR-ABL1* mutations in patients with advanced phase of CML or Ph^+ ALL. Resistance was associated with a single amino acid substitution (T315I) in 6 of 9 patients (Gorre et al., 2001). The T315I mutation disrupts hydrogen bond interaction and sterically impairs binding of imatinib, which results in insensitivity to imatinib as well as to nilotinib, dasatinib, and bosutinib (Schindler et al., 2000; Gorre et al., 2001; Shah et al., 2004; O'Hare et al., 2005; Puttini et al., 2006).

There is also a subset of patients in which two (or more) different mutations in *BCR-ABL1* kinase could be detected (Jabbour et al., 2006; Khorashad et al., 2013). This arises either due to the presence of compound mutations (variants containing ≥2 mutations within the same *BCR-ABL1* allele that presumably arise sequentially) or due to polyclonal resistance (presence of multiple *BCR-ABL1* mutant clones). Sequential therapy with different TKI may lead to the development of compound mutations limiting the effectiveness of retreating patients with TKIs that have previously failed (Shah et al., 2007). Compound mutations are present more often in the late CML-CP and CML-AP (Akram et al., 2017). Polyclonal resistance was also seen in some patients (Shah et al., 2002). In some cases, mutant clones were probably present prior to treatment at levels below the threshold for detection and expanded under selective imatinib pressure (Shah et al., 2002). This supports the clonal selection model in which *BCR-ABL1* mutations pre-exist and expand under selective pressure (Roche-Lestienne et al., 2002; Shah et al., 2002).

BCR-ABL1 **gene amplification and overexpression of Bcr-Abl protein**

BCR-ABL1 gene amplification and BCR-ABL overexpression are less common mechanisms of clinical resistance (Gorre et al., 2001; Hochhaus et al., 2002). Upregulation of the BCR-ABL kinase due to amplification of the *BCR-ABL1* gene was first reported in the cell lines Ba/F3 BCR-ABL-r, LAMA84-r, and AR230-r exposed to gradually increasing concentrations of imatinib (Mahon et al., 2000). The *BCR-ABL1* gene amplification was identified also in K562 cells (Gribble et al., 2000). Amplification of the *BCR-ABL1* gene (2-fold higher number of *BCR-ABL1* gene copies in resistant cells compared to sensitive cells) was described as a mechanism of imatinib resistance in K562 cells in our study (Hrdinova et al., 2021). Several case reports describe amplification of the *BCR-ABL1* gene as a clinical mechanism of resistance (Campbell et al., 2002; Morel et al., 2003). It was shown that amplification can be a result of the

Ph chromosome duplication and/or due to intrachromosomal amplification (Campbell et al., 2002; Gargallo et al., 2003; Al-Achkar et al., 2013).

It seems that BCR-ABL protein levels are associated with the emergence of mutant subclones (Barnes et al., 2005). Cells expressing high levels of BCR-ABL are less sensitive to imatinib and it takes a shorter time to develop resistant mutant clones than for cells expressing low levels of BCR-ABL (Barnes et al., 2005). This could probably be related to genomic instability caused by increased amounts of BCR-ABL, which promotes the accumulation of additional chromosomal aberrations and mutations (Barnes et al., 2005; Koptyra et al., 2008). However, in practice, clinical resistance occurs more likely due to point mutations than the *BCR-ABL1* gene amplification and overexpression.

1.6.2. BCR-ABL independent mechanisms of resistance to TKI

Overexpression of P-glycoprotein (multidrug resistance protein 1 (MDR1))

Imatinib is a substrate for the efflux transporter P-glycoprotein (Mahon et al., 2000). Mahon and colleagues were the first who demonstrated that overexpression of P-glycoprotein in imatinib-resistant LAMA84 cell line contributes to imatinib resistance together with the amplification of *BCR-ABL1* gene (Mahon et al., 2000). P-glycoprotein was also found to be expressed at varying levels in primary CML cells (Mahon et al., 2003; Thomas et al., 2004). Cells expressing P-glycoprotein have lower imatinib intracellular concentrations (Illmer et al., 2004; Thomas et al., 2004). P-glycoprotein overexpression could contribute to imatinib resistance in primary leukemic cells (Mahon et al., 2003). It was suggested that P-glycoprotein expression could play an important role in imatinib resistance during the first months of imatinib treatment or during the CML progression (Galimberti et al., 2005). However, it should be mentioned that another study using K562 cells did not confirm that P-glycoprotein overexpression plays a significant role in resistance to imatinib *in vitro* (Ferrao et al., 2003). Similarly, inhibition of P-glycoprotein in primitive CML cells did not enhance imatinib activity and efficiency (Hatziieremia et al., 2009).

Pharmacokinetic parameters of imatinib uptake

Imatinib plasma levels vary among patients, which suggests that imatinib concentration inside the cells may not be effective enough (Peng et al., 2004). Imatinib is metabolized by cytochrome P450 enzymes, primarily by the Cytochrome P450 Family 3 Subfamily A Member 4 (CYP3A4) (Gréen et al., 2010). Differential CYP3A4 gene expression and agents modifying CYP3A4 enzymatic activity affect imatinib levels in plasma (Peng et al., 2004).

Alpha-1 acid glycoprotein (AGP) binds imatinib at physiological concentrations in plasma, thus preventing the active drug from entering into leukemic cells and affecting its intracellular distribution, which restricts therapeutic activity of imatinib and leads to imatinib resistance (Gambacorti-Passerini et al., 2000, 2003b). The observations indicated that measuring imatinib plasma concentrations in patients represents rather unreliable way to estimate an actual imatinib concentration reached inside the leukemic cells circulating in the patient's body. (Gambacorti-Passerini et al., 2003b).

Organic cation transporter 1 (OCT1, SLC22A1)

The differential expression of the influx transporter OCT1 influences intracellular imatinib levels and thus contributes to imatinib resistance (Thomas et al., 2004). Inhibitors of OCT1 significantly decrease the uptake of imatinib (Thomas et al., 2004). OCT1 expression was determined in cell lines and in primary cells from CML patients (Thomas et al., 2004). Patients with low OCT1 activity had lower imatinib intracellular concentrations and lower probability to achieve cytogenetic and molecular response (White et al., 2007). Patients with higher OCT1 activity achieve molecular response regardless of imatinib dose (White et al., 2007).

Clonal evolution, genomic instability, and epigenetic modifications

Clonal evolution is an acquisition of additional non-random chromosomal abnormalities in Ph positive cells during CML progression. Clonal evolution correlates with lower response to imatinib and predicts shorter time to imatinib failure (O'Dwyer et al., 2002, 2004; Cortes et al., 2003; Schoch et al., 2003; Jabbour et al., 2006). In a comprehensive study performed on 300 patients, new additional chromosomal aberrations were found in 58% of resistant patients, while *BCR-ABL1* kinase domain mutations were detected in 45% of resistant patients (Lahaye et al., 2005). These observations led to theory that CML can intrinsically evolve in advanced stages and that resistance to imatinib is not caused by a single mechanism (Lahaye et al., 2005).

Genomic instability is a result of genetic alternations caused by a combination of increased DNA damage and insufficient DNA repair. BCR-ABL kinase perturbs several DNA repair pathways thereby increasing genomic instability (Nowicki et al., 2004).

BCR-ABL kinase increases levels of reactive oxygen species (ROS), which cause oxidative DNA damage resulting in double-strand breaks (DSBs) (Sattler et al., 2000; Nowicki et al., 2004). BCR-ABL stimulates homologous recombination repair (HRR) and nonhomologous end-joining (NHEJ) to fix DSBs (Nowicki et al., 2004). However, BCR-ABL also reduces the fidelity of DSBs repair by HRR and NHEJ, since HRR products contain mutations and NHEJ products

contain deletions (Nowicki et al., 2004; Dierov et al., 2009). Moreover, BCR-ABL-induced ROS causing DNA damage can generate additional mutations in the *BCR-ABL1* kinase domain leading to imatinib resistance (Koptyra et al., 2006). Finally, the BCR-ABL kinase stimulates expression and increases activity of the most inaccurate DNA polymerase, DNA polymerase β, which may replace other polymerases and introduce point mutations (Canitrot et al., 1999).

Epigenetic modification is a mechanism of imatinib resistance based on alterations in the acetylation pattern of non-histone proteins (Lee et al., 2007). For example, in imatinib-resistant K562 cell line, aberrant acetylation of p53, Ku70, and HSP90 proteins was found (Lee et al., 2007). Imatinib-resistant cells showed upregulation of histone deacetylases and down-regulation of histone acetyltransferases. Thereby, the amounts of acetylated p53 and Ku70 were reduced and HSP90 was highly acetylated (Lee et al., 2007). This was accompanied by downregulation of the BCL2-associated X (BAX) protein and upregulation of the B-cell lymphoma-2 (BCL-2) protein. These results highlight the significance of acetylation as a regulatory mechanism controlling the activity of apoptosis related proteins in another example of BCR-ABL independent mechanism of imatinib resistance. Imatinib-resistant cells were more sensitive to a histone deacetylase inhibitor, suberoylanilide hydroxamic acid (Lee et al., 2007).

Impaired signaling pathways in CML contributing to imatinib resistance

Multiple signaling pathways can be potentiated by BCR-ABL such as JAK/STAT, PI3K/AKT, RAF/MEK/ERK, and thus can contribute to better proliferation of CML cells in imatinib and eventually lead to acquired resistance to imatinib (or other TKI).

STAT3 activation plays a role in extrinsic and intrinsic BCR-ABL independent resistance (Traer et al., 2012; Eiring et al., 2014). Cocultivation of TKI sensitive progenitor BCR-ABL$^+$ cells with the human bone marrow stromal cell line HS5 contributed to survival of CML progenitor cells through soluble bone marrow-derived factors which promoted STAT3 activation via Tyr705 phosphorylation (Bewry et al., 2008; Traer et al., 2012; Eiring et al., 2014). STAT3 was found to be activated in CML primary cells isolated from patients resistant to TKI as well is in established CML cell lines (Eiring et al., 2015b). It was suggested that activation of STAT3 is critical for BCR-ABL kinase independent TKI resistance (Eiring et al., 2015b). Inhibition of STAT3 by specific inhibitors (SF-1-066, BP-5-087, or LLL12) enhanced apoptosis of resistant CML cell lines and primary cells isolated from patients resistant to TKI (Eiring et al., 2015b; Patel et al., 2021).

PI3K/AKT signaling regulates proliferation and growth of CML cells (Skorski et al., 1995a). PI3K/AKT/mammalian target of rapamycin (mTOR) activation was described *in vitro* in BCR-ABL$^+$ cell line LAMA84 and in primary leukemia cells during the imatinib treatment (Burchert et al., 2005). It was suggested that PI3K/AKT signaling mediates cell survival in early phases of imatinib resistance until the first occurrence of *BCR-ABL1* mutation (Burchert et al., 2005). Inhibition of mTOR prevents imatinib-induced AKT activation and halts the development of imatinib resistance (Burchert et al., 2005). Downstream of PI3K/AKT, the transcription factor forkhead box O1 (FOXO1) contributes to resistance via its retention in the cytoplasm (Wagle et al., 2016). Elevated levels of FOXO1 were also found in primary cells from relapsed patients without *BCR-ABL1* mutations (Wagle et al., 2016). Drug combination involving TKI and PI3K inhibitors may represent a novel therapeutic strategy to target cells with BCR-ABL kinase independent resistance (Wagle et al., 2016).

RAF/MEK/ERK signaling is increased in BCR-ABL independent imatinib-resistant CML cell lines due to upregulation of PKCη (Ma et al., 2014). PKCη is also upregulated in BCR-ABL independent imatinib-resistant patient samples (Ma et al., 2014). Enhanced MAPK activity was found in primary CD34$^+$ cells during the imatinib treatment (Chu et al., 2004). Combined treatment by imatinib and the MEK inhibitor trametinib synergistically kills BCR-ABL$^+$ cells and prolongs survival of mouse models of BCR-ABL independent resistance (Ma et al., 2014). Another study performed on drug-resistant CML cells expressing *BCR-ABL1* T315I mutation showed that imatinib, nilotinib, and dasatinib activate RAF/MEK/ERK pathway in a RAS dependent manner (Packer et al., 2011). Combination of nilotinib and a MEK inhibitor induced synthetic lethality and killed drug-resistant cells (Packer et al., 2011).

Src family kinases (HCK, LYN, and FYN) are implicated in BCR-ABL signaling by phosphorylation of the BCR-ABL SH3-SH2 linker region (Meyn et al., 2006). Phosphorylation within the SH3-SH2 region is important for BCR-ABL transforming activity and for stabilization of the active BCR-ABL conformation, which does not bind imatinib (Meyn et al., 2006). Activation and/or overexpression of Src family kinases is involved in CML progression to BP and in imatinib resistance (Donato et al., 2003). Upregulation of LYN and HCK was found in K562 cell line and also in the blasts from imatinib-resistant patients (Donato et al., 2003). Comparative analysis of patient samples collected before and after imatinib therapy failure suggested that LYN and HCK kinases are activated and/or overexpressed during CML progression (Donato et al., 2003).

1.7. Deregulated pathways in imatinib-resistant CML cells identified in our studies

Na^+/H^+ exchanger regulatory factor (NHERF1), Wingless-related integration site (WNT) signaling, and calcium homeostasis

NHERF1 is a multifunctional protein with two postsynaptic density protein 95 (PSD-95)/drosophila discs large tumor suppressor (Dlg1)/zonula occludens (ZO-1) (PDZ) domains (Reczek et al., 1997). The NHERF1 protein interacts directly by the PDZ2 domain with the C-terminus of a subset of frizzled receptors (FZD2,4,7) and thus regulates WNT signaling (Wheeler et al., 2011). The canonical WNT/β-catenin pathway controls renewal and maintenance of HSCs and LSCs (Zhao et al., 2007). β-catenin plays a role in an intrinsic resistance upon BCR-ABL inhibition by imatinib (Eiring et al., 2015a). Silencing of β-catenin expression by siRNA inhibited proliferation and clonogenicity of CML cells synergistically with imatinib (Coluccia et al., 2007). Noncanonical WNT/Ca^{2+}/nuclear factor of activated T cells (NFAT) signaling is responsible for maintenance of Ph^+ cells, and inhibition of this pathway sensitizes Ph^+ cells to imatinib (Gregory et al., 2010). In addition, inhibition of the pathway effector calcineurin by cyclosporin A (CsA) sensitized imatinib-resistant cells to imatinib (Gregory et al., 2010).

The NHERF1 protein post-transcriptionally controls expression and function of the multidrug resistance-associated protein 2 (MRP2) (Li et al., 2010). NHERF1 functions as a negative regulator of the Na^+/H^+ exchanger 3 (NHE3), which regulates intracellular pH (Lamprecht et al., 1998; He and Yun, 2010). NHERF1 also modulates activation of the transient receptor potential channels TRPC4 and TRPC5, thereby influencing Ca^{2+} concentration in the cytosol (Tang et al., 2000; Obukhov and Nowycky, 2004). Cellular Ca^{2+} homeostasis mediates various cellular processes, such as proliferation, migration, and apoptosis (Hennings et al., 1980; Piwocka et al., 2006). However, only few studies describe the link between calcium and leukemogenesis in CML. For example, BCR-ABL^+ cells exhibited a decrease in the amount of free releasable Ca^{2+} in ER as well as weaker store-operated calcium entry (SOCE), which resulted in inhibition of calcium-dependent apoptotic signaling (Piwocka et al., 2006; Cabanas et al., 2018). The decrease in SOCE was accompanied by reduced translocation of NFAT to the nucleus (Cabanas et al., 2018). Peripheral mononuclear cells from CML patients also exhibit decreased intracellular calcium fluxes after inositol trisphosphate (InsP3), ATP, and ionomycin treatment (Ciarcia et al., 2010). Our results showed decreased Ca^{2+} levels in imatinib-resistant cells, which were concomitant with selective susceptibility of these cells to modulators of intracellular calcium

concentration, calcium signaling inhibitors, and calcium channel blockers (Toman et al., 2016). Thus, using a model cell line resistant to imatinib we proposed that Ca^{2+} homeostasis can be exploited as a potential therapeutic target in imatinib resistance (Toman et al., 2016).

Insulin-like growth factor 1 receptor (IGF1R) signaling, STAT3 signaling, and Interferon Induced Transmembrane Protein 3 (IFITM3)

The growth hormone insulin-like growth factor 1 (IGF1) and its receptor IGF1R play supportive roles in proliferation and viability of CML cells. Expression of IGF1R increases with CML progression (Shi et al., 2010; Xie et al., 2015). IGF1 is detected at higher levels in patients with CML-BP (Lakshmikuttyamma et al., 2008). It was shown that BCR-ABL can activate IGF1 via HCK and STAT5b (Lakshmikuttyamma et al., 2008). Inhibition of these proteins decreases proliferation and induces apoptosis in CML-BC cell lines (Lakshmikuttyamma et al., 2008). IFG1R also regulates the self-renewal of CML cells (Xie et al., 2015). Inhibition of IGF1R and insulin receptor substrate (IRS-1/2) either with picropodophyllin (PPP) or NT157 reduces proliferation of Ba/F3 cells transduced either with wild-type *BCR-ABL1* or with *BCR-ABL1* carrying imatinib-resistant mutations including T315I (Shi et al., 2010; Scopim-Ribeiro et al., 2021). PPP also efficiently decreases the viability of CML primary cells isolated from imatinib-resistant patients (Shi et al., 2010).

IGF1R signaling increases *STAT3* mRNA expression and STAT3 phosphorylation (Xu et al., 2017; Das et al., 2018; Bie et al., 2021). The STAT3 transcription factor can be phosphorylated and activated by the Bcr-Abl kinase directly, or indirectly via BCR-ABL modulation of JAK and MEK pathways (Ilaria and Van Etten, 1996). STAT3 regulates cell proliferation, survival, and drug resistance, and its inhibition either by siRNA or by LLL-3 reduced CML cell viability and induced apoptosis (Ma et al., 2010; Mencalha et al., 2010). Targeting STAT3 in a BCR-ABL-independent model of resistance either by shRNA or by SF-1-066 or BP-5-087 in combination with imatinib reduced the survival of TKI resistant CML cell lines (Eiring et al., 2015b). These observations were further supported by a recent study, which utilized the STAT3 inhibitor LLL12 to sensitize drug-resistant cells to imatinib treatment (Patel et al., 2021). This study also revealed that STAT3 promoted metabolic shift in TKI resistant cells, which led to their increased dependence on glycolysis (Patel et al., 2021).

IGF1R signaling induces expression of IFITM2 protein in gastric cancer cells via STAT3 (Xu et al., 2017). Knockdown of *IFITM2* gene decreased proliferation, invasion, and migration of gastric cancer cells (Xu et al., 2017). IFITM3 protein is another member of the interferon-induced

transmembrane protein family, which is involved in antiviral defense (Bailey et al., 2014). IFITM3 expression is partially regulated by STAT3 due to predicted STAT3 binding site in the IFITM3 promoter; yet PI3K can also regulate IFITM3 expression (https://www.genecards.org/cgi-bin/carddisp.pl?gene=IFITM3&keywords=ifitm3) (Stelzer et al., 2016; Lee et al., 2018a). Human embryonic stem cells and human induced pluripotent stem cells have elevated levels of distinct interferon-stimulated genes, including IFITM3 to function as an innate antiviral protection (Wu et al., 2018). Inhibition of viral entry by IFITM3 is caused by IFITM3-mediated accumulation of cholesterol in multivesicular bodies and late endosomes (Amini-Bavil-Olyaee et al., 2013). Overexpression of IFITM3 was found in AML patients and in gastric, lung, oral, and breast human cancer cell lines (Yang et al., 2013; Hu et al., 2014; Zhang et al., 2017; Gan et al., 2019; Liu et al., 2019). IFITM3 plays role in cancer progression, cell proliferation, migration, and invasion (Yang et al., 2013; Hu et al., 2014; Zhang et al., 2017; Gan et al., 2019). IFITM3 promotes PI3K signaling by accumulation of phosphatidylinositol-3,4,5-triphosphate (PIP3) in the cell membrane, which is followed by subsequent integration of PIP3 into lipid raft signaling complexes (Lee et al., 2020). IFITM3 regulates STAT3 phosphorylation as was shown in a study where knockdown of IFITM3 inhibited STAT3 phosphorylation and reduced cell growth (Yang et al., 2013; Gan et al., 2019). High expression levels of IFITM3 protein are associated with adverse prognosis in AML and in B cell malignancies including B-ALL and mantle cell lymphoma (Liu et al., 2019; Lee et al., 2020).

STAT3 in oncogene dependent metabolism, lipid metabolism, and drug resistance

In addition to the well-known oncogenic roles of STAT3 in transcriptional regulation of genes involved in cell proliferation, survival, and chemoresistance (Xiong et al., 2014), STAT3 regulates transcription of genes involved in central metabolic pathways (Wang et al., 2018; Gao et al., 2020; Patel et al., 2021) and exerts nontranscriptional functions in regulating mitochondrial oxidative phosphorylation (Gough et al., 2009; Wegrzyn et al., 2009).

STAT3 phosphorylated on Ser727 is imported into the inner mitochondrial membrane via the complex I subunit gene associated with retinoid-IFN-induced mortality 19 (GRIM-19) of the electron transport chain (Tammineni et al., 2013). STAT3 present in the mitochondria is required for the activity of the complexes I, II, and V (ATP synthase) of the electron transport chain, where it stimulates oxidative phosphorylation and respiration (Gough et al., 2009; Wegrzyn et al., 2009). As a result, ATP production is increased, which provides energy for rapid growth and division of tumor cells (Gough et al., 2009)

Tumor cells can also alter their lipid metabolism to maximize the utilization of energy (Ye et al., 2016; Cao, 2019). Cancer cells possess upregulated fatty acid synthesis and elevated beta-oxidation of fatty acids (Yoshii et al., 2015; Wang et al., 2018). STAT3 regulates expression of the fatty acid synthase (FASN) (Gao et al., 2020), which mediates *de novo* synthesis of fatty acids and was shown to promotes tumor growth and survival (Flavin et al., 2010). JAK/STAT3 pathway regulates beta-oxidation of fatty acids, which is crucial for breast cancer stem cells stemness and resistance to drugs (Wang et al., 2018). STAT3 regulates mRNA expression of the fatty acid transporter CD36 in LSC and chronic lymphocytic leukemia (CLL) cells (Ye et al., 2016; Rozovski et al., 2018; Su et al., 2020). It was revealed that CD36-expressing LSC occupy preferably the bone marrow adipose tissue to evade chemotherapy (Ye et al., 2016). Increased expression of CD36 was also found in our imatinib-resistant cells $K562^{IR}$ (Hrdinova et al., 2021). Recent data suggest that *de novo* synthesis of fatty acid, fatty acid uptake, and beta-oxidation of fatty acids are important for tumor progression. Dysregulated lipid metabolism in cancer contributes to cancer progression and represents a promising target in anticancer therapy (Fu et al., 2021).

1.8. Exosomes

Exosomes are small (cca 30-150 nm) membrane-bound vesicles derived from the endosomal compartment (Harding et al., 1983; Pan et al., 1985). Exosomes were originally proposed to eliminate cellular waste and described as transferrin receptor-containing vesicles (Harding et al., 1983; Pan et al., 1985; Johnstone et al., 1987). Exosomes arise from membranes of multivesicular endosomes (MVB) by inward budding and accumulate inside large MVB (Pan et al., 1985). When MVE fuse with the plasma membrane, exosomes are released into the extracellular space (Pan et al., 1985).

Recent studies confirm that exosomes influence numerous physiological and pathological processes including leukemia (CML) (Mathivanan et al., 2010; Becker et al., 2016). Depending on their composition, CML-derived exosomes affect proliferation of CML cells, support neoangiogenesis, and contribute to transfer of drug resistance traits between CML cells (Taverna et al., 2012; Raimondo et al., 2015; Min et al., 2018).

1.8.1. Exosomal biogenesis and cargo loading

Exosome biogenesis is initiated within the endosomal system. Early endosomes mature into late endosomes and multivesicular bodies (MVB) (Rink et al., 2005). Maturation of an early

endosome to a late endosome is accompanied by a switch in RAB proteins within the endosomal membrane, where RAB5 is replaced with RAB7 (Rink et al., 2005). This process leads to invaginations in the endosomal membrane and the generation of intraluminal vesicles (ILV) (Raiborg et al., 2002; Sachse et al., 2002). Formation of ILV occurs via two pathways; the first pathway involves the endosomal sorting complex required for transport (ESCRT) and the second pathway is independent of ESCRT (Katzmann et al., 2001; Trajkovic et al., 2008).

In the first pathway, the ESCRT complex and accessory proteins such as the AAA-type ATPase vacuolar protein sorting-associated protein (VPS) 4 and the ALG-2-interacting protein X (ALIX) are important for membrane remodeling and MVB/ILV biogenesis (Babst et al., 1998, 2002; Katzmann et al., 2001, 2003; Strack et al., 2003; Teo et al., 2004). Protein monoubiquitination serves as a sorting signal to the MVB pathway (Katzmann et al., 2001; Raiborg et al., 2002). ESCRT-0 and ESCRT-I complexes recognize monoubiquitinated protein cargo and sort it to MVB vesicles (Katzmann et al., 2001; Raiborg et al., 2002; Bache et al., 2003). Similarly, RNA packing into exosomes requires complexes with RNA binding proteins during the biogenesis of exosomes (Statello et al., 2018). ESCRT-0, ESCRT-I, and ECSRT-II form stable heterooligomers which recognize not only ubiquitin but also the phospholipid phosphatidylinositol 3-phosphate (PtdIns3P) enriched at the endosomal surface (Katzmann et al., 2003; Teo et al., 2006). ESCRT-II binds ESCRT-III and initiates formation of the ESCRT-III complex (Babst et al., 2002; Teo et al., 2004). ESCRT-III is assembled sequentially and is required for endosomal membrane deformation and formation of ILV (Hanson et al., 2008; Teis et al., 2008). ESCRT-III recruits accessory proteins such as Alix (Odorizzi et al., 2003; Strack et al., 2003). ALIX in turn recruits ubiquitin carboxyl-terminal hydrolase 4 (DOA4) responsible for deubiquitination of cargo just prior to the cargo delivery into ILV (Luhtala and Odorizzi, 2004). This process is followed by final dissociation of ESCRT proteins from the endosomal membrane catalyzed by ESCRT-III AAA-type ATPase VPS4 (Babst et al., 1998, 2002; Katzmann et al., 2001).

The second, ESCRT independent pathway involves ceramide and is dependent on membrane raft microdomains and lateral segregation of cargo (Trajkovic et al., 2008). Inhibition of neutral sphingomyelinases reduced the release of exosomes (Trajkovic et al., 2008). In addition, the tetraspanins CD63 and CD9 were shown to be involved in protein transport to ILV (Buschow et al., 2009; van Niel et al., 2011).

MVB can fuse with lysosomes to destroy their cargo or be transported to the plasma membrane and release exosomes out of the cell (Villarroya-Beltri et al., 2016) (Figure 4). ISGylation is a

posttranslational ubiquitin-like modification, which regulates MVB fate (Villarroya-Beltri et al., 2016). ISGylation promotes the fusion of MVB with lysosomes, thereby degrading MVB content and decreasing exosomes secretion (Villarroya-Beltri et al., 2016).

Secretion of exosomes can be constitutive or inducible depending on cell type (Savina et al., 2003; Wei et al., 2017).

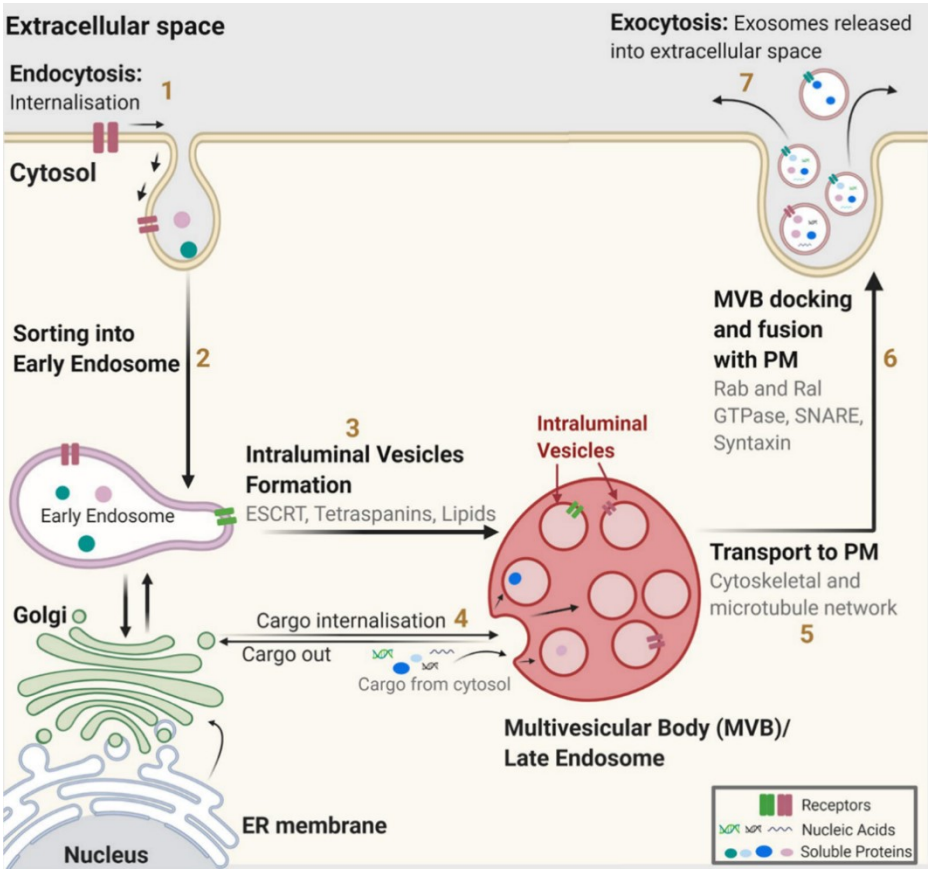

Figure 4. Exosome biogenesis. Internalized cargo (1) is sorted into early endosomes (2), which then mature into the multivesicular body (3) with internalized cargo in intraluminal vesicles (4). Multivesicular body with intraluminal vesicles is transported to the plasma membrane (5), fuses with the latter it, and exosomes are released into the extracellular space. (Modified from Gurung et al., 2021).

1.8.2. Exosome uptake

Once released into the extracellular environment, exosomes interact with target cells. Upon reaching the target cells, exosomes can be internalized by the recipient cell in different ways. Exosomes can trigger juxtacrine signaling by interaction with the cell receptors, fuse directly with the plasma membrane of the recipient cell, or can be internalized by various mechanisms of endocytosis.

1.8.2.1. Juxtacrine signaling

Ligands on the exosome surface bind directly to the receptors on the recipient cell, as was shown for Fas ligand (FasL) and TNF-related apoptosis-inducing ligand (TRAIL) (Stenqvist et al.,

2013). Exosomes from placental explant cultures bearing FasL and TRAIL ligands were capable of triggering apoptosis of recipient Jurkat cells and also activated peripheral blood mononuclear cells (PBMC) (Stenqvist et al., 2013). The same mechanism was shown for exosomes derived from ovarian tumor cells, which bore FasL and induced apoptosis of T cells (Taylor et al., 2003). Exosomes derived from dendritic cells also express FasL, together with tumor necrosis factor (TNF) and TRAIL on their surface (Munich et al., 2012). These exosomes directly kill tumor cells (B16 melanoma, KLN205 squamous lung carcinoma, and MC38 colon carcinoma cells) and activate natural killer cells via TNF (Munich et al., 2012). Specific receptors mediating exosome uptake have not been found, however, there are several candidate proteins, such as the phosphatidylserine receptor T cell immunoglobulin domain and mucin domain (TIM)1/4 and ICAM-1 (Segura et al., 2005, 2007; Miyanishi et al., 2007)**.**

1.8.2.2. Fusion with the plasma membrane

Fusion with the plasma membrane is a process in which the membrane of vesicles merges with the membrane of a target cell as it was shown for monocyte or human monocytic THP-1 cell line-derived exosomes, which fused with activated platelets (Del Conde et al., 2005). A lipid-mixing assay, which relies on the interactions between two fluorescently labeled phospholipids incorporated into exosomal membrane was used to study the fusion of vesicles with activated platelets (Del Conde et al., 2005). Lipids and proteins were transferred from exosomes to recipient cells (Del Conde et al., 2005). Similarly, dendritic cell-to-cell communication is mediated by exosomes which fuse with the plasma membrane and release exosome content (miRNA) into the cytosol of target dendritic cell (Montecalvo et al., 2012). Exosomes from multiple myeloma cells fuse with the plasma membrane of bone marrow mesenchymal stromal cells (BMSC) in addition to other mechanisms of exosome uptake (Zheng et al., 2019).

1.8.2.3. Internalization of exosomes

It has been suggested that exosome internalization is the primary mechanism of exosome uptake by recipient cells (Tian et al., 2010, 2013; Zheng et al., 2019; Joshi et al., 2020). A variety of mechanisms of exosome uptake exists including clathrin- or caveolin- dependent endocytosis, macropinocytosis, phagocytosis, and lipid raft-mediated endocytosis. It was shown that exosome internalization is temperature-dependent and involves actin polymerization (Barrès et al., 2010; Tian et al., 2010; Escrevente et al., 2011).

Clathrin-mediated endocytosis was shown to be a mechanism of exosomal uptake in various cell types such as ovarian cancer cells, the human HCT116 and COLO205 colon cancer cell lines,

and cardiomyocytes (Escrevente et al., 2011; Horibe et al., 2018; Eguchi et al., 2019). Dependence on clathrin-mediated exosome internalization was demonstrated by inhibition of clathrin-mediated endocytosis with inhibitors such as Pitstop2 and chlorpromazine (Escrevente et al., 2011; Horibe et al., 2018). Similarly, dynamin-2 inhibition reduced exosome uptake by BMSC (Tian et al., 2014).

Caveolae-dependent endocytosis of exosomes was demonstrated in the human colon cancer cell line COLO205 (Horibe et al., 2018). Similarly, exosomes derived from a multiple myeloma cell line were internalized by BMSC primarily by caveolin-dependent endocytosis (Zheng et al., 2019). However, it was also shown that caveolin-1 negatively regulates exosome internalization at least partially through suppression of ERK1/2 activation (Svensson et al., 2013).

Lipid raft-mediated endocytosis in exosome uptake was observed in human umbilical vein endothelial cells (HUVEC), the glioblastoma U87 MG cells, the breast carcinoma cells BT-549, and the ovarian carcinoma SKOV3 cells (Escrevente et al., 2011; Koumangoye et al., 2011; Svensson et al., 2013). Internalization of glioblastoma-derived exosomes involves nonclassical lipid raft-dependent endocytosis (Svensson et al., 2013). Depletion of cholesterol by methyl-β-cyclodextrin (MβCD) inhibited exosome internalization (Koumangoye et al., 2011; Svensson et al., 2013). In addition, exosome internalization is impaired when cells producing exosomes are pretreated by sphingolipid biosynthesis inhibitors, which modify the lipid composition of the budding exosomes (Izquierdo-Useros et al., 2009). Exosomal uptake was also reduced by pretreatment of HUVEC cells with filipin III (He et al., 2019).

Phagocytosis as a mechanism of exosome uptake is predominantly used by immune cells, such as dendritic cells and macrophages (Feng et al., 2010; Montecalvo et al., 2012). Exosome internalization by phagocytosis is dependent on the actin cytoskeleton and PI3K (Feng et al., 2010).

Macropinocytosis is also involved in the internalization of exosomes (Fitzner et al., 2011; Costa Verdera et al., 2017). The presence of phosphatidylserine on the surface of exosomes derived from oligodendrocytes activated micropinocytosis in microglia (Fitzner et al., 2011). Macropinocytosis of exosomes is dependent on PI3K and Na^+ (Fitzner et al., 2011; Tian et al., 2014; Costa Verdera et al., 2017). Inhibition of Na^+/H^+ exchanger (by EIPA or amiloride) or inhibition of PI3K (by LY294002 or by wortmannin) blocks micropinocytosis (Fitzner et al., 2011; Tian et al., 2014; Costa Verdera et al., 2017).

Interestingly, in HeLa cells, in ovarian carcinoma cells and in BMSC, the uptake of exosomes is mediated by more than one mechanism (Escrevente et al., 2011; Costa Verdera et al., 2017; Zheng et al., 2019).

1.8.3. Molecular composition of exosomes

Exosomes are small vesicles with specific protein and lipid composition, which also carry DNA, mRNA, miRNA, and mtDNA (Théry et al., 1999, 2001; Valadi et al., 2007; Guescini et al., 2010; Llorente et al., 2013; Kahlert et al., 2014; Thakur et al., 2014). First proteomic analyses of exosomes were performed on exosomes derived from dendritic cells, followed by proteomic analysis of exosomes of different origin, which are collected in the ExoCarta database of exosomal proteins and mRNA (Théry et al., 1999, 2001; Mathivanan and Simpson, 2009). Exosomes are enriched in distinct lipids such as glycosphingolipids, sphingomyelin, cholesterol, and phosphatidylserine as it was shown in exosomes released by PC-3 prostate cancer cells (Llorente et al., 2013). The discovery of mRNA and miRNA in exosomes derived from mouse and human mast cell lines (MC/9 and HMC-1) is considered the second breakthrough in exosome research after the discovery of their role in cell to cell communication (Raposo et al., 1996; Valadi et al., 2007). It was shown that mRNA contained in mast cell-derived exosomes is transferred to recipient cells and that this transferred mRNA can be translated into proteins, suggesting that exosomal mRNA is functional (Valadi et al., 2007). The discovery of DNA present in exosomes revealed that serum exosomes from patients with pancreatic cancer contain genomic DNA spanning all chromosomes (Kahlert et al., 2014). DNA was also present in exosomes isolated from healthy donor human plasma, vascular smooth muscle cells (VSMC), or from cell culture supernatants of HEK293and K562 cell lines (Cai et al., 2013). Double stranded DNA fragments are found inside the exosomes rather than outside as it was shown in exosomes treated by outside added DNAse (Cai et al., 2013) (Figure 5). Exosomes are capable to transfer *BCR-ABL1* DNA from K562 to HEK293 and neutrophils (Cai et al., 2013). This supports the theory of exosomal transfer of functional DNA between cells and its pathophysiological significance (Cai et al., 2013).

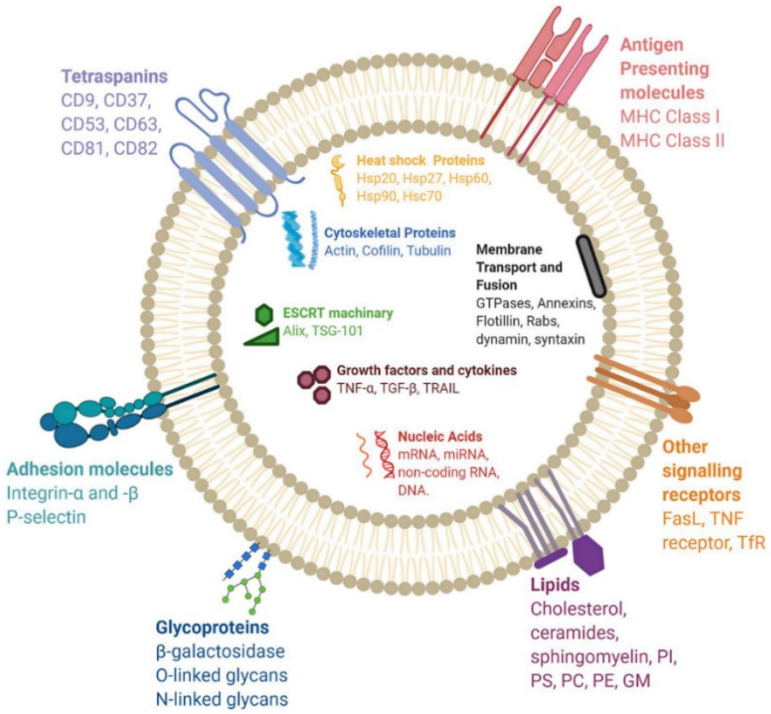

Figure 5. Exosome composition. Exosomes are composed of proteins, lipids, and nucleic acids. Proteins include transmembrane proteins (tetraspanins, antigen-presenting molecules, receptors, adhesion molecules, and glycoproteins) and luminal proteins (ESCRT components, heat shock proteins, cytokines, growth factors, and cytoskeletal proteins). Lipids include cholesterol, sphingomyelin, ceramide, phosphatidylinositol (PI), phosphatidylserine (PS), phosphatidylcholine (PC), phosphatidylethanolamine (PE), and gangliosides (GM). Nucleic acids include mRNA, miRNA, DNA, and non-coding RNA. (Modified from Gurung et al., 2021).

1.8.4. Exosomes and chronic myeloid leukemia

Exosomes have been considered to be an integral part of the extracellular microenvironment and a way of cell-to-cell communication in normal physiological state. However, emerging evidence indicates that exosomes play also important roles in different types of cancer diseases by influencing tumor growth, angiogenesis, metastasis, drug resistance, tumor niche formation, escape from the immune system, and neoplastic transformation (Huber et al., 2005; Peinado et al., 2012; Taverna et al., 2012; Abd Elmageed et al., 2014; Chen et al., 2014; Costa-Silva et al., 2015). Exosomes transfer oncogenic proteins and nucleic acids from tumor cells to recipient cells to modulate their activity (Skog et al., 2008; Peinado et al., 2012).

1.8.4.1. CML exosomes in the crosstalk with the BM microenvironment

BM is the major site of adult hematopoiesis. The BM microenvironment maintains normal hematopoiesis by integrated crosstalk among cells (Calvi et al., 2003; Zhang et al., 2003; Stier et al., 2005; Hooper et al., 2009). BM microenvironment consists of very diverse populations of specific cell types such as HSC, broad and still incompletely characterized mesenchymal stromal cells (MSC), many types of vascular and sinusoidal endothelial cells, leukemia stem cells (in the case of leukemic bone marrow), osteoblasts, osteoclasts, bone lining cells, macrophages,

perivascular CXCL12-abundant reticular cells (CAR), neurons, adipocytes, and the extracellular matrix (Behrmann et al., 2020). Normal hematopoietic stem cells reside in BM and are supported by specialized and highly organized endosteal and vascular stem cell niches (Zhang et al., 2003; Kiel et al., 2005; Tamma and Ribatti, 2017). Communication with other cells is important for HSC proliferation, survival, and self-renewal (Goloviznina et al., 2016). Genetic alterations in HSC or progenitor cells can transform these cells into LSC that retain self-renewal capacity, undergo uncontrolled proliferation, and differentiation into leukemic blasts (Biernaux et al., 1995; Jaiswal et al., 2014; Xie et al., 2014; Lee-Six et al., 2018). LSC reside in the same niche as healthy HSC, so they benefit from BM niche support and even modify BM to induce a more favorable microenvironment for the outgrowth and dissemination of leukemia cells so they become the predominant cell population (Colmone et al., 2008; Schepers et al., 2013; Duarte et al., 2018). The tumor microenvironment is important for cancer progression because it provides crucial signaling crosstalk. This crosstalk is mediated through direct cell-to-cell contact, secretion of regulatory proteins such as cytokines and growth factors, or through other factors. Among those, exosomes belong to the most important mediators of communication (Colmone et al., 2008; Schepers et al., 2013; Hornick et al., 2016; Duarte et al., 2018; Kumar et al., 2018; Gao et al., 2019). Exosomes are involved in hematologic cancers where they sustain proliferative signals, participate in evasion from the immune system, mediate angiogenesis and resistance to death (Mineo et al., 2012; Taverna et al., 2012; Hong et al., 2014; Raimondo et al., 2015; Min et al., 2018; Hrdinova et al., 2021). However, still a lot of information about the precise role of CML-derived exosomes in disease progression, immune system escape, and drug resistance is missing and needs to be elucidated. CML exosomes participate in BM niche remodeling towards malignant leukemic niche (Gao et al., 2019; Jafarzadeh et al., 2019). In CML mouse model and in BMSC from CML patients, osteogenic differentiation and proliferation capacity were impaired by CML-derived exosomes (Gao et al., 2019). Secreted exosomes were endocytosed by BMSC and decreased their capacity of osteogenic differentiation as it was shown by downregulation of a major osteogenic marker, the runt-related transcription factor 2 (RUNX2) (Gao et al., 2019). Exosomes released by CML cells were enriched in certain tumor suppressive miRNAs, especially miR-320, which suppressed osteogenesis via inhibition of β-catenin (Gao et al., 2019). Ablation of osteoblasts impaired normal HSC self-renewal and accelerated the development of leukemia (Bowers et al., 2015). Exosomes derived from the K562 cell line increased production of inflammatory and macrophage polarization molecules (IL-10, nitric oxide (NO), and TNFα) and decreased production of ROS in stromal cells and macrophages (Jafarzadeh et al., 2019). Exosomes derived from the CML cell line LAMA84 induced expression of IL-8 in HS5 bone

marrow stromal cells and also promoted adhesion of LAMA84 cells to HS5 stromal cells and thus enhanced CML cell survival and favored retention of CML cells within the bone marrow (Corrado et al., 2014, 2016). IL-8 treatment promoted LAMA84 cell survival by activating AKT kinase (Corrado et al., 2014). Further studies showed that LAMA84-derived exosomes and exosomes derived from CML patients contain a critical autocrine growth factor, amphiregulin (AREG), which activates the epidermal growth factor receptor (EGFR) signaling in HS5 stromal cells (Corrado et al., 2016). Contradictory results showed that K562-derived exosomes decreased adhesivness of stromal cells via miR-711 delivery (Jiang et al., 2020).

Endothelial cells are active players in the formation of new blood vessels both in health and diseases like leukemia (Li et al., 2004; Pezeshkian et al., 2013). In the study performed on CML cell line-derived exosomes and a model cell line of endothelial cells (HUVEC), fluorescently labeled exosomes derived from LAMA84 CML cell line were internalized by HUVEC cells and stimulated neoangiogenesis through modulation of HUVEC motility and tube formation (Taverna et al., 2012). LAMA84-derived exosomes increased expression of the adhesion molecules ICAM-1 and vascular cell adhesion molecule-1 (VCAM-1) via IL-8 in target HUVEC cells (Taverna et al., 2012). Similar proangiogenic effects were achieved by K562-derived exosomes (Mineo et al., 2012; Umezu et al., 2013). Further, it was shown that tube formation in HUVEC cells is mediated through Src kinase activation and miR-92a transfer (Mineo et al., 2012; Umezu et al., 2013). Data obtained from cell lines were confirmed *in vivo* in nude mice subcutaneously injected either with plugs containing a synthetic extracellular matrix (Matrigel) and K562-derived exosomes, or with exosomes isolated from CML patients (Mineo et al., 2012; Taverna et al., 2012).

Cancer cells evade the host immune system by known phenomenon called immune escape or immune evasion by several immunological mechanisms. One of these mechanisms which facilitates tumor progression is the suppression of **immunocompetent cells**. However, there is only one study describing the role of CML-derived exosomes in modulating the immune cell functions (Jafarzadeh et al., 2019). Little more information is known about the role of AML-derived exosomes. AML-derived exosomes carrying high levels of TGF-β1 suppressed NK cell cytotoxicity by down-regulating expression of natural killer group 2 member D (NKG2D) in normal natural killer cells (Szczepanski et al., 2011). CML-derived exosomes contain high levels of TGF-β1 too (Raimondo et al., 2015).

CML exosomes can also reprogram macrophages to M2-like phenotype. Such phenotypical change is associated with increased production of TNFα, IL-10 and downregulation of inducible

nitric oxide synthase (iNOS) transcript levels. This further led to reduction of NO and ROS levels in macrophages treated with CML exosomes (Jafarzadeh et al., 2019). CML exosomes can thus induce changes in macrophages and drive their polarization towards leukemia-associated macrophages (Jafarzadeh et al., 2019).

1.8.4.2. Exosomes and proliferation of CML cells

Exosomes are capable of mediating direct cell-to-cell communication via an autocrine mechanism. Exosomes released by LAMA84 cell line directly promoted the proliferation of LAMA84 cells by transforming growth factor beta 1 (TGF- β1)-mediated activation of ERK, AKT, and nuclear factor kappa-light-chain-enhancer of activated B cells (NF-kB) (Raimondo et al., 2015). Exosomes from LAMA84 cells increased the expression of anti-apoptotic (survivin, BCL-xL and BCL-2-like protein 2 (BCL-W)) and decreased the expression of pro-apoptotic (BAD, BAX and BCL2 binding component 3 (PUMA)) proteins and their respective mRNAs in recipient cells (Raimondo et al., 2015).

Recently, it was shown that BMSC derived exosomes promoted tumor growth by increasing expression of BCL-2, decreasing expression of caspase-3, and inducing imatinib resistance in BALB/c nu/nu mice (Zhang et al., 2020). However, results obtained *in vivo* contradicted the *in vitro* results because it was found that *in vitro* BMSC exosomes are able to inhibit proliferation of CML cells (Zhang et al., 2020).

1.8.4.3. CML exosomes, horizontal transfer of *BCR-ABL1*, and chemoresistance

An increasing number of studies suggest that exosomes can mediate drug resistance in malignant cells (Steinbichler et al., 2019). Drug resistance is the main cause of leukemia therapy failure (Lahaye et al., 2005). Exosomes derived from the K562 cell line contain BCR-ABL protein, *BCR-ABL1* mRNA, and fragments of *BCR-ABL1* DNA (Cai et al., 2013, 2014; Kang et al., 2018; Hrdinova et al., 2021). *BCR-ABL1* DNA fragments can be transferred to recipient cells (HEK293, neutrophils) and induce CML-like disease in immunodeficient mice (Cai et al., 2013, 2014). Imatinib-resistant K562 cells were shown to transfer miR-365 via exosomes to imatinib-sensitive K562 cells leading to acquired imatinib resistance in the recipient cells (Min et al., 2018). Similarly, we found that exosomes derived from imatinib-resistant K562 cells significantly increased the survival of imatinib-sensitive K562 cells in the presence of imatinib (Hrdinova et al., 2021).

1.8.4.4. CML exosomes as biomarkers and as drug delivery vesicles

Research outputs from investigating the role of exosomes in leukemia progression can be applied in clinical use for their prognostic, therapeutic, and diagnostic values. Exosomes carrying specific molecules associated with cancer represent an attractive tool for biomarker discovery and screening. BCR-ABL1 fusion gene and protein are the fingerprints of CML so they are commonly used as biomarkers in CML cell lines and CML patient samples (Kang et al., 2018; Bernardi et al., 2019; Hrdinova et al., 2021). In addition, our results suggest that exosomal surface proteins (CD146, IFITM3, and CD36) from imatinib-resistant $K562^{IR}$ cells could be used as potential diagnostic markers of imatinib resistance in CML (Hrdinova et al., 2021). However, a recent study performed on exosomes isolated from plasma of CML patients responding and non-responding to imatinib showed different upregulated proteins as candidate biomarkers of imatinib resistance (Li et al., 2021)

Exosomes can also be used as a drug delivery system (Bellavia et al., 2017). Modified exosomes derived from HEK293T cells engineered to express IL3 fused to the exosomal lysosome-associated membrane protein 2 (LAMP2B) were loaded with imatinib and were capable of targeting leukemia cells *in vitro* and *in vivo*. Modified exosomes containing BCR-ABL siRNA were also able to deliver their content to imatinib-resistant CML cells and reduced their viability. BCR-ABL siRNA in exosomes also showed *in vivo* effect. Exosomes containing BCR-ABL siRNA reduced tumor growth in mice subcutaneously inoculated with imatinib-resistant CML cells (Bellavia et al., 2017).

2. Aims of the study

The main aim of the study was to use proteomic approach for comprehensive characterization of two model CML cell lines resistant to imatinib, in order to identify putative metabolic vulnerabilities associated with imatinib resistance, which can be exploited as potential therapeutic targets in the imatinib-resistant cells. Proteomic characterization of exosomes derived from imatinib-resistant K562 cells could elucidate the role of exosomes in the transfer of drug resistance traits among CML cells.

Specific aims were as follows:

1. Proteomic characterization of CML cells resistant to imatinib, covering two different mechanisms of resistance, and identification of metabolic adaptations in their proteomes which contribute to their proliferation in the presence of imatinib.

2. Evaluation of adaptational changes in the phenotypes of imatinib-resistant cells as metabolic vulnerabilities specific for cells resistant to imatinib, which can be targeted by clinically available drugs and exploited as potential therapeutic targets.

2. Elucidation of the effect of exosomes derived from $K562^{IR}$ cells resistant to imatinib on survival of cells sensitive to the drug.

3. Proteomic characterization of exosomes derived from K562 and $K562^{IR}$ cell lines with an emphasis on identification of clinically relevant markers of resistance to imatinib.

3. Materials and methods

Materials. All chemicals, unless otherwise stated, were purchased from Merck KgaA.

Methods. All methods which have already been published are in detail described in the publications.

Cell lines. The human CML-T1 and K562 cell lines (purchased from the German Collection of Microorganisms and Cell culture GmbH) were grown in Roswell Park Memorial Institute (RPMI) medium supplemented with 10% fetal bovine serum (FBS, Gibco, Thermo Fisher Scientific), 100 U/ml penicillin G, 100 μg/ml streptomycin and 7.5% sodium bicarbonate at 37˚C in a humidified incubator with 5% CO_2. CML-T1^{IR} and K562^{IR} resistant to imatinib were derived from original sensitive cell lines (CMLT-T1, K562) by prolonged cultivation in gradually increasing imatinib concentrations.

Mutational analysis of BCR-ABL1 kinase domain. CML-T1 and CML-T1^{IR} cells were first analyzed by Sanger sequencing as previously described (Poláková et al., 2010; Toman et al., 2016). The results were later completed by next-generation sequencing (NGS). K562 and K562^{IR} cells were analyzed directly by NGS (Hrdinova et al., 2021).

BCR-ABL1 gene copy number analysis in K562 and K562^{IR} cells. BCR-ABL1 copy number in K562 and K562^{IR} cells was determined by quantitative droplet digital PCR (ddPCR) method and a K562 specific assay based on the *BCR-ABL1* gene breakpoint sequence (Hrdinova et al., 2021).

Measurement of BCR-ABL1 transcript levels in K562 and K562^{IR} cells. Total RNA from K562 and K562^{IR} cells was isolated using TRIzol® reagent (Thermo Fisher Scientific, Inc.) according to the manufacturer's instructions. cDNA was synthesized by 200 U M-MLV reverse transcriptase (Promega Corporation) and random hexamer primers (Jena Bioscience GmbH) according to the instruction of the manufacturer, with incubation at 37˚C for 1 h and denaturation at 95˚C for 5 min. β-Glucuronidase (GUSB) was used as the control gene (Rulcová et al., 2007; Moravcová et al., 2009). The measurement of the expression levels of *BCR-ABL1* was performed according to the Europe Against Cancer protocol (Gabert et al., 2003).

Cell viability assays. CMLT1 and CML-T1^{IR} cells ($1x10^4$) were grown in the presence of increasing concentrations of the tested drugs imatinib, amiloride, 3′,4′-dichlorobenzamil hydrochloride (DCB), thapsigargin, ionomycin, verapamil, carboxyamidotriazole (CAI), FK-506, and CsA for 3 days. K562 and K562^{IR} cells ($5x10^4$) were cultured in the presence of increasing concentrations of selected inhibitors, i.e. imatinib, PPP, Stattic, NT157, and

cyclosporine H (CsH) for 3 days. Inhibitor toxicity was determined by measuring cell viability using the Vybrant™ MTT cell proliferation assay kit (Thermo Fisher Scientific, Inc.), following the manufacturer's instructions. Absorbance was detected at 570 nm using a microplate reader (Chameleon; Hidex Oy) or using a multimode microplate reader (Spark, Tecan Group, Ltd.). Data were analyzed using MikroWin 2000 software, v4.0 (Mikrotek Laborsysteme GmbH).

Multidrug resistance (MDR) assay. Measurement of drug efflux from CML-T1 and CML-T1^{IR} cells was performed using the Vybrant™ Multidrug Resistance Assay kit (Thermo Fisher Scientific, Inc.). CML-T1 and CML-T1^{IR} cells (5×10^4 cells/well) were grown in a 96-well plate for 24 h. Then the cells were treated with CsA and/or verapamil (at a final concentration ranging from 0.4 to 120 μg/ml). Untreated cells were used as a control. After 1 hour of treatment, calcein acetoxymethyl ester (calcein-AM) was added to 100 μl of each cell sample. After 30 min, the cells were washed twice with 200 μl of cold RPMI 1640 medium, and the fluorescence of the retained calcein was measured at 485 nm and 538 nm by spectrofluorometer FluoroMax-3 equipped with DataMax software (Jobin Yvon Horriba, Kyoto, Japan).

Cytosolic pH measurement. The assay was performed according to Kiedrowski (Kiedrowski, 2011). Cells were treated with 1 μM BCECF-AM (2',7'-bis-(2-carboxyethyl)-5-(and-6)-carboxyfluorescein) for 20 min at room temperature. To monitor the fluorescence of BCECF, the cells were exposed every 5 sec to excitation light (488 and 440 nm) and the fluorescence emission spectra up from 520 nm (F488 and F440) were measured by a spectrofluorometer FluoroMax-3 equipped with DataMax software (Jobin Yvon Horriba, France). Cytosolic pH values were calculated from F488/F440 ratios based on *in situ* calibration performed at the end of the experiments according to Kiedrowski (Kiedrowski, 2011).

Measurement of cytosolic Ca^{2+}. Calcium concentration in the cytosol was measured as previously described (Kinsella et al., 1997). Briefly, the cells were washed with modified Hank's balanced salt solution (HBSS) buffer (140 mM NaCl, 5 mM KCl, 2 mM $CaCl_2$, 3 mM $MgCl_2$, 10 mM 4-(2-hydroxyethyl)-1-piperazineethanesulfonic acid buffer (HEPES), 50 mM glucose pH 7.4) and treated with 3 μM Fura-2 acetoxymethyl ester (Fura-2/AM) for 30 min at 25°C in the dark, rinsed and allowed to rest for 30 min prior to fluorescence measurements by a FluoroMax-3 spectrofluorometer equipped with DataMax software (Jobin Yvon Horriba, Japan). The fluorescence intensity of Fura-2/AM (excitation at 340 and 380 nm, and emission at 510 nm) was recorded every 15 sec, with an integration time of 3 sec. Free intracellular Ca^{2+} concentration was determined proportionally to the ratio of fluorescence at 340/380 nm. Grynkiewicz equation

was used to calculate the actual Ca^{2+} concentration (Grynkiewicz et al., 1985). The K_d for Ca^{2+} binding to Fura-2/AM was 240 nM at the experimental temperature.

Sample preparation for two-dimensional electrophoresis (2-DE). CML-T1 and CML-T1^{IR} cells were washed twice with phosphate buffered saline (PBS) and lysed in a lysis buffer composed of 7 M urea, 2 M thiourea, 4% CHAPS, 60 mM dithiothreitol (DTT), 1% ampholytes (IPG buffer pH 4.0–7.0; GE Healthcare Life Sciences), and a protease inhibitor cocktail (Roche Diagnostics) for 20 min at room temperature. The cleared cell lysates (15,000 x g for 20 min at room temperature) were collected and the protein concentration was determined by the Bradford method (Bio-Rad Laboratories, Inc.). The protein concentration in all samples was equalized by dilution with the lysis buffer to 7.3 mg/ml.

Two-dimensional electrophoresis (2-DE). Each biological sample of CML-T1 and CML-T1^{IR} was run in six technical replicates. Isoelectric focusing was carried out using a Bio-Rad Protean IEF cell. Immobilized pH gradient (IPG) strips (pH 4.0–7.0; 24 cm, GE Healthcare Life Sciences) were rehydrated overnight, each in 450 µl of sample, representing 3.3 mg of protein. Isoelectric focusing was performed for 60 kVh, with the maximum voltage not exceeding 5 kV, the current limited to 50 mA/strip, and the temperature set to 18°C. The focused IPG strips were equilibrated and reduced in equilibration buffer A (6 M urea, 50 mM Tris pH 8.8, 30% glycerol, 2% SDS, and 450 mg DTT/50 ml of the buffer) for 15 min and subsequently alkylated in equilibration buffer B (6 M urea, 50 mM Tris pH 8.8, 30% glycerol, 2% SDS and 1.125 mg iodoacetamide/50 ml). The second dimension was performed in 10% polyacrylamide gel electrophoresis (PAGE) gels, equilibrated strips were secured in place by molten agarose. Electrophoresis was performed in a Tris-glycine-SDS system using a Protean Plus Dodeca Cell apparatus (Bio-Rad Laboratories, Inc.) with buffer circulation and external cooling (20°C). The twelve gels were run at a constant voltage of 200 V for 6 h. Following electrophoresis, the gels were washed three times for 15 min in deionized water to remove SDS. The washed gels were subsequently stained in Coomassie G-250 (SimplyBlue SafeStain, Invitrogen Life Technologies, Carlsbad, CA, USA) overnight, and then destained in deionized water.

Densitometry. Calibrated densitometer GS 800 was used to scan the stained gels (Bio-Rad, Inc.). Analysis of images was performed with Phoretix 2D software (Nonlinear Dynamics, Newcastle upon Tyne, UK) in semi-manual mode. Normalization was based on total spot density. Integrated spot density values (spot volumes) were calculated after background subtraction. Average spot volume values (averages from all the six gels in the group) for each spot were compared between

the groups. Protein spots were considered differentially expressed if the average difference of normalized spot volume was >1.5-fold and the statistical significance of the change determined by the t-test was $P<0.05$.

Matrix-assisted laser desorption/ionization (MALDI) MS, protein identification. Differentially expressed proteins were manually excised from gels, cut into small pieces, and washed with 25 mM ammonium bicarbonate in 50% acetonitrile (ACN) three times. The gels pieces were then dried in a SpeedVac concentrator (Eppendorf, Hamburg, Germany) and subsequently incubated with sequencing grade modified trypsin (6 ng/μl) (Promega) in 25 mM ammonium bicarbonate in 5% ACN overnight at 37°C. The resulting peptides were extracted with 50% ACN. Samples were then spotted on a steel target plate (Bruker Daltonics, Bremen, Germany) and allowed to dry at room temperature. Matrix solution composed of 3 mg α-cyano-4-hydroxycinnamic acid in 1 ml of 50% ACN containing 0.1% trifluoroacetic acid was then added. Positive-ion MALDI mass spectra were measured on an Autoflex II MALDI-TOF/TOF mass spectrometer (Bruker Daltonics) equipped with a solid nitrogen laser (337 nm) and FlexControl software in reflectron mode. The mass spectrometer was calibrated externally using Peptide Calibration Standard II (Bruker Daltonics). Spectra were acquired in the mass range of 800–3,000 Da. Flex analysis software was used to generate peak lists. Proteins were identified by searching against Swiss-Prot (2014 version) using the Mascot software. The search criteria were set as follows: mass tolerance 100 ppm, taxonomy *Homo sapiens*, 1 missed cleavage, the cysteine carbamidomethylation as a fixed modification, oxidation of methionine, and protein N-terminal acetylation as variable modifications. Proteins were considered as identified with a Mascot score threshold over 56 for $P<0.05$.

Gene microarray targeting WNT. Total RNA was isolated from CML-T1 and CML-T1^{IR} cells using TRIzol reagent (Thermo Fisher Scientific, Inc.) and a RNeasy Mini kit (Qiagen, Hilden, Germany) according to the manufacturer's instructions. cDNA was synthesized using M-MLV reverse transcriptase (Promega) and random hexamer primers (Jena Bioscience GmbH). The expression of 92 genes from the WNT signaling pathway and four control genes was analyzed on a TaqMan® array human WNT Pathway Fast 96-well plate (Invitrogen Life Technologies) by a StepOnePlus™ RT-PCR system (Applied Biosystems, Foster City, CA, USA) in triplicates for both CML-T1 and the CML-T1^{IR} cells. The genes (n=25), for which the amplification signals were not observed in one or more replicates simultaneously for CML-T1 and CML-T1^{IR}, were excluded from the analysis. GUSB was used as the control gene (White et al., 2015). Relative expression levels of the genes (n=67) were evaluated using the $2^{-\Delta\Delta Cq}$ formula according to

Livak *et al* (Livak and Schmittgen, 2001). Glyceraldehyde-3-phosphate dehydrogenase (GAPDH) was used for data control checking and provided highly similar results as obtained with GUSB.

Exosome isolation from K562 and K562^{IR} cells. K562 and K562^{IR} cells were cultured in RPMI medium with 10% exosome-depleted FBS for 5 days. Exosomes were isolated from 200 ml cell culture media according to the protocol as described (Théry et al., 2006; Hrdinova et al., 2021).

Exosome visualization by transmission electron microscopy. Exosomes were resuspended in Trump´s 4F:1G fixative and adsorbed on Formvar/carbon-coated grids which were conditioned with 1% Alcian blue in 1% acetic acid. The adsorbed exosomes were negatively stained with 2% phosphotungstic acid and then viewed at 100 kV with a JEM 2000 CX microscope (JEOL, Ltd.) equipped with an Olympus MegaviewTM II digital camera (Olympus Corporation).

Exosome size and concentration measurement using tunable resistive pulse sensing. Exosomal aliquot resuspended in phosphate-buffered saline (PBS) was placed in the NP150 nanopore (qNano; Izon Science). All samples were measured with the same applied voltage and at a defined membrane stretch at two pressure levels of 5 and 11 mbar. The calibration particles were measured immediately after the exosomal samples and under identical conditions.

Exosome fluorescent labeling and uptake monitoring. Freshly isolated exosomes were resuspended in PBS, labeled with carboxyfluorescein succinimidyl ester (CFSE) (Invitrogen; Thermo Fisher Scientific, Inc.), diluted to a final concentration of 20 μM, and incubated at room temperature in the dark for 25-30 min. The CFSE labeling process was stopped by adding 4 ml of cold complete media, supplemented with 10% FBS on ice for 5 min. Exosomes labeled with CFSE were diluted in PBS, collected by ultracentrifugation (100,000 x g for 70 min at 4˚C), and resuspended in 1.5 ml cell culture media with K562 cells ($5x10^5$ cells/ml). CFSE-positive cells were observed under a FluoView FV1000 confocal laser scanning microscope (Olympus Corporation) using an UPlanSAPO 60x NA1.35 oil immersion objective (magnification, x60). A 488 nm laser was used for CFSE excitation, and fluorescence emission was detected with a high sensitivity GaAsP detector at 500-600 nm. Fluorescent images were processed using the FluoView software (FV10 ASW v3.1; Olympus Corporation).

Exosomes and cell co-cultivation. The K562 cells were co-cultured with exosomes derived either from K562 or K562^{IR} cells for 4 h and then incubated with 2 μM imatinib for 48 h. Cell viability was assessed by a Vybrant® Cell Proliferation Assay kit (Thermo Fisher Scientific, Inc.). The absorbance was measured at 570 nm using a microplate reader (Chameleon; Hidex Oy).

Preparation of nuclear and cytoplasmic extracts. Cytoplasmic and nuclear extracts were prepared using the Nuclear and Cytoplasmic Extraction kit (NE-PER; Thermo Fisher Scientific, Inc.) according to the manufacturer's instructions with an additional modification in the final step of the nuclear protein extraction procedure, where the resulting pellets of the nuclear proteins were washed in ice cold PBS supplied with a protease inhibitor cocktail (Roche Diagnostics) and re-centrifuged at 16,000 x g to remove cytoplasmic protein contaminations.

Western blot analysis. CML-T1 cell pellets were lysed in lysis buffer containing 50 mM Tris pH 7.4., 1% Triton X100, a protease inhibitor cocktail, 1 tablet/10 ml (Roche Diagnostic) on ice for 20 min. K562 and $K62^{IR}$ cells were treated with PPP (100 nM), Stattic (5 µM), NT157 (0.5 µM), CsH (8 µM) for 24 h for detection of total proteins and for 4 h for detection of phosphoproteins. K562 and $K562^{IR}$ cell pellets were solubilized in CelLytic™ M lysis buffer containing protease inhibitor cocktail (1 tablet/10 ml; Roche Diagnostics) on ice for 20 min.

K562 and $K562^{IR}$ exosome pellets were lysed in 150 µl lysis buffer composed of 140 mM sodium chloride, 10mM HEPES, 0.15% Triton X100, and protease inhibitor cocktail (1 tablet/10 ml; Roche Diagnostic), and incubated on ice for 20 min. An Amicon Ultra 0.5. ml 3 kDa molecular weight cut-off (MWCO) centrifugal filter was used to pooled and concentrate exosome samples. Micro BCA™ protein assay kit (Pierce; Thermo Fisher Scientific) was used according to the manufacturer´s instructions to determine the protein concentration and the protein samples were frozen and stored at -80°C.

The cleared cell lysates from CML-T1, CML-$T1^{IR}$, K562, and $K562^{IR}$ were collected by centrifugation at 15,000 x g for 20 min at 4˚C, and the protein concentration was determined by the Bradford method (Bio-Rad Laboratories, Inc.).

CML-T1 and CML-$T1^{IR}$ lysed samples (60 µg) were combined with SDS loading buffer containing DTT and separated on Novex precast 4-20% gradient gels (Thermo Fisher Scientific). The lysed samples (30-60 µg) from K562 and $K562^{IR}$ cells and their respective exosomes were mixed with Laemmli sample buffer (Bio-Rad Laboratories, Inc.) containing 2-mercaptoethanol and separated on 4-15% or 7.5% (in the case of Bcr-Abl separation) precast gels (Mini PROTEAN® TGX™; Bio-Rad Laboratories, Inc.). The separated proteins were transferred onto polyvinylidene fluoride membranes using the iBlot system, according to the manufacturer's instructions (Thermo Fisher Scientific, Inc.). The membranes were blocked for 1 h in SuperBlock™ blocking buffer (Thermo Fisher Scientific, Inc.) and incubated overnight at 4˚C with primary antibodies diluted to 1:1,000 in PBST (PBS, 0.1% Tween-20) (Table I).

After extensive washing in PBST, the membranes were incubated with secondary antibodies diluted to 1:20,000 in PBST (PBS, 0.1% Tween-20) (Table I) for 90 min at room temperature. Protein bands in the case of CML-T1 and CML-T1^{IR} cells were detected with an enhanced chemiluminescence detection reagent (ECL; GE Healthcare Life Sciences) on X-ray film (Kodak, Rochester, NY, USA), developed, scanned, and quantified by the Quantity One software (Bio-Rad). Protein bands in the case of K562 and K562^{IR} cells and their respective exosomes were detected using a G:BOX imager (Syngene Europe), and quantified using ImageJ software, v1.8.0 (National Institutes of Health).

Table I. List of primary and secondary antibodies.

Antibody Specificity / Sensitivity	**Host**	**Clonality**	**Supplier**	**Cat. no.**
Primary				
β-actin	rabbit	monoclonal	Cell Signaling Technology, Inc.	4970
NFAT	rabbit	monoclonal	Cell Signaling Technology, Inc.	5862
NHERF1	rabbit	monoclonal	Cell Signaling Technology, Inc.	8601
MRP2/ABCC2	rabbit	monoclonal	Cell Signaling Technology, Inc.	12559
c-Abl	rabbit	polyclonal	Cell Signaling Technology, Inc.	2862S
Bcr-Abl (7C6)	mouse	monoclonal	Abcam	ab187831
GAPDH	rabbit	monoclonal	Merck KgaA	SAB5600208
IFITM3	rabbit	monoclonal	Cell Signaling Technology, Inc.	59212
CD146	mouse	monoclonal	BD Biosciences	563619
CD36	rabbit	monoclonal	Cell Signaling Technology, Inc.	14347S
STAT3	rabbit	monoclonal	Cell Signaling Technology, Inc.	4904S
phospho-STAT3 (Tyr705)	rabbit	monoclonal	Cell Signaling Technology, Inc.	9145S
phospho-STAT3 (Ser727)	rabbit	polyclonal	Cell Signaling Technology, Inc.	9134S
histone H3	rabbit	monoclonal	Cell Signaling Technology, Inc.	4499S
lamin B1	rabbit	monoclonal	Cell Signaling Technology, Inc.	12586S
IGF-I Receptor β	rabbit	monoclonal	Cell Signaling Technology, Inc.	9750S
phospho-IGF-I Receptor β (Tyr1135/1136)/Insulin Receptor β (Tyr1150/1151)	rabbit	monoclonal	Cell Signaling Technology, Inc.	3024S
IRS-1	rabbit	monoclonal	Cell Signaling Technology, Inc.	3407S
phospho-IRS-1 (Ser612)	rabbit	monoclonal	Cell Signaling Technology, Inc.	3203S
phospho-IRS-1 (Ser636/639)	rabbit	polyclonal	Cell Signaling Technology, Inc.	2388S
Akt (pan)	rabbit	monoclonal	Cell Signaling Technology, Inc.	4691S
p44/42 MAPK (Erk1/2)	rabbit	polyclonal	Cell Signaling Technology, Inc.	9102S
phospho-p44/42 MAPK (Erk1/2) (Thr202/Tyr204)	rabbit	monoclonal	Cell Signaling Technology, Inc.	4370S
p-Akt1 (5.Ser 473)	mouse	monoclonal	Santa Cruz Biotechnology	sc-293125

EXOAB antibody kit 1: CD63, CD81, CD9 and HSP70	rabbit	polyclonal	Systems Biosciences, LLC	EXOAB-KIT-1
Secondary				
horseradish peroxidase-conjugated anti-rabbit	goat	polyclonal	Cell Signaling Technology, Inc.	7074P2
horseradish peroxidase-conjugated anti-mouse	horse	polyclonal	Cell Signaling Technology, Inc.	7076P2

Sample preparation for tandem mass spectrometry (MS/MS) analysis: K562 cells and exosomes. Exosomes derived from K562 and K562^{IR} cells. A total of five pairs of independent exosomal isolations from both K562 and K562^{IR} cells were analyzed by MS/MS spectrometry. The filter-aided sample preparation method with some modifications was used (Wisniewski et al., 2009). Detailed description of proteomic sample preparation is described in the publication by Hrdinova *et al.* (Hrdinova et al., 2021).

K562 and K562^{IR} cell lysates. A total of 5 pairs of independent cell lysates from both K562 and K562^{IR} cells were subjected to MS/MS analysis. The filter-aided sample preparation method with some modifications was used (Wisniewski et al., 2009). Frozen cell pellets were resuspended in 100 mM ammonium bicarbonate, transferred to spin columns (Amicon Ultra 0.5 ml 10 kDa MWCO centrifugal filters; Merck KGaA), and centrifuged at 26,000 x g for 20 min at 4˚C. The samples were then washed twice with 400 µl 100 mM ammonium bicarbonate and centrifuged again (26,000 x g for 20 min at 4˚C). RapiGest™ (0.1%; Waters Corporation) dissolved in 100 µl 50 mM Tris/HCl (pH 7.5) was subsequently added to the samples in the spin columns, then the samples were incubated at 95˚C for 10 min. After allowing the samples to cool down, 200 µl 0.1% RapiGest™ in 50 mM Tris/HCl (pH 7.5) with 8 M guanidinium chloride was added, and the samples were subsequently incubated for 20 min at room temperature. Samples were washed twice by 0,4 µl 100 mM ammonium bicarbonate (26 000 x g, 20 min at 4 °C). Benzonase (SRP6593-5KU, Sigma-Aldrich) was added to the final concentration 150U/ml, and samples were incubated on ice for 1 hour. The samples were then centrifuged at 18,000 x g for 25 min at 25˚C. Sample aliquots (10 µl) were taken for protein concentration quantification using the QuantiPro™ BCA Assay kit (Sigma-Aldrich; Merck KGaA). Subsequently, the samples were reduced with 100 µl 100 mM (Tris)2-carboxyethyl phosphine hydrochloride for 30 min at 55˚C in a thermoshaker (Biosan, Ltd.) set at 600 rpm, alkylated with 100 µl 300 mM iodoacetamide at

37˚C for 30 min in the dark, then centrifuged at 12,000 x g for 35 min at 25˚C. Next, the samples were digested overnight at 37˚C using 2 μg sequencing-grade trypsin (Promega Corporation). The digested samples were then transferred into a new microtube for subsequent centrifugation (12,000 x g for 35 min at room temperature). Empore™ Solid Phase Extraction cartridges (C18; standard density, bed I.D., 4 mm) (3M Company) were used to desalt the peptide mixtures. Peptides were eluted in 60% ACN/0.1% trifluoroacetic acid (TFA), then dried in a SpeedVac. Prior to MS analysis, the samples were resuspended in 30 μl 2% ACN/0.1% TFA.

Liquid chromatography (LC) MS/MS (LC-MS/MS) of K562, K562^{IR} cells, and their respective exosomes.

LC-MS/MS analysis. The LC separation of exosome and cell samples was carried out by an UltiMate™ 3000 RSLCnano system controlled by Chromeleon software (Dionex; Thermo Fisher Scientific, Inc.). Aliquots (1 μl) of each sample (10X diluted) were loaded onto a capillary trap column (PepMap100 C18, 3 μm, 100 Å, 0.075x20 mm Dionex; Thermo Fisher Scientific, Inc.) at 5 μl/min for 5 min. Afterward, the peptides were separated on an analytical column (PepMap RSLC C18, 2 μm, 100 Å, 0.075x150 mm Dionex; Thermo Fisher Scientific, Inc.) by a gradient formed by the mobile phase A [0.1% formic acid (FA)] and mobile phase B [80% ACN/0.1% FA], running from 4 to 34% over 68 min, and from 34 to 55% of mobile phase B over 21 min, at a flow rate of 0.3 μl/min at 40 °C. Subsequently, the eluted peptides were electrosprayed directly into Nanospray Flex ion source (Thermo Fisher Scientific, Inc.) and detected by Q-Exactive™ mass spectrometer. Full positive ion MS spectra (350-1,650 m/z) were acquired using a $1x10^6$ automatic gain control (AGC) target in the Orbitrap at 70,000 resolution. The top 12 precursors with charge state $\geq$2 and threshold intensity of $5x10^4$ counts were selected for higher-energy collisional dissociation fragmentation, with a dynamic exclusion window of 30 sec. The isolation window of 1.6 Da and normalized collision energy 27% was used. Each MS/MS spectrum was acquired at a resolution of 17,500, with a $1x10^5$ AGC target and a maximum 100 msec injection time.

Label-free quantification (LFQ): Raw data processing. Analysis of the acquired raw files was performed against the *Homo sapiens* subset of the SwissProt database (exosomes: downloaded on 4th July 2019; 26,468 sequences, K562 cells: downloaded on 8th July 2020; 26,549 sequences) by the MaxQuant software, v1.5.3.30 (Cox and Mann, 2008) [Andromeda was used as the search engine (Cox et al., 2011)]. Tryptic peptides at least 7 amino acids in length, with up to two missed cleavages were evaluated in configuration of mass tolerance 4.5 ppm at the MS level, and 0.5 Da at the MS/MS level. The oxidation of methionine was set as a variable

modification, and the carbamidomethylation of cysteine was set as a fixed modification. For the peptide spectra matches and protein identification using a target decoy approach, a false discovery rate (FDR) of 1% was used. The default parameters of the MaxLFQ algorithm (Cox et al., 2014), with the minimum ratio count set to 2 were used for relative quantification.

LFQ: Data analysis. The 'proteinGroups.txt' MaxQuant output file was uploaded into Perseus v1.5.2.6 (Tyanova et al., 2016). Potential, contaminants, decoy hits, and proteins only identified by site were removed. Protein groups quantified in at least four of five replicates for exosomes and in at least three of five replicates for K562 cells were considered for further $\log_2$ transformation of the LFQ intensities. Missing values were imputed from a normal distribution [Gaussian distribution width, 0.3 standard deviation (SD) and downshift 1.8 SD of the original data]. Exosomal data was normalized by the open source tool Normalyzer (http://www.quantitativeproteomics.org/normalyzerde) using the variance stabilization normalization method (Chawade et al., 2014). The Student's t-test (permutation-based FDR 0.05, S0=0.1) was used for statistical analysis. Finally, proteins from this group with a fold change at least 1.5 were considered as being significantly different ($P<0.05$). Inter-run reproducibility of individual LC-MS analyses was evaluated by Pearson's correlation test. Proteins with expected or known cell-surface localization were selected using GenieScore, an algorithm for the prediction of surface localization (Waas et al., 2020). The Exocarta database (http://www.exocarta.org/) was used to compare the proteins identified with those already found in exosomes.

Flow cytometry analysis. K562 and $K562^{IR}$ cells ($1.5x10^6$ cells) were washed in washing buffer composed of PBS supplemented with 0.1% bovine serum albumin (BSA) and 2 mM ethylenediaminetetraacetic acid (EDTA), centrifuged at 300 x g for 10 min at room temperature, and then resuspended in washing buffer. Aliquots (50 µl) the K562 and $K562^{IR}$ cell suspension (10^5 cells/tube) were transferred to tubes and incubated with 1 µl Anti-IFITM3 AF405 (cat. no. ITA8095; 1:50; G-Biosciences; Geno Technology, Inc.), 1 µl anti-CD146 AF647 (cat. no. 563619; 1:50; BD Biosciences) and 2 µl Anti-Hu CD36 FITC (cat. no. 1F-451-T100; 1:25; EXBIO Praha, a.s.) in the dark for 30 min at room temperature. The samples were then washed with 1 ml of washing buffer prior to centrifugation (300 x g for 5 min at 25˚C). Cell pellets were resuspended in 250 µl of washing buffer and the samples were analyzed by flow cytometry, in triplicate, using BD FACSCanto™ II Cell Analyzer (BD Biosciences). The data was analyzed by BD FACSDiva software (v6.1.3; BD Biosciences). Mean fluorescence intensity (MFI) was

determined for the whole sample, and the fraction of positively stained cells (P2) was determined as the percentage of the parent population.

Sample preparation for RT-PCR. K562 and $K562^{IR}$ cells were cultured in 5 mL RPMI 1640 medium, supplemented with 2 μM imatinib in the case of $K562^{IR}$ cells. $K562^{IR}$ cells were treated with Stattic (5 μM) or NT157 (0.5 μM) for 24 h.

RT-PCR. mRNA from K562 and $K562^{IR}$ cells treated with Stattic or NT157 was isolated using TRIzol® Reagent (Invitrogen™). First, 2 mL of each cell culture was centrifuged at 300 g for 5 min at RT. The supernatant was discarded, and the cell pellets were resuspended with 5 mL of PBS and centrifuged at 300 g for 5 min at RT. The cell pellet was resuspended in 1 mL of PBS, transferred to 1.5 mL Eppendorf tube, and washed under the same conditions. The supernatant was discarded and the cell pellets were resuspended in 300 μL of TRIzol® Reagent (Invitrogen™) by pipetting up and down several times. After 5 min incubation at RT 67 μL of chloroform was added. Samples were vigorously shaken by hand for 15 s and additionally incubated for 3 min at RT. Next, the samples were centrifuged at 12,000 g for 15 min at 4°C. The sample content was thus separated into multiple layers. The upper aqueous phase containing RNA was carefully removed and transferred into a new Eppendorf tube. Then 133 μL of 100% isopropanol was added, the samples were incubated for 10 min at RT and afterward centrifuged at 12,000 g for 10 min at 4°C. The supernatant was removed and the RNA was washed with 300 μL of 75% ethanol. The samples were vortexed and subsequently centrifuged at 7,500 g for 5 min at 4°C. The supernatant was discarded and the pellets were let to air dry for 10 min. Finally, the isolated RNA was resuspended in 50 μL of DNA/RNA free water (TopBio), incubated at 55°C in a heat block for 10 min, and stored at -80°C for further application. The contaminant DNA was removed by application of DNA-free™ Kit (Ambion, Life Technologies). Five μL of 10X DNase I Buffer and 1 μL of rDNase I were added to the thawed RNA samples. The reaction mixture was gently mixed and incubated at 37°C for 30 min. The reaction was terminated by adding 5 μL of DNase Inactivation Reagent for 2 min at RT with occasional gently mixing. The samples were then centrifuged at 10,000 g for 1.5 min at RT and the supernatant was transferred to a new Eppendorf tube. The RNA concentration was determined by Nanodrop. The transcription reaction was prepared following SuperScript® IV Reverse Transcriptase protocol (Invitrogen, Thermo Fischer Scientific). First, the reaction mixture for primer annealing was prepared by adding 1 μL of 50 μM Oligo $d(T)_{20}$ primer, 1 μL of 10 mM dNTP mix (Invitrogen, Thermo Fischer Scientific), 2 μg of total RNA, and sufficient amount of nuclease-free water. The sample was briefly vortexed, spun in the table centrifuge, and incubated for 5 min at 65°C. The

mixture was then cooled for 1 min on ice. Next, 7 µL of RT reaction mixture composed of 4 µL 5X SSIV Buffer, 1 µL 100 mM DTT, Rnase OUT^{TM} Recombinant RNase Inhibitor (Invitrogen, Thermo Fischer Scientific) and 1 µL of SuperScript® IV Reverse Transcriptase (200U/µL) were added. Negative controls lacking the SuperScript® IV Reverse Transcriptase were also included. The thermal protocol included 10 min incubation at 55°C and 10 min inactivation at 80°C. The cDNA samples were stored at -20°C before RT-PCR reaction. For RT-PCR, PowerUP Sybrgreen master mix (Applied Biosystems), predesigned KICqStart® Primers (Merck), and PCR water (TopBio) were Utilized. First, lyophilized KICqStart® Primers were resuspended in an appropriate volume of PCR water in order to obtain 100 µM solutions. Forward and reverse primers were combined into 10 µM F+R primer solutions. Each RT-PCR reaction with 5 µL final volume contained 2.5 µL PowerUP Sybrgreen master mix, 0.5 µL 10 µM F+R primer solution and 2 µL cDNA or PCR water (no template controls). Individual PCR reactions were prepared into 384 well plate by automated pipetting robot (Opentrons). The thermal protocol included precincubation at 95°C for 5 min and 40 cycles of amplification (95°C 15 sec, 60°C 20 sec, 72°C 30 sec) performed by Roche 480.

Table II. List of primers.

Name	**Forward**	**Reverse**
AKT1	AAGTACTCTTTCCAGACCC	TTCTCCAGCTTGAGGTC
IFITM3	GCCTATGGATAGATCAGGAG	TTTTTAGCACCAGAAACACG
IGF1R	AAAGACAAAATCCCCATCAG	TGCAGGAAATTCTCAAAGAC
IRS-1	CAGAATGAAGACCTAAATGACC	ATGCATCGTACCATCTACTG
STAT3	GGTACATCATGGGCTTTATC	TTTGCTGCTTTCACTGAATC
ACTB	GACGACATGGAGAAAATCTG	ATGATCTGGGTCATCTTCTC

Statistical analysis. The data are expressed as the mean ± SD, from at least three replicates. Statistical analysis was performed using the GraphPad Prism v8.0 software (GraphPad Software, Inc.). Relative resistance of CML-T1, CML-T1^{IR}, K562, and K562^{IR} cells to imatinib was evaluated using an unpaired Student's t-test. The toxicity of inhibitors (PPP, Stattic, NT157, CsH) was evaluated using an unpaired Student's t-test. For the investigation of cell survival following exosome exposure, one-way ANOVA with Tukey's post hoc test was used to determine the statistical significance. $P<0.05$ was considered to indicate a statistically significant difference. For investigation of IFITM3 mRNA expression, one-way ANOVA with Dunnett's multiple comparisons test was used.

4. Results

4.1. Targeting metabolism of CML cells with a point mutation in *BCR-ABL1*

Our first model study on CML cells resistant to imatinib was performed on CML-T1^{IR} cells, where the resistance is associated with a point mutation in the kinase domain of *BCR-ABL1* gene. To describe molecular changes associated with the resistant phenotype of CML-T1^{IR} cells, proteomic analysis using 2-DE electrophoresis (6 replicates for each state) followed by MALDI MS identification of differentially expressed spots was performed.

Development of imatinib-resistant CML-T1^{IR} subclone. CML-T1^{IR} cells were derived by prolonged cultivation of the original sensitive CML-T1 cells in increasing concentration of imatinib (Toman et al., 2016). The half-maximal effective imatinib concentration (EC_{50}), determined from reduction of cell viability, was 0.45±0.015 μM for the parental CML-T1 cells (Figure 6). The resistant CML-T1^{IR} cells fully proliferated in the presence of 20 μM imatinib, which had no cytotoxic effect.

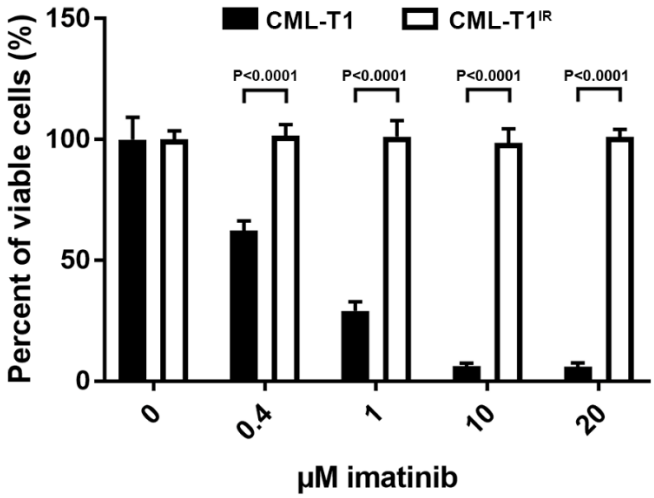

Figure 6. Viability of CML-T1 and CML-T1^{IR} cells. Viability of CML-T1 and CML-T1^{IR} cells in the presence of imatinib. Cells were cultured in the presence of imatinib for 3 days and the viability was determined using the MTT assay. Error bars indicate ± SD of three or more independent measurements. IR, resistant to imatinib.

Mutation analysis of CML-T1^{IR} cells. The typical mechanism of resistance to imatinib (and other TKIs) is a point mutation in the kinase domain of the *BCR-ABL1* gene (Gorre et al., 2001; Hochhaus et al., 2002). Mutational analysis of the *BCR-ABL1* gene in CML-T1^{IR} cells was performed and a causal mutation Y253H causing resistance was detected in 69% of *BCR-ABL1* transcripts in CML-T1^{IR} cells (Toman et al., 2016).

Proteomic analysis reveals upregulation of two NHERF1 variants in the CML-T1^{IR} cells. We hypothesized that in addition to imatinib-resistant mutation in the *BCR-ABL1* gene, CML-T1^{IR} cells may adapt their metabolism and/or intracellular signaling pathways for better proliferation in the presence of imatinib (Kominsky et al., 2009; Adamia et al., 2013). If there are specific molecular alterations driven by imatinib-resistant phenotype, some of them may be exploited as targets for selective inhibition of the resistant cells by clinically available inhibitors, which bears a potential for future combined therapies. To identify these alterations, two-dimensional (2-DE) proteomic analysis of CML-T1 and CML-T1^{IR} cells was performed. A total of eight proteins significantly differed in their quantities (Figure 7A) (Table III). The most upregulated protein in CML-T1^{IR} cells was NHERF1 also known as the solute carrier family 9 isoform A3 regulatory factor 1 (SLC9A3R1). NHERF1 was identified in two variants with different isoelectric points but comparable molecular weights (Table III, Figure 7B). Upregulation of NHERF1 was confirmed by Western blot (Figure 7C). In addition to NHERF1, increased expression of calreticulin, microtubule associated proteins, and protein chaperones were detected in the CML-T1^{IR} cells (Table III).

Table III. Differentially expressed proteins in the CML-T1^{IR} cells.

Upregulated proteins in CML-T1^{IR} cells								
Gene name	Protein IDs	Protein names	Fold change	P-value	Sequence coverage (%)	Mascot score	MW (Da)	pI
SLC9A3R1	O14745	Na^+/H^+ exchange regulatory cofactor NHERF1	2.84	<0.009	21	57	39,130	5.55
SLC9A3R1	O14745	Na^+/H^+ exchange regulatory cofactor NHERF1	>10	<0.001	32	84	39,130	5.55
RUVBL2	Q9Y230	RuvB-like 2	6.8	<0.015	29	81	51,296	5.49
CALR	P27797	Calreticulin	1.8	<0.023	24	71	48,283	4.29
ADA	P00813	Adenosine deaminase	2.9	<0.009	36	87	41,024	5.63
TPM4	P67936	Tropomyosin α-4 chain	1.56	<0.036	63	198	28,619	4.67
HSPB1	P04792	Heat shock protein β-1	>10	<0.001	35	136	22,826	5.98
Downregulated proteins in CML-T1^{IR} cells								

Gene name	Protein IDs	Protein names	Fold change	P-value	Sequence coverage (%)	Mascot score	MW (Da)	pI
RUVBL2	Q9Y230	RuvB-like 2	-2.17	<0.02	38	149	51,296	5.49
VAT1	Q99536	Synaptic vesicle membrane protein VAT-1 homolog	-3.7	<0.039	34	60	42,122	5.88
MAPRE1	Q15691	Microtubule-associated protein RP/EB family member	-1.86	<0.005	53	89	30,151	5.02
HSPB1	P04792	Heat shock protein β-1	-2.2	<0.001	44	75	22,826	5.98
Positive fold change indicates upregulation, negative fold change indicated downregulation in CML-T1^{IR} cells. MW, molecular weight.								

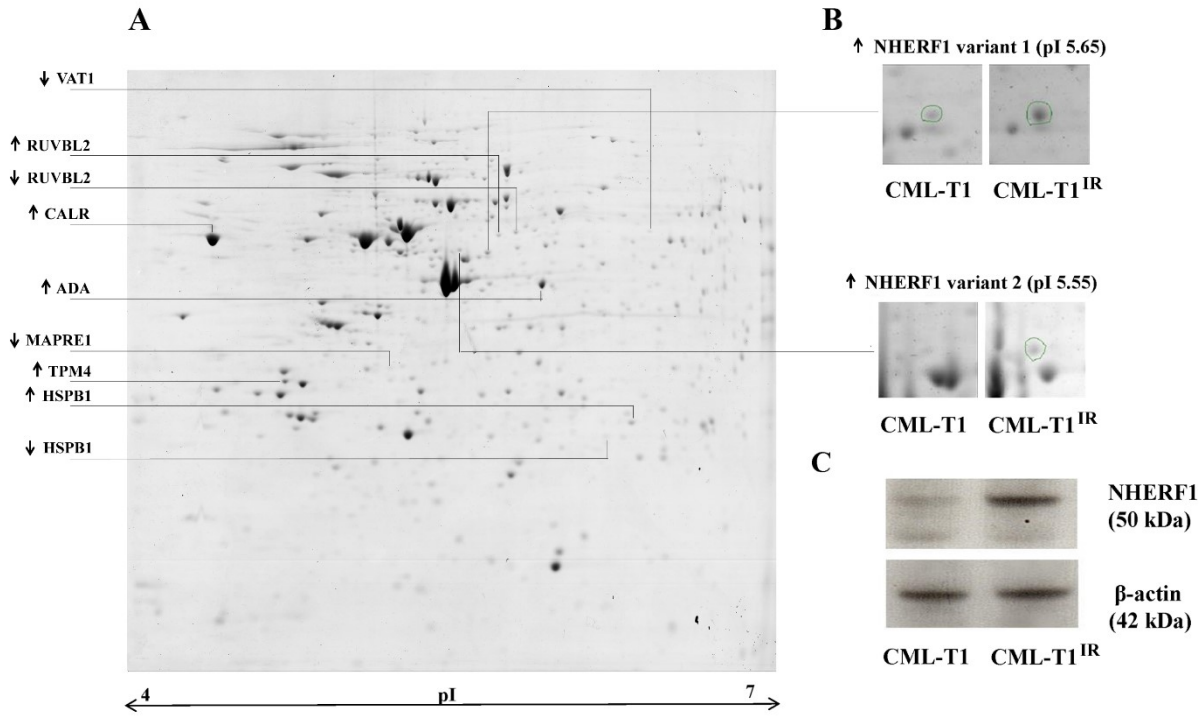

Figure 7. 2-DE proteomic analysis of CML-T1 and CML-T1^{IR} cells. (A) Differentially expressed proteins from CML-T1^{IR} cells representing spots in 2-DE are indicated by the arrows (↓ downregulated, ↑ upregulated). (B) Two variants of NHERF1 protein were upregulated in CML-T1^{IR} cells. (C) Verification of differential expression of NHERF1 protein in the cell lysates from CML-T1 and CML-T1^{IR} cells by Western blot.

NHERF1: functional analysis. NHERF1 is a scaffolding protein interacting with various intracellular proteins and modulating their activity, stability, and expression (Reczek et al., 1997; Ardura and Friedman, 2011). In hepatocytes, NHERF1 modulates expression and function of the multidrug resistance protein MRP2 (Li et al., 2010). NHERF1 regulates negatively the activity of NHE3, thus modulating intracellular pH (Lamprecht et al., 1998; He and Yun, 2010). NHERF1 is able to influence Ca^{2+} concentration in the cytosol via non-selective cation channels TRPC4 and TRPC5 (Tang et al., 2000; Obukhov and Nowycky, 2004; Storch et al., 2017). In addition, NHERF1 directly interacts with a subset of FZD receptors and negatively regulates the canonical WNT signaling pathway (Wheeler et al., 2011). Based on the aforementioned NHERF1 functions, consequences of NHERF1 upregulation in CML-T1^{IR} cells were examined to identify specific molecular alterations, which could potentially be exploited as a therapeutic target.

NHERF1 upregulation does not correlate with expression and function of the multidrug resistance proteins MRP2 and MDR1 in CML-T1^{IR} cells. It was evaluated whether upregulated NHERF1 contributes to CML-T1^{IR} cell growth in imatinib by controlling MRP2 expression and function as it was shown previously in hepatocytes (Li et al., 2010; Karvar et al., 2014). MDR assay was used to study efflux of a fluorescent probe calcein from cells by the multidrug exporters MDR1 and MRP2 (Bosch and Croop, 1996; Canitrot et al., 1996). No efflux of calcein from CML-T1 and CML-T1^{IR} cells was detected. MDR export inhibitors CsA and verapamil did not affect calcein efflux suggesting that MRP2 and MDR1 are not active in CML-T1 and CML-T1^{IR} cells (Figure 8A)**.** In addition, the MRP2 transporter was undetectable by Western blot in lysates of CML-T1 and CML-T1^{IR} cells (Figure 8B). In conclusion, neither MRP2 nor MDR1 contribute to the growth of CML-T1^{IR} cells in imatinib and NHERF1 upregulation is not related to MRP2 or MDR1 activity in CML-T1^{IR} cells.

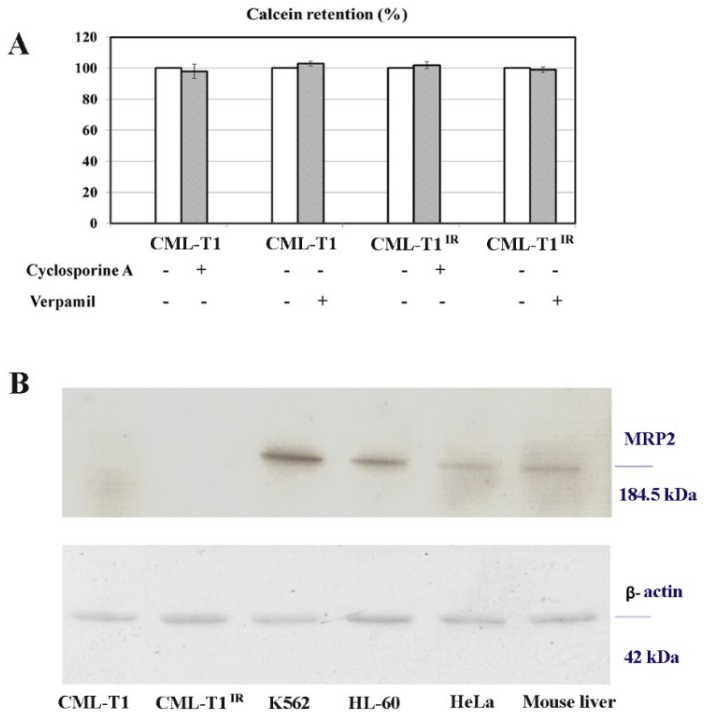

Figure 8. Multidrug resistance (MDR) assay and MRP2 protein expression in CML-T1 and CML-T1^{IR} cells compared to other cell lines. (A) Measurement of calcein retention to determine MDR exporter activity in the CML-T1 and CML-T1^{IR} cells. Cyclosporine A (CsA) and verapamil were used as MDR inhibitors. No activity of MDR was detected in CML-T1 and CML-T1^{IR} cells as a result of 100 % calcein retention in the cells. (B) MRP2 protein expression in cell lysates from CML-T1, CML-T1^{IR}, K562, and HL-60. Mouse liver tissue was used as a positive control.

Intracellular concentrations of H^+ and Ca^{2+} ions differ between CML-T1 and CML-T1^{IR} cells. Based on the known interaction between NHERF1 and NHE3 affecting cellular pH (Lamprecht et al., 1998; He and Yun, 2010), it was examined whether increased expression of NHERF1 affects intracellular pH in CML-T1^{IR} cells. Intracellular pH was found to be higher in the CML-T1^{IR} cells (pH 7.25) compared to imatinib-sensitive CML-T1 cells (pH 7.18) (Figure 9A).

It was described that NHERF1 regulates the activity of the non-selective cation channels TRPC4 and TRPC5, therefore it was examined whether increased expression of NHERF1 or pH shift in the cytosol affects cytosolic Ca^{2+} concentration in CML-T1^{IR} cells (Tang et al., 2000; Obukhov and Nowycky, 2004; Garciarena et al., 2013). Our measurements using Fura-2/AM fluorescent probe demonstrated a 50% decrease in Ca^{2+} concentration in the cytosol of CML-T1^{IR} cells compared to the parental line (Figure 9B). In summary, CML-T1^{IR} cells adapted to growth in imatinib by increased pH and decreased Ca^{2+} concentration in cytosol compared to parental CML-T1 cells sensitive to imatinib.

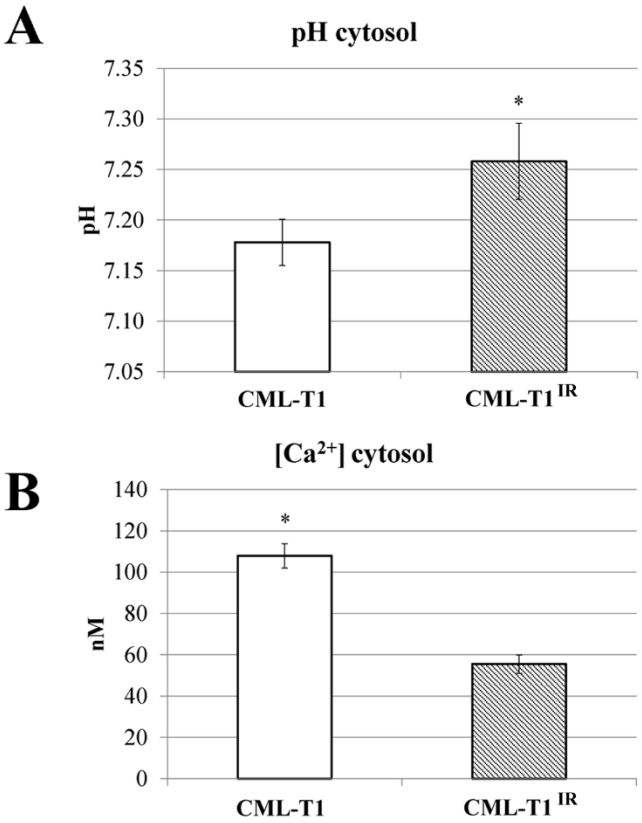

Figure 9. Intracellular pH and Ca^{2+}concentration in CML-T1 and CML-T1^{IR} cells. (A) Intracellular pH was measured by BCECF fluorescence intensity and (B) Ca^{2+}concentration was measured using Fura-2/AM fluorescent probe. The mean values ± were calculated from three independent experiments.

Calcium channel blockers and inhibitors of calcium signaling selectively inhibit the viability of CML-T1^{IR} cells. We hypothesized that higher cytosolic pH due to differential Na^+/H^+ exchange and/or reduction of Ca^{2+} cytosolic concentration are crucial for the survival of CML-T1^{IR} cells in the presence of imatinib (Pinton et al., 2000; Rich et al., 2000). To examine whether the inhibition of Na^+/H^+ exchange selectively affects CML-T1^{IR} cells, NHE3 was targeted by the specific inhibitor amiloride. Since it is known that Na^+/Ca^{2+} exchanger (NCX) may also alter pH and Ca^{2+} concentration in the cells, NCX was inhibited by 3',4'-dichlorobenzamil (DCB) (Condrescu et al., 2002; Iwamoto et al., 2007). However, cell viability assays using the two named inhibitors revealed no selective effect on CML-T1^{IR} cells. CML-T1 and the CML-T1^{IR} cells survived in comparable concentrations of amiloride and DCB EC_{50} values of 15 µM for amiloride and 7 µM for DCB (Figure 10).

To examine whether altered Ca^{2+} homeostasis is essential for the survival of CML-T1^{IR} cells in imatinib, CML-T1 and CML-T1^{IR} cells were exposed to increasing concentrations of inhibitors of Ca^{2+} signaling and transport, namely thapsigargin, ionomycin, verapamil, and CAI (Figure 10).

Thapsigargin increases the cytosolic Ca^{2+} concentration by inhibition of sarco/endoplasmic reticulum Ca^{2+} ATPase (SERCA) activity. SERCA normally transports cytosolic Ca^{2+} into the endoplasmic reticulum (ER) (Thastrup et al., 1990). Ionomycin increases intracellular Ca^{2+} by facilitating Ca^{2+} transport across the plasma membrane and/or by releasing Ca^{2+} from intracellular stores such as ER (Beeler et al., 1979). Verapamil is a clinically approved drug inhibiting voltage-dependent L-type Ca^{2+} channels (Nawrath and Wegener, 1997). CAI is an inhibitor of voltage-dependent and receptor-mediated Ca^{2+} entry (Hupe et al., 1991). CAI was previously shown to have an antiproliferative effect on the human embryonic kidney 293 (HEK 293) and Huh-7 human hepatoma cell lines (Enfissi et al., 2004; Mignen et al., 2005). In addition, it was demonstrated that CAI inhibits the growth of CML cells resistant to imatinib (Alessandro et al., 2008).

The toxicity of aforementioned compounds to CML-T1 and CML-$T1^{IR}$ cells was tested *in vitro* using cell viability assays. All the tested inhibitors showed stronger toxicity to CML-$T1^{IR}$ cells (Figure 10). Among them, thapsigargin was the most effective in the inhibition of CML-$T1^{IR}$ cell growth. Thapsigargin EC_{50} concentration was 75 nM for CML-$T1^{IR}$ cells while the EC_{50} for CML-T1 cells was not reached at 1.2 μM. CML-$T1^{IR}$ cells were 5-fold more sensitive to ionomycin (EC_{50} 200 nM for CML-$T1^{IR}$ cells and >1.6 μM for CML-T1 cells), ~3-fold more sensitive to verapamil (EC_{50} 30 nM for CML-$T1^{IR}$ cells and 90 nM for CML-T1 cells) and 2.5-fold more sensitive to CAI (EC_{50} 200 nM for CML-$T1^{IR}$ cells and 1.6 μM for CML-T1 cells).

Altered Ca^{2+} homeostasis influences many intracellular processes including WNT signaling. It was shown that CsA and tacrolimus (FK-506) modulate calcium homeostasis (Rovira et al., 2000; Maguire et al., 2013) and inhibit prosurvival signaling mediated by WNT signaling in drug-resistant cells (Gregory et al., 2010). Therefore, the effect of CsA and FK-506 on proliferation of CML-T1 and CML-$T1^{IR}$ cells was evaluated. In cell viability assays, CsA and FK-506 inhibited CML-$T1^{IR}$ proliferation at significantly lower concentrations (3- and 1.8-fold, respectively) compared to the CML-T1 cells. CsA EC_{50} was 4 μM for CML-$T1^{IR}$ cells and 12 μM for CML-T1 cells; FK-506 EC_{50} was 50 nM for CML-$T1^{IR}$ cells and 90 nM for CML-T1 cells (Figure 10).

In summary, CML-$T1^{IR}$ cells are more vulnerable to disruption of Ca^{2+} homeostasis (and to a lesser extent also to inhibition of WNT signaling), but not to inhibition of NHE3 or NCX exchangers. The most effective inhibition of CML-$T1^{IR}$ cell growth was achieved by the agents that cause depletion of the intracellular Ca^{2+} stores corresponding with an increase in cytosolic

Ca^{2+} concentration (thapsigargin, ionomycin). Ca^{2+} channel blocker verapamil and Ca^{2+} signaling antagonist CAI also exhibited a strong effect. Therefore, the aforementioned inhibitors could be used to selectively target CML-$T1^{IR}$ cells, which suggests their clinical potential in personalized treatment of CML resistant to TKI.

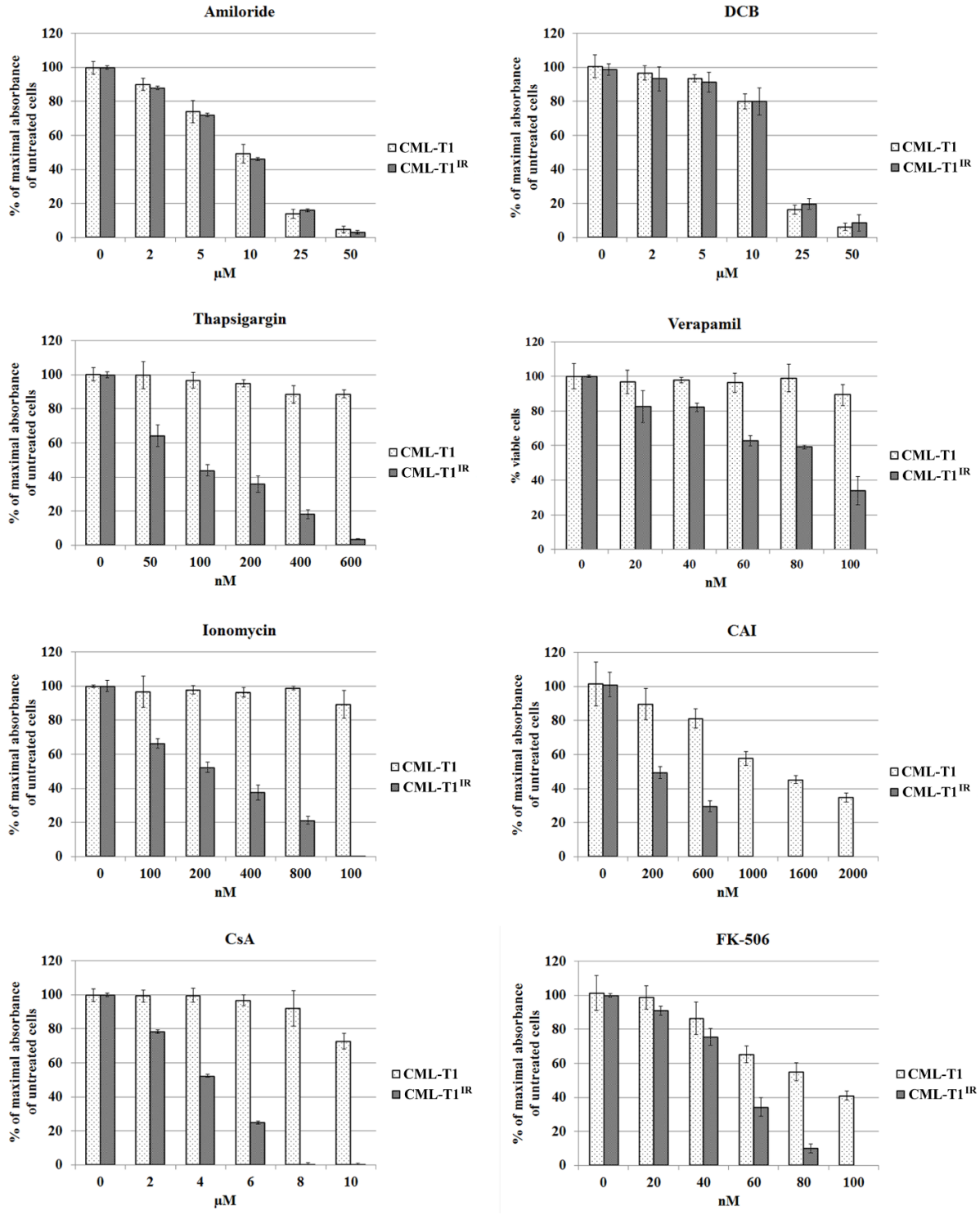

Figure 10. Effects of selected inhibitors on CML-T1 and CML-$T1^{IR}$ cell viability cultured in the presence of inhibitors for 3 days. Cell viability was determined using the MTT assay. Each graph represents measurements of at least three biological samples, which were performed in three technical replicates. DCB, 2',4'-dichlorobenzamil hydrochloride; CAI, carboxyamidotriazole.

WNT signaling pathway is dysregulated in CML-T1^{IR} cells. NHERF1 negatively regulates Wnt signaling via its direct interaction with FZD receptors (Wheeler et al., 2011). WNT signaling pathway can potentially serve as a therapeutic target (An et al., 2013). Therefore, it was examined whether NHERF1 upregulation (accompanied by altered cytosolic ion concentration) in CML-T1^{IR} cells is associated with altered WNT signaling. The activity of the WNT pathway was analyzed using RT-PCR WNT microarray to determine the relative expression of WNT target genes and regulatory molecules (Figure 11A). Canonical WNT/β-catenin pathway genes transducin-like enhancer protein 1 (TLE1), transducin-like enhancer protein 4 (TLE4), transcription factor 7 like 2 (TCF7L2), lymphoid enhancer-binding factor-1 (LEF1), MYC, and ras homolog family member U (RHOU) were downregulated in CML-T1^{IR} cells. Negative regulators of the canonical WNT pathway, kringle containing transmembrane protein 1 (KREMEN1), and secreted frizzled-related protein 5 (SFRP5) were upregulated in CML-T1^{IR} cells indicating that canonical Wnt/β-catenin-dependent pathway was suppressed in CML-T1^{IR} cells. In addition, the expression of genes involved in the non-canonical WNT/Ca^{2+}/NFAT pathway was evaluated. The amount of mRNA encoding FZD8 receptor was decreased in CML-T1^{IR} cells. This result is contradictory to the observation made by Gregory *et al* who demonstrated that the Ca^{2+}/calmodulin-dependent protein kinase II (CaMKII)/Ca^{2+}/NFAT WNT signaling pathway maintains survival of BCR-ABL^{+} CML cells via FZD8 receptor (Gregory et al., 2010).

To further verify the WNT/Ca^{2+}/NFAT signaling pathway status, the presence of an effector of this pathway, NFAT transcription factor, was determined in the cytoplasm and in the nuclei of CML-T1 and CML-T1^{IR} cells by Western blot. NFAT transcription factor was not detected in CML-T1^{IR} cells (Figure 11B). This suggests that WNT/Ca^{2+}/NFAT signaling pathway is diminished in CML-T1^{IR} cells and thus cannot contribute to cell survival in the presence of imatinib in our CML-T1 cell model.

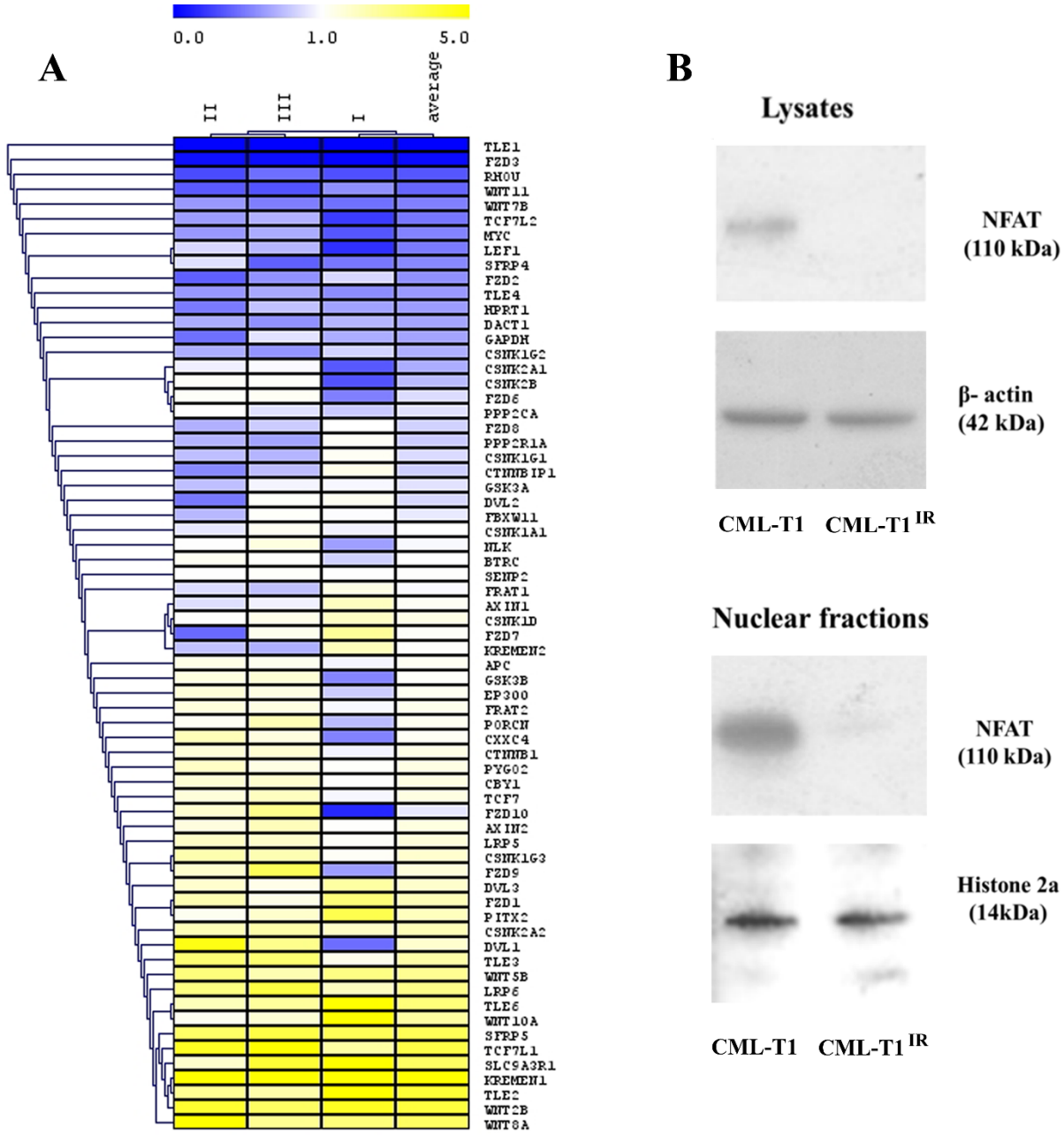

Figure 11. WNT signaling pathway array and expression levels of NFAT protein in CML-T1 and CML-T1^{IR} cells. (A) The heatmap of WNT gene expression shows downregulated (blue) or upregulated (yellow) genes in CML-T1^{IR} cells compared to CML-T1 cells. (B) NFAT protein expression was determined by Western blot in the cell lysates and in the nuclei of CML-T1 and CML-T1^{IR} cells.

4.2. Targeting metabolism of CML cell line with the *BCR-ABL1* gene amplification

In the second part of this work, a model example of cell line representing type of imatinib resistance without point mutation in the *BCR-ABL1* gene was examined. K562^{IR} cells have no mutations in the *BCR-ABL1* gene, instead, the ddPCR analysis revealed that acquired resistance

to imatinib in K562^{IR} is caused by the *BCR-ABL1* gene amplification. Analogically to our approach in the previous chapter describing CML-T1 and CML-T1^{IR} cells, a comparative analysis of K562 and its imatinib-resistant counterpart K562^{IR} was performed. Due to rapid development of new techniques, a modern LFQ proteomic analysis was used instead of 2-DE electrophoresis and MALDI MS identification.

Development of imatinib-resistant K562^{IR} subclone. The resistant K562^{IR} cells were derived by prolonged cultivation of the original sensitive K562 cells in increasing concentration of imatinib (Hrdinova et al., 2021). The half-maximal effective concentration (EC_{50}) of imatinib was 0.25-0.35 μM for sensitive K562 cells (Figure 12). Imatinib-resistant K562^{IR} fully proliferated in 2 μM imatinib.

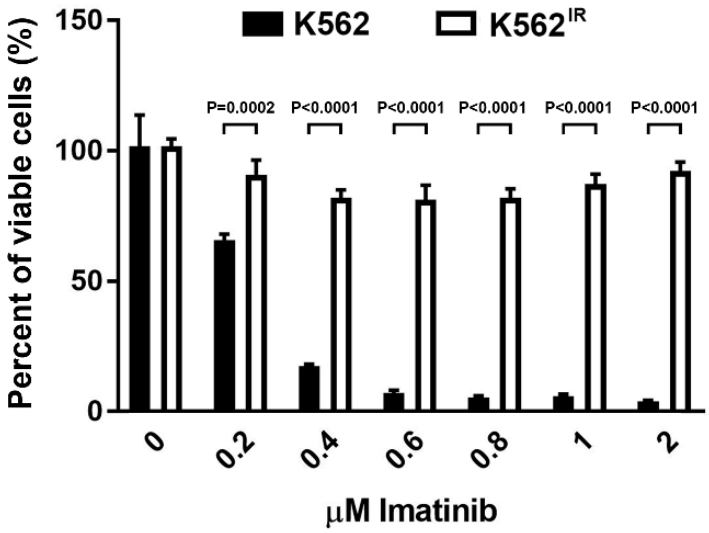

Figure 12. Viability of K562 and K562^{IR} cells. Relative viability of K562 and K562^{IR} cells in the presence of imatinib. Cells were cultured in the presence of imatinib for 3 days and the viability was determined using the MTT assay. Error bars indicate ± SD of three independent measurements. IR, resistant to imatinib.

Mutation analysis and BCR-ABL1 gene expression. Mutational analysis of the *BCR-ABL1* gene in K562^{IR} cells was performed as previously in CML-T1^{IR} cells (Toman et al., 2016). In the case of K562^{IR} cells, no mutations in the kinase domain were found. It is known that patients with TKI resistance lacking *BCR-ABL1* kinase domain mutations typically have an amplification of the *BCR-ABL1* gene (Gorre et al., 2001). Therefore, ddPCR was used to identify the number of *BCR-ABL1* copies. A 2-fold higher number of *BCR-ABL1* gene copies was found in K562^{IR} cells compared to imatinib-sensitive K562 cells (data not shown). As amplification of the *BCR-ABL1* gene may result in *BCR-ABL1* mRNA and BCR-ABL protein overexpression, amounts of mRNA and protein were compared between K562 and K562^{IR} cells. The *BCR-ABL1* mRNA (Figure 13A), as well as BCR-ABL protein (Figure 13B) levels were increased in K562^{IR} cells. In

addition, expression of MRP2 protein, a MDR exporter with not clearly understood relation to imatinib resistance, was examined by Western blot in K562 and K562^{IR} cells (Figure 13C) (Breedveld et al., 2005; Au et al., 2014).

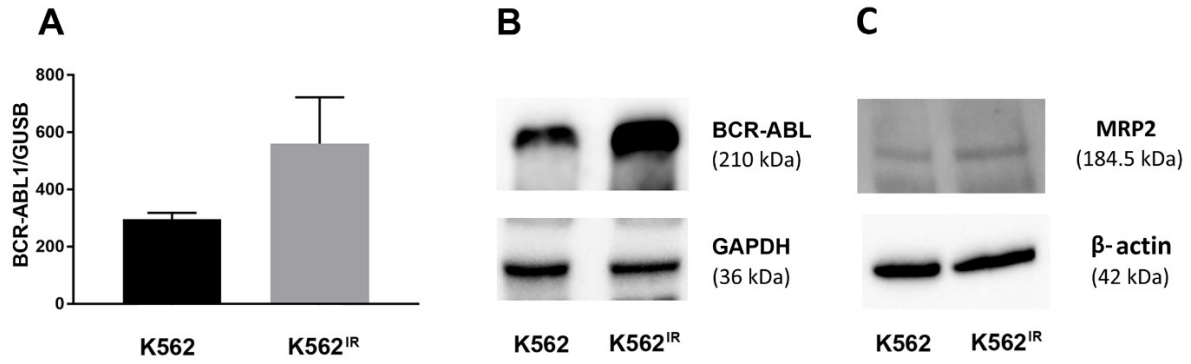

Figure 13. Expression levels of BCR-ABL1 mRNA, BCR-ABL protein, and MRP2 transporter. BCR-ABL1 mRNA expression levels were determined by real time-quantitative PCR (A) and protein levels were determined by Western blot (B). The expression of MRP2 was determined by Western blot (C). Error bars indicate ± SD of three independent measurements. IR, resistant to imatinib.

LFQ proteomic analysis of K562 cells. K562 and K562^{IR} cells were subjected to LFQ proteomic analysis to identify differences in proteome composition reflecting adaptive molecular changes in their metabolism and/or signaling pathways. A total of 10 samples obtained from five independent cultivation replicates of both K562 and K562^{IR} cells were analyzed using LC-MS/MS (Q-Exactive). With the FDR set to 0.01, a minimum of 1,829 and a maximum of 2,516 proteins were identified in each sample. A total of 3,141 unique proteins were identified. To determine the quantitative robustness of label-free analysis, the quantitative similarity of all the LC-MS/MS runs was examined. Correlation analysis revealed good inter-sample reproducibility, with Pearson's correlation coefficients in the range of 0.942-0.991 (Figure 14). The LFQ analysis provided semi-quantitative data for 2,118 proteins (Table SI).

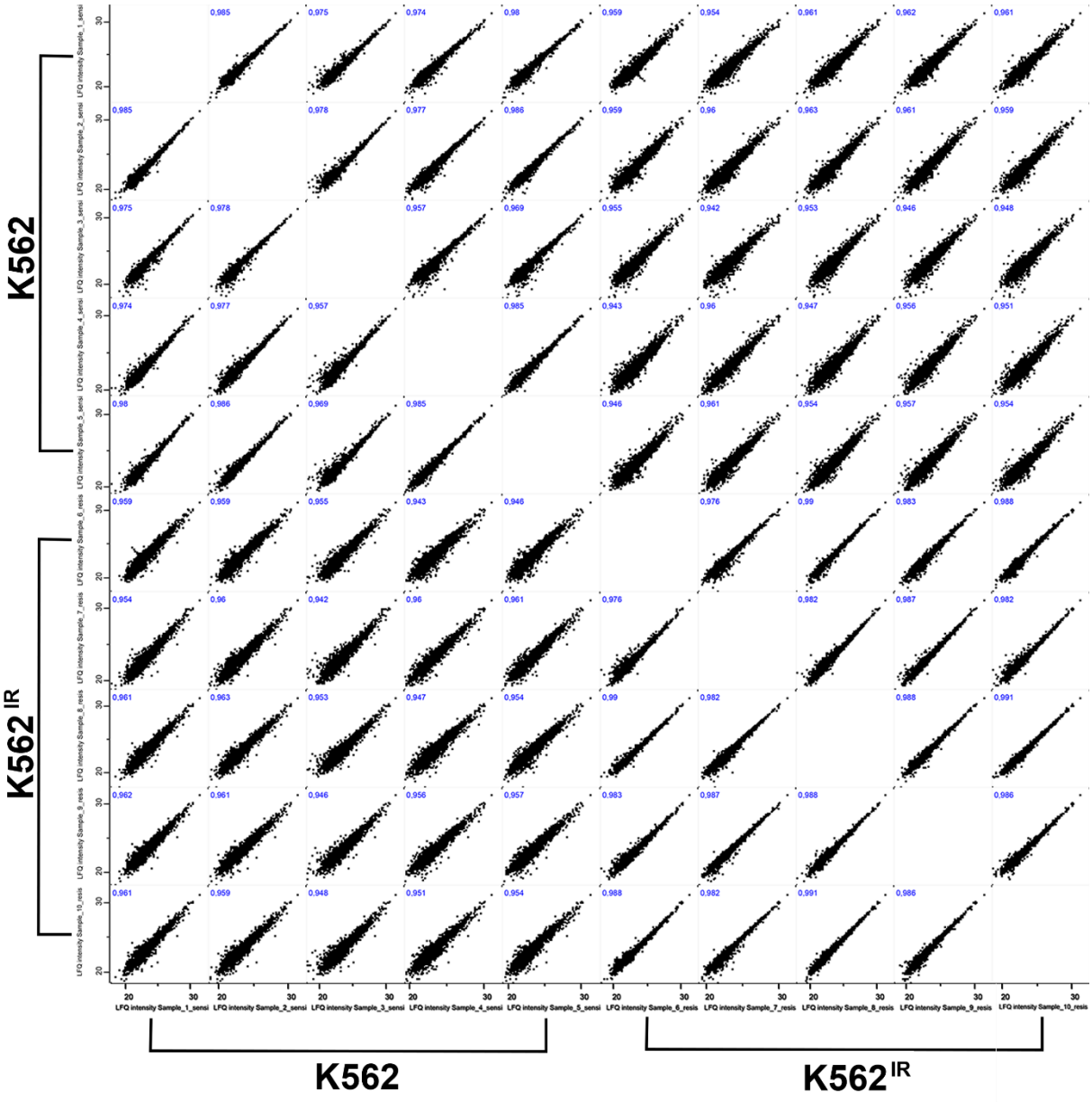

Figure 14. LFQ-MS peptide signal intensity correlations between individual LC-MS analysis of K562 and K562^{IR} cells. The figure is a composite image of the correlation plots from the LFQ-MS peptide signal intensities between all the LC-MS runs from the proteomic analysis. Pearson's correlation coefficients in the range of 0.942-0.991 revealed good inter-sample reproducibility. LFQ, label-free quantification; LC, liquid chromatography; MS, mass spectrometry; IR, resistant to imatinib.

Differentially expressed proteins in K562 cells. A total of 392 proteins with significantly different quantities were identified in K562^{IR} cells compared to K562 cells (fold change >1.5) (Figure 15, Table SII). Of these 392 proteins, 235 proteins were found as upregulated and 157 proteins as downregulated in K562^{IR} cells. From the group of the most upregulated proteins (fold change > 4) (Table IV), STAT3 protein (5.4-fold) was further investigated due to its critical role in leukemia cell growth, transformation, and drug resistance (Eiring et al., 2014, 2015b; Patel et al., 2021). In addition to STAT3, major upregulation (fold change > 4) of mitochondrial proteins cytochrome c oxidase subunit NDUFA4 (5.4-fold), NADH dehydrogenase [ubiquinone] 1 alpha

subcomplex subunit 8 (4.4-fold), and NADPH:adrenodoxin oxidoreductase, mitochondrial) (4.1-fold) was observed. Proteins involved in cholesterol and fatty acid metabolisms such as the ATP-binding cassette sub-family D member 3 (4.9-fold) and the very long-chain acyl-CoA synthetase (4.6-fold) were also strongly upregulated in $K562^{IR}$ cells.

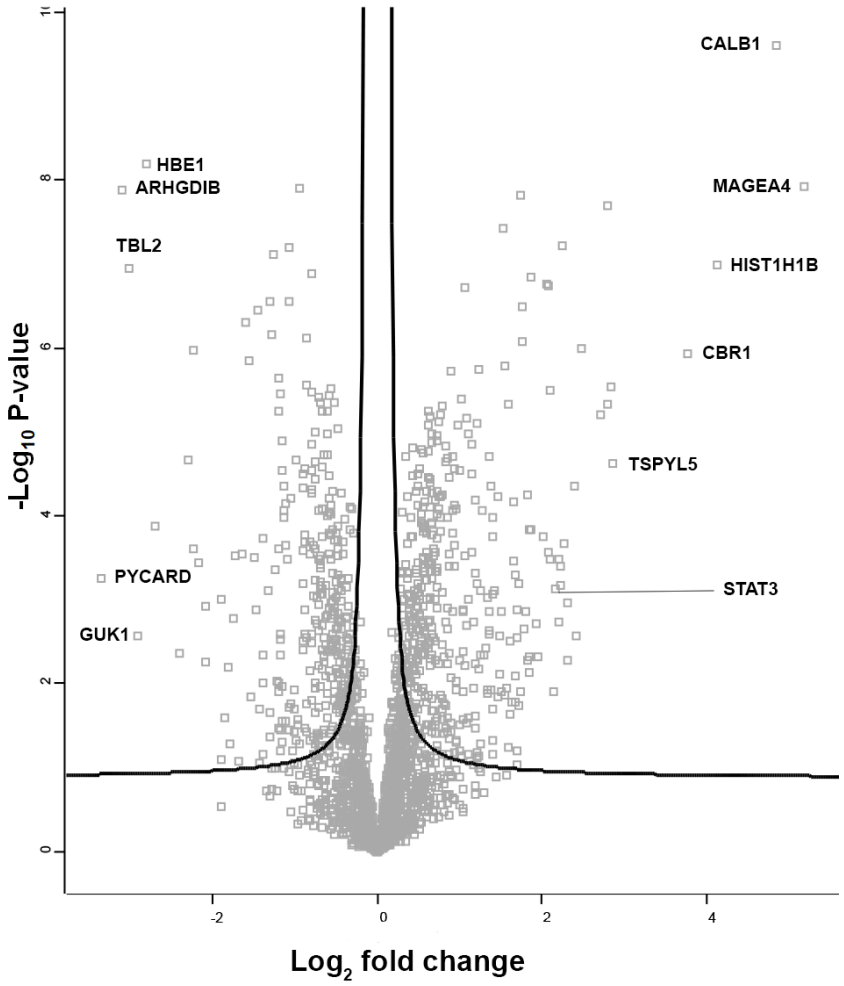

Figure 15. Differentially expressed proteins were identified using label-free quantification proteomic analysis of K562 and $K562^{IR}$ cells. Proteins with positive log_2 fold change were upregulated in $K562^{IR}$ cells, while negative fold change indicated downregulated proteins in $K562^{IR}$ cells. Only the proteins above the black line indicating statistical significance (false discovery rate <0.05, S0=0.1) were considered.

Table IV. Differentially expressed proteins in $K562^{IR}$ cells compared to K562 cells, fold change > 4

Upregulated in $K562^{IR}$ cells						
Protein names	**Protein IDs**	**Gene names**	**Fold change**	**Unique peptides**	**MS/MS Count**	**Permutation based FDR**
Melanoma-associated antigen 4	P43358	MAGEA4	36.2	8	56	<0.001
Calbindin	P05937	CALB1	28.9	5	27	<0.001
Histone H1.5	P16401	HIST1H1B	17.6	4	16	<0.001
Carbonyl reductase [NADPH] 1	P16152	CBR1	13.5	6	27	<0.001
Testis-specific Y-encoded-like protein 5	Q86VY4	TSPYL5	7.2	4	16	<0.001
Cytoskeleton-associated protein 4	Q07065	CKAP4	7.1	7	23	<0.001
Mannose-6-phosphate isomerase	P34949	MPI	6.9	3	14	<0.001
Eukaryotic initiation factor 4A-II	Q14240	EIF4A2	6.9	3	10	<0.001
Alpha-synuclein	P37840	SNCA	6.5	5	12	<0.001
Retinal dehydrogenase 1	P00352	ALDH1A1	5.5	5	22	<0.001
Cytochrome c oxidase subunit NDUFA4	O00483	NDUFA4	5.4	4	13	0.003
Nitric oxide synthase-interacting protein	Q9Y314	NOSIP	5.3	6	20	<0.001
Plectin	Q15149	PLEC	4.9	23	43	0.0051
ATP-binding cassette sub-family D member 3	P28288	ABCD3	4.9	4	10	0.001
Annexin A3	P12429	ANXA3	4.8	5	13	<0.001
Erythrocyte band 7 integral membrane protein	P27105	STOM	4.7	4	26	<0.001
Proteasome assembly chaperone 1	O95456	PSMG1	4.7	3	16	<0.001
Endothelial cell-selective	Q96AP7	ESAM	4.7	5	16	<0.001

adhesion molecule						
Beta-galactosidase	P16278	GLB1	4.6	8	33	0.002
Very long-chain acyl-CoA synthetase	O14975	SLC27A2	4.6	10	17	<0.001
Signal transducer and activator of transcription 3	P40763	STAT3	4.5	7	18	<0.001
NADH dehydrogenase [ubiquinone] 1 alpha subcomplex subunit 8	P51970	NDUFA8	4.4	5	7	0.012
Tyrosine-protein kinase ABL1	P00519	ABL1	4.3	6	14	<0.001
Tetraspanin-13	O95857	TSPAN13	4.3	2	8	<0.001
LINE-1 retrotransposable element ORF1 protein	Q9UN81	L1RE1	4.2	4	17	<0.001
Hematopoietic lineage cell-specific protein	P14317	HCLS1	4.2	5	13	<0.001
NADPH:adrenodoxin oxidoreductase. mitochondrial	P22570	FDXR	4.1	15	68	<0.001
Syntaxin-3	Q13277	STX3	4.0	3	10	<0.001
Downregulated in K562^{IR} cells						
Tumor protein D52	P55327	TPD52	-4.2	4	9	0.006
Receptor-type tyrosine-protein phosphatase C	P08575	PTPRC	-4.3	7	14	0.001
Coiled-coil-helix-coiled-coil-helix domain-containing protein 2	Q9Y6H1	CHCHD2	-4.5	4	16	<0.001
Nucleoside diphosphate-linked moiety X motif 19. mitochondrial	A8MXV4	NUDT19	-4.7	9	26	<0.001
Protein-glutamine gamma-glutamyltransferase 2	P21980	TGM2	-4.7	5	9	<0.001
Glutamine synthetase	P15104	GLUL	-4.9	4	14	<0.001

Bifunctional methylenetetrahydrofolate dehydrogenase/cyclohydrolase. mitochondrial	P13995	MTHFD2	-5.3	7	23	0.004
Hemoglobin subunit delta	P02042	HBD	-6.5	9	43	<0.001
Hemoglobin subunit epsilon	P02100	HBE1	-7.0	9	104	<0.001
Guanylate kinase	Q16774	GUK1	-7.5	3	12	0.003
Transducin beta-like protein 2	Q9Y4P3	TBL2	-8.1	5	11	<0.001
Rho GDP-dissociation inhibitor 2	P52566	ARHGDIB	-8.6	5	28	<0.001
Apoptosis-associated speck-like protein containing a CARD	Q9ULZ3	PYCARD	-10.2	4	15	<0.001
Positive fold change indicates upregulation, negative fold change indicated downregulation in $K562^{IR}$ cells. FDR, false discovery rate; MS, mass spectrometry						

Upregulation of the STAT3 transcription factor in $K562^{IR}$ cells: functional analysis. The strongly upregulated proteins were further investigated with a particular focus on proteins involved in signaling pathways controlling cell survival, proliferation, and drug resistance. The transcription factor STAT3 met these criteria. STAT3 is a member of the family of transcription factors activated by cytokines, growth factors, oncogenes, and non-receptor kinases (Levy and Darnell, 2002). STAT3 and other STAT transcription factors normally reside in the cytoplasm. Upon cellular stimulation, STAT transcription factors are activated by phosphorylation on a conserved tyrosine residue (Tyr705 in the case of STAT3), dimerize, and translocate to the nucleus to start transcription of their respective target genes (Schindler et al., 1992; Darnell et al., 1994). Phosphorylation of Ser727 in STAT3 enhances its transcriptional activity (Wen et al., 1995). Constitutive activation of STATs has been described in solid tumors as well as in hematological malignancies. In CML cells, STAT3 can be phosphorylated by BCR-ABL kinase (Ilaria and Van Etten, 1996). Activated STAT3 also contributes to resistance to BCR-ABL inhibitors (Bewry et al., 2008; Eiring et al., 2014; Patel et al., 2021). The presence of the candidate protein (STAT3) was confirmed in the cells using Western blot analysis with specific antibodies (Figure 16).

Expression of STAT3, pSTAT3 (Tyr705), and pSTAT3 (Ser727) is increased in lysates and nuclei of $K562^{IR}$ cells. The expression of STAT3 protein and its phosphorylated forms pSTAT3 (Tyr705) and pSTAT3 (Ser727) was evaluated in cell lysates of K562 and $K562^{IR}$ cells. Western

blot data confirmed the upregulation of STAT3, pSTAT3 (Tyr705), and pSTAT3 (Ser727) in cell lysates (Figure 16).

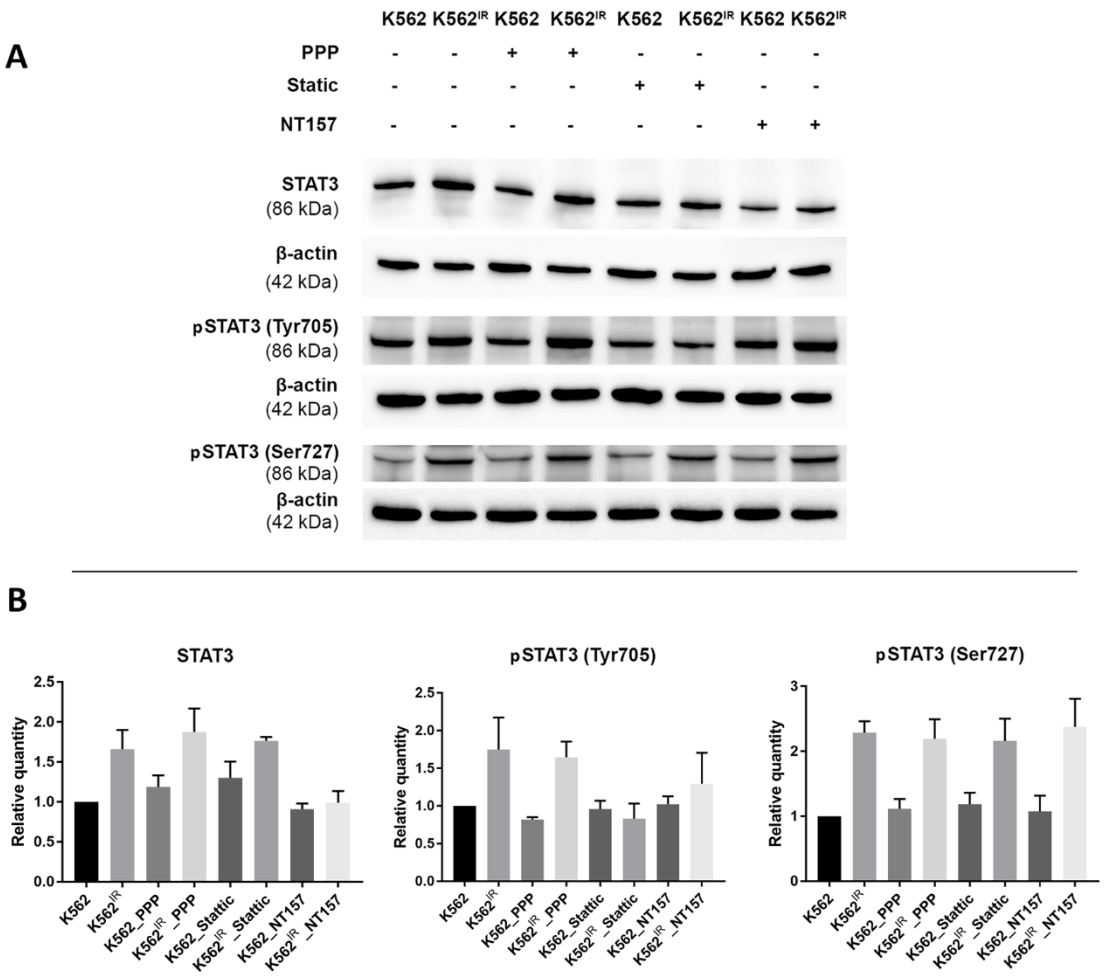

Figure 16. Western blot analysis and relative quantification of STAT3, pSTAT3 (Tyr705), pSTAT3 (Ser727) in K562 and K562^{IR} cell lysates and after treatment by selected inhibitors. (A) Expression of STAT3, pSTAT3 (Tyr705), pSTAT3 (Ser727) in K562 and K562^{IR} cell lysates and after treatment by selected inhibitors PPP (100 nM), Stattic (5μM) and NT157 (0.5 μM) was determined by Western blot. Protein samples (30 μg) were separated on precast 4-15% SDS-PAGE gels. (B) Relative quantification of STAT3, pSTAT3 (Tyr705), pSTAT3 (Ser727) protein expression. Error bars indicate ± SD of three independent measurements. IR, resistant to imatinib.

The expression of STAT3 and pSTAT3 (Tyr705) was also evaluated in the nuclei of K562 and K562^{IR} cells. Increased expression of STAT3 and its phosphorylated form pSTAT3 (Tyr705) was observed in the nuclei of K562^{IR} cells (Figure 17). Transcription factor STAT3 controls the expression of many target genes in the nucleus (Carpenter and Lo, 2014).

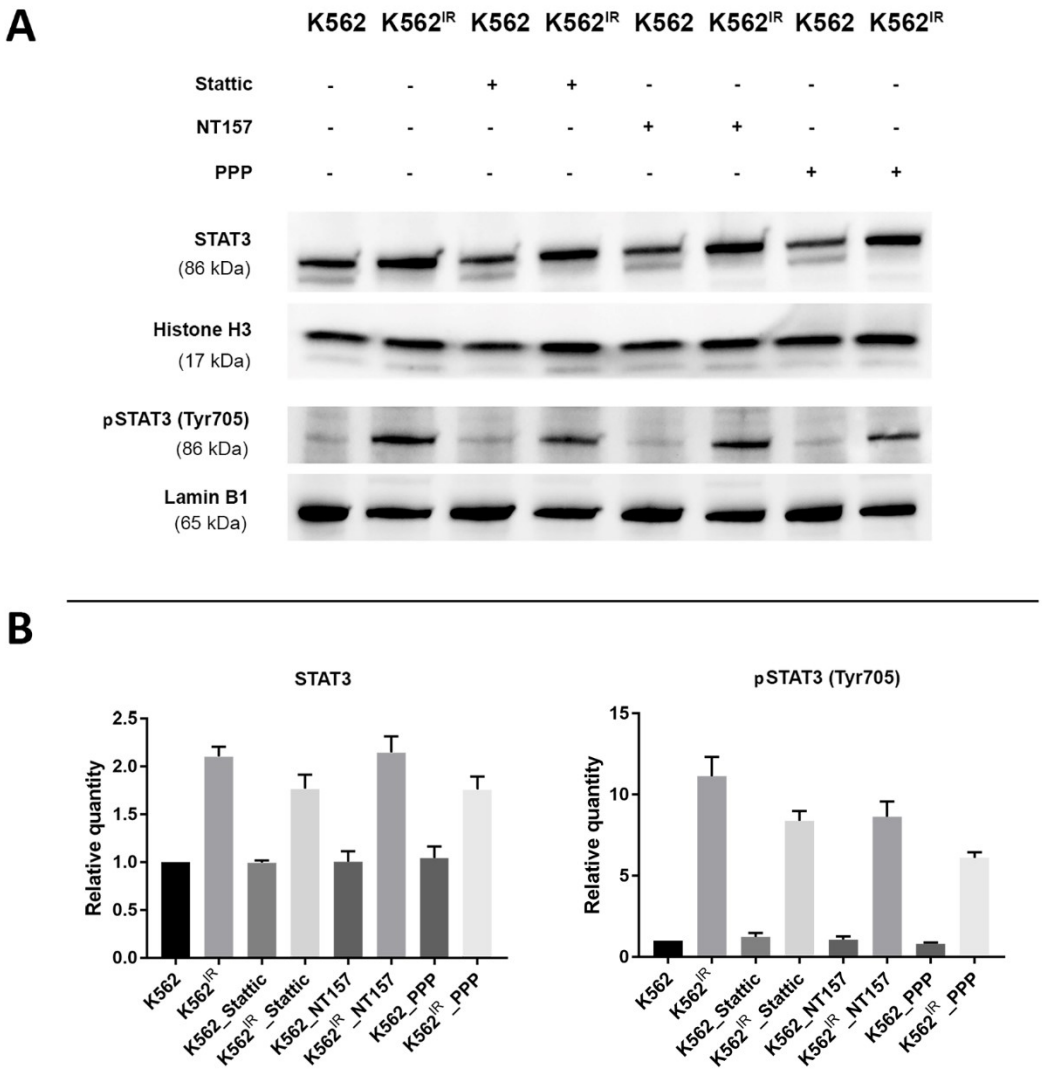

Figure 17. Western blot analysis and relative quantification of STAT3 and pSTAT3 (Tyr705) in the nuclei of K562 and K562^{IR} cells and after treatment by selected inhibitors. (A) Expression of STAT3 and its phosphorylated form pSTAT3 (Tyr705) in the nuclei of K562 and K562^{IR} cells and after treatment by inhibitors PPP (100 nM), Stattic (5μM), and NT157 (0.5 μM) was determined by Western blot. Protein samples (30 μg) were separated on precast 4-15% SDS-PAGE gel.(B) Relative quantification of STAT3 and pSTAT3 (Tyr705) protein expression. Error bars indicate ± SD of three independent measurements. IR, resistant to imatinib.

STAT3 inhibition by Stattic selectively decreases the viability of K562^{IR} cells. STAT3 mediates drug resistance in CML cells and its inhibition by specific inhibitors in combination with imatinib showed a great antiproliferative effect (Eiring et al., 2015b; Patel et al., 2021). To evaluate STAT3 as a molecular target with therapeutic potential, specific STAT3 inhibitor Stattic was used. Markedly increased sensitivity of K562^{IR} cells to Stattic compared to K562 cells was observed. While the EC_{50} for K562 cells was 1.6 μM, the EC_{50} for K562^{IR} cells was 0.3 μM. (Figure 18**)**. Phosphorylation of pSTAT3 (Tyr705) was decreased after Stattic treatment in cell lysates of K562^{IR} cells (Figure 16). Stattic treatment also slightly decreased the levels of pSTAT3 (Tyr705) in the nuclei of K562^{IR} cells **(**Figure 17).

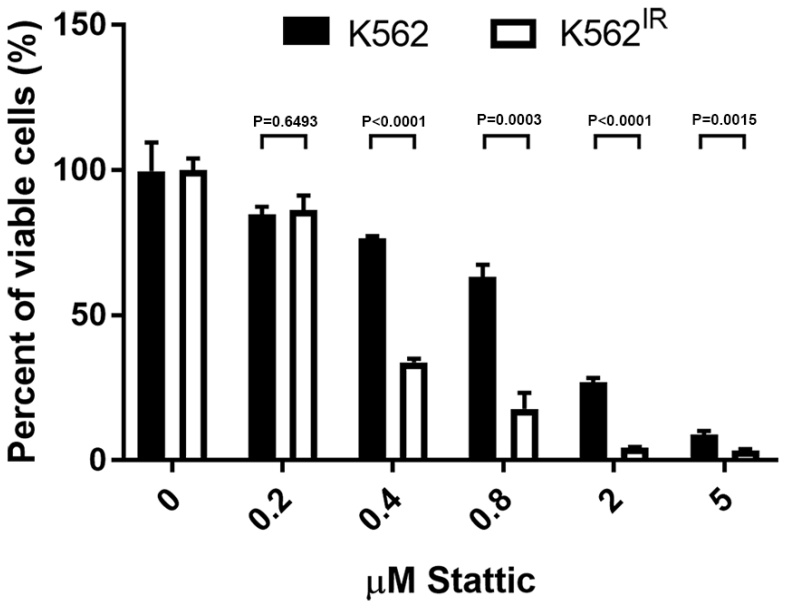

Figure 18. Viability of K562 and K562^{IR} cells cultured in the presence of Stattic for 3 days. Cell viability was determined using the MTT assay. Error bars indicate ± SD of three independent experiments.

STAT3 and IGF1R: functional analysis. Besides its direct phosphorylation by Bcr-Abl, STAT3 can also be activated by phosphorylation via IGF1R signaling (Ilaria and Van Etten, 1996; Zong et al., 2000; Xu et al., 2017; Das et al., 2018; Lee et al., 2018b; Zhu et al., 2019). It was shown previously that the IGF1R pathway maintains viability and proliferation of imatinib-resistant CML cells (Shi et al., 2010). Therefore, the expression of the IGF1R β receptor and its phosphorylated form pIGF1R β (Tyr1135/1136) was examined in K562 and K562^{IR} cells by Western blot (Figure 19). Western blot detection showed comparable levels of total IGF1R β receptor as well as phosphorylated pIGF1R β (Tyr1135/1136) in K562^{IR} and K562 cells.

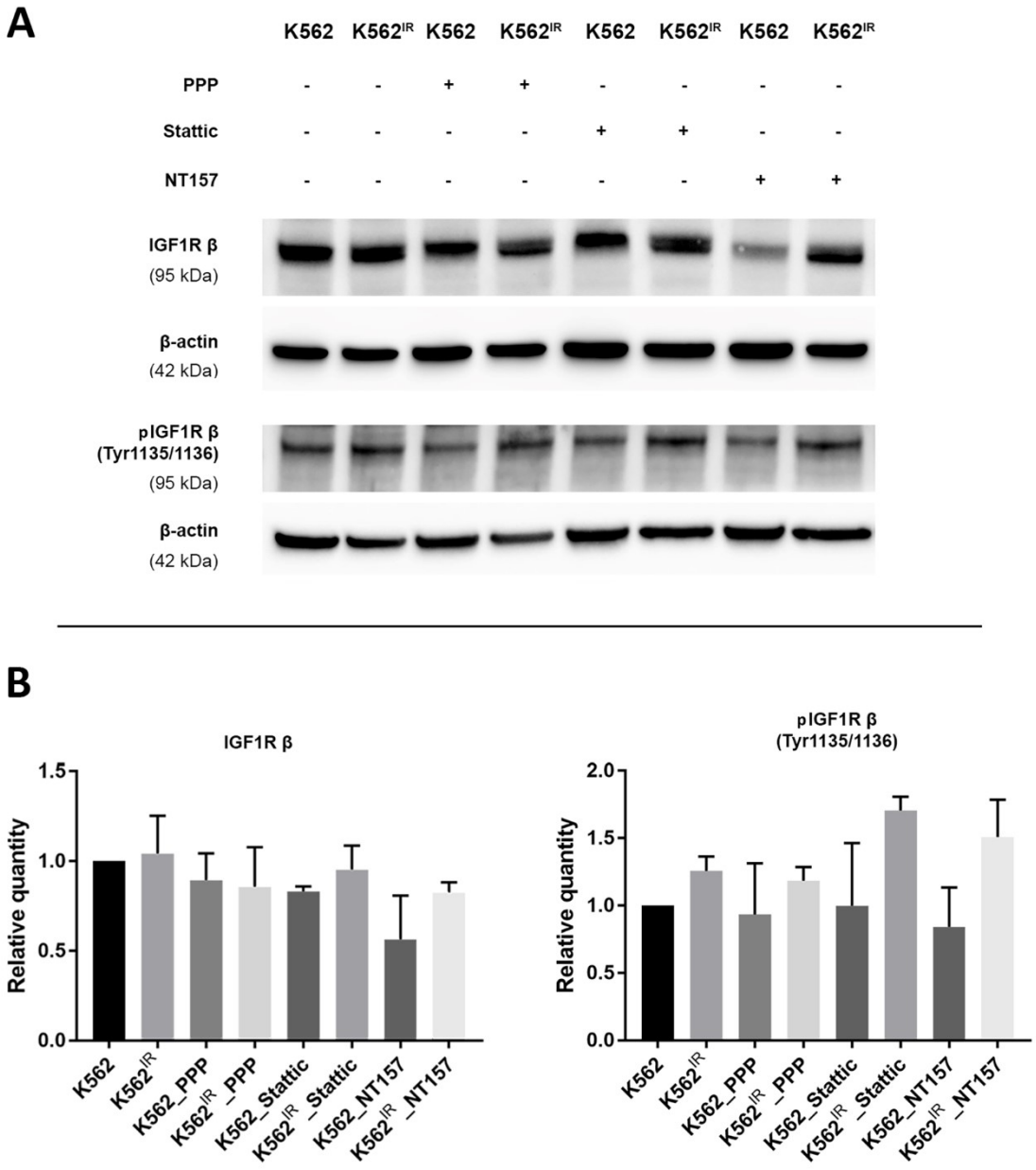

Figure 19. Western blot analysis and relative quantification of IGF1R β and pIGF1R β (Tyr1135/1136) in K562 and K562^{IR} cells. (A) Expression of IGF1R β and pIGF1R β (Tyr1135/1136) in K562 and K562^{IR} cells *was determined by Western blot. Effects of selected inhibitors PPP (100 nM), Stattic (5 μM) and NT157 (0.5 μM) on the expression of IGF1R β and pIGF1R β (Tyr1135/1136) were observed. Protein samples (30 μ) were separated on precast 4-15% SDS-PAGE gels. (B) Relative quantification of IGF1R β and pIGF1R β (Tyr1135/1136) expression in K562 and K562^{IR} cells. Error bars indicate ± SD of three independent measurements. IR, resistant to imatinib.*

IGF1R inhibition by PPP selectively inhibits the viability of K562^{IR} cells. Previously, PPP, a selective inhibitor of IGF1R was shown to be effective in eliminating BaF3 cells transfected either with wild-type *BCR-ABL1* or mutant *BCR-ABL1* with E255K or T315I point mutation (Shi et al., 2010). To address whether the inhibition of IGF1R receptor selectively affects the viability of the K562^{IR} cells, we targeted IGF1R receptor by PPP. K562 and K562^{IR} cells were exposed to PPP and markedly decreased viability of K562^{IR} compared to K562 cells was observed. The EC_{50} for K562^{IR} cells was 0.3 μM while the EC_{50} for K562 was 0.6 μM (Figure 20).

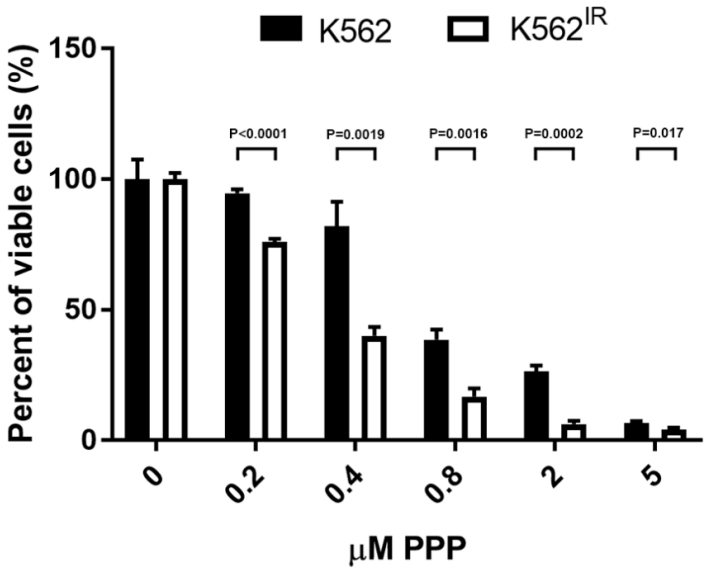

Figure 20. Viability of K562 and K562^{IR} cells cultured in the presence of picropodophylin (PPP) for 3 days. Cell viability was assessed using the MTT assay. Error bars indicate ± SD of three independent experiments.

Dual inhibition of STAT3 and IGF1R signaling by NT157 inhibitor selectively affects the viability of K562^{IR} cells. To address whether a combined inhibition of STAT3 and IGF1R signaling is more potent against the viability of resistant cells, NT157, a dual inhibitor of STAT3 and IGF1R/IRS-1/2 signaling was used. Previously, it was found that NT157 is effective in the elimination of BCR-ABL^{+} cells including cells harboring T315I mutation (Scopim-Ribeiro et al., 2021). Our results show that NT157 treatment reduced cell proliferation in a dose-dependent manner, EC_{50} for K562 cells was 0.35 μM, EC_{50} for K562^{IR} cells is cca 0.25 μM (Figure 21). NT157 treatment reduced levels of total STAT3 protein in cell lysates of K562 and K562^{IR} cells (Figure 16) and also slightly decreased the levels of pSTAT3 (Tyr705) in the nuclei of K562^{IR} cells **(**Figure 17).

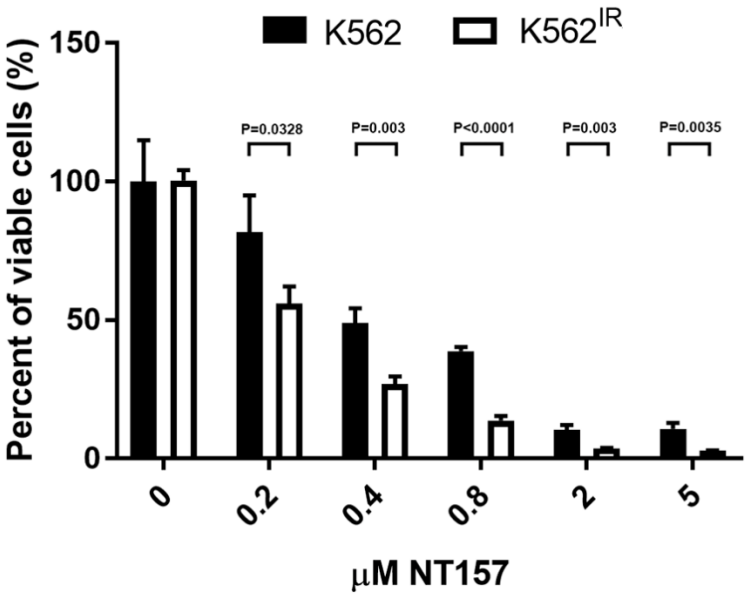

Figure 21. Viability of K562 and K562^{IR} cells cultured in the presence of NT157 for 3 days. The viability was determined using the MTT assay. Error bars indicate ± SD of three independent experiments.

PPP and NT157 treatment modulate the expression and phosphorylation of IRS-1, pIRS-1 (Ser612), and pIRS-1 (Ser636/639). Effects of PPP and NT157 on adaptor protein IRS-1 and its phosphorylated forms were explored by Western blot analysis. PPP induced inhibitory phosphorylation of IRS-1 on Ser612 and Ser636/639 in K562 and K562^{IR} cells (Figure 22). Addition of NT157 to the cell culture increased the levels of total IRS-1 protein in K562 and K562^{IR} cells. This result corresponds with previous results showing the presence of IRS-1 in K562 cells after treatment with NT157 (Scopim-Ribeiro et al., 2021). However, these results are in contrast to previously published data from studies on melanoma cells (Flashner-Abramson et al., 2016) and colorectal cells (Sanchez-Lopez et al., 2016). The mechanism by which NT157 suppresses IRS-1 adaptor protein is an induction of inhibitory serine phosphorylation of IRS-1 followed by its subsequent degradation (Reuveni et al., 2013). Western blot analysis revealed that NT157 (0.5 μM) treatment induced inhibitory phosphorylation of the adaptor protein IRS-1 at Ser612 and Ser636/639 in K562 and K562^{IR} (Figure 22). These results indicate that NT157 suppresses IGF1R signaling through the established mechanism of IRS-1 serine phosphorylation and subsequent degradation.

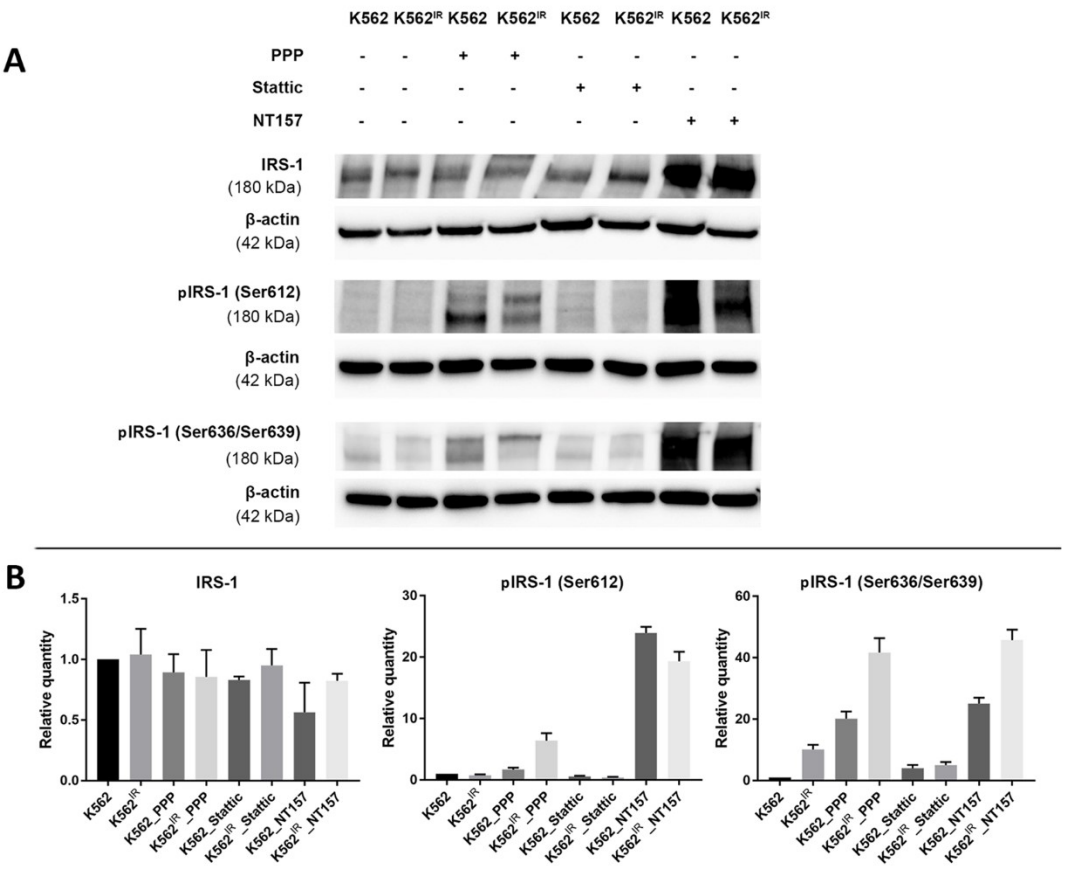

Figure 22. Western blot and relative quantification of IRS-1, pIRS-1 (Ser612), and IRS-1 (Ser636/639) in K562 and K562^{IR} cells. (A) Expression of IRS-1, pIRS-1 (Ser612), and IRS-1 (Ser636/639) in K562 and K562^{IR} cells was determined by Western blot. Effects of selected inhibitors PPP (100 nM), Stattic (5 μM) and NT157 (0.5 μM) on the expression of IRS-1, pIRS-1 (Ser612), and IRS-1 (Ser636/639) were observed. (B) Relative quantification of expression of IRS-1 and pIRS-1 (Ser612), and IRS-1 (Ser636/639) in K562 and K562^{IR} cells. Error bars indicate ± SD of three independent measurements. IR, resistant to imatinib.

PPP and NT157 treatment modulate the expression and phosphorylation of intracellular proteins. Effects of PPP and NT157 on proteins involved in cell signaling were evaluated by Western blot analysis. PPP slightly reduced the levels of phosphorylated pAKT (Ser473) in lysates of K562^{IR} cells. PPP also potentiated activation of ERK1/2 kinase by phosphorylation (Figure 23). NT157 also lowered detectable amount of phosphorylated AKT (Ser473) in lysates of K562^{IR} cells. NT157 treatment induced ERK1/2 activation in K562 and K562^{IR} cells by phosphorylation (Figure 23). These results are in agreement with previously published data obtained on prostate cancer cells where NT157 treatment suppressed AKT activation but potentiated ERK1/2 phosphorylation (Ibuki et al., 2014).

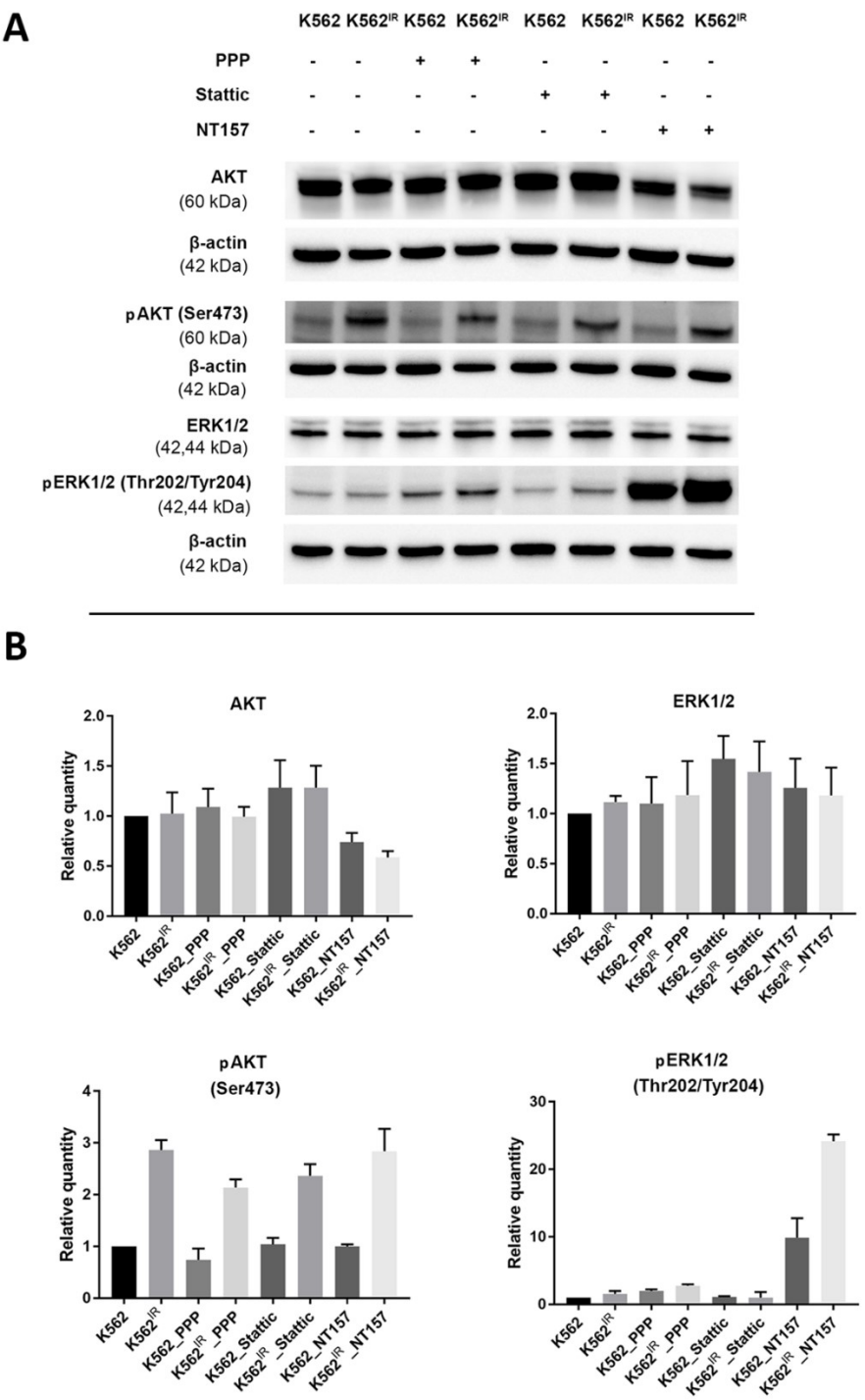

Figure 23. Western blot analysis and relative quantification of AKT, AKT (Ser473), ERK1/2, ERK1/2 (Thr202/Tyr204) in K562 and K562^{IR} cells. (A) Expression of selected proteins AKT, AKT (Ser473), ERK1/2, ERK1/2 (Thr202/Tyr204) in cell lysates of K562 and K562^{IR} cells and after treatment of cells with selected inhibitors PPP (100 nM), Stattic (5 μM) and NT157 (0.5 μM). Protein samples (30 μ) were separated on precast 4-15% SDS-PAGE gels. (B) Relative quantification of expression of AKT, AKT (Ser473), ERK1/2, ERK1/2 (Thr202/Tyr204) in cell lysates of K562 and K562^{IR} cells. Error bars indicate ± SD of three independent measurements. IR, resistant to imatinib.

Stattic and NT157 decrease the expression of IFITM3 protein and mRNA. The data from our parallel work on the analysis of exosomes released from K562 and K562^{IR} cells revealed markedly increased levels of the IFITM3 protein in exosomes derived from K562^{IR} cells as well as in the lysates of the source K562^{IR} cells as proven by Western blots (Figure 33) and verified

by FACS analysis (Hrdinova et al., 2021). Previously, it was demonstrated that expression of the IFITM2 protein, another member of the IFITM family of proteins, can be modulated via IGF1R/STAT3 signaling axis (Xu et al., 2017). To address whether IGF1R/STAT3 pathway is capable of modulating IFITM3 expression in K562^{IR} cells, K562^{IR} cells were treated with STAT3 inhibitor Stattic (5μM) and NT157 (0.5 μM) in different time points with subsequent Western blots detection of IFITM3 in cell lysates (**Chyba! Nenalezen zdroj odkazů.**). The results demonstrated that both Stattic and NT157 decrease expression of IFITM3 protein after 24h incubation. Similar observations were obtained by RT-PCR for IFITM3 mRNA (Figure 25).

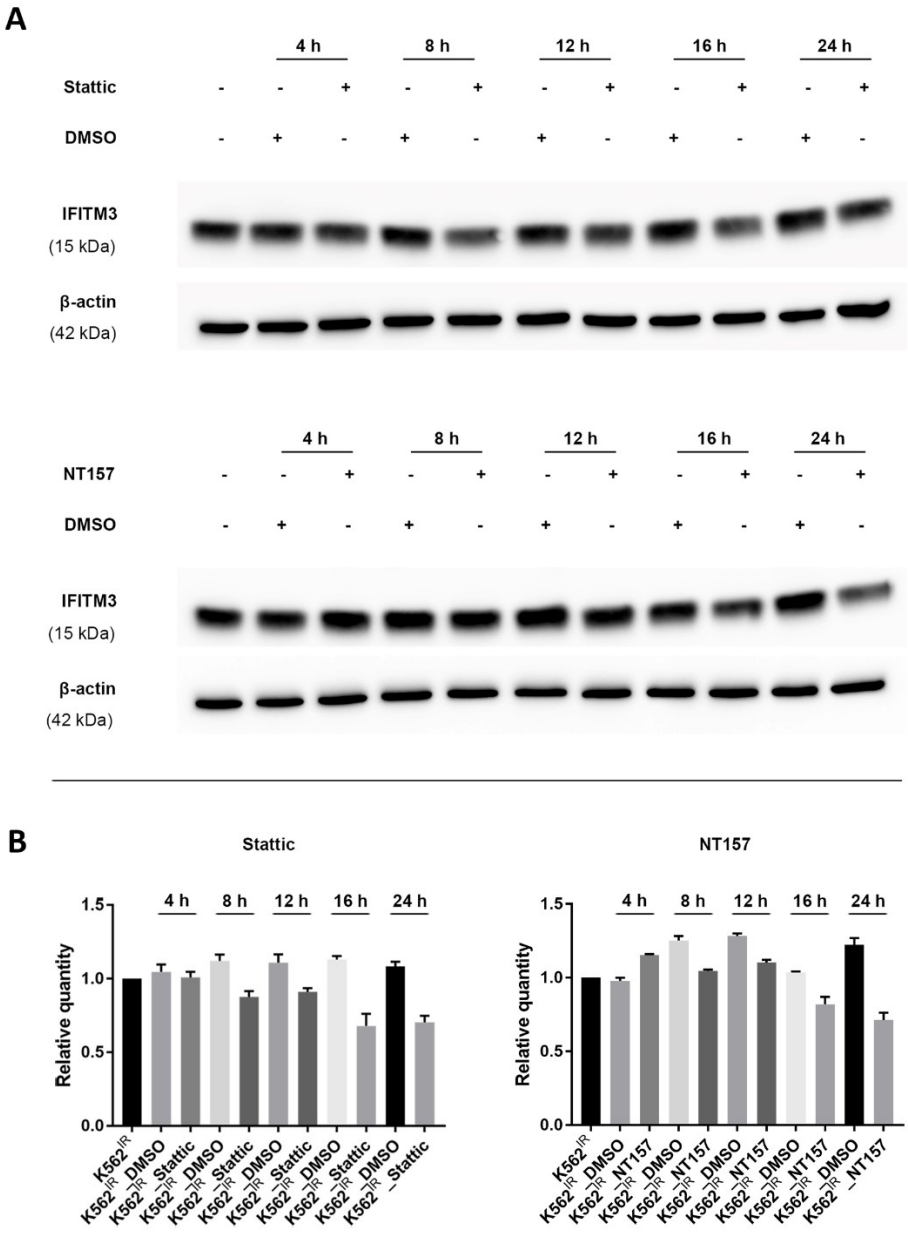

Figure 24. Western blot analysis and relative quantification of IFITM3 expression after Stattic and NT157 treatment. (A) K562^{IR} cells were treated with Stattic (5 μM) and NT157 (0.5 μM) in different time points. Protein samples (30 μg) were separated on precast 4-15% SDS-PAGE gels.(B) Relative quantification of expression of IFITM3 protein in K562^{IR} cells after Stattic and NT157 treatment. Error bars indicate ± SD of three independent measurements. IR, resistant to imatinib.

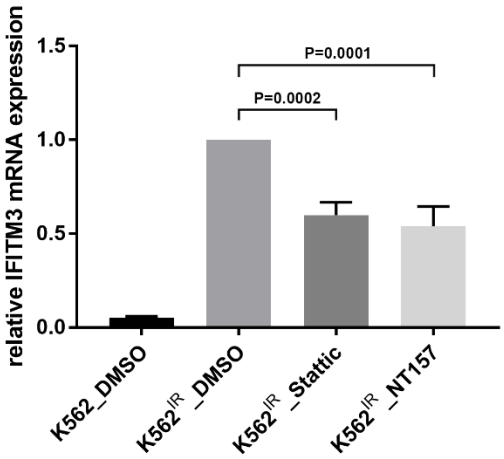

Figure 25. IFITM3 mRNA expression in the K562, K562^{IR} cells and in K562^{IR} cells treated with Stattic or NT157. mRNA expression levels were determined by RT-PCR analysis and normalized to the values obtained from the untreated K562^{IR} cells. Error bars indicate ± SD of three independent measurements. IR, resistant to imatinib.

Stattic and NT157 are responsible for distinct transcriptional profile of K562^{IR} cells. Relative expression of several genes involved in IGF1R and STAT3 signaling was analyzed using RT-PCR, the summary of results is given in Table V. Expression of *IGF1R* mRNA was found to be 2-fold increased in K562^{IR} cells compared to K562 cells. Treatment of K562^{IR} cells with NT157 resulted in almost 2-fold decrease in expression of *IGF1R* mRNA. Stattic did not markedly alter *IGF1R* mRNA expression in K562^{IR} cells. Steady state *IRS-1* mRNA expression was decreased 2-fold in K562^{IR} cells compared to K562 cells. Treatment of K562^{IR} cells with NT157 resulted in a 3-fold increase of *IRS-1* mRNA expression. Constitutive expression of *STAT3* mRNA was increased 2-fold in K562^{IR} cells compared to K562 cells. 24h pretreatment of K562^{IR} cells with the NT157 inhibitor resulted in (almost 2-fold) reduction of *STAT3* mRNA expression. Interestingly, Stattic did not affects the levels of *STAT3* mRNA in K562^{IR} cells. Basal *IFITM3* expression was significantly elevated in K562^{IR} cells compared to K562 cells and treatment of K562^{IR} cells by Stattic and NT157 lowered *IFITM3* mRNA almost 2-fold. Expression of *AKT1* mRNA in K562^{IR} cells was 30% lower than in control K562 cells. The Amount of *AKT1* mRNA was decreased in K562^{IR} cells after treatment with NT157 (Table V). Taken together, our data show that NT157 affects more molecular targets essential for the proliferation of K562^{IR} cells than Stattic and indicate its better therapeutic potential in a hypothetical model of combined therapy of CML resistant to imatinib.

Table V. Changes in the expression of selected genes (AKT1, IFITM3, IGF1R, IRS-1, STAT3). *The heatmap shows genes with downregulated expression (blue) or upregulated (red) in the K562^{IR} cells compared to K562 cells and K562^{IR} cells treated with inhibitors Stattic and NT157.*

	S_DMSO	R_DMSO	R_Stattic	R_NT157
AKT1	0.7186361	1	0.897095	0.371989
IFITM3	0.0551689	1	0.598048	0.644685
IGF1R	0.5321851	1	0.717806	0.522439
IRS1	1.6548112	1	0.578344	3.872683
STAT3	0.5625292	1	1.011619	0.601513

>0,9
>0,5
>0,25
1
<1,1
<2
<4

CsH decreased IFITM3 expression and viability of K562^{IR} cells. Previous articles suggested that CsH, an inhibitor of the formyl peptide receptor, is capable of downregulating IFITM3 expression (de Paulis et al., 1996; Wu et al., 2018). To determine whether CsH can modulate the expression of IFITM3 in K562^{IR} cells, K562^{IR} cells were treated with CsH. We found that 8 µM CsH strongly decreased IFITM3 expression in K562^{IR} cells (Figure 26). To address whether inhibition of IFITM3 by CsH is crucial for K562^{IR} survival, K562^{IR} cells were incubated with CsH and assayed for cell viability. CsH treatment reduced the viability of K562^{IR} cells more selectively (EC_{50} 16 µM) in comparison with K562 cells (Figure 27).

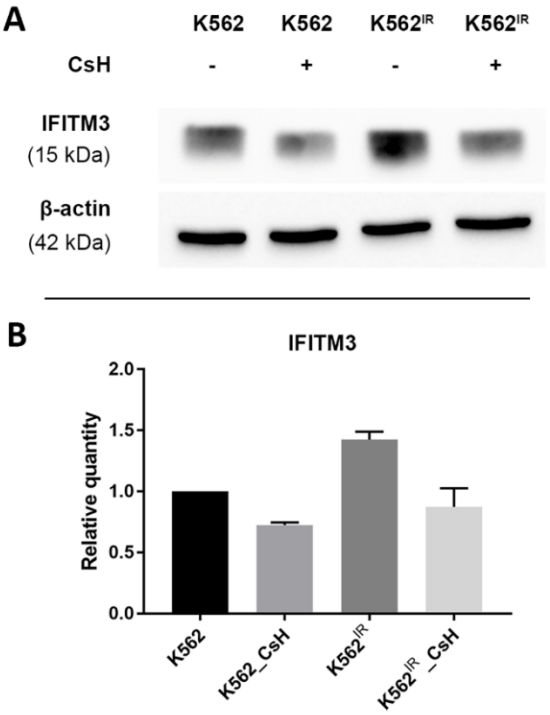

Figure 26. Western blot analysis and relative quantification of IFITM3 expression after treatment with cyclosporin H (CsH). (A) Expression of IFITM3 protein in K562 and K562^{IR} cell lysates after treatment with CsH. Protein samples (30 µg) were separated on precast 4-15% SDS-PAGE gels. (B) Relative quantification of expression of IFITM3 protein in K562 and K562^{IR} cells after CsH treatment. Error bars indicate ± SD of three independent measurements. IR, resistant to imatinib.

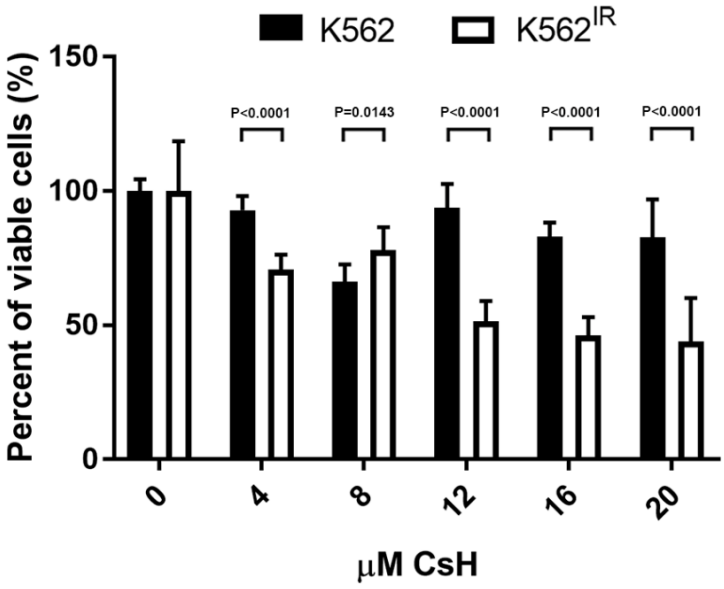

Figure 27. Relative viability of the K562 and K562^{IR} cells cultured in the presence of cyclosporin H for 3 days. The viability was determined using the MTT assay. Error bars indicate ± SD of three independent experiments. IR, resistant to imatinib.

4.3. Analysis of exosomes released by K562 and K562^{IR} cells

To expand our knowledge about leukemia cell biology represented by model K562 and K562^{IR} CML cell lines and to understand better the mechanisms of their survival in imatinib with emphasis on cell-to-cell communication, exosomes from K562 and K562^{IR} cells were isolated and their putative role in resistance to imatinib was examined. Using LFQ proteomic analysis exosomal protein composition was compared with a special focus on the identification of exosome surface markers clinically relevant as potential diagnostic markers.

Exosome characterization. K562 and K562^{IR} exosomes were isolated from cell culture supernatants by ultracentrifugation. Transmission electron microscopy was used to verify the purity and size of exosomes. Exosomes were observed as round or cup-shaped vesicles with the size ranging between 50-150 nm in diameter (Figure 28A). The observations were confirmed by tunable resistive pulse sensing (TRPS) using qNano instrument analysis which showed the mode diameter of exosomes in size between 100-110 nm. The number of exosomes produced by $1.8x10^8$ of K562^{IR} cells ($1.7x10^{11}$ particles/ml) was ~ about 2 times higher compared to the number of exosomes produced by $1.8x10^8$ of K562 cells ($8x10^{10}$ particles/ml) (Figure 28B). To verify the purity of the exosome isolation procedure, Western blot was used to confirm the presence of 'exosomal markers' i.e. proteins frequently found in exosomes (CD9, CD81, CD63, and HSP70, using GAPDH as a loading control) (Kowal et al., 2016) (Figure 28C).

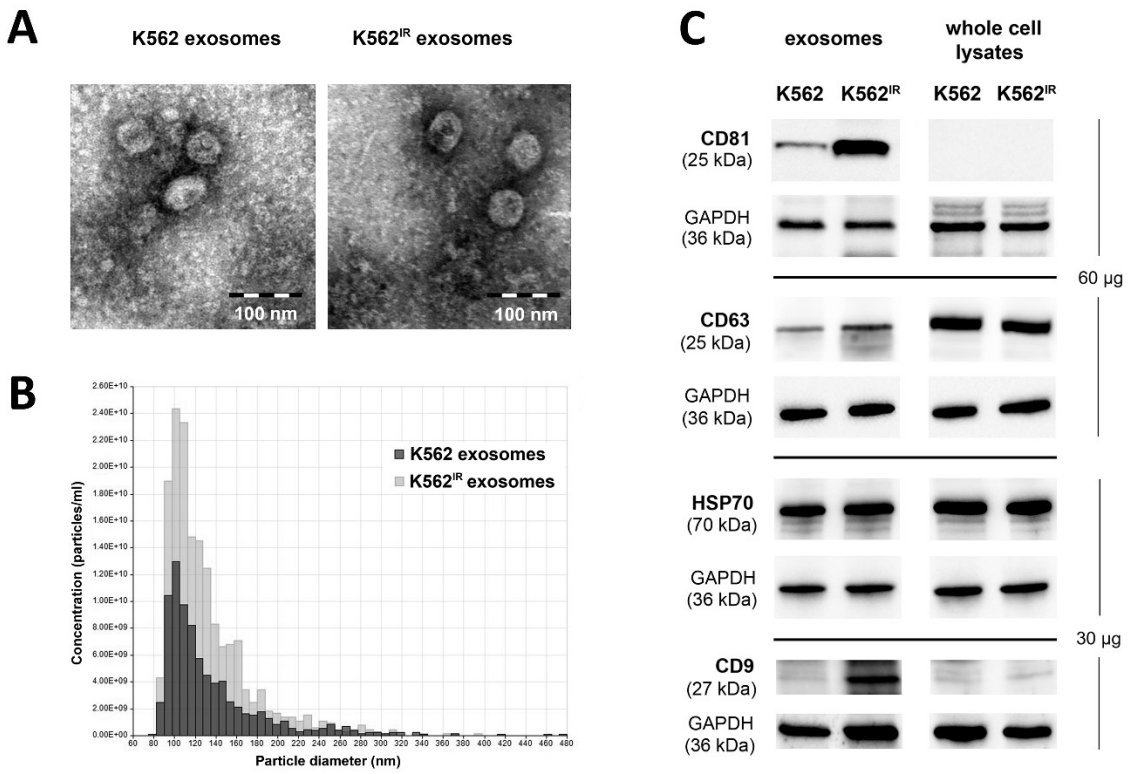

Figure 28. Exosome characterization. (A) Exosomes derived from K562 and K562^{IR} cells were visualized using transmission electron microscopy. Exosomes were round or cup-shaped vesicles with size ranging between 50-150 nm. Scale bar indicates 100 nm. (B) Size distribution of the K562 and K562^{IR} exosomes analyzed using qNano. The qNano analysis confirmed comparable size distributions of the vesicles with sizes dominantly between 100-110 nm. (C) Presence of exosomal markers in K562 and K562^{IR} derived exosomes and cell lysates. Expression of exosomal markers was determined by Western blot. For Bcr-Abl, CD9, and HSP70, 30 µg of total protein was loaded, for CD63 and CD81 60 µg of total protein was loaded. Exosomes and cell lysates probed with the same antibody were always loaded together on the same gel/membrane. Irrelevant lanes have been cropped from the figure IR, resistant to imatinib.

K562^{IR} exosomes are internalized by K562 cells. It was shown previously that exosomes derived from K562 cells can be internalized by various cell types, such as macrophages, bone marrow stromal cells, endothelial cells, and leukemic cells (Mineo et al., 2012; Taverna et al., 2012; Tadokoro et al., 2013; Corrado et al., 2014; Raimondo et al., 2015; Jafarzadeh et al., 2019). Recently, it was shown that exosomes derived from CML cells resistant to imatinib are internalized by imatinib-sensitive CML cells and are capable of inducing drug-resistant phenotype to recipient cells (Min et al., 2018).

In this study, the fusion of CFSE labeled exosomes, derived from K562 or K562^{IR} cells, with recipient K562 cells was confirmed after 4 h incubation (Figure 29). K562 cells with internalized CFSE-positive exosomes were visualized by confocal microscopy starting 1 h after exosomes addition, and the maximum of exosome internalization occurred within 4 hours as determined in a pilot time course experiment (data not shown).

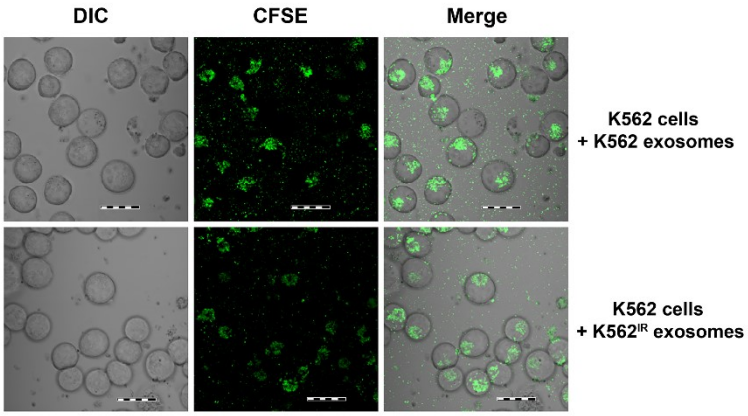

Figure 29. Internalization of K562 exosomes and K562^{IR} exosomes by K562 cells visualized by confocal microscopy. K562^{IR} and K562 derived exosomes were labeled with CFSE (green), were internalized into K562 cells, and were visualized after 4-h incubation. Scale bar, 20 µm. CFSE, carboxyfluorescein succinimidyl ester; IR, resistant to imatinib.

K562^{IR} exosomes increase survival of K562 cells in 2 µM imatinib. It was shown previously that exosomes derived from imatinib-resistant K562 cells were able to confer resistant trait to imatinib-sensitive K562 cells (Min et al., 2018). To verify this observation, exosomes derived either from K562^{IR} or from K562 cells were incubated with K562 cells for 4 h with the subsequent addition of imatinib (2 µM) to the media followed by 2 days cultivation. Subsequent cell viability assays revealed that K562^{IR} derived exosomes significantly increased survival of imatinib-sensitive K562 cells in 2 µM imatinib compared to K562 cells treated either with K562-derived exosomes or without any exosomes (Figure 30). In the original work by *Min et al* mentioned above, miR-365 was identified as the main molecule responsible for this prosurvival effect. However, administration of whole exosomes had an additional beneficial prosurvival effect compared to miR-365 alone, suggesting that other molecules play role in this process. Thus, it could be hypothesized that the exosomes derived from our K562^{IR} cells with the unique molecular composition also carry molecules beneficial for better survival of recipient K562 cells in imatinib. To identify protein candidates associated putatively with exosomal transfer of imatinib resistance, LFQ analysis of exosomes derived from K562 and K562^{IR} cells was performed and the respective exosomal protein profiles were compared quantitatively. We focused on the identification of specifically enriched molecules, which could be associated with imatinib resistance, and/or better proliferation of the recipient, imatinib-sensitive cells. We also searched for unique proteins localized on the surface of K562^{IR} exosomes to identify possible clinically relevant diagnostic markers associated with imatinib resistance. For this purpose, a detailed combined proteomic approach combining LFQ, WB, and FACS analysis was performed.

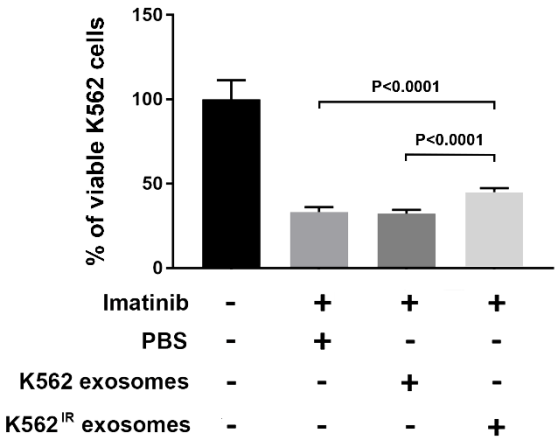

Figure 30. Incubation of K562^{IR} exosomes with K562 cells increased the viability of K562 cells in the presence of 2 μM imatinib. One-way ANOVA with Tukey's post-hoc test was used. The mean values ± SD were calculated from three independent experiments. IR, imatinib-resistant.

LFQ proteomic analysis of the exosomes. Exosomes isolated from K562 and K562^{IR} cells were analyzed by LC-MS/MS (Q-Exactive). A total of five pairs of the respective exosome samples were obtained from independent isolations of exosomes from K562 and K562^{IR} cells. In total, 3,218 exosomal proteins were identified. The number of proteins identified in each sample ranged from 1,072 to 1,751 with FDR set to 0.01. The LFQ proteomic analysis provided semi-quantitative data for 1,241 proteins (Table SIII). To determine the reproducibility of LFQ analysis, the quantitative accuracy was examined by Pearson correlation analysis which showed good inter-sample reproducibility (Pearson's correlation coefficients in the range of 0.723-0.971 (Figure 31). The majority (2,693 of 3,218, 83.7 %) of all the identified proteins were listed in the database of exosomal proteomes Exocarta (http://www.exocarta.org), whereas, 525 novel exosomal proteins were identified.

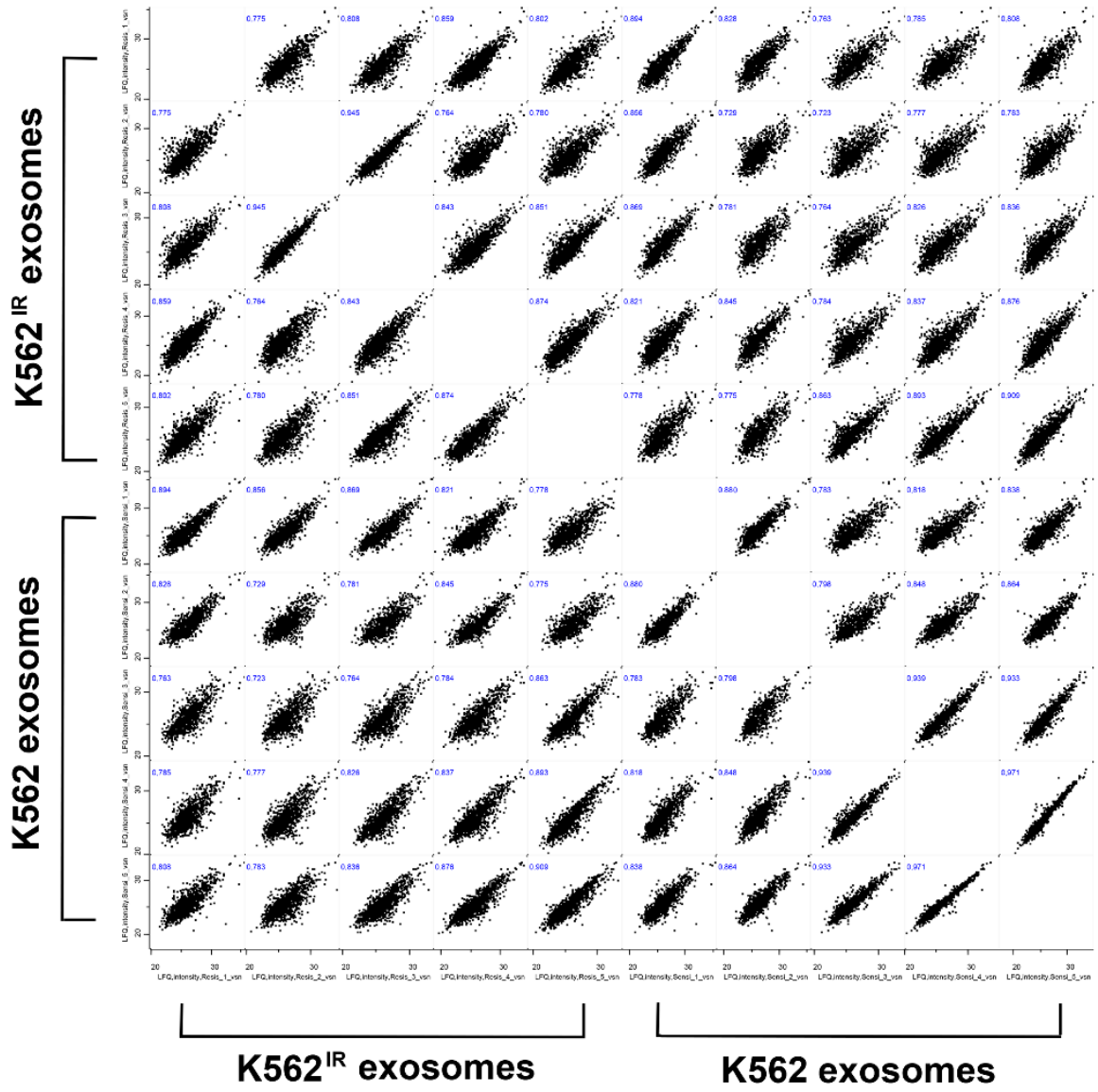

Figure 31. LFQ-MS peptide signal intensity correlations between individual LC-MS analysis of K562 and K562^{IR} exosomes. The figure is a composite image of the correlation plots from LFQ-MS peptide signal intensities between all the LC-MS runs from the proteomic analysis. Pearson's correlation coefficients in the range of 0.723-0.971 revealed good inter-sample reproducibility. LFQ, label-free quantification; LC, liquid chromatography; MS, mass spectrometry; IR, imatinib-resistant.

Identification of differentially abundant proteins in exosomes. In exosomes derived from K562^{IR} cells, 35 proteins with significantly different abundances were identified compared to exosomes from the parental sensitive cells (fold change >1.5) (Figure 32, Table VI). Among these, 28 proteins were enriched, while the abundance of 7 proteins was lowered in K562^{IR} exosomes. The most enriched proteins identified in K562^{IR} exosomes included interferon-induced transmembrane protein 3 (IFITM3), desmoglein-2 (DSG2), cell-surface glycoprotein MUC18 (CD146), and platelet glycoprotein 4 (CD36). By contrast, proteins with significantly lowered abundance were collagen α -1 (XV) chain, galectin-3-binding protein (LGALS3BP), laminin

subunit β-1 (LAMB1), bone marrow stromal antigen 2 (BST2), and epidermal growth factor-like protein 7 (EGFL7).

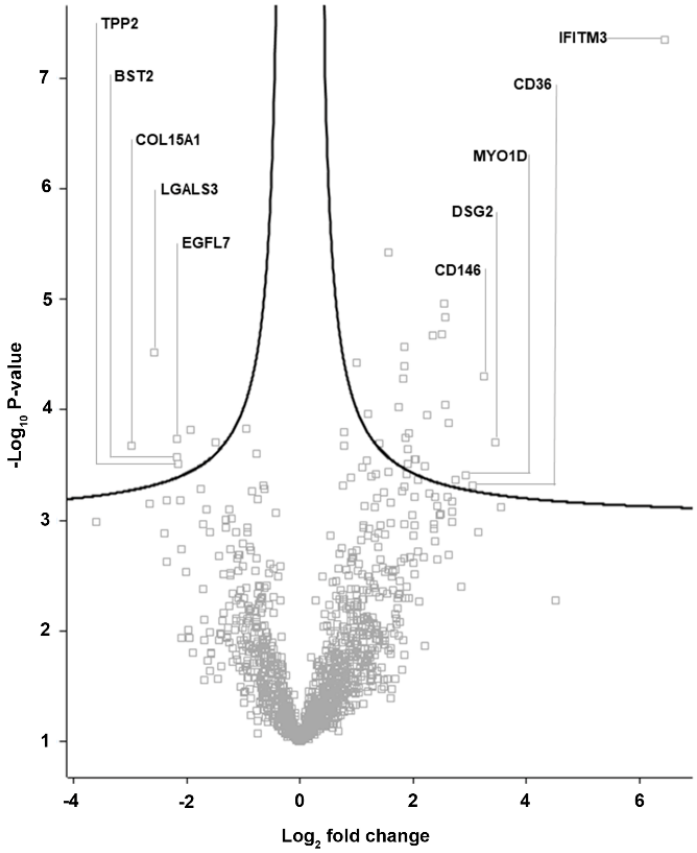

Figure 32. Differentially abundant proteins present in exosomes were identified using LFQ proteomic analysis of K562 and K562^{IR} exosomes. Proteins with positive log$_2$ fold change were upregulated in K562^{IR} exosomes, proteins with negative fold-change were downregulated in K562^{IR} exosomes. Only the proteins above the black line indicating statistical significance (false discovery rate <0.05, S0=0.1) were considered.

Table VI. Differentially abundant proteins in the K562^{IR} exosomes.

Upregulated protein in K562^{IR} exosomes						
Protein names	Protein IDs	Gene names	Fold change	Unique peptides	MS/MS	Permutation-based FDR
Interferon-induced transmembrane protein 3	Q01628	IFITM3	87.5	1	24	<0.001
Desmoglein-2	Q14126	DSG2	10.9	10	33	0.002
Cell surface glycoprotein MUC18	P43121	MCAM	9.6	11	28	<0.001
Platelet glycoprotein 4	P16671	CD36	8.4	7	18	0.005
Unconventional myosin-Id	O94832	MYO1D	7.6	21	41	0.004
CD2-associated protein	Q9Y5K6	CD2AP	6.7	29	105	0.004
Multivesicular body subunit 12A	Q96EY5	MVB12A	6.2	2	19	0.001
Golgi integral membrane protein 4	O00461	GOLIM4	6.0	18	37	<0.001
Protein TFG	Q92734	TFG	5.9	3	9	<0.001

Melanoma-associated antigen 4	P43358	MAGEA4	5.8	9	20	<0.001
Spastin	Q9UBP0	SPAST	5.7	9	19	<0.001
Melanotransferrin	P08582	MFI2	5.1	10	19	<0.001
Charged multivesicular body protein 4a	Q9BY43	CHMP4A	4.8	9	35	0.001
Tetraspanin-18	Q96SJ8	TSPAN18	4.6	3	13	0.003
Rab11 family-interacting protein 1	Q6WKZ4	RAB11FIP1	4.1	16	37	0.003
STAM-binding protein	O95630	STAMBP	4.1	9	16	0.003
Rac GTPase-activating protein 1	Q9H0H5	RACGAP1	3.8	10	18	0.002
Hepatocyte growth factor-regulated tyrosine kinase substrate	O14964	HGS	3.8	15	45	0.003
Protein tweety homolog 2	Q9BSA4	TTYH2	3.7	3	13	0.002
Toll-interacting protein	Q9H0E2	TOLLIP	3.7	4	24	0.002
Syntenin-1	O00560	SDCBP	3.6	22	207	<0.001
Hemoglobin subunit ε	P02100	HBE1	3.6	11	56	<0.001
Vacuolar protein sorting-associated protein 4A	Q9UN37	VPS4A	3.5	11	76	<0.001
Charged multivesicular body protein 4b	Q9H444	CHMP4B	3.3	15	86	<0.001
Crk-like protein	P46109	CRKL	3.0	12	56	<0.001
L-aminoadipate-semialdehyde dehydrogenase-phosphopantetheinyl transferase	Q9NRN7	AASDHPPT	2.6	6	10	0.002
Hemoglobin subunit ζ	P02008	HBZ	2.3	13	217	0.001
Heat shock protein 105 kDa	Q92598	HSPH1	2.0	19	79	<0.001
Downregulated proteins in K562^{IR} exosomes						
Protein names	Protein IDs	Gene names	Fold change	Unique peptides	MS/MS	Permutation-based FDR
DNA topoisomerase 2-β	Q02880	TOP2B	-2.8	7	23	0.002
Tyrosine-protein kinase receptor UFO	P30530	AXL	-3.8	7	21	0.002
Tripeptidyl-peptidase 2	P29144	TPP2	-4.4	57	211	0.003
Epidermal growth factor-like protein 7	Q9UHF1	EGFL7	-4.5	4	10	0.002
Bone marrow stromal antigen 2	Q10589	BST2	-4.5	6	17	0.003
Galectin-3-binding protein	Q08380	LGALS3BP	-5.9	6	17	0.001
Collagen α-1(XV) chain	P39059	COL15A1	-7.9	15	102	0.002
Positive fold change indicates upregulation, negative fold change indicated downregulation in K562^{IR} exosomes. FDR, false discovery rate; MS, mass spectrometry						

The most enriched proteins (at least 5-fold) in K562^{IR} derived exosomes were further examined with a special focus on their potential to represent diagnostically exploitable exosomal (or cell) markers associated with resistance to imatinib. Three candidate proteins were identified by an algorithm for prediction of surface localization GenieScore (Waas et al., 2020): IFITM3, CD146 (MUC18), and CD36. The presence of IFITM3, CD146, and CD36 was confirmed by Western blot using specific antibodies in the exosomes and in their respective cells of origin (Figure 33Figure 33). Western blot analysis confirmed enrichment of all three proteins in K562^{IR} derived exosomes as well as in the lysates of K562^{IR} cells. These results indicate their putative diagnostic potential as the differential profile of IFITM3, CD146 and CD36 protein abundance between K562 and K562^{IR} derived exosomes corresponds with their respective expression in K562 and K562^{IR} cells.

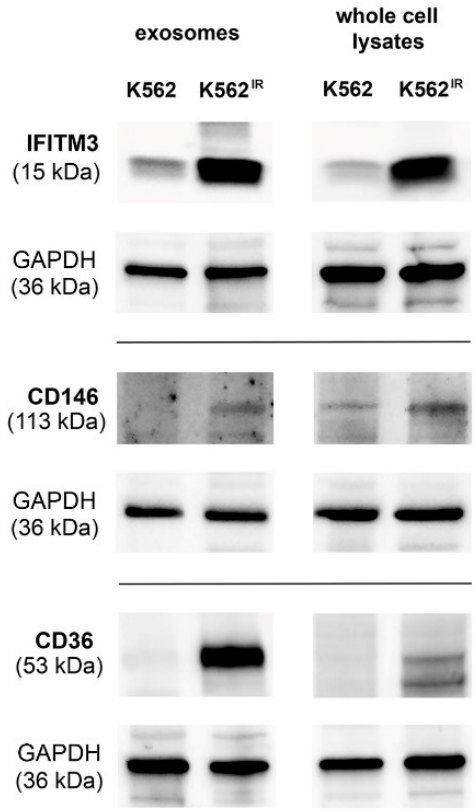

Figure 33. Confirmation of differential enrichment of IFITM3, CD146, and CD36 in the exosomes and cells by Western blot with specific antibodies. Samples (60 µg) were separated on 4-15% precast SDS PAGE gels. Irrelevant lanes have been cropped from the figure. IFITM3, interferon-induced transmembrane protein 3; IR, imatinib-resistant.

CML oncoprotein BCR-ABL is present in exosomes from imatinib-resistant K562^{IR} cells. We hypothesized whether exosomes derived from K562^{IR} cells are enriched in the CML oncoprotein BCR-ABL. Western blot analysis demonstrated the presence of BCR-ABL protein in exosomes from both K562 and K562^{IR} cells. The amount of BCR-ABL protein was strongly enriched in K562^{IR} derived exosomes reflecting its increased expression in K562^{IR} cells (Figure 34).

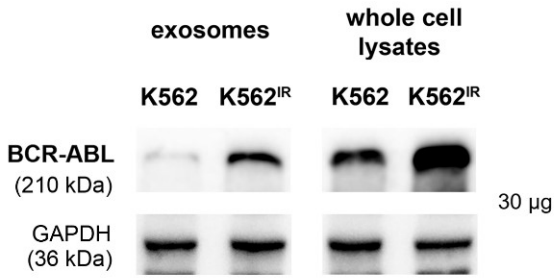

Figure 34. Expression of the CML oncoprotein BCR-ABL in exosomes and cell lysates from K562 and K562^{IR} cells. Expression of BCR-ABL was determined by Western blot analysis. 30 µg of total protein was loaded for both exosomes and lysates.

CD146 and IFITM3 are specific cell-surface markers of K562^{IR} cells. To evaluate the potential of IFITM3, CD146, and CD36 to represent cell surface markers associated with imatinib resistance, flow cytometric analysis of live K562 and K562^{IR} cells was performed. Flow cytometry demonstrated markedly increased cell-surface expression of IFITM3 and CD146. Expression of CD36 was increased to a lesser extent (Figure 35). K562^{IR} cells were positive in 96.2% for CD146 and 51.6% for IFITM3, whereas K562 cells were positive in 0.7% for CD146 and 4% for IFITM3 respectively. CD36 was detected in 10.5% of K562^{IR} compared to 3% of K562 cells (Figure 35).

Flow cytometric analysis demonstrated that the expression of CD146 clearly distinguishes K562^{IR} cell population from K562 cells and that CD146 could be used as a cell-surface marker of imatinib-resistant K562^{IR} cells. IFITM3 also appeared as a promising resistance-associated marker. However, the specific role of these proteins taking an active part in imatinib resistance, as well as their potential to influence the phenotype of the recipient sensitive K562 cells remains to be elucidated.

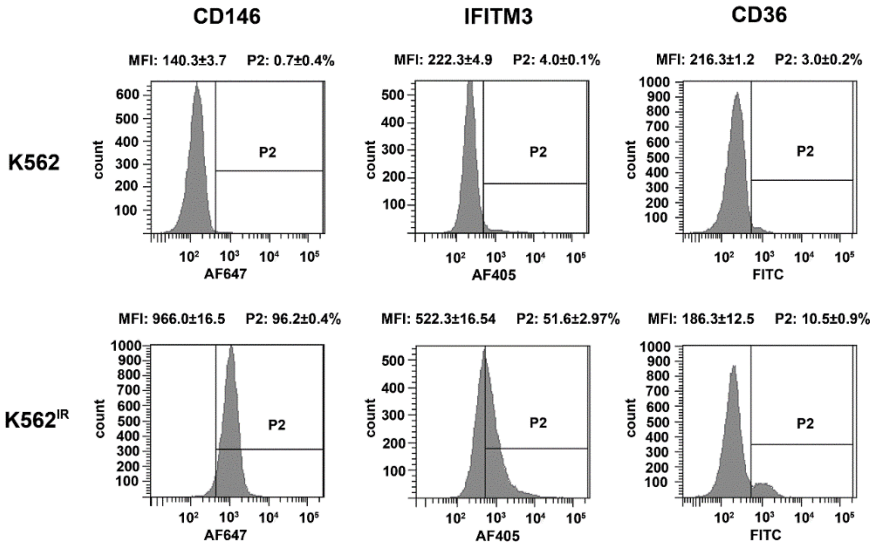

Figure 35. Analysis of cell surface expression of IFITM3, CD146, and CD36. Increased expression of CD146, IFITM3, and CD36 on the cell surface of K562 and K562^{IR} cells was confirmed by flow cytometry. The mean and P2 values ± SD were calculated from three independent experiments. Representative graphs from repeated experiments are shown. The gate was set using unstained controls. IFITM3, interferon-induced transmembrane protein 3; MFI, mean fluorescence intensity; IR, imatinib-resistant.

5. Discussion

Despite the fact that the approval of imatinib (and other TKI) for clinical use revolutionized the treatment of CML, improving the prognosis and quality of life of affected patients, the development of pharmacological resistance in CML therapy remains a major problem which still needs to be addressed.

Although imatinib was designed to restrain BCR-ABL activity exclusively, it becomes clear that even an acquired resistance achieved mostly by point mutations in *BCR-ABL1* gene or *BCR-ABL1* gene amplification in CML cells is accompanied by additional (BCR-ABL dependent or independent) auxiliary mechanisms and changes within the cell metabolism to establish an adapted, growth of drug-resistant CML cells in the presence of imatinib. Metabolic adaptations of leukemic cells leading to acquired TKI resistance are a result of numerous specific molecular alterations which converge to create a new drug-resistant cell phenotype differing from the phenotype of the original cells. One mutation in *BCR-ABL1* is not the whole image of imatinib-resistant cell. Instead, it should be viewed that although one single mutation in *BCR-ABL1* gene disables imatinib from action, the resulting complex metabolism of imatinib-resistant CML cells is not necessarily identical to the original, imatinib sensitive cells. Indeed, this work highlights specific metabolic features developed by imatinib-resistant cells to fully proliferate in imatinib, using two CML cell lines serving as examples of imatinib resistance that commonly occur in clinical reality. Proteomic characterization of these changes in drug-resistant CML cells provides useful information for identification and evaluation of promising potential therapeutic targets and can open new perspectives for improved, personalized, combined, and molecularly targeted therapies (Petrak et al., 2009; Lorkova et al., 2015; Toman et al., 2016). Recently, exosomes were also shown to play an important role in cancer development, progression, and drug resistance. However, the role of exosomes in hematological malignancies, especially in CML is not well elucidated.

The aim of this study was to characterize two leukemic CML model cell lines sensitive (CML-T1, K562) and resistant (CML-T1^{IR} and K562^{IR}) to imatinib with different mechanisms of resistance, as well as exosomes released by imatinib-sensitive and imatinib-resistant K562 cells in order to evaluate potential therapeutic targets in drug-resistant cells and to elucidate the role of exosomes in resistance to imatinib with emphasis on identification of clinically relevant diagnostic markers.

The two resistant CML cell lines, CML-T1^{IR} and K562^{IR} differ in the mechanism of resistance to imatinib. CML-T1^{IR} cells carry the mutation Y253H in the *BCR-ABL1* gene. Mutations in the

kinase domain of the *BCR-ABL1* gene are the most common cause of imatinib resistance in CML patients (Gorre et al., 2001). In contrast, the second CML cell line used in this study, $K562^{IR}$, does not carry a mutation in the *BCR-ABL1* gene. Instead, imatinib-resistant $K562^{IR}$ cells harbored a 2-fold higher number of *BCR-ABL1* gene copies compared to imatinib-sensitive K562 cells. Thus, the mechanism of resistance to imatinib in $K562^{IR}$ cells was an amplification of the *BCR-ABL1* gene, which resulted in overexpression of *BCR-ABL1* mRNA and protein levels. This mechanism of resistance was previously described in a subset of CML patients (Gadzicki et al., 2005; Chandran et al., 2019). Considering additional or alternative putative mechanisms contributing to imatinib resistance, MRP2 protein was detected in K562 and $K562^{IR}$ cells. Previously, overexpression of MRP2 was detected in imatinib-resistant K562 cells (He et al., 2017). However, MRP2 relationship to imatinib resistance is not well elucidated and it is not clear whether MRP2 contributes to imatinib resistance (Breedveld et al., 2005; Au et al., 2014).

5.1. Targeting metabolism of CML cell line with a point mutation in BCR-ABL1

Using 2-DE analysis, proteome profiles of CML-T1 and CML-$T1^{IR}$ cells were compared to identify their metabolic vulnerabilities to selectively affect viability of CML-$T1^{IR}$ cells harboring a point mutation in the BCR-ABL1 gene, presumably the main cause of resistance to imatinib in this model. Eight differentially expressed proteins including strongly upregulated multifunctional protein NHERF1 in CML-$T1^{IR}$ cells were identified. We suggest that overexpression of NHERF1 adapts the metabolism of CML-$T1^{IR}$ cells by shifting cytosolic pH, altering cytosolic calcium levels, and modulating the WNT signaling pathway. Based on known interaction between NHERF1 and NHE3 influencing cellular pH (Donowitz et al., 2005; He and Yun, 2010) and NHERF1 regulation of activity of nonselective Ca^{2+} permeable cation channels (Tang et al., 2000), intracellular pH and Ca^{2+} concentration were examined. Intracellular (cytosolic) pH was increased in CML-$T1^{IR}$ cells compared to CML-T1 cells. On the contrary, Ca^{2+} concentration was decreased in the cytosol of CML-$T1^{IR}$ cells compared to CML-T1 cells. Previously, it was found primary CML cells exhibited decreased Ca^{2+} concentration in the cytosol (Ciarcia et al., 2010). We hypothesized that increased pH and decreased concentration of Ca^{2+} could be crucial for better survival of CML-$T1^{IR}$ cells in the presence of imatinib. Therefore, NHE3 inhibition by amiloride was examined for its potential to selectively impair the viability of CML-$T1^{IR}$ cells. Since NCX exchanger also alters pH and Ca^{2+} concentration in the cells (Condrescu et al., 2002;

Iwamoto et al., 2007), NCX inhibition by its inhibitor DCB was studied. However, none of these two inhibitors showed any specific toxic effect against CML-T1^{IR} cells and their viability remained similar to CML-T1 in corresponding concentrations of amiloride and DCB.

The altered cytosolic concentration of Ca^{2+} may change expression of certain subsets of proteins and affect signaling pathways such as WNT/Ca^{2+}/NFAT pathway (Gregory et al., 2010). Previously, it was demonstrated that WNT/Ca^{2+}/NFAT pathway is important for survival of CML cells resistant to imatinib (Gregory et al., 2010). CsA, an inhibitor of the transcription factor NFAT eliminates imatinib-resistant CML cells (Gregory et al., 2010). Accordingly to this study (Gregory et al., 2010), NFAT inhibitors (CsA and FK-506) were used in our experiments. CsA and FK-506 significantly inhibited the proliferation of CML-T1^{IR} cells. However, the observed effect appeared to be independent of the transcription factor NFAT because NFAT was strongly downregulated in CML-T1^{IR} nuclei.

Therefore, we proposed that a selective effect of CsA and FK-506 on the metabolism of CML-T1^{IR} cells is mediated through modulation of their calcium homeostasis. There is evidence that CsA and FK-506 affect Ca^{2+} homeostasis directly (Bilmen et al., 2002; Chelu et al., 2004). CsA inhibits the activity of the ER ATPase SERCA, a membrane pump responsible for direct Ca^{2+} influx into ER from the cytosol (Bilmen et al., 2002). FK-506 stimulates the activity of the ryanodine receptor (RYR), which causes release of Ca^{2+} from ER to the cytosol (Chelu et al., 2004). Direct effect of these inhibitors (CsA and FK-506) on Ca^{2+} homeostasis may explain their selective toxicity to CML-T1^{IR} cells in the absence of the transcription factor NFAT.

To further verify that the specific balance in Ca^{2+} homeostasis is crucial for the survival of CML-T1^{IR} cells, CML-T1^{IR} cells were treated by inhibitors of Ca^{2+} transport and Ca^{2+} signaling, namely thapsigargin, ionomycin, verapamil, and CAI. These modulators of cytosolic calcium levels, calcium signaling inhibitors, and calcium channel blockers showed selective toxicity to CML-T1^{IR} cells compared to CML-T1 cells. The most selective effect on CML-T1^{IR} cells was observed using thapsigargin and ionomycin. These agents cause elevation of cytosolic Ca^{2+} ions to toxic levels i.e. by depletion of Ca^{2+} ions from ER, which leads to ER stress, unfolded protein response, and apoptosis (Beeler et al., 1979; Thastrup et al., 1990; Krebs et al., 2015). FK-506 (tacrolimus) and verapamil are known inhibitors of multidrug export (Arceci et al., 1992; Mahon et al., 2003). Our results suggest that not only Ca^{2+} levels in the cytoplasm but also in ER are crucial for the survival of CML-T1^{IR} cells in imatinib. The hypothesis can be supported by our results from 2-DE proteomic analysis, where an ER-resident protein, calreticulin, was upregulated in CML-T1^{IR} cells. Calreticulin is a Ca^{2+} binding chaperone in the ER. CML-T1^{IR}

cells require increased levels of calreticulin to preserve Ca^{2+} homeostasis in ER. Thus, thapsigargin, an inhibitor of Ca^{2+} entry to ER, and ionomycin, calcium ionophore increasing intracellular Ca^{2+} concentration, showed selective toxicity to CML-T1^{IR} (Beeler et al., 1979; Thastrup et al., 1990).

In addition to the selective experimental inhibitors, thapsigargin and ionomycin, three clinically established drugs, CsA, FK-506 (tacrolimus), and verapamil possess similar toxic effects to CML-T1^{IR} cells. The observed toxic effect to CML-T1^{IR} cells can probably be caused by disruption of Ca^{2+} homeostasis between ER and the cytosol by verapamil and tacrolimus (Chelu et al., 2004; Triggle, 2006).

Ca^{2+} ions are important second messengers, which are involved in many diverse cellular processes including muscle contraction, cell migration, and growth (Berridge et al., 2000). Ca^{2+} homeostasis can also be maintained by mitochondria-ER contacts via membrane microdomains between mitochondria and ER called mitochondria-associated membranes (MAMs) (Rizzuto et al., 1998; Sassano et al., 2017). Special attention should also be paid to these tight contacts where Ca^{2+} flux could be critically affected by the drugs used in our study with detrimental effects on CML-T1^{IR} cell viability. Our nonpublished results confirmed elevated markers of ER stress upon drugs causing Ca^{2+} depletion from ER stores (not shown). Taking together, Ca^{2+} homeostasis in CML is not well elucidated and its deregulation is described in a few studies including ours (Ciarcia et al., 2010; Toman et al., 2016; Cabanas et al., 2018).

5.2. Targeting metabolism of CML cell line with *BCR-ABL1* gene amplification

The second chapter of this work is dedicated to the identification and verification of potential therapeutic targets which could be exploited for selective elimination of K562^{IR} cells resistant to imatinib. The *BCR-ABL1* gene amplification and overexpression of the constitutively active BCR-ABL kinase represents another, less common model of imatinib resistance. More powerful LFQ method for proteomic analysis of K562 and K562^{IR} cells was applied to obtain more in-depth view of adaptive changes in the metabolism of imatinib-resistant K562^{IR} cells. The LFQ proteomic analysis identified a total of 3141 proteins and provided relative quantification for 2118 proteins. Among 392 proteins that were found to be differentially expressed, we focused on significantly upregulated proteins involved in signaling pathways mediating survival and proliferation of cells. The transcription factor STAT3 was markedly upregulated in K562^{IR} cells

(4.5-fold). STAT3 has been previously associated with drug resistance in CML (Eiring et al., 2014, 2015b; Patel et al., 2021).

STAT3 is a member of the family of signal transducer and activator of transcription proteins (Darnell, 1997; Levy and Darnell, 2002). The STAT3 transcription factors can be activated by a variety of cytokines, growth factors, oncogenes, and non-receptor kinases (Herrington et al., 2000; Reddy et al., 2000; Ihle, 2001). Irrespective of the activating kinase, STAT3 is phosphorylated on the conserved residue (Tyr705) directly by the intrinsic kinase activity of the activated receptor kinase or by the tyrosine kinase receptor-associated JAK (Heinrich et al., 1998, 2003; Quesnelle et al., 2007). In CML cells, STAT3 is phosphorylated by the BCR-ABL kinase (Ilaria and Van Etten, 1996). Activated STAT3 also contributes to resistance to BCR-ABL inhibitors (Bewry et al., 2008; Eiring et al., 2014; Patel et al., 2021). Critical role of STAT3 in drug resistance in CML was demonstrated by its inhibition using selective inhibitors BP-5-087 and LLL12 in combination with imatinib (Eiring et al., 2015b; Patel et al., 2021). This combined treatment led to reduced survival of drug-resistant CML cells including resistant primary CML cells (Eiring et al., 2015b; Patel et al., 2021). Using specific antibodies, it was possible in our study to verify upregulated expression of STAT3 and its phosphorylated forms STAT3 (Tyr705) and STAT3 (Ser727) in lysates and nuclei from $K562^{IR}$ cells. We further confirmed the differential expression of STAT3 by RT-PCR using specific primers. *STAT3* mRNA expression was increased almost 2-fold in $K562^{IR}$ cells compared to K562 cells. Among other differentially expressed proteins identified by LFQ in $K562^{IR}$ cells, the cytoskeletal protein spectrin beta, non-erythrocytic1 (SPTBN1), one of the negative transcriptional regulators of STAT3 (Lin et al., 2014), was found to be downregulated. Application of specific STAT3 inhibitor Stattic results in selective impairment of $K562^{IR}$ cell viability in the presence of imatinib. Our results clearly indicated selective toxicity of Stattic against $K562^{IR}$ cells and therefore confirmed the previous observations that inhibition of STAT3 by various inhibitors reduced survival of resistant CML cell lines and primary CML cells (Eiring et al., 2015b; Patel et al., 2021). We then focused on examining signaling pathways that could regulate STAT3 activity in $K562^{IR}$ cells and thus support their self-renewal, proliferation, and survival. One such candidate was IGF1R signaling pathway (Xie et al., 2015). IGF1R signaling is required for normal hematopoiesis as well as for leukemogenesis (Akahane et al., 1987; Hizuka et al., 1987; Kurtz et al., 1988). IGF1R signaling can be induced by BCR-ABL in CML cells and plays a supportive role in proliferation and CML cell viability (Lakshmikuttyamma et al., 2008; Shi et al., 2010). Aberrant activation of autocrine IGF1R signaling may facilitate the transformation from CP to BP (Lakshmikuttyamma et al.,

2008). IGF1 expression appeared to be directly correlated with CML progression and is increased in patients with CML-BP (Lakshmikuttyamma et al., 2008; Shi et al., 2010). IGF1R signaling is critical for survival of cells resistant to imatinib as well as to other inhibitors (Shi et al., 2010). Inhibition of IGF1R using the selective inhibitor PPP in combination with imatinib decreased the viability and induced apoptosis in various CML cell lines, BaF3 cells transfected with wild-type *BCR-ABL1*, *BCR-ABL1* carrying the mutation E255K or cross-resistant *BCR-ABL1* with the mutation T315I, as well as in primary cells collected from imatinib-resistant patients (Shi et al., 2010). Therefore, the expression of IGF1R, its activated phosphorylated form pIGF1R (Tyr1135/1136), and adapter protein insulin receptor substrate 1 (IRS-1) were evaluated in our model K562 and $K562^{IR}$ cells. No significant differences were found in the expression of total IGF1R and IRS-1 proteins between K562 and $K562^{IR}$ cells. However, *IGF1R* mRNA expression was increased 2-fold in $K562^{IR}$ compared to K562 cells. Levels of IGF1R and pIGF1R (Tyr1135/1136) did not change after treatment with PPP, but PPP induced inhibitory phosphorylation of IRS-1 adaptor protein. Some other downstream targets of IGF1R pathway such as phosphorylated form of activated AKT kinase (Ser473) appeared to be stimulated in $K562^{IR}$ cells. Treatment of $K562^{IR}$ cells with PPP resulted in the downregulation of phosphorylated AKT kinase (Ser473). Finally, selective toxicity of PPP was observed against $K562^{IR}$ in the series of cell viability assays which corresponds with other previously published data showing toxicity of PPP to imatinib-resistant primary CML cells as well as to imatinib-sensitive CML cell lines (K562, KBM-5, MEG01, and BV173) (Shi et al., 2010). However, these data did not compare the differential cytotoxicity of PPP to sensitive and resistant CML cells as we did in our study. Interestingly, PPP treatment did not show any selective toxicity to BaF3 cells transfected with *BCR-ABL1* carrying E255K or T315I mutations, when compared to BaF3 cells transfected with wild-type *BCR-ABL1* (Shi et al., 2010). The reason for this observation could be a different mechanism of imatinib resistance and metabolic adaptation in our model cell line, $K562^{IR}$, in comparison with transfected Ba/F3 cells. Our model cell line $K562^{IR}$ was found to have *BCR-ABL1* gene amplification whereas Ba/F3 cells harbor a mutation in the *BCR-ABL1* gene. Thus, selective toxicity of PPP to $K562^{IR}$ cells could be specific for our K562 cellular model. Alternatively, observed cytotoxic effect of PPP could be independent of IGF1R inhibition as was described previously (Wu et al., 2013; Waraky et al., 2014).

We also speculated whether dual inhibition of aforementioned signaling nods with suggested prosurvival effects on the viability of $K562^{IR}$ cells in the presence of imatinib – STAT3 and IGF1R/IRS-1 – could induce stronger toxic effects in $K562^{IR}$ cells and we explored this

combination to evaluate its better therapeutic significance. Recent studies in melanoma, colorectal cancer and $JAK2^{V617F}$- positive myeloproliferative neoplasms showed promising results obtained with a novel inhibitor NT157. This compound is targeting both the adaptor protein IRS-1 and STAT3 (Flashner-Abramson et al., 2016; Sanchez-Lopez et al., 2016; Fenerich et al., 2020). Promising results were obtained with NT157 in the treatment of BCR-ABL-positive cells. NT157 decreased the cell viability and proliferation and induced apoptosis of BCR-ABL-positive K562 cells (Scopim-Ribeiro et al., 2021). It was also shown that inhibition of IRS-1/2 by NT157 induced apoptosis of BaF3 cells transfected either with wild-type *BCR-ABL1* or mutant *BCR-ABL1* T315I (Scopim-Ribeiro et al., 2021). NT157 treatment inhibited colony formation in primary CML cells in contrast to normal hematopoietic cells (Scopim-Ribeiro et al., 2021). NT157 activity was also demonstrated in primary cells from one CML patient harboring mutant *BCR-ABL1* T315I (Scopim-Ribeiro et al., 2021). Our results from cell viability assays not only confirm these data but also indicate that NT157 was more potent against $K562^{IR}$ cells compared with K562 cells.

Recently, it was found that IGF1/IGF1R/STAT3 signaling induced expression of IFITM2 protein in gastric cancer cells (Xu et al., 2017). IFITM2 protein is a member of the IFITM protein family including at least two other members, IFITM1 and IFITM3. IFITM3 protein was found strongly enriched in exosomes derived from $K562^{IR}$ cells as identified by LFQ in this work (Hrdinova et al., 2021). Increased levels of IFITM3 protein were verified in exosomes derived from $K562^{IR}$ cells and also in $K562^{IR}$ cells by Western blot (Hrdinova et al., 2021). Using GeneCards database it was possible to predict a STAT3 binding site in IFITM3 promoter (https://www.genecards.org/cgi-bin/carddisp.pl?gene=IFITM3&keywords=ifitm3) (Stelzer et al., 2016). We hypothesized that IFITM3 gene is regulated by the STAT3 transcription factor. Using the inhibitors Stattic and NT157, it was possible to show that expression of IFITM3 protein in $K562^{IR}$ cells decreased after 24 hours of incubation with respective inhibitors. These data were further supported by PCR data showing decrease in *IFITM3* mRNA expression after treatment of $K562^{IR}$ cells with Stattic and NT157. The result suggests that IFITM3 protein and mRNA expression are at least partially regulated by the STAT3 transcription factor. Other separate part of this thesis showed that the level of IFITM3 expression in $K562^{IR}$ cells was decreased by CsH, a specific inhibitor of formyl peptide receptor (FPR1). FPR1 belongs to the class of G protein-coupled receptors, which can be stimulated by binding of formyl Met-Leu-Phe peptide. Such peptides can typically be a product of bacterial infection, or, due to evolutionary mechanisms, can be released by defective mitochondria as a damage-associated molecular patterns (DAMPs)

upon cellular stress (Grazioli and Pugin, 2018). It is known that DAMPs can stimulate chronic inflammation in malignant cells resulting in deregulated interferon response (Hernandez et al., 2016). Thus, it can be speculated whether interferon-induced IFITM3 protein upregulation in $K562^{IR}$ can also be a result of chronic inflammation induced by DAMPs released by mitochondria. Indeed, CsH is used to enhance lentivirus transduction of human hematopoietic cells, which normally express interferon-stimulated genes including IFITM3 to prevent IFITM3 antiviral function (de Paulis et al., 1996; Wu et al., 2018). Moreover, CsH selectively decreased viability of imatinib-resistant $K562^{IR}$ cells, suggesting importance of this protein not only as a surface marker of resistant cells but also for $K562^{IR}$ cell survival.

5.3. Analysis of exosomes from imatinib resistant CML cells

In the last chapter of this work, a comparative study was dedicated to analyze protein composition of exosomes released by K562 and $K562^{IR}$ cells. In our working hypothesis, exosomes released by imatinib-resistant $K562^{IR}$ can carry prosurvival signal providing phenotypical changes in recipient cells to escape apoptosis-inducing effects of imatinib. The LFQ analysis was used to obtain more detailed data on exosome protein composition. To verify our working hypothesis, $K562^{IR}$ derived exosomes were incubated with K562 cells prior to their exposure to 2 µM imatinib. The results from these repeated experiments showed that $K562^{IR}$ derived exosomes increased slightly but significantly the survival of K562 cells in the presence of 2 µM imatinib.

This supports the previously published observation made by *Min et al* (Min et al., 2018) and highlights the role of exosomes in the horizontal transfer of putative prosurvival information between cancer cells. The significance of exosome-mediated survival in the development of resistance to imatinib in CML patients remains to be elucidated. It is expected that more complex and complicated situation occurs *in vivo* in patients. Exosomes from leukemic cells circulate throughout the whole body, overcome biological barriers and take part in complex signaling networks especially in the compartment of BM, where they communicate with other cell types such as endothelial cells, macrophages, or stromal cells (Mineo et al., 2012; Taverna et al., 2012; Corrado et al., 2014; Jafarzadeh et al., 2019). It should also be mentioned that the processes of exosome release and internalization occur rather continuously *in vivo*. Furthermore, the role of exosome-mediated survival may differ among CML patients with respect to different molecular mechanisms of imatinib resistance which may affect the proliferation rate of cells, protein expression profiles, the rate of exosome production, and the resulting exosomal composition.

Therefore, data presented here may be associated uniquely with imatinib resistance caused by the *BCR-ABL1* gene overexpression in our model K562^{IR} cells.

Exosomal role in cancer progression and drug resistance can also mean that exosomes could serve as biomarkers for monitoring disease progression and development of drug resistance (Maacha et al., 2019; Steinbichler et al., 2019). The specific protein composition of K562 and K562^{IR} derived exosomes was characterized in detail to identify candidate resistance-associated markers on the surface of K562^{IR} exosomes and K562^{IR} cells. The LFQ proteomic analysis identified over 3,000 proteins in exosomes with relative quantification for 1,241 of these proteins. The presented dataset is probably the largest set of proteins identified in leukemic exosomes. A total of 35 proteins were classified as differentially abundant. Attention was paid to proteins localized or expected to be present on cell surface because such molecules could be exploited clinically as markers to monitor disease progression or drug resistance, or eventually represent potential targets for future drugs. The significantly upregulated proteins (i.e., >7-fold according to LFQ data) identified in K562^{IR} exosomes with predicted surface localization were IFITM3, CD146, and CD36. These proteins with putative diagnostic potential have been previously linked to cancer progression (Lehmann et al., 1989; Watson-Hurst and Becker, 2006; Wu and Dickerson, 2014; Ye et al., 2016; Zhang et al., 2017; Landberg et al., 2018; Liu et al., 2019).

The IFITM3 protein belongs to the interferon-induced transmembrane protein family, which plays role in antiviral defense (Bailey et al., 2014). Recently, it was demonstrated that human embryonic stem cells and human induced pluripotent stem cells have elevated levels of selected interferon-stimulated genes including IFITM3 to function as an innate antiviral protection (Wu et al., 2018). In addition, high levels of IFITM3 protein have been found in AML patients and in human cell lines derived from lung, gastric, oral, and breast tumors (Yang et al., 2013; Hu et al., 2014; Zhang et al., 2017; Gan et al., 2019; Liu et al., 2019). IFITM3 protein is involved in cancer progression (Hu et al., 2014; Zhang et al., 2017) and shows pro-proliferative and pro-migratory effects (Yang et al., 2013; Gan et al., 2019). In patients with AML and B-cell malignancies, high levels of IFITM3 expression correlates with poor prognosis (Liu et al., 2019; Lee et al., 2020).

The transmembrane glycoprotein CD146 was first described in malignant melanoma where its expression correlated with the development of metastasis and poor prognosis (Lehmann et al., 1989). Overexpression of CD146 protein has been linked to tumor progression, metastasis and angiogenesis in various types of malignancies such as melanoma, lung, ovarian and breast cancers (Watson-Hurst and Becker, 2006; Wu and Dickerson, 2014; Lei et al., 2015). CD146 also promotes drug resistance (Liang et al., 2017; Tripathi et al., 2017).

CD36 has been described as a hematopoietic marker in a subpopulation of leukemia stem cells, primary primitive (less differentiated) cells, and CML-BP cells (Ye et al., 2016; Landberg et al., 2018). It is thus possible that increased expression of CD36 protein could potentially mark a fraction of $K562^{IR}$ cells which are less differentiated.

Elevated expression of these three putative markers in $K562^{IR}$ derived exosomes and $K562^{IR}$ cells were confirmed by Western blot using specific antibodies. Flow cytometric analysis of live cells was further performed to confirm a higher abundance of IFITM3, CD146, and CD36 on the cell surface of $K562^{IR}$ cells so they could represent diagnostically accessible markers of resistance to imatinib. It was demonstrated that CD146 could serve as a valid positive marker of $K562^{IR}$ cells. Thus, CD146 is an exploitable molecule for distinguishing $K562^{IR}$ populations by flow cytometry. Expression of IFITM3 and CD36 proteins on the cell surface exhibited lower differences between the K562 and $K562^{IR}$ cells and thus are less suitable for distinguishing between K562 and $K562^{IR}$ cells.

In concordance with this, CD146 has already been described as promising target in CD146-positive cancers, such as melanoma, and its therapeutic potential is evaluated using anti-CD146 antibodies (Nollet et al., 2017; Stalin et al., 2017). Similarly to CD146 inhibition, studies with knockdown of IFITM3 protein in breast cancer cell lines and in oral squamous cell carcinoma supported its potential for future targeted therapeutic strategies (Yang et al., 2013; Gan et al., 2019). At least hypothetically, CD146 and IFITM3 proteins (expressed specifically on the surface of $K562^{IR}$ cells), could serve as markers or molecular targets for therapy of imatinib-resistant CML.

The exact mechanism by which incubation of $K562^{IR}$ derived exosomes with K562 cells enhances their survival in imatinib is not explained in our study. However, some mechanisms may be proposed. It could be hypothesized that exosomes carry BCR-ABL kinase into K562 cells and alter BCR-ABL kinase/imatinib ratio in the K562 cells leading to their better survival.

Alternatively, $K562^{IR}$ exosomes could carry additional molecules responsible for better survival of recipient cells such as DNAs, RNAs, and proteins. Previously, it was shown that miR-365 present in $K562^{IR}$ exosomes is partly responsible for chemoresistance (Min et al., 2018). However, the beneficial effect of miR-365 alone was weaker compared to the exosomes derived from imatinib-resistant cells (Min et al., 2018). These findings emphasize that other molecules mediate this effect. It could be hypothesized that IFITM3 and CD146 could be another candidate molecules contributing to enhanced survival e.g. through regulation and activation of STAT3

and AKT signaling pathways (Johnston and Grandis, 2011; Wang et al., 2020). IFITM3 regulates PI3K signaling in B cells and knockdown of IFITM3 suppressed STAT3 phosphorylation *in vitro* (Lee et al., 2020; Wang et al., 2020). CD146 mediates chemoresistance through activation of the AKT kinase in breast cancer and in small cell lung cancer (Liang et al., 2017; Tripathi et al., 2017). However, it remains to be elucidated whether IFITM3 and/or CD146 proteins carried by exosomes from $K562^{IR}$ cells can modulate the aforementioned molecules in target cells to promote their survival in the presence of imatinib.

The proteomic studies performed on imatinib-resistant CML cells (CML-T1 and K562) provide a proof of concept for basic research in a future model of personalized CML therapy including TKI-resistant causes. Moreover, this concept is applicable in the research of other drug-resistant diseases. However, there are few major drawbacks complicating the application of this personalized concept of CML therapy. CML cell lines (CML-T1 and K562) represent a clonal cellular model which could differ from CML cells proliferating in a variable and complex environment *in vivo* in patient´s body as it was shown in a recent study (Li et al., 2021). For example, it remains to be experimentally verified whether altered Ca^{2+} homeostasis which we found to be important for CML-T1 cells survival, could also be detected in primary CML cells isolated from imatinib-resistant patients. Similarly, a study detecting the surface proteins IFITM3 and CD146 (identified as markers in $K562^{IR}$ cells) could also be performed using CML primary cells or plasma obtained from imatinib-resistant patients. Unfortunately, acquisition of primary CML cells from patients with imatinib resistance is complicated by different factors. Firstly, it is due to quick replacement of TKI drugs in CML therapy without the bone marrow sampling when the patients do not respond (Hochhaus et al., 2020). Secondly, verification of expression of putative protein markers such as IFITM3 and CD146 or measurement of altered Ca^{2+} homeostasis may be limited by the amount of isolated Ph^{+} cells and/or by challenges in techniques of primary cell expansion. Thirdly, patients may differ in mechanisms of imatinib resistance. In addition, the results presented here may be specific for mechanisms of imatinib resistance described in our model cell lines, i.e. *BCR-ABL1* gene mutation or amplification. Therefore, a prospective study should include the expansion of leukemia cells isolated from patients with a different mechanism of imatinib resistance. Validation of IFITM3 and CD146 surface marker expression *in vivo* would be necessary prior to propose IFITM3 and CD146 as novel markers of imatinib resistance or as potential therapeutic targets in imatinib-resistant CML.

6. Conclusions

- Proteomic analysis of CML cells sensitive and resistant to imatinib imatinib revealed potential therapeutic targets in imatinib-resistant cells. Proteomic analysis of exosomes derived from imatinib resistant cells identified membrane surface markers which reflect their expression on the surface of imatinib resistant cells ant thus could serve as clinically relevant diagnostic markers associated with imatinib resistance.

- Proteomic analysis of CML-T1^{IR} cells revealed upregulated NHERF1 protein and its consequent effects on cellular pH and Ca^{2+} homeostasis were evaluated.
- Increased pH and decreased Ca^{2+} measured in the cytosol of CML-T1^{IR} cells has a profound therapeutic potential.
- The modulators of intracellular calcium, namely thapsigargin, ionomycin, verapamil, CAI, CsA, and FK-506 were significantly more potent in inhibition of proliferation of CML-T1^{IR} compared to the sensitive parental cell line.

- Proteomic analysis of K562^{IR} cells revealed upregulated STAT3 transcription factor which was previously described as important for drug-resistant cells.
- STAT3 inhibition by Stattic or inhibition of IGF1R signaling by PPP, as well as dual targeting IRS-1/2 and STAT3 by NT157 led to selective elimination of imatinib-resistant K562^{IR} cells.
- The expression of IFITM3 protein is at least partly regulated by the transcription factor STAT3 as was demonstrated by reduced expression of IFITM3 after treatment of K562^{IR} cells with Stattic or NT157.
- IFITM3 expression in K562^{IR} cells is decreased by CsH in K562^{IR} cells and the viability of K562^{IR} cells is reduced by CsH.

- Our proteomic analysis of exosomes derived from K562^{IR} cells identified upregulation of IFITM3, CD146, and CD36 proteins.
- Upregulation of IFITM3 and CD146 proteins in K562^{IR} cells was confirmed by flow cytometry and these proteins could be used as markers of imatinib resistance in K562^{IR} cells in our studies.

7. Publications

This Ph.D. thesis consists of 2 publications and the unpublished results from a manuscript in preparation, chronologically ordered below. Individual papers are attached at the end of the thesis.

1) Proteomic analysis of imatinib-resistant CML-T1 cells reveals calcium homeostasis as a potential therapeutic target

Toman O, **Kabickova T**, Vit O, Fiser R, Polakova KM, Zach J, Linhartova J, Vyoral D, Petrak J. Oncol Rep. 2016 Sep;36(3):1258-68. doi: 10.3892/or.2016.4945. Epub 2016 Jul 18.PMID: 27430982. IF 3.906

- I am listed as a co-author. I performed Western blots and cell viability assays. I revised the manuscript.

2) Exosomes released by imatinib-resistant K562 cells contain specific membrane markers, IFITM3, CD146 and CD36 and increase the survival of imatinib-sensitive cells in the presence of imatinib

Hrdinova T, Toman O, Dresler J, Klimentova J, Salovska B, Pajer P, Bartos O, Polivkova V, Linhartova J, Machova Polakova K, Kabickova H, Brodska B, Krijt M, Zivny J, Vyoral D, Petrak J. Int J Oncol. 2021 Feb;58(2):238-250. doi: 10.3892/ijo.2020.5163. Epub 2020 Dec 23.PMID: 33491750. IF 5.650

- I am listed as a first author. I designed, performed, and analyzed the majority of the experiments. I wrote and revised the manuscript.

3) Unpublished results from manuscript in preparation

- I designed, performed, and analyzed the majority of the experiments.

Other publication not included in my thesis:

Circulating Small Noncoding RNAs Have Specific Expression Patterns in Plasma and Extracellular Vesicles in Myelodysplastic Syndromes and Are Predictive of Patient Outcome.

Hrustincova A, Krejcik Z, Kundrat D, Szikszai K, Belickova M, Pecherkova P, Klema J, Vesela J, Hruba M, Cermak J, **Hrdinova T**, Krijt M, Valka J, Jonasova A, Merkerova MD. Cells. 2020 Mar 26;9(4):794. doi: 10.3390/cells9040794.PMID: 32224889. IF 6.600

Detection and quantitation of iron in ferritin, transferrin and labile iron pool (LIP) in cardiomyocytes using 55Fe and storage phosphorimaging

Krijt M, Jirkovska A, **Kabickova T**, Melenovsky V, Petrak J, Vyoral D. Biochim Biophys Acta Gen Subj. 2018 Dec;1862(12):2895-2901. doi: 10.1016/j.bbagen.2018.09.005. Epub 2018 Sep 10.PMID: 30279145. IF 2.590

8. Availability of data and materials

The supplementary material: Table SI, SII, SIII generated and analyzed during the current study have been deposited to:

https://biocev.lf1.cuni.cz/disertacni-prace-terezy-hrdinove

Table SI_K562 cells_List of relatively quantified proteins

Table SII_K562 cells_List of differentially expressed proteins

Table SIII_K562 exosomes_List of relatively quantified proteins

9. References

Abd Elmageed, Z. Y., Yang, Y., Thomas, R., Ranjan, M., Mondal, D., Moroz, K., et al. (2014). Neoplastic reprogramming of patient-derived adipose stem cells by prostate cancer cell-associated exosomes. *Stem Cells* 32, 983–997. doi:10.1002/stem.1619.

Abelson, H. T., and Rabstein, L. S. (1970). Lymphosarcoma: virus-induced thymic-independent disease in mice. *Cancer Res.* 30, 2213–2222.

Abraham, S. A., Hopcroft, L. E. M., Carrick, E., Drotar, M. E., Dunn, K., Williamson, A. J. K., et al. (2016). Dual targeting of p53 and c-MYC selectively eliminates leukaemic stem cells. *Nature* 534, 341–346. doi:10.1038/nature18288.

Adamia, S., Pilarski, P. M., Bar-Natan, M., Stone, R. M., and Griffin, J. D. (2013). Alternative splicing in chronic myeloid leukemia (CML): a novel therapeutic target? *Curr. Cancer Drug Targets* 13, 735–748. doi:10.2174/15680096113139990083.

Adnan-Awad, S., Kim, D., Hohtari, H., Javarappa, K. K., Brandstoetter, T., Mayer, I., et al. (2021). Characterization of p190-Bcr-Abl chronic myeloid leukemia reveals specific signaling pathways and therapeutic targets. *Leukemia* 35, 1964–1975. doi:10.1038/s41375-020-01082-4.

Adrián, F. J., Ding, Q., Sim, T., Velentza, A., Sloan, C., Liu, Y., et al. (2006). Allosteric inhibitors of Bcr-abl-dependent cell proliferation. *Nat. Chem. Biol.* 2, 95–102. doi:10.1038/nchembio760.

Akahane, K., Tojo, A., Urabe, A., and Takaku, F. (1987). Pure erythropoietic colony and burst formations in serum-free culture and their enhancement by insulin-like growth factor I. *Exp. Hematol.* 15, 797–802.

Akram, A. M., Iqbal, Z., Akhtar, T., Khalid, A. M., Sabar, M. F., Qazi, M. H., et al. (2017). Presence of novel compound BCR-ABL mutations in late chronic and advanced phase imatinib sensitive CML patients indicates their possible role in CML progression. *Cancer Biol. Ther.* 18, 214–221. doi:10.1080/15384047.2017.1294289.

Al-Achkar, W., Wafa, A., Moassass, F., Klein, E., and Liehr, T. (2013). Multiple copies of BCR-ABL fusion gene on two isodicentric Philadelphia chromosomes in an imatinib mesylate-resistant chronic myeloid leukemia patient. *Oncol. Lett.* 5, 1579–1582. doi:10.3892/ol.2013.1225.

Alessandro, R., Fontana, S., Giordano, M., Corrado, C., Colomba, P., Flugy, A. M., et al. (2008). Effects of carboxyamidotriazole on in vitro models of imatinib-resistant chronic myeloid leukemia. *J. Cell. Physiol.* 215, 111–121. doi:10.1002/jcp.21290.

Amarante-Mendes, G. P., Jascur, T., Nishioka, W. K., Mustelin, T., and Green, D. R. (1997). Bcr - Abl-mediated resistance to apoptosis is independent of PI 3-kinase activity. *Cell Death Differ.* 4, 548–554. doi:10.1038/sj.cdd.4400276.

Amarante-Mendes, G. P., Naekyung Kim, C., Liu, L., Huang, Y., Perkins, C. L., Green, D. R., et al. (1998). Bcr-Abl exerts its antiapoptotic effect against diverse apoptotic stimuli through blockage of mitochondrial release of cytochrome C and activation of caspase-3.

Blood 91, 1700–1705.

Amini-Bavil-Olyaee, S., Choi, Y. J., Lee, J. H., Shi, M., Huang, I.-C., Farzan, M., et al. (2013). The antiviral effector IFITM3 disrupts intracellular cholesterol homeostasis to block viral entry. *Cell Host Microbe* 13, 452–464. doi:10.1016/j.chom.2013.03.006.

An, S. M., Ding, Q. P., and Li, L. (2013). Stem cell signaling as a target for novel drug discovery: recent progress in the WNT and Hedgehog pathways. *Acta Pharmacol. Sin.* 34, 777–783. doi:10.1038/aps.2013.64.

Apperley, J. F., Cortes, J. E., Kim, D.-W., Roy, L., Roboz, G. J., Rosti, G., et al. (2009). Dasatinib in the treatment of chronic myeloid leukemia in accelerated phase after imatinib failure: the START a trial. *J. Clin. Oncol. Off. J. Am. Soc. Clin. Oncol.* 27, 3472–3479. doi:10.1200/JCO.2007.14.3339.

Arceci, R. J., Stieglitz, K., and Bierer, B. E. (1992). Immunosuppressants FK506 and rapamycin function as reversal agents of the multidrug resistance phenotype. *Blood* 80, 1528–1536.

Ardura, J. A., and Friedman, P. A. (2011). Regulation of G protein-coupled receptor function by Na+/H+ exchange regulatory factors. *Pharmacol. Rev.* 63, 882–900. doi:10.1124/pr.110.004176.

Au, A., Baba, A. A., Azlan, H., Norsa'adah, B., and Ankathil, R. (2014). Clinical impact of ABCC1 and ABCC2 genotypes and haplotypes in mediating imatinib resistance among chronic myeloid leukaemia patients. *J. Clin. Pharm. Ther.* 39, 685–690. doi:10.1111/jcpt.12197.

Babst, M., Katzmann, D. J., Snyder, W. B., Wendland, B., and Emr, S. D. (2002). Endosome-associated complex, ESCRT-II, recruits transport machinery for protein sorting at the multivesicular body. *Dev. Cell* 3, 283–289. doi:10.1016/s1534-5807(02)00219-8.

Babst, M., Wendland, B., Estepa, E. J., and Emr, S. D. (1998). The Vps4p AAA ATPase regulates membrane association of a Vps protein complex required for normal endosome function. *EMBO J.* 17, 2982–2993. doi:10.1093/emboj/17.11.2982.

Bache, K. G., Brech, A., Mehlum, A., and Stenmark, H. (2003). Hrs regulates multivesicular body formation via ESCRT recruitment to endosomes. *J. Cell Biol.* 162, 435–442. doi:10.1083/jcb.200302131.

Bailey, C. C., Zhong, G., Huang, I.-C., and Farzan, M. (2014). IFITM-Family Proteins: The Cell's First Line of Antiviral Defense. *Annu. Rev. Virol.* 1, 261–283. doi:10.1146/annurev-virology-031413-085537.

Barnes, D. J., Palaiologou, D., Panousopoulou, E., Schultheis, B., Yong, A. S. M., Wong, A., et al. (2005). Bcr-Abl expression levels determine the rate of development of resistance to imatinib mesylate in chronic myeloid leukemia. *Cancer Res.* 65, 8912–8919. doi:10.1158/0008-5472.CAN-05-0076.

Barrès, C., Blanc, L., Bette-Bobillo, P., André, S., Mamoun, R., Gabius, H.-J., et al. (2010). Galectin-5 is bound onto the surface of rat reticulocyte exosomes and modulates vesicle uptake by macrophages. *Blood* 115, 696–705. doi:10.1182/blood-2009-07-231449.

Bartram, C. R., de Klein, A., Hagemeijer, A., van Agthoven, T., Geurts van Kessel, A., Bootsma, D., et al. (1983). Translocation of c-ab1 oncogene correlates with the presence of a Philadelphia chromosome in chronic myelocytic leukaemia. *Nature* 306, 277–280. doi:10.1038/306277a0.

Bazzoni, G., Carlesso, N., Griffin, J. D., and Hemler, M. E. (1996). Bcr/Abl expression stimulates integrin function in hematopoietic cell lines. *J. Clin. Invest.* 98, 521–528. doi:10.1172/JCI118820.

Becker, A., Thakur, B. K., Weiss, J. M., Kim, H. S., Peinado, H., and Lyden, D. (2016). Extracellular Vesicles in Cancer: Cell-to-Cell Mediators of Metastasis. *Cancer Cell* 30, 836–848. doi:10.1016/j.ccell.2016.10.009.

Beeler, T. J., Jona, I., and Martonosi, A. (1979). The effect of ionomycin on calcium fluxes in sarcoplasmic reticulum vesicles and liposomes. *J. Biol. Chem.* 254, 6229–6231.

Behrmann, L., Wellbrock, J., and Fiedler, W. (2020). The bone marrow stromal niche: a therapeutic target of hematological myeloid malignancies. *Expert Opin. Ther. Targets* 24, 451–462. doi:10.1080/14728222.2020.1744850.

Bellavia, D., Raimondo, S., Calabrese, G., Forte, S., Cristaldi, M., Patinella, A., et al. (2017). Interleukin 3- receptor targeted exosomes inhibit in vitro and in vivo Chronic Myelogenous Leukemia cell growth. *Theranostics* 7, 1333–1345. doi:10.7150/thno.17092.

Bellodi, C., Lidonnici, M. R., Hamilton, A., Helgason, G. V., Soliera, A. R., Ronchetti, M., et al. (2009). Targeting autophagy potentiates tyrosine kinase inhibitor-induced cell death in Philadelphia chromosome-positive cells, including primary CML stem cells. *J. Clin. Invest.* 119, 1109–1123. doi:10.1172/JCI35660.

Ben-Neriah, Y., Bernards, A., Paskind, M., Daley, G. Q., and Baltimore, D. (1986a). Alternative 5' exons in c-abl mRNA. *Cell* 44, 577–586. doi:10.1016/0092-8674(86)90267-9.

Ben-Neriah, Y., Daley, G. Q., Mes-Masson, A. M., Witte, O. N., and Baltimore, D. (1986b). The chronic myelogenous leukemia-specific P210 protein is the product of the bcr/abl hybrid gene. *Science* 233, 212–214. doi:10.1126/science.3460176.

Bernardi, S., Foroni, C., Zanaglio, C., Re, F., Polverelli, N., Turra, A., et al. (2019). Feasibility of tumor-derived exosome enrichment in the onco-hematology leukemic model of chronic myeloid leukemia. *Int. J. Mol. Med.* 44, 2133–2144. doi:10.3892/ijmm.2019.4372.

Berridge, M. J., Lipp, P., and Bootman, M. D. (2000). The versatility and universality of calcium signalling. *Nat. Rev. Mol. Cell Biol.* 1, 11–21. doi:10.1038/35036035.

Bewry, N. N., Nair, R. R., Emmons, M. F., Boulware, D., Pinilla-Ibarz, J., and Hazlehurst, L. A. (2008). Stat3 contributes to resistance toward BCR-ABL inhibitors in a bone marrow microenvironment model of drug resistance. *Mol. Cancer Ther.* 7, 3169–3175. doi:10.1158/1535-7163.MCT-08-0314.

Bie, C., Chen, Y., Tang, H., Li, Q., Zhong, L., Peng, X., et al. (2021). Insulin-Like Growth Factor 1 Receptor Drives Hepatocellular Carcinoma Growth and Invasion by Activating Stat3-Midkine-Stat3 Loop. *Dig. Dis. Sci.* doi:10.1007/s10620-021-06862-1.

Biernaux, C., Loos, M., Sels, A., Huez, G., and Stryckmans, P. (1995). Detection of major bcr-abl gene expression at a very low level in blood cells of some healthy individuals. *Blood* 86, 3118–3122.

Bilmen, J. G., Wootton, L. L., and Michelangeli, F. (2002). The inhibition of the sarcoplasmic/endoplasmic reticulum Ca2+-ATPase by macrocyclic lactones and cyclosporin A. *Biochem. J.* 366, 255–263. doi:10.1042/BJ20020431.

Bocchia, M., Gentili, S., Abruzzese, E., Fanelli, A., Iuliano, F., Tabilio, A., et al. (2005). Effect of a p210 multipeptide vaccine associated with imatinib or interferon in patients with chronic myeloid leukaemia and persistent residual disease: a multicentre observational trial. *Lancet (London, England)* 365, 657–662. doi:10.1016/S0140-6736(05)17945-8.

Bocchia, M., Sicuranza, A., Abruzzese, E., Iurlo, A., Sirianni, S., Gozzini, A., et al. (2018). Residual Peripheral Blood CD26(+) Leukemic Stem Cells in Chronic Myeloid Leukemia Patients During TKI Therapy and During Treatment-Free Remission. *Front. Oncol.* 8, 194. doi:10.3389/fonc.2018.00194.

Bonifazi, F., de Vivo, A., Rosti, G., Guilhot, F., Guilhot, J., Trabacchi, E., et al. (2001). Chronic myeloid leukemia and interferon-alpha: a study of complete cytogenetic responders. *Blood* 98, 3074–3081. doi:10.1182/blood.v98.10.3074.

Bonnet, D., and Dick, J. E. (1997). Human acute myeloid leukemia is organized as a hierarchy that originates from a primitive hematopoietic cell. *Nat. Med.* 3, 730–737. doi:10.1038/nm0797-730.

Bosch, I., and Croop, J. (1996). P-glycoprotein multidrug resistance and cancer. *Biochim. Biophys. Acta* 1288, F37-54. doi:10.1016/0304-419x(96)00022-4.

Boschelli, D. H., Ye, F., Wang, Y. D., Dutia, M., Johnson, S. L., Wu, B., et al. (2001). Optimization of 4-phenylamino-3-quinolinecarbonitriles as potent inhibitors of Src kinase activity. *J. Med. Chem.* 44, 3965–3977. doi:10.1021/jm0102250.

Bower, H., Björkholm, M., Dickman, P. W., Höglund, M., Lambert, P. C., and Andersson, T. M.-L. (2016). Life Expectancy of Patients With Chronic Myeloid Leukemia Approaches the Life Expectancy of the General Population. *J. Clin. Oncol. Off. J. Am. Soc. Clin. Oncol.* 34, 2851–2857. doi:10.1200/JCO.2015.66.2866.

Bowers, M., Zhang, B., Ho, Y., Agarwal, P., Chen, C.-C., and Bhatia, R. (2015). Osteoblast ablation reduces normal long-term hematopoietic stem cell self-renewal but accelerates leukemia development. *Blood* 125, 2678–2688. doi:10.1182/blood-2014-06-582924.

Branford, S., Rudzki, Z., Walsh, S., Grigg, A., Arthur, C., Taylor, K., et al. (2002). High frequency of point mutations clustered within the adenosine triphosphate-binding region of BCR/ABL in patients with chronic myeloid leukemia or Ph-positive acute lymphoblastic leukemia who develop imatinib (STI571) resistance. *Blood* 99, 3472–3475. doi:10.1182/blood.v99.9.3472.

Branford, S., Rudzki, Z., Walsh, S., Parkinson, I., Grigg, A., Szer, J., et al. (2003). Detection of BCR-ABL mutations in patients with CML treated with imatinib is virtually always accompanied by clinical resistance, and mutations in the ATP phosphate-binding loop (P-loop) are associated with a poor prognosis. *Blood* 102, 276–283. doi:10.1182/blood-2002-

09-2896.

Brasher, B. B., and Van Etten, R. A. (2000). c-Abl has high intrinsic tyrosine kinase activity that is stimulated by mutation of the Src homology 3 domain and by autophosphorylation at two distinct regulatory tyrosines. *J. Biol. Chem.* 275, 35631–35637. doi:10.1074/jbc.M005401200.

Breedveld, P., Pluim, D., Cipriani, G., Wielinga, P., van Tellingen, O., Schinkel, A. H., et al. (2005). The effect of Bcrp1 (Abcg2) on the in vivo pharmacokinetics and brain penetration of imatinib mesylate (Gleevec): implications for the use of breast cancer resistance protein and P-glycoprotein inhibitors to enable the brain penetration of imatinib in pa. *Cancer Res.* 65, 2577–2582. doi:10.1158/0008-5472.CAN-04-2416.

Brümmendorf, T. H., Cortes, J. E., de Souza, C. A., Guilhot, F., Duvillié, L., Pavlov, D., et al. (2015). Bosutinib versus imatinib in newly diagnosed chronic-phase chronic myeloid leukaemia: results from the 24-month follow-up of the BELA trial. *Br. J. Haematol.* 168, 69–81. doi:10.1111/bjh.13108.

Buchdunger, E., Cioffi, C. L., Law, N., Stover, D., Ohno-Jones, S., Druker, B. J., et al. (2000). Abl protein-tyrosine kinase inhibitor STI571 inhibits in vitro signal transduction mediated by c-kit and platelet-derived growth factor receptors. *J. Pharmacol. Exp. Ther.* 295, 139–145.

Buchdunger, E., Zimmermann, J., Mett, H., Meyer, T., Müller, M., Druker, B. J., et al. (1996). Inhibition of the Abl protein-tyrosine kinase in vitro and in vivo by a 2-phenylaminopyrimidine derivative. *Cancer Res.* 56, 100–104.

Burchert, A., Wang, Y., Cai, D., von Bubnoff, N., Paschka, P., Müller-Brüsselbach, S., et al. (2005). Compensatory PI3-kinase/Akt/mTor activation regulates imatinib resistance development. *Leukemia* 19, 1774–1782. doi:10.1038/sj.leu.2403898.

Buschow, S. I., Nolte-'t Hoen, E. N. M., van Niel, G., Pols, M. S., ten Broeke, T., Lauwen, M., et al. (2009). MHC II in dendritic cells is targeted to lysosomes or T cell-induced exosomes via distinct multivesicular body pathways. *Traffic* 10, 1528–1542. doi:10.1111/j.1600-0854.2009.00963.x.

Cabanas, H., Harnois, T., Magaud, C., Cousin, L., Constantin, B., Bourmeyster, N., et al. (2018). Deregulation of calcium homeostasis in Bcr-Abl-dependent chronic myeloid leukemia. *Oncotarget* 9, 26309–26327. doi:10.18632/oncotarget.25241.

Cai, J., Han, Y., Ren, H., Chen, C., He, D., Zhou, L., et al. (2013). Extracellular vesicle-mediated transfer of donor genomic DNA to recipient cells is a novel mechanism for genetic influence between cells. *J. Mol. Cell Biol.* 5, 227–238. doi:10.1093/jmcb/mjt011.

Cai, J., Wu, G., Tan, X., Han, Y., Chen, C., Li, C., et al. (2014). Transferred BCR/ABL DNA from K562 extracellular vesicles causes chronic myeloid leukemia in immunodeficient mice. *PLoS One* 9, e105200. doi:10.1371/journal.pone.0105200.

Calvi, L. M., Adams, G. B., Weibrecht, K. W., Weber, J. M., Olson, D. P., Knight, M. C., et al. (2003). Osteoblastic cells regulate the haematopoietic stem cell niche. *Nature* 425, 841–846. doi:10.1038/nature02040.

Campbell, L. J., Patsouris, C., Rayeroux, K. C., Somana, K., Januszewicz, E. H., and Szer, J. (2002). BCR/ABL amplification in chronic myelocytic leukemia blast crisis following imatinib mesylate administration. *Cancer Genet. Cytogenet.* 139, 30–33. doi:10.1016/s0165-4608(02)00615-5.

Canitrot, Y., Lahmy, S., Buquen, J. J., Canitrot, D., and Lautier, D. (1996). Functional study of multidrug resistance with fluorescent dyes. Limits of the assay for low levels of resistance and application in clinical samples. *Cancer Lett.* 106, 59–68. doi:10.1016/0304-3835(96)04301-7.

Canitrot, Y., Lautier, D., Laurent, G., Fréchet, M., Ahmed, A., Turhan, A. G., et al. (1999). Mutator phenotype of BCR--ABL transfected Ba/F3 cell lines and its association with enhanced expression of DNA polymerase beta. *Oncogene* 18, 2676–2680. doi:10.1038/sj.onc.1202619.

Cao, Y. (2019). Adipocyte and lipid metabolism in cancer drug resistance. *J. Clin. Invest.* 129, 3006–3017. doi:10.1172/JCI127201.

Capdeville, R., Buchdunger, E., Zimmermann, J., and Matter, A. (2002). Glivec (STI571, imatinib), a rationally developed, targeted anticancer drug. *Nat. Rev. Drug Discov.* 1, 493–502. doi:10.1038/nrd839.

Carlesso, N., Frank, D. A., and Griffin, J. D. (1996). Tyrosyl phosphorylation and DNA binding activity of signal transducers and activators of transcription (STAT) proteins in hematopoietic cell lines transformed by Bcr/Abl. *J. Exp. Med.* 183, 811–820. doi:10.1084/jem.183.3.811.

Carpenter, R. L., and Lo, H.-W. (2014). STAT3 Target Genes Relevant to Human Cancers. *Cancers (Basel).* 6, 897–925. doi:10.3390/cancers6020897.

Carroll, M., Ohno-Jones, S., Tamura, S., Buchdunger, E., Zimmermann, J., Lydon, N. B., et al. (1997). CGP 57148, a tyrosine kinase inhibitor, inhibits the growth of cells expressing BCR-ABL, TEL-ABL, and TEL-PDGFR fusion proteins. *Blood* 90, 4947–4952.

Chandran, R. K., Geetha, N., Sakthivel, K. M., Aswathy, C. G., Gopinath, P., Raj, T. V. A., et al. (2019). Genomic amplification of BCR-ABL1 fusion gene and its impact on the disease progression mechanism in patients with chronic myelogenous leukemia. *Gene* 686, 85–91. doi:10.1016/j.gene.2018.11.005.

Chawade, A., Alexandersson, E., and Levander, F. (2014). Normalyzer: a tool for rapid evaluation of normalization methods for omics data sets. *J. Proteome Res.* 13, 3114–3120. doi:10.1021/pr401264n.

Chelu, M. G., Danila, C. I., Gilman, C. P., and Hamilton, S. L. (2004). Regulation of ryanodine receptors by FK506 binding proteins. *Trends Cardiovasc. Med.* 14, 227–234. doi:10.1016/j.tcm.2004.06.003.

Chen, W., Liu, X., Lv, M., Chen, L., Zhao, J., Zhong, S., et al. (2014). Exosomes from drug-resistant breast cancer cells transmit chemoresistance by a horizontal transfer of microRNAs. *PLoS One* 9, e95240. doi:10.1371/journal.pone.0095240.

Chu, S., Holtz, M., Gupta, M., and Bhatia, R. (2004). BCR/ABL kinase inhibition by imatinib

mesylate enhances MAP kinase activity in chronic myelogenous leukemia CD34+ cells. *Blood* 103, 3167–3174. doi:10.1182/blood-2003-04-1271.

Chuang, T. H., Xu, X., Kaartinen, V., Heisterkamp, N., Groffen, J., and Bokoch, G. M. (1995). Abr and Bcr are multifunctional regulators of the Rho GTP-binding protein family. *Proc. Natl. Acad. Sci. U. S. A.* 92, 10282–10286. doi:10.1073/pnas.92.22.10282.

Ciarcia, R., d'Angelo, D., Pacilio, C., Pagnini, D., Galdiero, M., Fiorito, F., et al. (2010). Dysregulated calcium homeostasis and oxidative stress in chronic myeloid leukemia (CML) cells. *J. Cell. Physiol.* 224, 443–453. doi:10.1002/jcp.22140.

Cilloni, D., and Saglio, G. (2012). Molecular pathways: BCR-ABL. *Clin. cancer Res. an Off. J. Am. Assoc. Cancer Res.* 18, 930–937. doi:10.1158/1078-0432.CCR-10-1613.

Clark, R. E., Dodi, I. A., Hill, S. C., Lill, J. R., Aubert, G., Macintyre, A. R., et al. (2001). Direct evidence that leukemic cells present HLA-associated immunogenic peptides derived from the BCR-ABL b3a2 fusion protein. *Blood* 98, 2887–2893. doi:10.1182/blood.v98.10.2887.

Colmone, A., Amorim, M., Pontier, A. L., Wang, S., Jablonski, E., and Sipkins, D. A. (2008). Leukemic cells create bone marrow niches that disrupt the behavior of normal hematopoietic progenitor cells. *Science* 322, 1861–1865. doi:10.1126/science.1164390.

Coluccia, A. M. L., Vacca, A., Duñach, M., Mologni, L., Redaelli, S., Bustos, V. H., et al. (2007). Bcr-Abl stabilizes beta-catenin in chronic myeloid leukemia through its tyrosine phosphorylation. *EMBO J.* 26, 1456–1466. doi:10.1038/sj.emboj.7601485.

Condrescu, M., Opuni, K., Hantash, B. M., and Reeves, J. P. (2002). Cellular regulation of sodium-calcium exchange. *Ann. N. Y. Acad. Sci.* 976, 214–223. doi:10.1111/j.1749-6632.2002.tb04744.x.

Corbin, A. S., Agarwal, A., Loriaux, M., Cortes, J., Deininger, M. W., and Druker, B. J. (2011). Human chronic myeloid leukemia stem cells are insensitive to imatinib despite inhibition of BCR-ABL activity. *J. Clin. Invest.* 121, 396–409. doi:10.1172/JCI35721.

Corbin, A. S., Buchdunger, E., Pascal, F., and Druker, B. J. (2002). Analysis of the structural basis of specificity of inhibition of the Abl kinase by STI571. *J. Biol. Chem.* 277, 32214–32219. doi:10.1074/jbc.M111525200.

Corrado, C., Raimondo, S., Saieva, L., Flugy, A. M., De Leo, G., and Alessandro, R. (2014). Exosome-mediated crosstalk between chronic myelogenous leukemia cells and human bone marrow stromal cells triggers an interleukin 8-dependent survival of leukemia cells. *Cancer Lett.* 348, 71–76. doi:10.1016/j.canlet.2014.03.009.

Corrado, C., Saieva, L., Raimondo, S., Santoro, A., De Leo, G., and Alessandro, R. (2016). Chronic myelogenous leukaemia exosomes modulate bone marrow microenvironment through activation of epidermal growth factor receptor. *J. Cell. Mol. Med.* 20, 1829–1839. doi:10.1111/jcmm.12873.

Cortes, J. E., Gambacorti-Passerini, C., Deininger, M. W., Mauro, M. J., Chuah, C., Kim, D.-W., et al. (2018). Bosutinib Versus Imatinib for Newly Diagnosed Chronic Myeloid Leukemia: Results From the Randomized BFORE Trial. *J. Clin. Oncol. Off. J. Am. Soc.*

Clin. Oncol. 36, 231–237. doi:10.1200/JCO.2017.74.7162.

Cortes, J. E., Kantarjian, H. M., Brümmendorf, T. H., Kim, D.-W., Turkina, A. G., Shen, Z.-X., et al. (2011). Safety and efficacy of bosutinib (SKI-606) in chronic phase Philadelphia chromosome-positive chronic myeloid leukemia patients with resistance or intolerance to imatinib. *Blood* 118, 4567–4576. doi:10.1182/blood-2011-05-355594.

Cortes, J. E., Kantarjian, H., Shah, N. P., Bixby, D., Mauro, M. J., Flinn, I., et al. (2012a). Ponatinib in refractory Philadelphia chromosome-positive leukemias. *N. Engl. J. Med.* 367, 2075–2088. doi:10.1056/NEJMoa1205127.

Cortes, J. E., Kim, D.-W., Kantarjian, H. M., Brümmendorf, T. H., Dyagil, I., Griskevicius, L., et al. (2012b). Bosutinib versus imatinib in newly diagnosed chronic-phase chronic myeloid leukemia: results from the BELA trial. *J. Clin. Oncol. Off. J. Am. Soc. Clin. Oncol.* 30, 3486–3492. doi:10.1200/JCO.2011.38.7522.

Cortes, J. E., Kim, D.-W., Pinilla-Ibarz, J., le Coutre, P., Paquette, R., Chuah, C., et al. (2013). A phase 2 trial of ponatinib in Philadelphia chromosome-positive leukemias. *N. Engl. J. Med.* 369, 1783–1796. doi:10.1056/NEJMoa1306494.

Cortes, J. E., Talpaz, M., Giles, F., O'Brien, S., Rios, M. B., Shan, J., et al. (2003). Prognostic significance of cytogenetic clonal evolution in patients with chronic myelogenous leukemia on imatinib mesylate therapy. *Blood* 101, 3794–3800. doi:10.1182/blood-2002-09-2790.

Cortes, J., Kim, D.-W., Raffoux, E., Martinelli, G., Ritchie, E., Roy, L., et al. (2008). Efficacy and safety of dasatinib in imatinib-resistant or -intolerant patients with chronic myeloid leukemia in blast phase. *Leukemia* 22, 2176–2183. doi:10.1038/leu.2008.221.

Cortez, D., Reuther, G., and Pendergast, A. M. (1997). The Bcr-Abl tyrosine kinase activates mitogenic signaling pathways and stimulates G1-to-S phase transition in hematopoietic cells. *Oncogene* 15, 2333–2342. doi:10.1038/sj.onc.1201400.

Costa-Silva, B., Aiello, N. M., Ocean, A. J., Singh, S., Zhang, H., Thakur, B. K., et al. (2015). Pancreatic cancer exosomes initiate pre-metastatic niche formation in the liver. *Nat. Cell Biol.* 17, 816–826. doi:10.1038/ncb3169.

Costa Verdera, H., Gitz-Francois, J. J., Schiffelers, R. M., and Vader, P. (2017). Cellular uptake of extracellular vesicles is mediated by clathrin-independent endocytosis and macropinocytosis. *J. Control. Release* 266, 100–108. doi:10.1016/j.jconrel.2017.09.019.

Cox, J., Hein, M. Y., Luber, C. A., Paron, I., Nagaraj, N., and Mann, M. (2014). Accurate proteome-wide label-free quantification by delayed normalization and maximal peptide ratio extraction, termed MaxLFQ. *Mol. Cell. Proteomics* 13, 2513–2526. doi:10.1074/mcp.M113.031591.

Cox, J., and Mann, M. (2008). MaxQuant enables high peptide identification rates, individualized p.p.b.-range mass accuracies and proteome-wide protein quantification. *Nat. Biotechnol.* 26, 1367–1372. doi:10.1038/nbt.1511.

Cox, J., Neuhauser, N., Michalski, A., Scheltema, R. A., Olsen, J. V, and Mann, M. (2011). Andromeda: a peptide search engine integrated into the MaxQuant environment. *J.*

Proteome Res. 10, 1794–1805. doi:10.1021/pr101065j.

Daley, G. Q., and Baltimore, D. (1988). Transformation of an interleukin 3-dependent hematopoietic cell line by the chronic myelogenous leukemia-specific P210bcr/abl protein. *Proc. Natl. Acad. Sci. U. S. A.* 85, 9312–9316. doi:10.1073/pnas.85.23.9312.

Daley, G. Q., Van Etten, R. A., and Baltimore, D. (1990). Induction of chronic myelogenous leukemia in mice by the P210bcr/abl gene of the Philadelphia chromosome. *Science* 247, 824–830. doi:10.1126/science.2406902.

Darnell, J. E. J. (1997). STATs and gene regulation. *Science* 277, 1630–1635. doi:10.1126/science.277.5332.1630.

Darnell, J. E. J., Kerr, I. M., and Stark, G. R. (1994). Jak-STAT pathways and transcriptional activation in response to IFNs and other extracellular signaling proteins. *Science* 264, 1415–1421. doi:10.1126/science.8197455.

Das, S. K., Pradhan, A. K., Bhoopathi, P., Talukdar, S., Shen, X.-N., Sarkar, D., et al. (2018). The MDA-9/Syntenin/IGF1R/STAT3 Axis Directs Prostate Cancer Invasion. *Cancer Res.* 78, 2852–2863. doi:10.1158/0008-5472.CAN-17-2992.

de Groot, R. P., Raaijmakers, J. A., Lammers, J. W., Jove, R., and Koenderman, L. (1999). STAT5 activation by BCR-Abl contributes to transformation of K562 leukemia cells. *Blood* 94, 1108–1112.

de Paulis, A., Ciccarelli, A., de Crescenzo, G., Cirillo, R., Patella, V., and Marone, G. (1996). Cyclosporin H is a potent and selective competitive antagonist of human basophil activation by N-formyl-methionyl-leucyl-phenylalanine. *J. Allergy Clin. Immunol.* 98, 152–164. doi:10.1016/s0091-6749(96)70237-3.

Deininger, M. W., Goldman, J. M., Lydon, N., and Melo, J. V (1997). The tyrosine kinase inhibitor CGP57148B selectively inhibits the growth of BCR-ABL-positive cells. *Blood* 90, 3691–3698.

Deininger, M. W., Vieira, S., Mendiola, R., Schultheis, B., Goldman, J. M., and Melo, J. V (2000). BCR-ABL tyrosine kinase activity regulates the expression of multiple genes implicated in the pathogenesis of chronic myeloid leukemia. *Cancer Res.* 60, 2049–2055.

Del Conde, I., Shrimpton, C. N., Thiagarajan, P., and López, J. A. (2005). Tissue-factor-bearing microvesicles arise from lipid rafts and fuse with activated platelets to initiate coagulation. *Blood* 106, 1604–1611. doi:10.1182/blood-2004-03-1095.

del Peso, L., González-García, M., Page, C., Herrera, R., and Nuñez, G. (1997). Interleukin-3-induced phosphorylation of BAD through the protein kinase Akt. *Science* 278, 687–689. doi:10.1126/science.278.5338.687.

Dengler, R., Münstermann, U., al-Batran, S., Hausner, I., Faderl, S., Nerl, C., et al. (1995). Immunocytochemical and flow cytometric detection of proteinase 3 (myeloblastin) in normal and leukaemic myeloid cells. *Br. J. Haematol.* 89, 250–257. doi:10.1111/j.1365-2141.1995.tb03297.x.

Diekmann, D., Brill, S., Garrett, M. D., Totty, N., Hsuan, J., Monfries, C., et al. (1991). Bcr

encodes a GTPase-activating protein for p21rac. *Nature* 351, 400–402. doi:10.1038/351400a0.

Dierks, C., Beigi, R., Guo, G.-R., Zirlik, K., Stegert, M. R., Manley, P., et al. (2008). Expansion of Bcr-Abl-positive leukemic stem cells is dependent on Hedgehog pathway activation. *Cancer Cell* 14, 238–249. doi:10.1016/j.ccr.2008.08.003.

Dierov, J., Sanchez, P. V, Burke, B. A., Padilla-Nash, H., Putt, M. E., Ried, T., et al. (2009). BCR/ABL induces chromosomal instability after genotoxic stress and alters the cell death threshold. *Leukemia* 23, 279–286. doi:10.1038/leu.2008.308.

Donato, N. J., Wu, J. Y., Stapley, J., Gallick, G., Lin, H., Arlinghaus, R., et al. (2003). BCR-ABL independence and LYN kinase overexpression in chronic myelogenous leukemia cells selected for resistance to STI571. *Blood* 101, 690–698. doi:10.1182/blood.V101.2.690.

Donowitz, M., Cha, B., Zachos, N. C., Brett, C. L., Sharma, A., Tse, C. M., et al. (2005). NHERF family and NHE3 regulation. *J. Physiol.* 567, 3–11. doi:10.1113/jphysiol.2005.090399.

Druker, B. J., Talpaz, M., Resta, D. J., Peng, B., Buchdunger, E., Ford, J. M., et al. (2001). Efficacy and safety of a specific inhibitor of the BCR-ABL tyrosine kinase in chronic myeloid leukemia. *N. Engl. J. Med.* 344, 1031–1037. doi:10.1056/NEJM200104053441401.

Druker, B. J., Tamura, S., Buchdunger, E., Ohno, S., Segal, G. M., Fanning, S., et al. (1996). Effects of a selective inhibitor of the Abl tyrosine kinase on the growth of Bcr-Abl positive cells. *Nat. Med.* 2, 561–566. doi:10.1038/nm0596-561.

Duarte, D., Hawkins, E. D., Akinduro, O., Ang, H., De Filippo, K., Kong, I. Y., et al. (2018). Inhibition of Endosteal Vascular Niche Remodeling Rescues Hematopoietic Stem Cell Loss in AML. *Cell Stem Cell* 22, 64-77.e6. doi:10.1016/j.stem.2017.11.006.

Efficace, F., Baccarani, M., Breccia, M., Alimena, G., Rosti, G., Cottone, F., et al. (2011). Health-related quality of life in chronic myeloid leukemia patients receiving long-term therapy with imatinib compared with the general population. *Blood* 118, 4554–4560. doi:10.1182/blood-2011-04-347575.

Eguchi, S., Takefuji, M., Sakaguchi, T., Ishihama, S., Mori, Y., Tsuda, T., et al. (2019). Cardiomyocytes capture stem cell-derived, anti-apoptotic microRNA-214 via clathrin-mediated endocytosis in acute myocardial infarction. *J. Biol. Chem.* 294, 11665–11674. doi:10.1074/jbc.RA119.007537.

Eiring, A. M., Khorashad, J. S., Anderson, D. J., Yu, F., Redwine, H. M., Mason, C. C., et al. (2015a). β-Catenin is required for intrinsic but not extrinsic BCR-ABL1 kinase-independent resistance to tyrosine kinase inhibitors in chronic myeloid leukemia. *Leukemia* 29, 2328–2337. doi:10.1038/leu.2015.196.

Eiring, A. M., Kraft, I. L., Page, B. D., O'Hare, T., Gunning, P. T., and Deininger, M. W. (2014). STAT3 as a mediator of BCR-ABL1-independent resistance in chronic myeloid leukemia. *Leuk. Suppl.* 3, S5-6. doi:10.1038/leusup.2014.3.

Eiring, A. M., Page, B. D. G., Kraft, I. L., Mason, C. C., Vellore, N. A., Resetca, D., et al. (2015b). Combined STAT3 and BCR-ABL1 inhibition induces synthetic lethality in therapy-resistant chronic myeloid leukemia. *Leukemia* 29, 586–597. doi:10.1038/leu.2014.245.

Enfissi, A., Prigent, S., Colosetti, P., and Capiod, T. (2004). The blocking of capacitative calcium entry by 2-aminoethyl diphenylborate (2-APB) and carboxyamidotriazole (CAI) inhibits proliferation in Hep G2 and Huh-7 human hepatoma cells. *Cell Calcium* 36, 459–467. doi:10.1016/j.ceca.2004.04.004.

Escrevente, C., Keller, S., Altevogt, P., and Costa, J. (2011). Interaction and uptake of exosomes by ovarian cancer cells. *BMC Cancer* 11, 108. doi:10.1186/1471-2407-11-108.

Faden, R. R., Chalkidou, K., Appleby, J., Waters, H. R., and Leider, J. P. (2009). Expensive cancer drugs: a comparison between the United States and the United Kingdom. *Milbank Q.* 87, 789–819. doi:10.1111/j.1468-0009.2009.00579.x.

Fefer, A., Cheever, M. A., Thomas, E. D., Boyd, C., Ramberg, R., Glucksberg, H., et al. (1979). Disappearance of Ph1-positive cells in four patients with chronic granulocytic leukemia after chemotherapy, irradiation and marrow transplantation from an identical twin. *N. Engl. J. Med.* 300, 333–337. doi:10.1056/NEJM197902153000702.

Fenerich, B. A., Fernandes, J. C., Rodrigues Alves, A. P. N., Coelho-Silva, J. L., Scopim-Ribeiro, R., Scheucher, P. S., et al. (2020). NT157 has antineoplastic effects and inhibits IRS1/2 and STAT3/5 in JAK2(V617F)-positive myeloproliferative neoplasm cells. *Signal Transduct. Target. Ther.* 5, 5. doi:10.1038/s41392-019-0102-5.

Feng, D., Zhao, W.-L., Ye, Y.-Y., Bai, X.-C., Liu, R.-Q., Chang, L.-F., et al. (2010). Cellular internalization of exosomes occurs through phagocytosis. *Traffic* 11, 675–687. doi:10.1111/j.1600-0854.2010.01041.x.

Ferrao, P. T., Frost, M. J., Siah, S.-P., and Ashman, L. K. (2003). Overexpression of P-glycoprotein in K562 cells does not confer resistance to the growth inhibitory effects of imatinib (STI571) in vitro. *Blood* 102, 4499–4503. doi:10.1182/blood-2003-01-0083.

Fitzner, D., Schnaars, M., van Rossum, D., Krishnamoorthy, G., Dibaj, P., Bakhti, M., et al. (2011). Selective transfer of exosomes from oligodendrocytes to microglia by macropinocytosis. *J. Cell Sci.* 124, 447–458. doi:10.1242/jcs.074088.

Flashner-Abramson, E., Klein, S., Mullin, G., Shoshan, E., Song, R., Shir, A., et al. (2016). Targeting melanoma with NT157 by blocking Stat3 and IGF1R signaling. *Oncogene* 35, 2675–2680. doi:10.1038/onc.2015.229.

Flavin, R., Peluso, S., Nguyen, P. L., and Loda, M. (2010). Fatty acid synthase as a potential therapeutic target in cancer. *Future Oncol.* 6, 551–562. doi:10.2217/fon.10.11.

Frazer, R., Irvine, A. E., and McMullin, M. F. (2007). Chronic Myeloid Leukaemia in The 21st Century. *Ulster Med. J.* 76, 8–17.

Fu, Y., Zou, T., Shen, X., Nelson, P. J., Li, J., Wu, C., et al. (2021). Lipid metabolism in cancer progression and therapeutic strategies. *MedComm* 2, 27–59. doi:10.1002/mco2.27.

Gabert, J., Beillard, E., van der Velden, V. H. J., Bi, W., Grimwade, D., Pallisgaard, N., et al. (2003). Standardization and quality control studies of "real-time" quantitative reverse transcriptase polymerase chain reaction of fusion gene transcripts for residual disease detection in leukemia - a Europe Against Cancer program. *Leukemia* 17, 2318–2357. doi:10.1038/sj.leu.2403135.

Gadzicki, D., von Neuhoff, N., Steinemann, D., Just, M., Busche, G., Kreipe, H., et al. (2005). BCR-ABL gene amplification and overexpression in a patient with chronic myeloid leukemia treated with imatinib. *Cancer Genet. Cytogenet.* 159, 164–167. doi:10.1016/j.cancergencyto.2004.09.021.

Gainor, J. F., and Chabner, B. A. (2015). Ponatinib: Accelerated Disapproval. *Oncologist* 20, 847–848. doi:10.1634/theoncologist.2015-0253.

Galimberti, S., Cervetti, G., Guerrini, F., Testi, R., Pacini, S., Fazzi, R., et al. (2005). Quantitative molecular monitoring of BCR-ABL and MDR1 transcripts in patients with chronic myeloid leukemia during Imatinib treatment. *Cancer Genet. Cytogenet.* 162, 57–62. doi:10.1016/j.cancergencyto.2005.01.015.

Gambacorti-Passerini, C. B., Gunby, R. H., Piazza, R., Galietta, A., Rostagno, R., and Scapozza, L. (2003a). Molecular mechanisms of resistance to imatinib in Philadelphia-chromosome-positive leukaemias. *Lancet. Oncol.* 4, 75–85. doi:10.1016/s1470-2045(03)00979-3.

Gambacorti-Passerini, C., Barni, R., le Coutre, P., Zucchetti, M., Cabrita, G., Cleris, L., et al. (2000). Role of alpha1 acid glycoprotein in the in vivo resistance of human BCR-ABL(+) leukemic cells to the abl inhibitor STI571. *J. Natl. Cancer Inst.* 92, 1641–1650. doi:10.1093/jnci/92.20.1641.

Gambacorti-Passerini, C., Zucchetti, M., Russo, D., Frapolli, R., Verga, M., Bungaro, S., et al. (2003b). Alpha1 acid glycoprotein binds to imatinib (STI571) and substantially alters its pharmacokinetics in chronic myeloid leukemia patients. *Clin. cancer Res. an Off. J. Am. Assoc. Cancer Res.* 9, 625–632.

Gan, C. P., Sam, K. K., Yee, P. S., Zainal, N. S., Lee, B. K. B., Abdul Rahman, Z. A., et al. (2019). IFITM3 knockdown reduces the expression of CCND1 and CDK4 and suppresses the growth of oral squamous cell carcinoma cells. *Cell. Oncol. (Dordr).* 42, 477–490. doi:10.1007/s13402-019-00437-z.

Gao, P., Wang, L.-L., Liu, J., Dong, F., Song, W., Liao, L., et al. (2020). Dihydroartemisinin inhibits endothelial cell tube formation by suppression of the STAT3 signaling pathway. *Life Sci.* 242, 117221. doi:10.1016/j.lfs.2019.117221.

Gao, X., Wan, Z., Wei, M., Dong, Y., Zhao, Y., Chen, X., et al. (2019). Chronic myelogenous leukemia cells remodel the bone marrow niche via exosome-mediated transfer of miR-320. *Theranostics* 9, 5642–5656. doi:10.7150/thno.34813.

Garcia-Gutiérrez, V., Luna, A., Alonso-Dominguez, J. M., Estrada, N., Boque, C., Xicoy, B., et al. (2021). Safety and efficacy of asciminib treatment in chronic myeloid leukemia patients in real-life clinical practice. *Blood Cancer J.* 11, 16. doi:10.1038/s41408-021-00420-8.

Garciarena, C. D., Youm, J. B., Swietach, P., and Vaughan-Jones, R. D. (2013). H^+-activated Na^+ influx in the ventricular myocyte couples Ca^{2+}-signalling to intracellular pH. *J. Mol. Cell. Cardiol.* 61, 51–59. doi:10.1016/j.yjmcc.2013.04.008.

Gargallo, P. M., Cuello, M. T., Aranguren, P. N., and Larripa, I. B. (2003). Amplification of the BCR/ABL fusion gene clustered on a masked Philadelphia chromosome in a patient with myeloblastic crisis of chronic myelocytic leukemia. *Cancer Genet. Cytogenet.* 143, 140–144. doi:10.1016/s0165-4608(02)00854-3.

Gesbert, F., and Griffin, J. D. (2000). Bcr/Abl activates transcription of the Bcl-X gene through STAT5. *Blood* 96, 2269–2276.

Giustacchini, A., Thongjuea, S., Barkas, N., Woll, P. S., Povinelli, B. J., Booth, C. A. G., et al. (2017). Single-cell transcriptomics uncovers distinct molecular signatures of stem cells in chronic myeloid leukemia. *Nat. Med.* 23, 692–702. doi:10.1038/nm.4336.

Golas, J. M., Arndt, K., Etienne, C., Lucas, J., Nardin, D., Gibbons, J., et al. (2003). SKI-606, a 4-anilino-3-quinolinecarbonitrile dual inhibitor of Src and Abl kinases, is a potent antiproliferative agent against chronic myelogenous leukemia cells in culture and causes regression of K562 xenografts in nude mice. *Cancer Res.* 63, 375–381.

Golemovic, M., Verstovsek, S., Giles, F., Cortes, J., Manshouri, T., Manley, P. W., et al. (2005). AMN107, a novel aminopyrimidine inhibitor of Bcr-Abl, has in vitro activity against imatinib-resistant chronic myeloid leukemia. *Clin. cancer Res. an Off. J. Am. Assoc. Cancer Res.* 11, 4941–4947. doi:10.1158/1078-0432.CCR-04-2601.

Goloviznina, N. A., Verghese, S. C., Yoon, Y. M., Taratula, O., Marks, D. L., and Kurre, P. (2016). Mesenchymal Stromal Cell-derived Extracellular Vesicles Promote Myeloid-biased Multipotent Hematopoietic Progenitor Expansion via Toll-Like Receptor Engagement. *J. Biol. Chem.* 291, 24607–24617. doi:10.1074/jbc.M116.745653.

Gomez, G. A., Sokal, J. E., and Walsh, D. (1981). Prognostic features at diagnosis of chronic myelocytic leukemia. *Cancer* 47, 2470–2477. doi:10.1002/1097-0142(19810515)47:10<2470::aid-cncr2820471026>3.0.co;2-0.

Gordon, M. Y., Dowding, C. R., Riley, G. P., Goldman, J. M., and Greaves, M. F. (1987). Altered adhesive interactions with marrow stroma of haematopoietic progenitor cells in chronic myeloid leukaemia. *Nature* 328, 342–344. doi:10.1038/328342a0.

Gorre, M. E., Mohammed, M., Ellwood, K., Hsu, N., Paquette, R., Rao, P. N., et al. (2001). Clinical resistance to STI-571 cancer therapy caused by BCR-ABL gene mutation or amplification. *Science* 293, 876–880. doi:10.1126/science.1062538.

Gough, D. J., Corlett, A., Schlessinger, K., Wegrzyn, J., Larner, A. C., and Levy, D. E. (2009). Mitochondrial STAT3 supports Ras-dependent oncogenic transformation. *Science* 324, 1713–1716. doi:10.1126/science.1171721.

Graham, S. M., Jørgensen, H. G., Allan, E., Pearson, C., Alcorn, M. J., Richmond, L., et al. (2002). Primitive, quiescent, Philadelphia-positive stem cells from patients with chronic myeloid leukemia are insensitive to STI571 in vitro. *Blood* 99, 319–325. doi:10.1182/blood.v99.1.319.

Grazioli, S., and Pugin, J. (2018). Mitochondrial Damage-Associated Molecular Patterns: From Inflammatory Signaling to Human Diseases. *Front. Immunol.* 9, 832. doi:10.3389/fimmu.2018.00832.

Gréen, H., Skoglund, K., Rommel, F., Mirghani, R. A., and Lotfi, K. (2010). CYP3A activity influences imatinib response in patients with chronic myeloid leukemia: a pilot study on in vivo CYP3A activity. *Eur. J. Clin. Pharmacol.* 66, 383–386. doi:10.1007/s00228-009-0772-y.

Gregory, M. A., Phang, T. L., Neviani, P., Alvarez-Calderon, F., Eide, C. A., O'Hare, T., et al. (2010). Wnt/Ca2+/NFAT signaling maintains survival of Ph+ leukemia cells upon inhibition of Bcr-Abl. *Cancer Cell* 18, 74–87. doi:10.1016/j.ccr.2010.04.025.

Gribble, S. M., Roberts, I., Grace, C., Andrews, K. M., Green, A. R., and Nacheva, E. P. (2000). Cytogenetics of the chronic myeloid leukemia-derived cell line K562: karyotype clarification by multicolor fluorescence in situ hybridization, comparative genomic hybridization, and locus-specific fluorescence in situ hybridization. *Cancer Genet. Cytogenet.* 118, 1–8. doi:10.1016/s0165-4608(99)00169-7.

Groffen, J., Stephenson, J. R., Heisterkamp, N., de Klein, A., Bartram, C. R., and Grosveld, G. (1984). Philadelphia chromosomal breakpoints are clustered within a limited region, bcr, on chromosome 22. *Cell* 36, 93–99. doi:10.1016/0092-8674(84)90077-1.

Grynkiewicz, G., Poenie, M., and Tsien, R. Y. (1985). A new generation of Ca2+ indicators with greatly improved fluorescence properties. *J. Biol. Chem.* 260, 3440–3450.

Guescini, M., Guidolin, D., Vallorani, L., Casadei, L., Gioacchini, A. M., Tibollo, P., et al. (2010). C2C12 myoblasts release micro-vesicles containing mtDNA and proteins involved in signal transduction. *Exp. Cell Res.* 316, 1977–1984. doi:10.1016/j.yexcr.2010.04.006.

Gumireddy, K., Baker, S. J., Cosenza, S. C., John, P., Kang, A. D., Robell, K. A., et al. (2005). A non-ATP-competitive inhibitor of BCR-ABL overrides imatinib resistance. *Proc. Natl. Acad. Sci. U. S. A.* 102, 1992–1997. doi:10.1073/pnas.0408283102.

Gurung, S., Perocheau, D., Touramanidou, L., and Baruteau, J. (2021). The exosome journey: from biogenesis to uptake and intracellular signalling. *Cell Commun. Signal.* 19, 47. doi:10.1186/s12964-021-00730-1.

Hanson, P. I., Roth, R., Lin, Y., and Heuser, J. E. (2008). Plasma membrane deformation by circular arrays of ESCRT-III protein filaments. *J. Cell Biol.* 180, 389–402. doi:10.1083/jcb.200707031.

Harding, C., Heuser, J., and Stahl, P. (1983). Receptor-mediated endocytosis of transferrin and recycling of the transferrin receptor in rat reticulocytes. *J. Cell Biol.* 97, 329–339. doi:10.1083/jcb.97.2.329.

Harnois, T., Constantin, B., Rioux, A., Grenioux, E., Kitzis, A., and Bourmeyster, N. (2003). Differential interaction and activation of Rho family GTPases by p210bcr-abl and p190bcr-abl. *Oncogene* 22, 6445–6454. doi:10.1038/sj.onc.1206626.

Hatziieremia, S., Jordanides, N. E., Holyoake, T. L., Mountford, J. C., and Jørgensen, H. G. (2009). Inhibition of MDR1 does not sensitize primitive chronic myeloid leukemia CD34+

cells to imatinib. *Exp. Hematol.* 37, 692–700. doi:10.1016/j.exphem.2009.02.006.

He, B., Bai, Y., Kang, W., Zhang, X., and Jiang, X. (2017). LncRNA SNHG5 regulates imatinib resistance in chronic myeloid leukemia via acting as a CeRNA against MiR-205-5p. *Am. J. Cancer Res.* 7, 1704–1713.

He, L., Zhu, W., Chen, Q., Yuan, Y., Wang, Y., Wang, J., et al. (2019). Ovarian cancer cell-secreted exosomal miR-205 promotes metastasis by inducing angiogenesis. *Theranostics* 9, 8206–8220. doi:10.7150/thno.37455.

He, P., and Yun, C. C. (2010). Mechanisms of the regulation of the intestinal Na+/H+ exchanger NHE3. *J. Biomed. Biotechnol.* 2010, 238080. doi:10.1155/2010/238080.

Heinrich, P. C., Behrmann, I., Haan, S., Hermanns, H. M., Müller-Newen, G., and Schaper, F. (2003). Principles of interleukin (IL)-6-type cytokine signalling and its regulation. *Biochem. J.* 374, 1–20. doi:10.1042/BJ20030407.

Heinrich, P. C., Behrmann, I., Müller-Newen, G., Schaper, F., and Graeve, L. (1998). Interleukin-6-type cytokine signalling through the gp130/Jak/STAT pathway. *Biochem. J.* 334 (Pt 2, 297–314. doi:10.1042/bj3340297.

Heisterkamp, N., Stephenson, J. R., Groffen, J., Hansen, P. F., de Klein, A., Bartram, C. R., et al. (1983). Localization of the c-ab1 oncogene adjacent to a translocation break point in chronic myelocytic leukaemia. *Nature* 306, 239–242. doi:10.1038/306239a0.

Hennings, H., Michael, D., Cheng, C., Steinert, P., Holbrook, K., and Yuspa, S. H. (1980). Calcium regulation of growth and differentiation of mouse epidermal cells in culture. *Cell* 19, 245–254. doi:10.1016/0092-8674(80)90406-7.

Hernandez, C., Huebener, P., and Schwabe, R. F. (2016). Damage-associated molecular patterns in cancer: a double-edged sword. *Oncogene* 35, 5931–5941. doi:10.1038/onc.2016.104.

Herrington, J., Smit, L. S., Schwartz, J., and Carter-Su, C. (2000). The role of STAT proteins in growth hormone signaling. *Oncogene* 19, 2585–2597. doi:10.1038/sj.onc.1203526.

Hizuka, N., Sukegawa, I., Takano, K., Asakawa, K., Horikawa, R., Tsushima, T., et al. (1987). Characterization of insulin-like growth factor I receptors on human erythroleukemia cell line (K-562 cells). *Endocrinol. Jpn.* 34, 81–88. doi:10.1507/endocrj1954.34.81.

Hochhaus, A., Baccarani, M., Deininger, M., Apperley, J. F., Lipton, J. H., Goldberg, S. L., et al. (2008). Dasatinib induces durable cytogenetic responses in patients with chronic myelogenous leukemia in chronic phase with resistance or intolerance to imatinib. *Leukemia* 22, 1200–1206. doi:10.1038/leu.2008.84.

Hochhaus, A., Baccarani, M., Silver, R. T., Schiffer, C., Apperley, J. F., Cervantes, F., et al. (2020). European LeukemiaNet 2020 recommendations for treating chronic myeloid leukemia. *Leukemia* 34, 966–984. doi:10.1038/s41375-020-0776-2.

Hochhaus, A., Kantarjian, H. M., Baccarani, M., Lipton, J. H., Apperley, J. F., Druker, B. J., et al. (2007). Dasatinib induces notable hematologic and cytogenetic responses in chronic-phase chronic myeloid leukemia after failure of imatinib therapy. *Blood* 109, 2303–2309.

doi:10.1182/blood-2006-09-047266.

Hochhaus, A., Kreil, S., Corbin, A. S., La Rosee, P., Muller, M. C., Lahaye, T., et al. (2002). Molecular and chromosomal mechanisms of resistance to imatinib (STI571) therapy. *Leukemia* 16, 2190–2196. doi:10.1038/sj.leu.2402741.

Hoffmann, V. S., Baccarani, M., Hasford, J., Lindoerfer, D., Burgstaller, S., Sertic, D., et al. (2015). The EUTOS population-based registry: incidence and clinical characteristics of 2904 CML patients in 20 European Countries. *Leukemia* 29, 1336–1343. doi:10.1038/leu.2015.73.

Hong, C.-S., Muller, L., Whiteside, T. L., and Boyiadzis, M. (2014). Plasma exosomes as markers of therapeutic response in patients with acute myeloid leukemia. *Front. Immunol.* 5, 160. doi:10.3389/fimmu.2014.00160.

Hooper, A. T., Butler, J. M., Nolan, D. J., Kranz, A., Iida, K., Kobayashi, M., et al. (2009). Engraftment and reconstitution of hematopoiesis is dependent on VEGFR2-mediated regeneration of sinusoidal endothelial cells. *Cell Stem Cell* 4, 263–274. doi:10.1016/j.stem.2009.01.006.

Horibe, S., Tanahashi, T., Kawauchi, S., Murakami, Y., and Rikitake, Y. (2018). Mechanism of recipient cell-dependent differences in exosome uptake. *BMC Cancer* 18, 47. doi:10.1186/s12885-017-3958-1.

Horita, M., Andreu, E. J., Benito, A., Arbona, C., Sanz, C., Benet, I., et al. (2000). Blockade of the Bcr-Abl kinase activity induces apoptosis of chronic myelogenous leukemia cells by suppressing signal transducer and activator of transcription 5-dependent expression of Bcl-xL. *J. Exp. Med.* 191, 977–984. doi:10.1084/jem.191.6.977.

Hornick, N. I., Doron, B., Abdelhamed, S., Huan, J., Harrington, C. A., Shen, R., et al. (2016). AML suppresses hematopoiesis by releasing exosomes that contain microRNAs targeting c-MYB. *Sci. Signal.* 9, ra88. doi:10.1126/scisignal.aaf2797.

Hrdinova, T., Toman, O., Dresler, J., Klimentova, J., Salovska, B., Pajer, P., et al. (2021). Exosomes released by imatinib-resistant K562 cells contain specific membrane markers, IFITM3, CD146 and CD36 and increase the survival of imatinib-sensitive cells in the presence of imatinib. *Int. J. Oncol.* 58, 238–250. doi:10.3892/ijo.2020.5163.

Hu, J., Wang, S., Zhao, Y., Guo, Q., Zhang, D., Chen, J., et al. (2014). Mechanism and biological significance of the overexpression of IFITM3 in gastric cancer. *Oncol. Rep.* 32, 2648–2656. doi:10.3892/or.2014.3522.

Hu, Y., Chen, Y., Douglas, L., and Li, S. (2009). beta-Catenin is essential for survival of leukemic stem cells insensitive to kinase inhibition in mice with BCR-ABL-induced chronic myeloid leukemia. *Leukemia* 23, 109–116. doi:10.1038/leu.2008.262.

Huber, V., Fais, S., Iero, M., Lugini, L., Canese, P., Squarcina, P., et al. (2005). Human colorectal cancer cells induce T-cell death through release of proapoptotic microvesicles: role in immune escape. *Gastroenterology* 128, 1796–1804. doi:10.1053/j.gastro.2005.03.045.

Hughes, T. P., Mauro, M. J., Cortes, J. E., Minami, H., Rea, D., DeAngelo, D. J., et al. (2019).

Asciminib in Chronic Myeloid Leukemia after ABL Kinase Inhibitor Failure. *N. Engl. J. Med.* 381, 2315–2326. doi:10.1056/NEJMoa1902328.

Hukku, S., Baboo, H. A., Venkataratnam, S., Vidyasagar, M. S., and Patel, N. L. (1983). Splenic irradiation in chronic myeloid leukemia. *Acta Radiol. Oncol.* 22, 9–12. doi:10.3109/02841868309134332.

Hupe, D. J., Boltz, R., Cohen, C. J., Felix, J., Ham, E., Miller, D., et al. (1991). The inhibition of receptor-mediated and voltage-dependent calcium entry by the antiproliferative L-651,582. *J. Biol. Chem.* 266, 10136–10142.

Ibuki, N., Ghaffari, M., Reuveni, H., Pandey, M., Fazli, L., Azuma, H., et al. (2014). The tyrphostin NT157 suppresses insulin receptor substrates and augments therapeutic response of prostate cancer. *Mol. Cancer Ther.* 13, 2827–2839. doi:10.1158/1535-7163.MCT-13-0842.

Ihle, J. N. (2001). The Stat family in cytokine signaling. *Curr. Opin. Cell Biol.* 13, 211–217. doi:10.1016/s0955-0674(00)00199-x.

Ilaria, R. L. J., and Van Etten, R. A. (1996). P210 and P190(BCR/ABL) induce the tyrosine phosphorylation and DNA binding activity of multiple specific STAT family members. *J. Biol. Chem.* 271, 31704–31710. doi:10.1074/jbc.271.49.31704.

Illmer, T., Schaich, M., Platzbecker, U., Freiberg-Richter, J., Oelschlägel, U., von Bonin, M., et al. (2004). P-glycoprotein-mediated drug efflux is a resistance mechanism of chronic myelogenous leukemia cells to treatment with imatinib mesylate. *Leukemia* 18, 401–408. doi:10.1038/sj.leu.2403257.

Inoue, K., Ogawa, H., Sonoda, Y., Kimura, T., Sakabe, H., Oka, Y., et al. (1997). Aberrant overexpression of the Wilms tumor gene (WT1) in human leukemia. *Blood* 89, 1405–1412.

Iwamoto, T., Watanabe, Y., Kita, S., and Blaustein, M. P. (2007). Na+/Ca2+ exchange inhibitors: a new class of calcium regulators. *Cardiovasc. Hematol. Disord. Drug Targets* 7, 188–198. doi:10.2174/187152907781745288.

Izquierdo-Useros, N., Naranjo-Gómez, M., Archer, J., Hatch, S. C., Erkizia, I., Blanco, J., et al. (2009). Capture and transfer of HIV-1 particles by mature dendritic cells converges with the exosome-dissemination pathway. *Blood* 113, 2732–2741. doi:10.1182/blood-2008-05-158642.

Jabbour, E., Kantarjian, H., Jones, D., Talpaz, M., Bekele, N., O'Brien, S., et al. (2006). Frequency and clinical significance of BCR-ABL mutations in patients with chronic myeloid leukemia treated with imatinib mesylate. *Leukemia* 20, 1767–1773. doi:10.1038/sj.leu.2404318.

Jackson, P., and Baltimore, D. (1989). N-terminal mutations activate the leukemogenic potential of the myristoylated form of c-abl. *EMBO J.* 8, 449–456.

Jafarzadeh, N., Safari, Z., Pornour, M., Amirizadeh, N., Forouzandeh Moghadam, M., and Sadeghizadeh, M. (2019). Alteration of cellular and immune-related properties of bone marrow mesenchymal stem cells and macrophages by K562 chronic myeloid leukemia

cell derived exosomes. *J. Cell. Physiol.* 234, 3697–3710. doi:10.1002/jcp.27142.

Jain, P., Kantarjian, H., Patel, K. P., Gonzalez, G. N., Luthra, R., Kanagal Shamanna, R., et al. (2016). Impact of BCR-ABL transcript type on outcome in patients with chronic-phase CML treated with tyrosine kinase inhibitors. *Blood* 127, 1269–1275. doi:10.1182/blood-2015-10-674242.

Jain, S. K., Langdon, W. Y., and Varticovski, L. (1997). Tyrosine phosphorylation of p120cbl in BCR/abl transformed hematopoietic cells mediates enhanced association with phosphatidylinositol 3-kinase. *Oncogene* 14, 2217–2228. doi:10.1038/sj.onc.1201049.

Jaiswal, S., Fontanillas, P., Flannick, J., Manning, A., Grauman, P. V, Mar, B. G., et al. (2014). Age-related clonal hematopoiesis associated with adverse outcomes. *N. Engl. J. Med.* 371, 2488–2498. doi:10.1056/NEJMoa1408617.

Jamieson, C. H. M., Ailles, L. E., Dylla, S. J., Muijtjens, M., Jones, C., Zehnder, J. L., et al. (2004). Granulocyte-macrophage progenitors as candidate leukemic stem cells in blast-crisis CML. *N. Engl. J. Med.* 351, 657–667. doi:10.1056/NEJMoa040258.

Jiang, Y.-H., Liu, J., Lin, J., Li, S.-Q., Xu, Y.-M., Min, Q.-H., et al. (2020). K562 cell-derived exosomes suppress the adhesive function of bone marrow mesenchymal stem cells via delivery of miR-711. *Biochem. Biophys. Res. Commun.* 521, 584–589. doi:10.1016/j.bbrc.2019.10.096.

Johnston, P. A., and Grandis, J. R. (2011). STAT3 signaling: anticancer strategies and challenges. *Mol. Interv.* 11, 18–26. doi:10.1124/mi.11.1.4.

Johnstone, R. M., Adam, M., Hammond, J. R., Orr, L., and Turbide, C. (1987). Vesicle formation during reticulocyte maturation. Association of plasma membrane activities with released vesicles (exosomes). *J. Biol. Chem.* 262, 9412–9420.

Jonuleit, T., van der Kuip, H., Miething, C., Michels, H., Hallek, M., Duyster, J., et al. (2000). Bcr-Abl kinase down-regulates cyclin-dependent kinase inhibitor p27 in human and murine cell lines. *Blood* 96, 1933–1939.

Joshi, B. S., de Beer, M. A., Giepmans, B. N. G., and Zuhorn, I. S. (2020). Endocytosis of Extracellular Vesicles and Release of Their Cargo from Endosomes. *ACS Nano* 14, 4444–4455. doi:10.1021/acsnano.9b10033.

Kahlert, C., Melo, S. A., Protopopov, A., Tang, J., Seth, S., Koch, M., et al. (2014). Identification of double-stranded genomic DNA spanning all chromosomes with mutated KRAS and p53 DNA in the serum exosomes of patients with pancreatic cancer. *J. Biol. Chem.* 289, 3869–3875. doi:10.1074/jbc.C113.532267.

Kang, K.-W., Jung, J.-H., Hur, W., Park, J., Shin, H., Choi, B., et al. (2018). The Potential of Exosomes Derived from Chronic Myelogenous Leukaemia Cells as a Biomarker. *Anticancer Res.* 38, 3935–3942. doi:10.21873/anticanres.12679.

Kantarjian, H., Giles, F., Wunderle, L., Bhalla, K., O'Brien, S., Wassmann, B., et al. (2006). Nilotinib in imatinib-resistant CML and Philadelphia chromosome-positive ALL. *N. Engl. J. Med.* 354, 2542–2551. doi:10.1056/NEJMoa055104.

Kantarjian, H. M., Giles, F., Gattermann, N., Bhalla, K., Alimena, G., Palandri, F., et al. (2007a). Nilotinib (formerly AMN107), a highly selective BCR-ABL tyrosine kinase inhibitor, is effective in patients with Philadelphia chromosome-positive chronic myelogenous leukemia in chronic phase following imatinib resistance and intolerance. *Blood* 110, 3540–3546. doi:10.1182/blood-2007-03-080689.

Kantarjian, H. M., O'Brien, S., Cortes, J. E., Shan, J., Giles, F. J., Rios, M. B., et al. (2003). Complete cytogenetic and molecular responses to interferon-alpha-based therapy for chronic myelogenous leukemia are associated with excellent long-term prognosis. *Cancer* 97, 1033–1041. doi:10.1002/cncr.11223.

Kantarjian, H., Pasquini, R., Hamerschlak, N., Rousselot, P., Holowiecki, J., Jootar, S., et al. (2007b). Dasatinib or high-dose imatinib for chronic-phase chronic myeloid leukemia after failure of first-line imatinib: a randomized phase 2 trial. *Blood* 109, 5143–5150. doi:10.1182/blood-2006-11-056028.

Kantarjian, H., Sawyers, C., Hochhaus, A., Guilhot, F., Schiffer, C., Gambacorti-Passerini, C., et al. (2002). Hematologic and cytogenetic responses to imatinib mesylate in chronic myelogenous leukemia. *N. Engl. J. Med.* 346, 645–652. doi:10.1056/NEJMoa011573.

Karvar, S., Suda, J., Zhu, L., and Rockey, D. C. (2014). Distribution dynamics and functional importance of NHERF1 in regulation of Mrp-2 trafficking in hepatocytes. *Am. J. Physiol. Cell Physiol.* 307, C727-37. doi:10.1152/ajpcell.00011.2014.

Katzmann, D. J., Babst, M., and Emr, S. D. (2001). Ubiquitin-dependent sorting into the multivesicular body pathway requires the function of a conserved endosomal protein sorting complex, ESCRT-I. *Cell* 106, 145–155. doi:10.1016/s0092-8674(01)00434-2.

Katzmann, D. J., Stefan, C. J., Babst, M., and Emr, S. D. (2003). Vps27 recruits ESCRT machinery to endosomes during MVB sorting. *J. Cell Biol.* 162, 413–423. doi:10.1083/jcb.200302136.

Kennedy, B. J. (1972). Hydroxyurea therapy in chronic myelogenous leukemia. *Cancer* 29, 1052–1056. doi:10.1002/1097-0142(197204)29:4<1052::aid-cncr2820290454>3.0.co;2-7.

Khorashad, J. S., Kelley, T. W., Szankasi, P., Mason, C. C., Soverini, S., Adrian, L. T., et al. (2013). BCR-ABL1 compound mutations in tyrosine kinase inhibitor-resistant CML: frequency and clonal relationships. *Blood* 121, 489–498. doi:10.1182/blood-2012-05-431379.

Khoury, H. J., Cortes, J. E., Kantarjian, H. M., Gambacorti-Passerini, C., Baccarani, M., Kim, D.-W., et al. (2012). Bosutinib is active in chronic phase chronic myeloid leukemia after imatinib and dasatinib and/or nilotinib therapy failure. *Blood* 119, 3403–3412. doi:10.1182/blood-2011-11-390120.

Kiedrowski, L. (2011). Cytosolic zinc release and clearance in hippocampal neurons exposed to glutamate--the role of pH and sodium. *J. Neurochem.* 117, 231–243. doi:10.1111/j.1471-4159.2011.07194.x.

Kiel, M. J., Yilmaz, O. H., Iwashita, T., Yilmaz, O. H., Terhorst, C., and Morrison, S. J. (2005). SLAM family receptors distinguish hematopoietic stem and progenitor cells and reveal endothelial niches for stem cells. *Cell* 121, 1109–1121. doi:10.1016/j.cell.2005.05.026.

Kinsella, B. T., O'Mahony, D. J., and Fitzgerald, G. A. (1997). The human thromboxane A2 receptor alpha isoform (TP alpha) functionally couples to the G proteins Gq and G11 in vivo and is activated by the isoprostane 8-epi prostaglandin F2 alpha. *J. Pharmacol. Exp. Ther.* 281, 957–964.

Kipreos, E. T., and Wang, J. Y. (1992). Cell cycle-regulated binding of c-Abl tyrosine kinase to DNA. *Science* 256, 382–385. doi:10.1126/science.256.5055.382.

Komatsu, N., Watanabe, T., Uchida, M., Mori, M., Kirito, K., Kikuchi, S., et al. (2003). A member of Forkhead transcription factor FKHRL1 is a downstream effector of STI571-induced cell cycle arrest in BCR-ABL-expressing cells. *J. Biol. Chem.* 278, 6411–6419. doi:10.1074/jbc.M211562200.

Kominsky, D. J., Klawitter, J., Brown, J. L., Boros, L. G., Melo, J. V, Eckhardt, S. G., et al. (2009). Abnormalities in glucose uptake and metabolism in imatinib-resistant human BCR-ABL-positive cells. *Clin. cancer Res. an Off. J. Am. Assoc. Cancer Res.* 15, 3442–3450. doi:10.1158/1078-0432.CCR-08-3291.

Koptyra, M., Cramer, K., Slupianek, A., Richardson, C., and Skorski, T. (2008). BCR/ABL promotes accumulation of chromosomal aberrations induced by oxidative and genotoxic stress. *Leukemia* 22, 1969–1972. doi:10.1038/leu.2008.78.

Koptyra, M., Falinski, R., Nowicki, M. O., Stoklosa, T., Majsterek, I., Nieborowska-Skorska, M., et al. (2006). BCR/ABL kinase induces self-mutagenesis via reactive oxygen species to encode imatinib resistance. *Blood* 108, 319–327. doi:10.1182/blood-2005-07-2815.

Koumangoye, R. B., Sakwe, A. M., Goodwin, J. S., Patel, T., and Ochieng, J. (2011). Detachment of breast tumor cells induces rapid secretion of exosomes which subsequently mediate cellular adhesion and spreading. *PLoS One* 6, e24234. doi:10.1371/journal.pone.0024234.

Kowal, J., Arras, G., Colombo, M., Jouve, M., Morath, J. P., Primdal-Bengtson, B., et al. (2016). Proteomic comparison defines novel markers to characterize heterogeneous populations of extracellular vesicle subtypes. *Proc. Natl. Acad. Sci. U. S. A.* 113, E968-77. doi:10.1073/pnas.1521230113.

Krämer, A., Hörner, S., Willer, A., Fruehauf, S., Hochhaus, A., Hallek, M., et al. (1999). Adhesion to fibronectin stimulates proliferation of wild-type and bcr/abl-transfected murine hematopoietic cells. *Proc. Natl. Acad. Sci. U. S. A.* 96, 2087–2092. doi:10.1073/pnas.96.5.2087.

Krause, D. S., Lazarides, K., von Andrian, U. H., and Van Etten, R. A. (2006). Requirement for CD44 in homing and engraftment of BCR-ABL-expressing leukemic stem cells. *Nat. Med.* 12, 1175–1180. doi:10.1038/nm1489.

Krebs, J., Agellon, L. B., and Michalak, M. (2015). Ca(2+) homeostasis and endoplasmic reticulum (ER) stress: An integrated view of calcium signaling. *Biochem. Biophys. Res. Commun.* 460, 114–121. doi:10.1016/j.bbrc.2015.02.004.

Kumar, B., Garcia, M., Weng, L., Jung, X., Murakami, J. L., Hu, X., et al. (2018). Acute myeloid leukemia transforms the bone marrow niche into a leukemia-permissive microenvironment through exosome secretion. *Leukemia* 32, 575–587.

doi:10.1038/leu.2017.259.

Kuntz, E. M., Baquero, P., Michie, A. M., Dunn, K., Tardito, S., Holyoake, T. L., et al. (2017). Targeting mitochondrial oxidative phosphorylation eradicates therapy-resistant chronic myeloid leukemia stem cells. *Nat. Med.* 23, 1234–1240. doi:10.1038/nm.4399.

Kurtz, A., Zapf, J., Eckardt, K. U., Clemons, G., Froesch, E. R., and Bauer, C. (1988). Insulin-like growth factor I stimulates erythropoiesis in hypophysectomized rats. *Proc. Natl. Acad. Sci. U. S. A.* 85, 7825–7829. doi:10.1073/pnas.85.20.7825.

Lahaye, T., Riehm, B., Berger, U., Paschka, P., Muller, M. C., Kreil, S., et al. (2005). Response and resistance in 300 patients with BCR-ABL-positive leukemias treated with imatinib in a single center: a 4.5-year follow-up. *Cancer* 103, 1659–1669. doi:10.1002/cncr.20922.

Lakshmikuttyamma, A., Pastural, E., Takahashi, N., Sawada, K., Sheridan, D. P., DeCoteau, J. F., et al. (2008). Bcr-Abl induces autocrine IGF-1 signaling. *Oncogene* 27, 3831–3844. doi:10.1038/onc.2008.8.

Lamprecht, G., Weinman, E. J., and Yun, C. H. (1998). The role of NHERF and E3KARP in the cAMP-mediated inhibition of NHE3. *J. Biol. Chem.* 273, 29972–29978. doi:10.1074/jbc.273.45.29972.

Landberg, N., von Palffy, S., Askmyr, M., Lilljebjorn, H., Sanden, C., Rissler, M., et al. (2018). CD36 defines primitive chronic myeloid leukemia cells less responsive to imatinib but vulnerable to antibody-based therapeutic targeting. *Haematologica* 103, 447–455. doi:10.3324/haematol.2017.169946.

Lee-Six, H., Øbro, N. F., Shepherd, M. S., Grossmann, S., Dawson, K., Belmonte, M., et al. (2018). Population dynamics of normal human blood inferred from somatic mutations. *Nature* 561, 473–478. doi:10.1038/s41586-018-0497-0.

Lee, J.-W., Geng, H., Dinson, D. S., Xiao, G., Cosgun, K. N., Chan, L. N., et al. (2018a). IFITM3-Mediated Regulation of Cell Membrane Dynamics Is Essential for Malignant B-Cell Transformation. *Blood* 132, 552 LP – 552. doi:10.1182/blood-2018-99-117472.

Lee, J. H., Choi, S. I., Kim, R. K., Cho, E. W., and Kim, I. G. (2018b). Tescalcin/c-Src/IGF1Rβ-mediated STAT3 activation enhances cancer stemness and radioresistant properties through ALDH1. *Sci. Rep.* 8, 10711. doi:10.1038/s41598-018-29142-x.

Lee, J., Robinson, M. E., Ma, N., Artadji, D., Ahmed, M. A., Xiao, G., et al. (2020). IFITM3 functions as a PIP3 scaffold to amplify PI3K signalling in B cells. *Nature* 588, 491–497. doi:10.1038/s41586-020-2884-6.

Lee, S. M., Bae, J. H., Kim, M. J., Lee, H. S., Lee, M. K., Chung, B. S., et al. (2007). Bcr-Abl-independent imatinib-resistant K562 cells show aberrant protein acetylation and increased sensitivity to histone deacetylase inhibitors. *J. Pharmacol. Exp. Ther.* 322, 1084–1092. doi:10.1124/jpet.107.124461.

Lehmann, J. M., Riethmuller, G., and Johnson, J. P. (1989). MUC18, a marker of tumor progression in human melanoma, shows sequence similarity to the neural cell adhesion molecules of the immunoglobulin superfamily. *Proc. Natl. Acad. Sci. U. S. A.* 86, 9891–9895. doi:10.1073/pnas.86.24.9891.

Lei, X., Guan, C.-W., Song, Y., and Wang, H. (2015). The multifaceted role of CD146/MCAM in the promotion of melanoma progression. *Cancer Cell Int.* 15, 3. doi:10.1186/s12935-014-0147-z.

Levinson, N. M., and Boxer, S. G. (2012). Structural and spectroscopic analysis of the kinase inhibitor bosutinib and an isomer of bosutinib binding to the Abl tyrosine kinase domain. *PLoS One* 7, e29828. doi:10.1371/journal.pone.0029828.

Levy, D. E., and Darnell, J. E. J. (2002). Stats: transcriptional control and biological impact. *Nat. Rev. Mol. Cell Biol.* 3, 651–662. doi:10.1038/nrm909.

Lewis, J. M., Baskaran, R., Taagepera, S., Schwartz, M. A., and Wang, J. Y. (1996). Integrin regulation of c-Abl tyrosine kinase activity and cytoplasmic-nuclear transport. *Proc. Natl. Acad. Sci. U. S. A.* 93, 15174–15179. doi:10.1073/pnas.93.26.15174.

Li, M.-Y., Zhao, C., Chen, L., Yao, F.-Y., Zhong, F.-M., Chen, Y., et al. (2021). Quantitative Proteomic Analysis of Plasma Exosomes to Identify the Candidate Biomarker of Imatinib Resistance in Chronic Myeloid Leukemia Patients. *Front. Oncol.* 11, 779567. doi:10.3389/fonc.2021.779567.

Li, M., Wang, W., Soroka, C. J., Mennone, A., Harry, K., Weinman, E. J., et al. (2010). NHERF-1 binds to Mrp2 and regulates hepatic Mrp2 expression and function. *J. Biol. Chem.* 285, 19299–19307. doi:10.1074/jbc.M109.096081.

Li, W., Johnson, S. A., Shelley, W. C., and Yoder, M. C. (2004). Hematopoietic stem cell repopulating ability can be maintained in vitro by some primary endothelial cells. *Exp. Hematol.* 32, 1226–1237. doi:10.1016/j.exphem.2004.09.001.

Li, Z., Qiao, Y., Liu, B., Laska, E. J., Chakravarthi, P., Kulko, J. M., et al. (2005). Combination of imatinib mesylate with autologous leukocyte-derived heat shock protein and chronic myelogenous leukemia. *Clin. cancer Res. an Off. J. Am. Assoc. Cancer Res.* 11, 4460–4468. doi:10.1158/1078-0432.CCR-05-0250.

Liang, Y.-K., Zeng, D., Xiao, Y.-S., Wu, Y., Ouyang, Y.-X., Chen, M., et al. (2017). MCAM/CD146 promotes tamoxifen resistance in breast cancer cells through induction of epithelial-mesenchymal transition, decreased ERalpha expression and AKT activation. *Cancer Lett.* 386, 65–76. doi:10.1016/j.canlet.2016.11.004.

Lin, L., Yao, Z., Bhuvaneshwar, K., Gusev, Y., Kallakury, B., Yang, S., et al. (2014). Transcriptional regulation of STAT3 by SPTBN1 and SMAD3 in HCC through cAMP-response element-binding proteins ATF3 and CREB2. *Carcinogenesis* 35, 2393–2403. doi:10.1093/carcin/bgu163.

Lipton, J. H., Chuah, C., Guerci-Bresler, A., Rosti, G., Simpson, D., Assouline, S., et al. (2016). Ponatinib versus imatinib for newly diagnosed chronic myeloid leukaemia: an international, randomised, open-label, phase 3 trial. *Lancet. Oncol.* 17, 612–621. doi:10.1016/S1470-2045(16)00080-2.

Liu, Y., Lu, R., Cui, W., Pang, Y., Liu, C., Cui, L., et al. (2019). High IFITM3 expression predicts adverse prognosis in acute myeloid leukemia. *Cancer Gene Ther.* doi:10.1038/s41417-019-0093-y.

Livak, K. J., and Schmittgen, T. D. (2001). Analysis of relative gene expression data using real-time quantitative PCR and the 2(-Delta Delta C(T)) Method. *Methods* 25, 402–408. doi:10.1006/meth.2001.1262.

Llorente, A., Skotland, T., Sylvänne, T., Kauhanen, D., Róg, T., Orłowski, A., et al. (2013). Molecular lipidomics of exosomes released by PC-3 prostate cancer cells. *Biochim. Biophys. Acta* 1831, 1302–1309. doi:10.1016/j.bbalip.2013.04.011.

Lombardo, L. J., Lee, F. Y., Chen, P., Norris, D., Barrish, J. C., Behnia, K., et al. (2004). Discovery of N-(2-chloro-6-methyl- phenyl)-2-(6-(4-(2-hydroxyethyl)- piperazin-1-yl)-2-methylpyrimidin-4- ylamino)thiazole-5-carboxamide (BMS-354825), a dual Src/Abl kinase inhibitor with potent antitumor activity in preclinical assays. *J. Med. Chem.* 47, 6658–6661. doi:10.1021/jm049486a.

Lorkova, L., Scigelova, M., Arrey, T. N., Vit, O., Pospisilova, J., Doktorova, E., et al. (2015). Detailed Functional and Proteomic Characterization of Fludarabine Resistance in Mantle Cell Lymphoma Cells. *PLoS One* 10, e0135314. doi:10.1371/journal.pone.0135314.

Luhtala, N., and Odorizzi, G. (2004). Bro1 coordinates deubiquitination in the multivesicular body pathway by recruiting Doa4 to endosomes. *J. Cell Biol.* 166, 717–729. doi:10.1083/jcb.200403139.

Lyman, G. H., and Henk, H. J. (2020). Association of Generic Imatinib Availability and Pricing With Trends in Tyrosine Kinase Inhibitor Use in Patients With Chronic Myelogenous Leukemia. *JAMA Oncol.* 6, 1969–1971. doi:10.1001/jamaoncol.2020.4660.

Ma, L., Shan, Y., Bai, R., Xue, L., Eide, C. A., Ou, J., et al. (2014). A therapeutically targetable mechanism of BCR-ABL-independent imatinib resistance in chronic myeloid leukemia. *Sci. Transl. Med.* 6, 252ra121. doi:10.1126/scitranslmed.3009073.

Ma, L., Zhou, M., Wen, S., Ni, C., Jiang, L., Fan, J., et al. (2010). Effects of STAT3 silencing on fate of chronic myelogenous leukemia K562 cells. *Leuk. Lymphoma* 51, 1326–1336. doi:10.3109/10428194.2010.483748.

Maacha, S., Bhat, A. A., Jimenez, L., Raza, A., Haris, M., Uddin, S., et al. (2019). Extracellular vesicles-mediated intercellular communication: roles in the tumor microenvironment and anti-cancer drug resistance. *Mol. Cancer* 18, 55. doi:10.1186/s12943-019-0965-7.

Maguire, O., Tornatore, K. M., O'Loughlin, K. L., Venuto, R. C., and Minderman, H. (2013). Nuclear translocation of nuclear factor of activated T cells (NFAT) as a quantitative pharmacodynamic parameter for tacrolimus. *Cytometry. A* 83, 1096–1104. doi:10.1002/cyto.a.22401.

Mahon, F.-X., Belloc, F., Lagarde, V., Chollet, C., Moreau-Gaudry, F., Reiffers, J., et al. (2003). MDR1 gene overexpression confers resistance to imatinib mesylate in leukemia cell line models. *Blood* 101, 2368–2373. doi:10.1182/blood.V101.6.2368.

Mahon, F.-X., Réa, D., Guilhot, J., Guilhot, F., Huguet, F., Nicolini, F., et al. (2010). Discontinuation of imatinib in patients with chronic myeloid leukaemia who have maintained complete molecular remission for at least 2 years: the prospective, multicentre Stop Imatinib (STIM) trial. *Lancet. Oncol.* 11, 1029–1035. doi:10.1016/S1470-2045(10)70233-3.

Mahon, F. X., Deininger, M. W., Schultheis, B., Chabrol, J., Reiffers, J., Goldman, J. M., et al. (2000). Selection and characterization of BCR-ABL positive cell lines with differential sensitivity to the tyrosine kinase inhibitor STI571: diverse mechanisms of resistance. *Blood* 96, 1070–1079.

Maru, Y., and Witte, O. N. (1991). The BCR gene encodes a novel serine/threonine kinase activity within a single exon. *Cell* 67, 459–468. doi:10.1016/0092-8674(91)90521-y.

Mathivanan, S., Ji, H., and Simpson, R. J. (2010). Exosomes: extracellular organelles important in intercellular communication. *J. Proteomics* 73, 1907–1920. doi:10.1016/j.jprot.2010.06.006.

Mathivanan, S., and Simpson, R. J. (2009). ExoCarta: A compendium of exosomal proteins and RNA. *Proteomics* 9, 4997–5000. doi:10.1002/pmic.200900351.

McGlave, P. B., Arthur, D. C., Kim, T. H., Ramsay, N. K., Hurd, D. D., and Kersey, J. (1982). Successful allogeneic bone-marrow transplantation for patients in the accelerated phase of chronic granulocytic leukaemia. *Lancet (London, England)* 2, 625–627. doi:10.1016/s0140-6736(82)92737-4.

McWhirter, J. R., Galasso, D. L., and Wang, J. Y. (1993). A coiled-coil oligomerization domain of Bcr is essential for the transforming function of Bcr-Abl oncoproteins. *Mol. Cell. Biol.* 13, 7587–7595. doi:10.1128/mcb.13.12.7587.

McWhirter, J. R., and Wang, J. Y. (1991). Activation of tyrosinase kinase and microfilament-binding functions of c-abl by bcr sequences in bcr/abl fusion proteins. *Mol. Cell. Biol.* 11, 1553–1565. doi:10.1128/mcb.11.3.1553.

Mencalha, A. L., Du Rocher, B., Salles, D., Binato, R., and Abdelhay, E. (2010). LLL-3, a STAT3 inhibitor, represses BCR-ABL-positive cell proliferation, activates apoptosis and improves the effects of Imatinib mesylate. *Cancer Chemother. Pharmacol.* 65, 1039–1046. doi:10.1007/s00280-009-1109-3.

Meyn, M. A. 3rd, Wilson, M. B., Abdi, F. A., Fahey, N., Schiavone, A. P., Wu, J., et al. (2006). Src family kinases phosphorylate the Bcr-Abl SH3-SH2 region and modulate Bcr-Abl transforming activity. *J. Biol. Chem.* 281, 30907–30916. doi:10.1074/jbc.M605902200.

Miao, Y. J., and Wang, J. Y. (1996). Binding of A/T-rich DNA by three high mobility group-like domains in c-Abl tyrosine kinase. *J. Biol. Chem.* 271, 22823–22830. doi:10.1074/jbc.271.37.22823.

Mignen, O., Brink, C., Enfissi, A., Nadkarni, A., Shuttleworth, T. J., Giovannucci, D. R., et al. (2005). Carboxyamidotriazole-induced inhibition of mitochondrial calcium import blocks capacitative calcium entry and cell proliferation in HEK-293 cells. *J. Cell Sci.* 118, 5615–5623. doi:10.1242/jcs.02663.

Million, R. P., and Van Etten, R. A. (2000). The Grb2 binding site is required for the induction of chronic myeloid leukemia-like disease in mice by the Bcr/Abl tyrosine kinase. *Blood* 96, 664–670.

Min, Q.-H., Wang, X.-Z., Zhang, J., Chen, Q.-G., Li, S.-Q., Liu, X.-Q., et al. (2018). Exosomes derived from imatinib-resistant chronic myeloid leukemia cells mediate a horizontal

transfer of drug-resistant trait by delivering miR-365. *Exp. Cell Res.* 362, 386–393. doi:10.1016/j.yexcr.2017.12.001.

Mineo, M., Garfield, S. H., Taverna, S., Flugy, A., De Leo, G., Alessandro, R., et al. (2012). Exosomes released by K562 chronic myeloid leukemia cells promote angiogenesis in a Src-dependent fashion. *Angiogenesis* 15, 33–45. doi:10.1007/s10456-011-9241-1.

Miyanishi, M., Tada, K., Koike, M., Uchiyama, Y., Kitamura, T., and Nagata, S. (2007). Identification of Tim4 as a phosphatidylserine receptor. *Nature* 450, 435–439. doi:10.1038/nature06307.

Molldrem, J., Dermime, S., Parker, K., Jiang, Y. Z., Mavroudis, D., Hensel, N., et al. (1996). Targeted T-cell therapy for human leukemia: cytotoxic T lymphocytes specific for a peptide derived from proteinase 3 preferentially lyse human myeloid leukemia cells. *Blood* 88, 2450–2457.

Montecalvo, A., Larregina, A. T., Shufesky, W. J., Stolz, D. B., Sullivan, M. L. G., Karlsson, J. M., et al. (2012). Mechanism of transfer of functional microRNAs between mouse dendritic cells via exosomes. *Blood* 119, 756–766. doi:10.1182/blood-2011-02-338004.

Moravcová, J., Rulcová, J., Poláková, K. M., and Klamová, H. (2009). Control genes in international standardization of real-time RT-PCR for BCR-ABL. *Leuk. Res.* 33, 582–584. doi:10.1016/j.leukres.2008.06.020.

Morel, F., Bris, M.-J. Le, Herry, A., Calvez, G. Le, Marion, V., Abgrall, J.-F., et al. (2003). Double minutes containing amplified bcr-abl fusion gene in a case of chronic myeloid leukemia treated by imatinib. *Eur. J. Haematol.* 70, 235–239. doi:10.1034/j.1600-0609.2003.00046.x.

Morstyn, G., Sullivan, J., Fairhead, S., Cowling, D., and Hurley, T. (1981). Effects of high dose busulphan on leukaemic progenitor cells in chronic myeloid leukaemia. *Aust. N. Z. J. Med.* 11, 609–614. doi:10.1111/j.1445-5994.1981.tb03534.x.

Munich, S., Sobo-Vujanovic, A., Buchser, W. J., Beer-Stolz, D., and Vujanovic, N. L. (2012). Dendritic cell exosomes directly kill tumor cells and activate natural killer cells via TNF superfamily ligands. *Oncoimmunology* 1, 1074–1083. doi:10.4161/onci.20897.

Nagar, B., Bornmann, W. G., Pellicena, P., Schindler, T., Veach, D. R., Miller, W. T., et al. (2002). Crystal structures of the kinase domain of c-Abl in complex with the small molecule inhibitors PD173955 and imatinib (STI-571). *Cancer Res.* 62, 4236–4243.

Nagar, B., Hantschel, O., Young, M. A., Scheffzek, K., Veach, D., Bornmann, W., et al. (2003). Structural basis for the autoinhibition of c-Abl tyrosine kinase. *Cell* 112, 859–871. doi:10.1016/s0092-8674(03)00194-6.

Narita, M., Masuko, M., Kurasaki, T., Kitajima, T., Takenouchi, S., Saitoh, A., et al. (2010). WT1 peptide vaccination in combination with imatinib therapy for a patient with CML in the chronic phase. *Int. J. Med. Sci.* 7, 72–81. doi:10.7150/ijms.7.72.

Nawrath, H., and Wegener, J. W. (1997). Kinetics and state-dependent effects of verapamil on cardiac L-type calcium channels. *Naunyn. Schmiedebergs. Arch. Pharmacol.* 355, 79–86. doi:10.1007/pl00004921.

Neshat, M. S., Raitano, A. B., Wang, H. G., Reed, J. C., and Sawyers, C. L. (2000). The survival function of the Bcr-Abl oncogene is mediated by Bad-dependent and -independent pathways: roles for phosphatidylinositol 3-kinase and Raf. *Mol. Cell. Biol.* 20, 1179–1186. doi:10.1128/mcb.20.4.1179-1186.2000.

Nichols, G. L., Raines, M. A., Vera, J. C., Lacomis, L., Tempst, P., and Golde, D. W. (1994). Identification of CRKL as the constitutively phosphorylated 39-kD tyrosine phosphoprotein in chronic myelogenous leukemia cells. *Blood* 84, 2912–2918.

Nollet, M., Stalin, J., Moyon, A., Traboulsi, W., Essaadi, A., Robert, S., et al. (2017). A novel anti-CD146 antibody specifically targets cancer cells by internalizing the molecule. *Oncotarget* 8, 112283–112296. doi:10.18632/oncotarget.22736.

Nosaka, T., Kawashima, T., Misawa, K., Ikuta, K., Mui, A. L., and Kitamura, T. (1999). STAT5 as a molecular regulator of proliferation, differentiation and apoptosis in hematopoietic cells. *EMBO J.* 18, 4754–4765. doi:10.1093/emboj/18.17.4754.

Nowell, P. C. (1962). The minute chromosome (Phl) in chronic granulocytic leukemia. *Blut* 8, 65–66. doi:10.1007/BF01630378.

Nowicki, M. O., Falinski, R., Koptyra, M., Slupianek, A., Stoklosa, T., Gloc, E., et al. (2004). BCR/ABL oncogenic kinase promotes unfaithful repair of the reactive oxygen species-dependent DNA double-strand breaks. *Blood* 104, 3746–3753. doi:10.1182/blood-2004-05-1941.

O'Brien, S. G., Guilhot, F., Larson, R. A., Gathmann, I., Baccarani, M., Cervantes, F., et al. (2003). Imatinib compared with interferon and low-dose cytarabine for newly diagnosed chronic-phase chronic myeloid leukemia. *N. Engl. J. Med.* 348, 994–1004. doi:10.1056/NEJMoa022457.

O'Dwyer, M. E., Mauro, M. J., Blasdel, C., Farnsworth, M., Kurilik, G., Hsieh, Y.-C., et al. (2004). Clonal evolution and lack of cytogenetic response are adverse prognostic factors for hematologic relapse of chronic phase CML patients treated with imatinib mesylate. *Blood* 103, 451–455. doi:10.1182/blood-2003-02-0371.

O'Dwyer, M. E., Mauro, M. J., Kurilik, G., Mori, M., Balleisen, S., Olson, S., et al. (2002). The impact of clonal evolution on response to imatinib mesylate (STI571) in accelerated phase CML. *Blood* 100, 1628–1633. doi:10.1182/blood-2002-03-0777.

O'Hare, T., Deininger, M. W. N., Eide, C. A., Clackson, T., and Druker, B. J. (2011). Targeting the BCR-ABL signaling pathway in therapy-resistant Philadelphia chromosome-positive leukemia. *Clin. cancer Res. an Off. J. Am. Assoc. Cancer Res.* 17, 212–221. doi:10.1158/1078-0432.CCR-09-3314.

O'Hare, T., Shakespeare, W. C., Zhu, X., Eide, C. A., Rivera, V. M., Wang, F., et al. (2009). AP24534, a pan-BCR-ABL inhibitor for chronic myeloid leukemia, potently inhibits the T315I mutant and overcomes mutation-based resistance. *Cancer Cell* 16, 401–412. doi:10.1016/j.ccr.2009.09.028.

O'Hare, T., Walters, D. K., Stoffregen, E. P., Jia, T., Manley, P. W., Mestan, J., et al. (2005). In vitro activity of Bcr-Abl inhibitors AMN107 and BMS-354825 against clinically relevant imatinib-resistant Abl kinase domain mutants. *Cancer Res.* 65, 4500–4505.

doi:10.1158/0008-5472.CAN-05-0259.

Obukhov, A. G., and Nowycky, M. C. (2004). TRPC5 activation kinetics are modulated by the scaffolding protein ezrin/radixin/moesin-binding phosphoprotein-50 (EBP50). *J. Cell. Physiol.* 201, 227–235. doi:10.1002/jcp.20057.

Odorizzi, G., Katzmann, D. J., Babst, M., Audhya, A., and Emr, S. D. (2003). Bro1 is an endosome-associated protein that functions in the MVB pathway in Saccharomyces cerevisiae. *J. Cell Sci.* 116, 1893–1903. doi:10.1242/jcs.00395.

Packer, L. M., Rana, S., Hayward, R., O'Hare, T., Eide, C. A., Rebocho, A., et al. (2011). Nilotinib and MEK inhibitors induce synthetic lethality through paradoxical activation of RAF in drug-resistant chronic myeloid leukemia. *Cancer Cell* 20, 715–727. doi:10.1016/j.ccr.2011.11.004.

Pan, B. T., Teng, K., Wu, C., Adam, M., and Johnstone, R. M. (1985). Electron microscopic evidence for externalization of the transferrin receptor in vesicular form in sheep reticulocytes. *J. Cell Biol.* 101, 942–948. doi:10.1083/jcb.101.3.942.

Park, C. S., Lewis, A. H., Chen, T. J., Bridges, C. S., Shen, Y., Suppipat, K., et al. (2019). A KLF4-DYRK2-mediated pathway regulating self-renewal in CML stem cells. *Blood* 134, 1960–1972. doi:10.1182/blood.2018875922.

Patel, S. B., Nemkov, T., Stefanoni, D., Benavides, G. A., Bassal, M. A., Crown, B. L., et al. (2021). Metabolic alterations mediated by STAT3 promotes drug persistence in CML. *Leukemia*. doi:10.1038/s41375-021-01315-0.

Peinado, H., Aleckovic, M., Lavotshkin, S., Matei, I., Costa-Silva, B., Moreno-Bueno, G., et al. (2012). Melanoma exosomes educate bone marrow progenitor cells toward a pro-metastatic phenotype through MET. *Nat. Med.* 18, 883–891. doi:10.1038/nm.2753.

Pelletier, S. D., Hong, D. S., Hu, Y., Liu, Y., and Li, S. (2004). Lack of the adhesion molecules P-selectin and intercellular adhesion molecule-1 accelerate the development of BCR/ABL-induced chronic myeloid leukemia-like myeloproliferative disease in mice. *Blood* 104, 2163–2171. doi:10.1182/blood-2003-09-3033.

Pendergast, A. M., Muller, A. J., Havlik, M. H., Maru, Y., and Witte, O. N. (1991). BCR sequences essential for transformation by the BCR-ABL oncogene bind to the ABL SH2 regulatory domain in a non-phosphotyrosine-dependent manner. *Cell* 66, 161–171. doi:10.1016/0092-8674(91)90148-r.

Pendergast, A. M., Quilliam, L. A., Cripe, L. D., Bassing, C. H., Dai, Z., Li, N., et al. (1993). BCR-ABL-induced oncogenesis is mediated by direct interaction with the SH2 domain of the GRB-2 adaptor protein. *Cell* 75, 175–185.

Peng, B., Hayes, M., Resta, D., Racine-Poon, A., Druker, B. J., Talpaz, M., et al. (2004). Pharmacokinetics and pharmacodynamics of imatinib in a phase I trial with chronic myeloid leukemia patients. *J. Clin. Oncol. Off. J. Am. Soc. Clin. Oncol.* 22, 935–942. doi:10.1200/JCO.2004.03.050.

Petrak, J., Toman, O., Simonova, T., Halada, P., Cmejla, R., Klener, P., et al. (2009). Identification of molecular targets for selective elimination of TRAIL-resistant leukemia

cells. From spots to in vitro assays using TOP15 charts. *Proteomics* 9, 5006–5015. doi:10.1002/pmic.200900335.

Pezeshkian, B., Donnelly, C., Tamburo, K., Geddes, T., and Madlambayan, G. J. (2013). Leukemia Mediated Endothelial Cell Activation Modulates Leukemia Cell Susceptibility to Chemotherapy through a Positive Feedback Loop Mechanism. *PLoS One* 8, e60823. doi:10.1371/journal.pone.0060823.

Pinton, P., Ferrari, D., Magalhães, P., Schulze-Osthoff, K., Di Virgilio, F., Pozzan, T., et al. (2000). Reduced loading of intracellular Ca(2+) stores and downregulation of capacitative Ca(2+) influx in Bcl-2-overexpressing cells. *J. Cell Biol.* 148, 857–862. doi:10.1083/jcb.148.5.857.

Piwocka, K., Vejda, S., Cotter, T. G., O'Sullivan, G. C., and McKenna, S. L. (2006). Bcr-Abl reduces endoplasmic reticulum releasable calcium levels by a Bcl-2-independent mechanism and inhibits calcium-dependent apoptotic signaling. *Blood* 107, 4003–4010. doi:10.1182/blood-2005-04-1523.

Pluk, H., Dorey, K., and Superti-Furga, G. (2002). Autoinhibition of c-Abl. *Cell* 108, 247–259. doi:10.1016/s0092-8674(02)00623-2.

Poláková, K. M., Polívková, V., Rulcová, J., Klamová, H., Jurcek, T., Dvoráková, D., et al. (2010). Constant BCR-ABL transcript level >or=0.1% (IS) in patients with CML responding to imatinib with complete cytogenetic remission may indicate mutation analysis. *Exp. Hematol.* 38, 20–26. doi:10.1016/j.exphem.2009.10.003.

Polte, T. R., and Hanks, S. K. (1995). Interaction between focal adhesion kinase and Crk-associated tyrosine kinase substrate p130Cas. *Proc. Natl. Acad. Sci. U. S. A.* 92, 10678–10682. doi:10.1073/pnas.92.23.10678.

Pophali, P. A., and Patnaik, M. M. (2016). The Role of New Tyrosine Kinase Inhibitors in Chronic Myeloid Leukemia. *Cancer J.* 22, 40–50. doi:10.1097/PPO.0000000000000165.

Puil, L., Liu, J., Gish, G., Mbamalu, G., Bowtell, D., Pelicci, P. G., et al. (1994). Bcr-Abl oncoproteins bind directly to activators of the Ras signalling pathway. *EMBO J.* 13, 764–773.

Puttini, M., Coluccia, A. M. L., Boschelli, F., Cleris, L., Marchesi, E., Donella-Deana, A., et al. (2006). In vitro and in vivo activity of SKI-606, a novel Src-Abl inhibitor, against imatinib-resistant Bcr-Abl+ neoplastic cells. *Cancer Res.* 66, 11314–11322. doi:10.1158/0008-5472.CAN-06-1199.

Qazilbash, M. H., Wieder, E., Thall, P. F., Wang, X., Rios, R., Lu, S., et al. (2017). PR1 peptide vaccine induces specific immunity with clinical responses in myeloid malignancies. *Leukemia* 31, 697–704. doi:10.1038/leu.2016.254.

Quesnelle, K. M., Boehm, A. L., and Grandis, J. R. (2007). STAT-mediated EGFR signaling in cancer. *J. Cell. Biochem.* 102, 311–319. doi:10.1002/jcb.21475.

Quintás-Cardama, A., and Cortes, J. E. (2006). Chronic myeloid leukemia: diagnosis and treatment. *Mayo Clin. Proc.* 81, 973–988. doi:10.4065/81.7.973.

Quintás-Cardama, A., Kantarjian, H. M., and Cortes, J. E. (2009). Mechanisms of primary and secondary resistance to imatinib in chronic myeloid leukemia. *Cancer Control* 16, 122–131. doi:10.1177/107327480901600204.

Raiborg, C., Bache, K. G., Gillooly, D. J., Madshus, I. H., Stang, E., and Stenmark, H. (2002). Hrs sorts ubiquitinated proteins into clathrin-coated microdomains of early endosomes. *Nat. Cell Biol.* 4, 394–398. doi:10.1038/ncb791.

Raimondo, S., Saieva, L., Corrado, C., Fontana, S., Flugy, A., Rizzo, A., et al. (2015). Chronic myeloid leukemia-derived exosomes promote tumor growth through an autocrine mechanism. *Cell Commun. Signal.* 13, 8. doi:10.1186/s12964-015-0086-x.

Raitano, A. B., Halpern, J. R., Hambuch, T. M., and Sawyers, C. L. (1995). The Bcr-Abl leukemia oncogene activates Jun kinase and requires Jun for transformation. *Proc. Natl. Acad. Sci. U. S. A.* 92, 11746–11750. doi:10.1073/pnas.92.25.11746.

Raposo, G., Nijman, H. W., Stoorvogel, W., Liejendekker, R., Harding, C. V, Melief, C. J., et al. (1996). B lymphocytes secrete antigen-presenting vesicles. *J. Exp. Med.* 183, 1161–1172. doi:10.1084/jem.183.3.1161.

Reczek, D., Berryman, M., and Bretscher, A. (1997). Identification of EBP50: A PDZ-containing phosphoprotein that associates with members of the ezrin-radixin-moesin family. *J. Cell Biol.* 139, 169–179. doi:10.1083/jcb.139.1.169.

Reddy, E. P., Korapati, A., Chaturvedi, P., and Rane, S. (2000). IL-3 signaling and the role of Src kinases, JAKs and STATs: a covert liaison unveiled. *Oncogene* 19, 2532–2547. doi:10.1038/sj.onc.1203594.

Renshaw, M. W., Lea-Chou, E., and Wang, J. Y. (1996). Rac is required for v-Abl tyrosine kinase to activate mitogenesis. *Curr. Biol.* 6, 76–83. doi:10.1016/s0960-9822(02)00424-4.

Reuveni, H., Flashner-Abramson, E., Steiner, L., Makedonski, K., Song, R., Shir, A., et al. (2013). Therapeutic destruction of insulin receptor substrates for cancer treatment. *Cancer Res.* 73, 4383–4394. doi:10.1158/0008-5472.CAN-12-3385.

Rich, I. N., Worthington-White, D., Garden, O. A., and Musk, P. (2000). Apoptosis of leukemic cells accompanies reduction in intracellular pH after targeted inhibition of the Na(+)/H(+) exchanger. *Blood* 95, 1427–1434.

Rink, J., Ghigo, E., Kalaidzidis, Y., and Zerial, M. (2005). Rab conversion as a mechanism of progression from early to late endosomes. *Cell* 122, 735–749. doi:10.1016/j.cell.2005.06.043.

Rizzuto, R., Pinton, P., Carrington, W., Fay, F. S., Fogarty, K. E., Lifshitz, L. M., et al. (1998). Close contacts with the endoplasmic reticulum as determinants of mitochondrial Ca2+ responses. *Science* 280, 1763–1766. doi:10.1126/science.280.5370.1763.

Roche-Lestienne, C., Soenen-Cornu, V., Grardel-Duflos, N., Laï, J.-L., Philippe, N., Facon, T., et al. (2002). Several types of mutations of the Abl gene can be found in chronic myeloid leukemia patients resistant to STI571, and they can pre-exist to the onset of treatment. *Blood* 100, 1014–1018. doi:10.1182/blood.v100.3.1014.

Ron, D., Zannini, M., Lewis, M., Wickner, R. B., Hunt, L. T., Graziani, G., et al. (1991). A region of proto-dbl essential for its transforming activity shows sequence similarity to a yeast cell cycle gene, CDC24, and the human breakpoint cluster gene, bcr. *New Biol.* 3, 372–379.

Ross, D. M., Branford, S., Seymour, J. F., Schwarer, A. P., Arthur, C., Yeung, D. T., et al. (2013). Safety and efficacy of imatinib cessation for CML patients with stable undetectable minimal residual disease: results from the TWISTER study. *Blood* 122, 515–522. doi:10.1182/blood-2013-02-483750.

Rovira, P., Mascarell, L., and Truffa-Bachi, P. (2000). The impact of immunosuppressive drugs on the analysis of T cell activation. *Curr. Med. Chem.* 7, 673–692. doi:10.2174/0929867003374778.

Rowley, J. D. (1973). Letter: A new consistent chromosomal abnormality in chronic myelogenous leukaemia identified by quinacrine fluorescence and Giemsa staining. *Nature* 243, 290–293. doi:10.1038/243290a0.

Rozovski, U., Harris, D. M., Li, P., Liu, Z., Jain, P., Ferrajoli, A., et al. (2018). STAT3-activated CD36 facilitates fatty acid uptake in chronic lymphocytic leukemia cells. *Oncotarget* 9, 21268–21280. doi:10.18632/oncotarget.25066.

Rulcová, J., Zmeková, V., Zemanová, Z., Klamová, H., and Moravcová, J. (2007). The effect of total-ABL, GUS and B2M control genes on BCR-ABL monitoring by real-time RT-PCR. *Leuk. Res.* 31, 483–491. doi:10.1016/j.leukres.2006.07.021.

Sachse, M., Urbé, S., Oorschot, V., Strous, G. J., and Klumperman, J. (2002). Bilayered clathrin coats on endosomal vacuoles are involved in protein sorting toward lysosomes. *Mol. Biol. Cell* 13, 1313–1328. doi:10.1091/mbc.01-10-0525.

Saglio, G., Kim, D.-W., Issaragrisil, S., le Coutre, P., Etienne, G., Lobo, C., et al. (2010). Nilotinib versus imatinib for newly diagnosed chronic myeloid leukemia. *N. Engl. J. Med.* 362, 2251–2259. doi:10.1056/NEJMoa0912614.

Salgia, R., Li, J. L., Lo, S. H., Brunkhorst, B., Kansas, G. S., Sobhany, E. S., et al. (1995a). Molecular cloning of human paxillin, a focal adhesion protein phosphorylated by P210BCR/ABL. *J. Biol. Chem.* 270, 5039–5047. doi:10.1074/jbc.270.10.5039.

Salgia, R., Pisick, E., Sattler, M., Li, J. L., Uemura, N., Wong, W. K., et al. (1996a). p130CAS forms a signaling complex with the adapter protein CRKL in hematopoietic cells transformed by the BCR/ABL oncogene. *J. Biol. Chem.* 271, 25198–25203. doi:10.1074/jbc.271.41.25198.

Salgia, R., Sattler, M., Pisick, E., Li, J. L., and Griffin, J. D. (1996b). p210BCR/ABL induces formation of complexes containing focal adhesion proteins and the protooncogene product p120c-Cbl. *Exp. Hematol.* 24, 310–313.

Salgia, R., Uemura, N., Okuda, K., Li, J. L., Pisick, E., Sattler, M., et al. (1995b). CRKL links p210BCR/ABL with paxillin in chronic myelogenous leukemia cells. *J. Biol. Chem.* 270, 29145–29150. doi:10.1074/jbc.270.49.29145.

Samanta, A. K., Chakraborty, S. N., Wang, Y., Schlette, E., Reddy, E. P., and Arlinghaus, R. B.

(2010). Destabilization of Bcr-Abl/Jak2 Network by a Jak2/Abl Kinase Inhibitor ON044580 Overcomes Drug Resistance in Blast Crisis Chronic Myelogenous Leukemia (CML). *Genes Cancer* 1, 346–359. doi:10.1177/1947601910372232.

Sanchez-Lopez, E., Flashner-Abramson, E., Shalapour, S., Zhong, Z., Taniguchi, K., Levitzki, A., et al. (2016). Targeting colorectal cancer via its microenvironment by inhibiting IGF-1 receptor-insulin receptor substrate and STAT3 signaling. *Oncogene* 35, 2634–2644. doi:10.1038/onc.2015.326.

Sassano, M. L., van Vliet, A. R., and Agostinis, P. (2017). Mitochondria-Associated Membranes As Networking Platforms and Regulators of Cancer Cell Fate. *Front. Oncol.* 7, 174. doi:10.3389/fonc.2017.00174.

Sattler, M., Mohi, M. G., Pride, Y. B., Quinnan, L. R., Malouf, N. A., Podar, K., et al. (2002). Critical role for Gab2 in transformation by BCR/ABL. *Cancer Cell* 1, 479–492. doi:10.1016/s1535-6108(02)00074-0.

Sattler, M., Salgia, R., Shrikhande, G., Verma, S., Uemura, N., Law, S. F., et al. (1997). Differential signaling after beta1 integrin ligation is mediated through binding of CRKL to p120(CBL) and p110(HEF1). *J. Biol. Chem.* 272, 14320–14326. doi:10.1074/jbc.272.22.14320.

Sattler, M., Verma, S., Shrikhande, G., Byrne, C. H., Pride, Y. B., Winkler, T., et al. (2000). The BCR/ABL tyrosine kinase induces production of reactive oxygen species in hematopoietic cells. *J. Biol. Chem.* 275, 24273–24278. doi:10.1074/jbc.M002094200.

Savina, A., Furlán, M., Vidal, M., and Colombo, M. I. (2003). Exosome release is regulated by a calcium-dependent mechanism in K562 cells. *J. Biol. Chem.* 278, 20083–20090. doi:10.1074/jbc.M301642200.

Sawyers, C. L., McLaughlin, J., and Witte, O. N. (1995). Genetic requirement for Ras in the transformation of fibroblasts and hematopoietic cells by the Bcr-Abl oncogene. *J. Exp. Med.* 181, 307–313. doi:10.1084/jem.181.1.307.

Schepers, K., Pietras, E. M., Reynaud, D., Flach, J., Binnewies, M., Garg, T., et al. (2013). Myeloproliferative neoplasia remodels the endosteal bone marrow niche into a self-reinforcing leukemic niche. *Cell Stem Cell* 13, 285–299. doi:10.1016/j.stem.2013.06.009.

Schindler, C., Shuai, K., Prezioso, V. R., and Darnell, J. E. J. (1992). Interferon-dependent tyrosine phosphorylation of a latent cytoplasmic transcription factor. *Science* 257, 809–813. doi:10.1126/science.1496401.

Schindler, T., Bornmann, W., Pellicena, P., Miller, W. T., Clarkson, B., and Kuriyan, J. (2000). Structural mechanism for STI-571 inhibition of abelson tyrosine kinase. *Science* 289, 1938–1942. doi:10.1126/science.289.5486.1938.

Schoch, C., Haferlach, T., Kern, W., Schnittger, S., Berger, U., Hehlmann, R., et al. (2003). Occurrence of additional chromosome aberrations in chronic myeloid leukemia patients treated with imatinib mesylate. *Leukemia* 17, 461–463. doi:10.1038/sj.leu.2402813.

Scopim-Ribeiro, R., Machado-Neto, J. A., Eide, C. A., Coelho-Silva, J. L., Fenerich, B. A., Fernandes, J. C., et al. (2021). NT157, an IGF1R-IRS1/2 inhibitor, exhibits antineoplastic

effects in pre-clinical models of chronic myeloid leukemia. *Invest. New Drugs* 39, 736–746. doi:10.1007/s10637-020-01028-8.

Sefton, B. M., Trowbridge, I. S., Cooper, J. A., and Scolnick, E. M. (1982). The transforming proteins of Rous sarcoma virus, Harvey sarcoma virus and Abelson virus contain tightly bound lipid. *Cell* 31, 465–474. doi:10.1016/0092-8674(82)90139-8.

Segura, E., Guérin, C., Hogg, N., Amigorena, S., and Théry, C. (2007). CD8+ dendritic cells use LFA-1 to capture MHC-peptide complexes from exosomes in vivo. *J. Immunol.* 179, 1489–1496. doi:10.4049/jimmunol.179.3.1489.

Segura, E., Nicco, C., Lombard, B., Véron, P., Raposo, G., Batteux, F., et al. (2005). ICAM-1 on exosomes from mature dendritic cells is critical for efficient naive T-cell priming. *Blood* 106, 216–223. doi:10.1182/blood-2005-01-0220.

Senechal, K., Halpern, J., and Sawyers, C. L. (1996). The CRKL adaptor protein transforms fibroblasts and functions in transformation by the BCR-ABL oncogene. *J. Biol. Chem.* 271, 23255–23261. doi:10.1074/jbc.271.38.23255.

Shah, N. P., Kantarjian, H. M., Kim, D.-W., Réa, D., Dorlhiac-Llacer, P. E., Milone, J. H., et al. (2008). Intermittent target inhibition with dasatinib 100 mg once daily preserves efficacy and improves tolerability in imatinib-resistant and -intolerant chronic-phase chronic myeloid leukemia. *J. Clin. Oncol. Off. J. Am. Soc. Clin. Oncol.* 26, 3204–3212. doi:10.1200/JCO.2007.14.9260.

Shah, N. P., Nicoll, J. M., Nagar, B., Gorre, M. E., Paquette, R. L., Kuriyan, J., et al. (2002). Multiple BCR-ABL kinase domain mutations confer polyclonal resistance to the tyrosine kinase inhibitor imatinib (STI571) in chronic phase and blast crisis chronic myeloid leukemia. *Cancer Cell* 2, 117–125. doi:10.1016/s1535-6108(02)00096-x.

Shah, N. P., Skaggs, B. J., Branford, S., Hughes, T. P., Nicoll, J. M., Paquette, R. L., et al. (2007). Sequential ABL kinase inhibitor therapy selects for compound drug-resistant BCR-ABL mutations with altered oncogenic potency. *J. Clin. Invest.* 117, 2562–2569. doi:10.1172/JCI30890.

Shah, N. P., Tran, C., Lee, F. Y., Chen, P., Norris, D., and Sawyers, C. L. (2004). Overriding imatinib resistance with a novel ABL kinase inhibitor. *Science* 305, 399–401. doi:10.1126/science.1099480.

Shi, P., Chandra, J., Sun, X., Gergely, M., Cortes, J. E., Garcia-Manero, G., et al. (2010). Inhibition of IGF-IR tyrosine kinase induces apoptosis and cell cycle arrest in imatinib-resistant chronic myeloid leukaemia cells. *J. Cell. Mol. Med.* 14, 1777–1792. doi:10.1111/j.1582-4934.2009.00795.x.

Shtivelman, E., Lifshitz, B., Gale, R. P., and Canaani, E. (1985). Fused transcript of abl and bcr genes in chronic myelogenous leukaemia. *Nature* 315, 550–554. doi:10.1038/315550a0.

Shtivelman, E., Lifshitz, B., Gale, R. P., Roe, B. A., and Canaani, E. (1986). Alternative splicing of RNAs transcribed from the human abl gene and from the bcr-abl fused gene. *Cell* 47, 277–284. doi:10.1016/0092-8674(86)90450-2.

Sillaber, C., Gesbert, F., Frank, D. A., Sattler, M., and Griffin, J. D. (2000). STAT5 activation

contributes to growth and viability in Bcr/Abl-transformed cells. *Blood* 95, 2118–2125.

Silver, R. T., Woolf, S. H., Hehlmann, R., Appelbaum, F. R., Anderson, J., Bennett, C., et al. (1999). An evidence-based analysis of the effect of busulfan, hydroxyurea, interferon, and allogeneic bone marrow transplantation in treating the chronic phase of chronic myeloid leukemia: developed for the American Society of Hematology. *Blood* 94, 1517–1536.

Skog, J., Würdinger, T., van Rijn, S., Meijer, D. H., Gainche, L., Sena-Esteves, M., et al. (2008). Glioblastoma microvesicles transport RNA and proteins that promote tumour growth and provide diagnostic biomarkers. *Nat. Cell Biol.* 10, 1470–1476. doi:10.1038/ncb1800.

Skorski, T., Kanakaraj, P., Nieborowska-Skorska, M., Ratajczak, M. Z., Wen, S. C., Zon, G., et al. (1995a). Phosphatidylinositol-3 kinase activity is regulated by BCR/ABL and is required for the growth of Philadelphia chromosome-positive cells. *Blood* 86, 726–736.

Skorski, T., Nieborowska-Skorska, M., Szczylik, C., Kanakaraj, P., Perrotti, D., Zon, G., et al. (1995b). C-RAF-1 serine/threonine kinase is required in BCR/ABL-dependent and normal hematopoiesis. *Cancer Res.* 55, 2275–2278.

Skorski, T., Wlodarski, P., Daheron, L., Salomoni, P., Nieborowska-Skorska, M., Majewski, M., et al. (1998). BCR/ABL-mediated leukemogenesis requires the activity of the small GTP-binding protein Rac. *Proc. Natl. Acad. Sci. U. S. A.* 95, 11858–11862. doi:10.1073/pnas.95.20.11858.

Smith, B. D., Kasamon, Y. L., Kowalski, J., Gocke, C., Murphy, K., Miller, C. B., et al. (2010). K562/GM-CSF immunotherapy reduces tumor burden in chronic myeloid leukemia patients with residual disease on imatinib mesylate. *Clin. cancer Res. an Off. J. Am. Assoc. Cancer Res.* 16, 338–347. doi:10.1158/1078-0432.CCR-09-2046.

Smith, K. M., Yacobi, R., and Van Etten, R. A. (2003). Autoinhibition of Bcr-Abl through its SH3 domain. *Mol. Cell* 12, 27–37. doi:10.1016/s1097-2765(03)00274-0.

Stalin, J., Nollet, M., Dignat-George, F., Bardin, N., and Blot-Chabaud, M. (2017). Therapeutic and Diagnostic Antibodies to CD146: Thirty Years of Research on Its Potential for Detection and Treatment of Tumors. *Antibodies (Basel, Switzerland)* 6. doi:10.3390/antib6040017.

Stam, K., Heisterkamp, N., Grosveld, G., de Klein, A., Verma, R. S., Coleman, M., et al. (1985). Evidence of a new chimeric bcr/c-abl mRNA in patients with chronic myelocytic leukemia and the Philadelphia chromosome. *N. Engl. J. Med.* 313, 1429–1433. doi:10.1056/NEJM198512053132301.

Statello, L., Maugeri, M., Garre, E., Nawaz, M., Wahlgren, J., Papadimitriou, A., et al. (2018). Identification of RNA-binding proteins in exosomes capable of interacting with different types of RNA: RBP-facilitated transport of RNAs into exosomes. *PLoS One* 13, e0195969. doi:10.1371/journal.pone.0195969.

Steinbichler, T. B., Dudas, J., Skvortsov, S., Ganswindt, U., Riechelmann, H., and Skvortsova, I.-I. (2019). Therapy resistance mediated by exosomes. *Mol. Cancer* 18, 58. doi:10.1186/s12943-019-0970-x.

Stelzer, G., Rosen, N., Plaschkes, I., Zimmerman, S., Twik, M., Fishilevich, S., et al. (2016). The GeneCards Suite: From Gene Data Mining to Disease Genome Sequence Analyses. *Curr. Protoc. Bioinforma.* 54, 1.30.1-1.30.33. doi:10.1002/cpbi.5.

Stenqvist, A.-C., Nagaeva, O., Baranov, V., and Mincheva-Nilsson, L. (2013). Exosomes secreted by human placenta carry functional Fas ligand and TRAIL molecules and convey apoptosis in activated immune cells, suggesting exosome-mediated immune privilege of the fetus. *J. Immunol.* 191, 5515–5523. doi:10.4049/jimmunol.1301885.

Stier, S., Ko, Y., Forkert, R., Lutz, C., Neuhaus, T., Grünewald, E., et al. (2005). Osteopontin is a hematopoietic stem cell niche component that negatively regulates stem cell pool size. *J. Exp. Med.* 201, 1781–1791. doi:10.1084/jem.20041992.

Storch, U., Forst, A.-L., Pardatscher, F., Erdogmus, S., Philipp, M., Gregoritza, M., et al. (2017). Dynamic NHERF interaction with TRPC4/5 proteins is required for channel gating by diacylglycerol. *Proc. Natl. Acad. Sci. U. S. A.* 114, E37–E46. doi:10.1073/pnas.1612263114.

Strack, B., Calistri, A., Craig, S., Popova, E., and Göttlinger, H. G. (2003). AIP1/ALIX is a binding partner for HIV-1 p6 and EIAV p9 functioning in virus budding. *Cell* 114, 689–699. doi:10.1016/s0092-8674(03)00653-6.

Su, T., Huang, C., Yang, C., Jiang, T., Su, J., Chen, M., et al. (2020). Apigenin inhibits STAT3/CD36 signaling axis and reduces visceral obesity. *Pharmacol. Res.* 152, 104586. doi:10.1016/j.phrs.2019.104586.

Svensson, K. J., Christianson, H. C., Wittrup, A., Bourseau-Guilmain, E., Lindqvist, E., Svensson, L. M., et al. (2013). Exosome uptake depends on ERK1/2-heat shock protein 27 signaling and lipid Raft-mediated endocytosis negatively regulated by caveolin-1. *J. Biol. Chem.* 288, 17713–17724. doi:10.1074/jbc.M112.445403.

Szczepanski, M. J., Szajnik, M., Welsh, A., Whiteside, T. L., and Boyiadzis, M. (2011). Blast-derived microvesicles in sera from patients with acute myeloid leukemia suppress natural killer cell function via membrane-associated transforming growth factor-beta1. *Haematologica* 96, 1302–1309. doi:10.3324/haematol.2010.039743.

Taagepera, S., McDonald, D., Loeb, J. E., Whitaker, L. L., McElroy, A. K., Wang, J. Y., et al. (1998). Nuclear-cytoplasmic shuttling of C-ABL tyrosine kinase. *Proc. Natl. Acad. Sci. U. S. A.* 95, 7457–7462. doi:10.1073/pnas.95.13.7457.

Tadokoro, H., Umezu, T., Ohyashiki, K., Hirano, T., and Ohyashiki, J. H. (2013). Exosomes derived from hypoxic leukemia cells enhance tube formation in endothelial cells. *J. Biol. Chem.* 288, 34343–34351. doi:10.1074/jbc.M113.480822.

Talpaz, M., McCredie, K., Kantarjian, H., Trujillo, J., Keating, M., and Gutterman, J. (1986). Chronic myelogenous leukaemia: haematological remissions with alpha interferon. *Br. J. Haematol.* 64, 87–95. doi:10.1111/j.1365-2141.1986.tb07576.x.

Talpaz, M., Shah, N. P., Kantarjian, H., Donato, N., Nicoll, J., Paquette, R., et al. (2006). Dasatinib in imatinib-resistant Philadelphia chromosome-positive leukemias. *N. Engl. J. Med.* 354, 2531–2541. doi:10.1056/NEJMoa055229.

Tamma, R., and Ribatti, D. (2017). Bone Niches, Hematopoietic Stem Cells, and Vessel Formation. *Int. J. Mol. Sci.* 18. doi:10.3390/ijms18010151.

Tammineni, P., Anugula, C., Mohammed, F., Anjaneyulu, M., Larner, A. C., and Sepuri, N. B. V. (2013). The import of the transcription factor STAT3 into mitochondria depends on GRIM-19, a component of the electron transport chain. *J. Biol. Chem.* 288, 4723–4732. doi:10.1074/jbc.M112.378984.

Tang, Y., Tang, J., Chen, Z., Trost, C., Flockerzi, V., Li, M., et al. (2000). Association of mammalian trp4 and phospholipase C isozymes with a PDZ domain-containing protein, NHERF. *J. Biol. Chem.* 275, 37559–37564. doi:10.1074/jbc.M006635200.

Tauchi, T., Miyazawa, K., Ohyashiki, K., and Toyama, K. (1996). A coiled-coil tetramerization domain of BCR-ABL is essential for the interactions of SH2-containing signal transduction molecules. *Hum. Cell* 9, 333–336.

Taverna, S., Flugy, A., Saieva, L., Kohn, E. C., Santoro, A., Meraviglia, S., et al. (2012). Role of exosomes released by chronic myelogenous leukemia cells in angiogenesis. *Int. J. cancer* 130, 2033–2043. doi:10.1002/ijc.26217.

Taylor, D. D., Gerçel-Taylor, C., Lyons, K. S., Stanson, J., and Whiteside, T. L. (2003). T-cell apoptosis and suppression of T-cell receptor/CD3-zeta by Fas ligand-containing membrane vesicles shed from ovarian tumors. *Clin. cancer Res. an Off. J. Am. Assoc. Cancer Res.* 9, 5113–5119.

Teis, D., Saksena, S., and Emr, S. D. (2008). Ordered assembly of the ESCRT-III complex on endosomes is required to sequester cargo during MVB formation. *Dev. Cell* 15, 578–589. doi:10.1016/j.devcel.2008.08.013.

Teo, H., Gill, D. J., Sun, J., Perisic, O., Veprintsev, D. B., Vallis, Y., et al. (2006). ESCRT-I core and ESCRT-II GLUE domain structures reveal role for GLUE in linking to ESCRT-I and membranes. *Cell* 125, 99–111. doi:10.1016/j.cell.2006.01.047.

Teo, H., Perisic, O., González, B., and Williams, R. L. (2004). ESCRT-II, an endosome-associated complex required for protein sorting: crystal structure and interactions with ESCRT-III and membranes. *Dev. Cell* 7, 559–569. doi:10.1016/j.devcel.2004.09.003.

Thakur, B. K., Zhang, H., Becker, A., Matei, I., Huang, Y., Costa-Silva, B., et al. (2014). Double-stranded DNA in exosomes: a novel biomarker in cancer detection. *Cell Res.* 24, 766–769. doi:10.1038/cr.2014.44.

Thastrup, O., Cullen, P. J., Drøbak, B. K., Hanley, M. R., and Dawson, A. P. (1990). Thapsigargin, a tumor promoter, discharges intracellular Ca2+ stores by specific inhibition of the endoplasmic reticulum Ca2(+)-ATPase. *Proc. Natl. Acad. Sci. U. S. A.* 87, 2466–2470. doi:10.1073/pnas.87.7.2466.

Thery, C., Amigorena, S., Raposo, G., and Clayton, A. (2006). Isolation and characterization of exosomes from cell culture supernatants and biological fluids. *Curr. Protoc. cell Biol.* Chapter 3, Unit 3.22. doi:10.1002/0471143030.cb0322s30.

Théry, C., Boussac, M., Véron, P., Ricciardi-Castagnoli, P., Raposo, G., Garin, J., et al. (2001). Proteomic analysis of dendritic cell-derived exosomes: a secreted subcellular

compartment distinct from apoptotic vesicles. *J. Immunol.* 166, 7309–7318. doi:10.4049/jimmunol.166.12.7309.

Théry, C., Regnault, A., Garin, J., Wolfers, J., Zitvogel, L., Ricciardi-Castagnoli, P., et al. (1999). Molecular characterization of dendritic cell-derived exosomes. Selective accumulation of the heat shock protein hsc73. *J. Cell Biol.* 147, 599–610. doi:10.1083/jcb.147.3.599.

Thomas, J., Wang, L., Clark, R. E., and Pirmohamed, M. (2004). Active transport of imatinib into and out of cells: implications for drug resistance. *Blood* 104, 3739–3745. doi:10.1182/blood-2003-12-4276.

Tian, T., Wang, Y., Wang, H., Zhu, Z., and Xiao, Z. (2010). Visualizing of the cellular uptake and intracellular trafficking of exosomes by live-cell microscopy. *J. Cell. Biochem.* 111, 488–496. doi:10.1002/jcb.22733.

Tian, T., Zhu, Y.-L., Hu, F.-H., Wang, Y.-Y., Huang, N.-P., and Xiao, Z.-D. (2013). Dynamics of exosome internalization and trafficking. *J. Cell. Physiol.* 228, 1487–1495. doi:10.1002/jcp.24304.

Tian, T., Zhu, Y.-L., Zhou, Y.-Y., Liang, G.-F., Wang, Y.-Y., Hu, F.-H., et al. (2014). Exosome uptake through clathrin-mediated endocytosis and macropinocytosis and mediating miR-21 delivery. *J. Biol. Chem.* 289, 22258–22267. doi:10.1074/jbc.M114.588046.

Toman, O., Kabickova, T., Vit, O., Fiser, R., Polakova, K. M., Zach, J., et al. (2016). Proteomic analysis of imatinib-resistant CML-T1 cells reveals calcium homeostasis as a potential therapeutic target. *Oncol. Rep.* 36, 1258–1268. doi:10.3892/or.2016.4945.

Traer, E., MacKenzie, R., Snead, J., Agarwal, A., Eiring, A. M., O'Hare, T., et al. (2012). Blockade of JAK2-mediated extrinsic survival signals restores sensitivity of CML cells to ABL inhibitors. *Leukemia* 26, 1140–1143. doi:10.1038/leu.2011.325.

Trajkovic, K., Hsu, C., Chiantia, S., Rajendran, L., Wenzel, D., Wieland, F., et al. (2008). Ceramide triggers budding of exosome vesicles into multivesicular endosomes. *Science* 319, 1244–1247. doi:10.1126/science.1153124.

Triggle, D. J. (2006). L-type calcium channels. *Curr. Pharm. Des.* 12, 443–457. doi:10.2174/138161206775474503.

Tripathi, S. C., Fahrmann, J. F., Celiktas, M., Aguilar, M., Marini, K. D., Jolly, M. K., et al. (2017). MCAM Mediates Chemoresistance in Small-Cell Lung Cancer via the PI3K/AKT/SOX2 Signaling Pathway. *Cancer Res.* 77, 4414–4425. doi:10.1158/0008-5472.CAN-16-2874.

Tyanova, S., Temu, T., Sinitcyn, P., Carlson, A., Hein, M. Y., Geiger, T., et al. (2016). The Perseus computational platform for comprehensive analysis of (prote)omics data. *Nat. Methods* 13, 731–740. doi:10.1038/nmeth.3901.

Uemura, N., Salgia, R., Ewaniuk, D. S., Little, M. T., and Griffin, J. D. (1999). Involvement of the adapter protein CRKL in integrin-mediated adhesion. *Oncogene* 18, 3343–3353. doi:10.1038/sj.onc.1202689.

Umezu, T., Ohyashiki, K., Kuroda, M., and Ohyashiki, J. H. (2013). Leukemia cell to endothelial cell communication via exosomal miRNAs. *Oncogene* 32, 2747–2755. doi:10.1038/onc.2012.295.

Valadi, H., Ekstrom, K., Bossios, A., Sjostrand, M., Lee, J. J., and Lotvall, J. O. (2007). Exosome-mediated transfer of mRNAs and microRNAs is a novel mechanism of genetic exchange between cells. *Nat. Cell Biol.* 9, 654–659. doi:10.1038/ncb1596.

Van Etten, R. A., Jackson, P., and Baltimore, D. (1989). The mouse type IV c-abl gene product is a nuclear protein, and activation of transforming ability is associated with cytoplasmic localization. *Cell* 58, 669–678. doi:10.1016/0092-8674(89)90102-5.

van Niel, G., Charrin, S., Simoes, S., Romao, M., Rochin, L., Saftig, P., et al. (2011). The tetraspanin CD63 regulates ESCRT-independent and -dependent endosomal sorting during melanogenesis. *Dev. Cell* 21, 708–721. doi:10.1016/j.devcel.2011.08.019.

Verfaillie, C. M., Hurley, R., Zhao, R. C., Prosper, F., Delforge, M., and Bhatia, R. (1997). Pathophysiology of CML: do defects in integrin function contribute to the premature circulation and massive expansion of the BCR/ABL positive clone? *J. Lab. Clin. Med.* 129, 584–591. doi:10.1016/s0022-2143(97)90192-x.

Villarroya-Beltri, C., Baixauli, F., Mittelbrunn, M., Fernández-Delgado, I., Torralba, D., Moreno-Gonzalo, O., et al. (2016). ISGylation controls exosome secretion by promoting lysosomal degradation of MVB proteins. *Nat. Commun.* 7, 13588. doi:10.1038/ncomms13588.

Waas, M., Snarrenberg, S. T., Littrell, J., Jones Lipinski, R. A., Hansen, P. A., Corbett, J. A., et al. (2020). SurfaceGenie: a web-based application for prioritizing cell-type specific marker candidates. *Bioinformatics*. doi:10.1093/bioinformatics/btaa092.

Wagle, M., Eiring, A. M., Wongchenko, M., Lu, S., Guan, Y., Wang, Y., et al. (2016). A role for FOXO1 in BCR-ABL1-independent tyrosine kinase inhibitor resistance in chronic myeloid leukemia. *Leukemia* 30, 1493–1501. doi:10.1038/leu.2016.51.

Wang, H., Tang, F., Bian, E., Zhang, Y., Ji, X., Yang, Z., et al. (2020). IFITM3/STAT3 axis promotes glioma cells invasion and is modulated by TGF-beta. *Mol. Biol. Rep.* 47, 433–441. doi:10.1007/s11033-019-05146-2.

Wang, J. Y., Ledley, F., Goff, S., Lee, R., Groner, Y., and Baltimore, D. (1984). The mouse c-abl locus: molecular cloning and characterization. *Cell* 36, 349–356. doi:10.1016/0092-8674(84)90228-9.

Wang, T., Fahrmann, J. F., Lee, H., Li, Y.-J., Tripathi, S. C., Yue, C., et al. (2018). JAK/STAT3-Regulated Fatty Acid β-Oxidation Is Critical for Breast Cancer Stem Cell Self-Renewal and Chemoresistance. *Cell Metab.* 27, 136-150.e5. doi:10.1016/j.cmet.2017.11.001.

Waraky, A., Akopyan, K., Parrow, V., Strömberg, T., Axelson, M., Abrahmsén, L., et al. (2014). Picropodophyllin causes mitotic arrest and catastrophe by depolymerizing microtubules via insulin-like growth factor-1 receptor-independent mechanism. *Oncotarget* 5, 8379–8392. doi:10.18632/oncotarget.2292.

Watson-Hurst, K., and Becker, D. (2006). The role of N-cadherin, MCAM and beta3 integrin in melanoma progression, proliferation, migration and invasion. *Cancer Biol. Ther.* 5, 1375–1382. doi:10.4161/cbt.5.10.3241.

Wegrzyn, J., Potla, R., Chwae, Y.-J., Sepuri, N. B. V, Zhang, Q., Koeck, T., et al. (2009). Function of mitochondrial Stat3 in cellular respiration. *Science* 323, 793–797. doi:10.1126/science.1164551.

Wei, Y., Wang, D., Jin, F., Bian, Z., Li, L., Liang, H., et al. (2017). Pyruvate kinase type M2 promotes tumour cell exosome release via phosphorylating synaptosome-associated protein 23. *Nat. Commun.* 8, 14041. doi:10.1038/ncomms14041.

Weisberg, E., Manley, P. W., Breitenstein, W., Brüggen, J., Cowan-Jacob, S. W., Ray, A., et al. (2005). Characterization of AMN107, a selective inhibitor of native and mutant Bcr-Abl. *Cancer Cell* 7, 129–141. doi:10.1016/j.ccr.2005.01.007.

Wen, Z., Zhong, Z., and Darnell, J. E. J. (1995). Maximal activation of transcription by Stat1 and Stat3 requires both tyrosine and serine phosphorylation. *Cell* 82, 241–250. doi:10.1016/0092-8674(95)90311-9.

Wheeler, D. S., Barrick, S. R., Grubisha, M. J., Brufsky, A. M., Friedman, P. A., and Romero, G. (2011). Direct interaction between NHERF1 and Frizzled regulates β-catenin signaling. *Oncogene* 30, 32–42. doi:10.1038/onc.2010.389.

White, D. L., Saunders, V. A., Dang, P., Engler, J., Venables, A., Zrim, S., et al. (2007). Most CML patients who have a suboptimal response to imatinib have low OCT-1 activity: higher doses of imatinib may overcome the negative impact of low OCT-1 activity. *Blood* 110, 4064–4072. doi:10.1182/blood-2007-06-093617.

White, H., Deprez, L., Corbisier, P., Hall, V., Lin, F., Mazoua, S., et al. (2015). A certified plasmid reference material for the standardisation of BCR-ABL1 mRNA quantification by real-time quantitative PCR. *Leukemia* 29, 369–376. doi:10.1038/leu.2014.217.

Wisniewski, J. R., Zougman, A., and Mann, M. (2009). Combination of FASP and StageTip-based fractionation allows in-depth analysis of the hippocampal membrane proteome. *J. Proteome Res.* 8, 5674–5678. doi:10.1021/pr900748n.

Wong, S., McLaughlin, J., Cheng, D., and Witte, O. N. (2003). Cell context-specific effects of the BCR-ABL oncogene monitored in hematopoietic progenitors. *Blood* 101, 4088–4097. doi:10.1182/blood-2002-11-3376.

Wu, G.-J., and Dickerson, E. B. (2014). Frequent and increased expression of human METCAM/MUC18 in cancer tissues and metastatic lesions is associated with the clinical progression of human ovarian carcinoma. *Taiwan. J. Obstet. Gynecol.* 53, 509–517. doi:10.1016/j.tjog.2014.03.003.

Wu, X., Dao Thi, V. L., Huang, Y., Billerbeck, E., Saha, D., Hoffmann, H.-H., et al. (2018). Intrinsic Immunity Shapes Viral Resistance of Stem Cells. *Cell* 172, 423-438.e25. doi:10.1016/j.cell.2017.11.018.

Wu, X., Sooman, L., Wickström, M., Fryknäs, M., Dyrager, C., Lennartsson, J., et al. (2013). Alternative cytotoxic effects of the postulated IGF-IR inhibitor picropodophyllin in vitro.

Mol. Cancer Ther. 12, 1526–1536. doi:10.1158/1535-7163.MCT-13-0091.

Wylie, A. A., Schoepfer, J., Jahnke, W., Cowan-Jacob, S. W., Loo, A., Furet, P., et al. (2017). The allosteric inhibitor ABL001 enables dual targeting of BCR-ABL1. *Nature* 543, 733–737. doi:10.1038/nature21702.

Xie, J., Chen, X., Zheng, J., Li, C., Stacy, S., Holzenberger, M., et al. (2015). IGF-IR determines the fates of BCR/ABL leukemia. *J. Hematol. Oncol.* 8, 3. doi:10.1186/s13045-015-0106-8.

Xie, M., Lu, C., Wang, J., McLellan, M. D., Johnson, K. J., Wendl, M. C., et al. (2014). Age-related mutations associated with clonal hematopoietic expansion and malignancies. *Nat. Med.* 20, 1472–1478. doi:10.1038/nm.3733.

Xiong, A., Yang, Z., Shen, Y., Zhou, J., and Shen, Q. (2014). Transcription Factor STAT3 as a Novel Molecular Target for Cancer Prevention. *Cancers (Basel).* 6, 926–957. doi:10.3390/cancers6020926.

Xu, L., Zhou, R., Yuan, L., Wang, S., Li, X., Ma, H., et al. (2017). IGF1/IGF1R/STAT3 signaling-inducible IFITM2 promotes gastric cancer growth and metastasis. *Cancer Lett.* 393, 76–85. doi:10.1016/j.canlet.2017.02.014.

Yamamoto, C., Nakashima, H., Ikeda, T., Kawaguchi, S.-I., Toda, Y., Ito, S., et al. (2019). Analysis of the cost-effectiveness of treatment strategies for CML with incorporation of treatment discontinuation. *Blood Adv.* 3, 3266–3277. doi:10.1182/bloodadvances.2019000745.

Yang, M., Gao, H., Chen, P., Jia, J., and Wu, S. (2013). Knockdown of interferon-induced transmembrane protein 3 expression suppresses breast cancer cell growth and colony formation and affects the cell cycle. *Oncol. Rep.* 30, 171–178. doi:10.3892/or.2013.2428.

Ye, H., Adane, B., Khan, N., Sullivan, T., Minhajuddin, M., Gasparetto, M., et al. (2016). Leukemic Stem Cells Evade Chemotherapy by Metabolic Adaptation to an Adipose Tissue Niche. *Cell Stem Cell* 19, 23–37. doi:10.1016/j.stem.2016.06.001.

Yoffe, G., Blick, M., Kantarjian, H., Spitzer, G., Gutterman, J., and Talpaz, M. (1987). Molecular analysis of interferon-induced suppression of Philadelphia chromosome in patients with chronic myeloid leukemia. *Blood* 69, 961–963.

Yoshii, Y., Furukawa, T., Saga, T., and Fujibayashi, Y. (2015). Acetate/acetyl-CoA metabolism associated with cancer fatty acid synthesis: overview and application. *Cancer Lett.* 356, 211–216. doi:10.1016/j.canlet.2014.02.019.

Yotnda, P., Firat, H., Garcia-Pons, F., Garcia, Z., Gourru, G., Vernant, J. P., et al. (1998). Cytotoxic T cell response against the chimeric p210 BCR-ABL protein in patients with chronic myelogenous leukemia. *J. Clin. Invest.* 101, 2290–2296. doi:10.1172/JCI488.

Zhang, D., Wang, H., He, H., Niu, H., and Li, Y. (2017). Interferon induced transmembrane protein 3 regulates the growth and invasion of human lung adenocarcinoma. *Thorac. cancer* 8, 337–343. doi:10.1111/1759-7714.12451.

Zhang, J., Niu, C., Ye, L., Huang, H., He, X., Tong, W.-G., et al. (2003). Identification of the

haematopoietic stem cell niche and control of the niche size. *Nature* 425, 836–841. doi:10.1038/nature02041.

Zhang, X., Yang, Y., Yang, Y., Chen, H., Tu, H., and Li, J. (2020). Exosomes from Bone Marrow Microenvironment-Derived Mesenchymal Stem Cells Affect CML Cells Growth and Promote Drug Resistance to Tyrosine Kinase Inhibitors. *Stem Cells Int.* 2020, 8890201. doi:10.1155/2020/8890201.

Zhao, C., Blum, J., Chen, A., Kwon, H. Y., Jung, S. H., Cook, J. M., et al. (2007). Loss of beta-catenin impairs the renewal of normal and CML stem cells in vivo. *Cancer Cell* 12, 528–541. doi:10.1016/j.ccr.2007.11.003.

Zhao, C., Chen, A., Jamieson, C. H., Fereshteh, M., Abrahamsson, A., Blum, J., et al. (2009). Hedgehog signalling is essential for maintenance of cancer stem cells in myeloid leukaemia. *Nature* 458, 776–779. doi:10.1038/nature07737.

Zheng, Y., Tu, C., Zhang, J., and Wang, J. (2019). Inhibition of multiple myeloma-derived exosomes uptake suppresses the functional response in bone marrow stromal cell. *Int. J. Oncol.* 54, 1061–1070. doi:10.3892/ijo.2019.4685.

Zhu, S., Soutto, M., Chen, Z., Blanca Piazuelo, M., Kay Washington, M., Belkhiri, A., et al. (2019). Activation of IGF1R by DARPP-32 promotes STAT3 signaling in gastric cancer cells. *Oncogene* 38, 5805–5816. doi:10.1038/s41388-019-0843-1.

Zong, C. S., Chan, J., Levy, D. E., Horvath, C., Sadowski, H. B., and Wang, L. H. (2000). Mechanism of STAT3 activation by insulin-like growth factor I receptor. *J. Biol. Chem.* 275, 15099–15105. doi:10.1074/jbc.M000089200.

10. Reprint of publications

1) Proteomic analysis of imatinib-resistant CML-T1 cells reveals calcium homeostasis as a potential therapeutic target

Toman O, **Kabickova T**, Vit O, Fiser R, Polakova KM, Zach J, Linhartova J, Vyoral D, Petrak J.

2) Exosomes released by imatinib-resistant K562 cells contain specific membrane markers, IFITM3, CD146 and CD36 and increase the survival of imatinib-sensitive cells in the presence of imatinib

Hrdinova T, Toman O, Dresler J, Klimentova J, Salovska B, Pajer P, Bartos O, Polivkova V, Linhartova J, Machova Polakova K, Kabickova H, Brodska B, Krijt M, Zivny J, Vyoral D, Petrak J.

Proteomic analysis of imatinib-resistant CML-T1 cells reveals calcium homeostasis as a potential therapeutic target

O. TOMAN[1], T. KABICKOVA[1,2], O. VIT[3], R. FISER[4], K. MACHOVA POLAKOVA[1,5], J. ZACH[1], J. LINHARTOVA[1], D. VYORAL[1,6] and J. PETRAK[1,3]

[1]Institute of Hematology and Blood Transfusion, CZ-12820 Prague 2; [2]Department of Cell Biology, Faculty of Natural Sciences, Charles University in Prague, CZ-12843 Prague; [3]BIOCEV, First Faculty of Medicine, Charles University in Prague, CZ-25250 Vestec; [4]Department of Genetics and Microbiology, Faculty of Natural Sciences, Charles University in Prague, CZ-12843 Prague; [5]Institute of Clinical and Experimental Hematology, First Faculty of Medicine, Charles University in Prague, CZ-128 53 Prague; [6]Institute of Pathological Physiology, First Faculty of Medicine, Charles University in Prague, CZ-12853 Prague, Czech Republic

Received February 25, 2016; Accepted March 26, 2016

DOI: 10.3892/or.2016.4945

Abstract. Chronic myeloid leukemia (CML) therapy has markedly improved patient prognosis after introduction of imatinib mesylate for clinical use. However, a subset of patients develops resistance to imatinib and other tyrosine kinase inhibitors (TKIs), mainly due to point mutations in the region encoding the kinase domain of the fused BCR-ABL oncogene. To identify potential therapeutic targets in imatinib-resistant CML cells, we derived imatinib-resistant CML-T1 human cell line clone (CML-T1/IR) by prolonged exposure to imatinib in growth media. Mutational analysis revealed that the Y235H mutation in BCR-ABL is probably the main cause of CML-T1/IR resistance to imatinib. To identify alternative therapeutic targets for selective elimination of imatinib-resistant cells, we compared the proteome profiles of CML-T1 and CML-T1/IR cells using 2-DE-MS. We identified eight differentially expressed proteins, with strongly upregulated Na^+/H^+ exchanger regulatory factor 1 (NHERF1) in the resistant cells, suggesting that this protein may influence cytosolic pH, Ca^{2+} concentration or signaling pathways such as Wnt in CML-T1/IR cells. We tested several compounds including drugs in clinical use that interfere with the aforementioned processes and tested their relative toxicity to CML-T1 and CML-T1/IR cells. Calcium channel blockers, calcium signaling antagonists and modulators of calcium homeostasis, namely thapsigargin, ionomycin, verapamil, carboxyamidotriazole and immunosuppressive drugs cyclosporine A and tacrolimus (FK-506) were selectively toxic to CML-T1/IR cells. The putative cellular targets of these compounds in CML-T1/IR cells are postulated in this study. We propose that Ca^{2+} homeostasis can be a potential therapeutic target in CML cells resistant to TKIs. We demonstrate that a proteomic approach may be used to characterize a TKI-resistant population of CML cells enabling future individualized treatment options for patients.

Correspondence to: Dr Ondrej Toman, Department of Physiology, Institute of Hematology and Blood Transfusion, U Nemocnice 1, CZ-12820 Prague 2, Czech Republic
E-mail: ondrej.toman@uhkt.cz

Abbreviations: CML, chronic myeloid leukemia; TKIs, tyrosine kinase inhibitors; NHERF-1, Na^+/H^+ exchanger regulatory factor 1; MDR, multidrug resistance; CaMKII, Ca^{2+}/calmodulin-dependent protein kinase II; PDZ, post synaptic density protein (PSD95); Dlg1, Discs, large (*Drosophila)* homolog 1; Zo-1, zonula occludens-1 protein; ABC, ATP-binding cassette transporters; NFAT, nuclear factor of activated T cells; DCB, 3',4'-dichlorobenzamil hydrochloride, TRPC, transient receptor potential calcium channel; SERCA, sarco/endoplasmic reticulum Ca^{2+} ATPase; CsA, cyclosporine A; RyR, ryanodine receptor

Key words: chronic myeloid leukemia, imatinib mesylate, drug resistance, proteomics, calcium homeostasis, endoplasmic reticulum, Wnt signaling, therapeutic targets

Introduction

Chronic myeloid leukemia (CML) is a myeloproliferative disorder characterized by the presence of the Philadelphia (Ph) chromosome (1), encoding a chimeric protein Bcr-Abl with constitutive tyrosine kinase activity (2). Bcr-Abl kinase activates multiple downstream signaling pathways essential for survival and proliferation of CML cells (3,4). Imatinib is the first tyrosine kinase inhibitor (TKI) drug approved for CML therapy which blocks the ATP-binding site of Bcr-Abl and inhibits its activity (5). Unfortunately, not all patients with CML benefit from imatinib treatment in CML therapy. Primary refractoriness to imatinib is present in 13% of patients (6). Secondary (acquired) resistance, where the TKI treatment during therapy effectively selects drug-resistant clones, is a major complication that leads to disease progression in 30-40% of imatinib-treated patients (7). The most frequent causes of acquired resistance to CML therapy are point mutations in the kinase domain of Bcr-Abl, which

prevent TKI drugs from effectively binding to Bcr-Abl (8). Other Bcr-Abl dependent mechanisms of resistance occur via amplification of the BCR-ABL gene and overexpression of the protein (9,10). Additional adaptive changes contributing to TKI resistance such as substitutive activation of the Src family of kinases (11), or activation of alternate cell signaling pathways such as PI3K/AKT/mTOR (12) have been documented.

Each causal change within a leukemic cell leading to TKI resistance is consequently accompanied by other adaptive molecular alterations resulting in a new drug-resistant cell phenotype. Proteomic characterization of such molecular alterations in resistant cancer cells enables identification of new molecular targets with therapeutic potential (13,14) and can be used for optimization of anticancer therapy (15). In order to identify the molecular alterations contributing to and associated with imatinib resistance in a model of CML, we performed proteomic analysis comparing imatinib-sensitive CML cells (CML-T1) with derived imatinib-resistant cells (CML-T1/IR). Among the most evident changes in the CML-T1/IR cells was upregulation of a multifunctional scaffolding protein Na^+/H^+ exchange regulatory factor 1 (NHERF1). Based on known NHERF1 functions, we evaluated the possible consequences of NHERF1 upregulation on the survival of the CML-T1/IR cells. We observed disrupted calcium homeostasis and demonstrated selective toxic effects of calcium transport and calcium signaling inhibitors in the imatinib-resistant CML cells. The pronounced toxicity of calcium homeostasis modulators emphasizes their therapeutic potential in CML therapy.

Materials and methods

Establishment of imatinib-resistant cells. CML-T1 cells (purchased from Leibniz Institut DSMZ, German Collection of Microorganisms and Cell Culture GmbH, Braunschweig, Germany) were grown in RPMI media in the presence of 10% fetal calf serum in a 37˚C humidified atmosphere with 5% CO_2. Resistant CML-T1 subclones, CML-T1/IR, were derived by prolonged cultivation in increasing concentrations of imatinib.

Mutation analysis in the kinase domain of BCR-ABL. Sanger sequencing was applied as previously described (16). Briefly, RNA was extracted from the CML-T1 and CML-T1/IR cells with TRIzol (Thermo Fisher Scientific, Inc., Waltham, MA, USA) and the complementary DNA was synthesized by M-MLV reverse transcriptase (Promega, Madison, WI, USA) using random hexamer primers (Jena Bioscience GmbH, Jena, Germany). The cDNA region encoding the kinase domain of the fused BCR-ABL was amplified using nested PCR. The resulting 914-bp amplicon was sequenced from both strands. Based on the conclusive observation of mutated BCR-ABL transcripts, we explored the analysis using next-generation deep sequencing (NGS) with IRON-II BCR-ABL plates (IRON, International Robustness of Next-Generation sequencing) on a 454 GS Junior system (Roche Applied Science, Penzberg, Germany) to reveal the presence of mutations below the detection limit of Sanger sequencing. The protocol and algorithm previously established for NGS data evaluation (17) were followed.

Sample preparation for 2-DE. CML-T1 and CML-T1/IR cells ($1x10^8$) were harvested by centrifugation, washed twice with PBS and homogenized in a lysis buffer [7 M urea, 2 M thiourea, 4% CHAPS, 60 mM DTT and 1% ampholytes (IPG buffer pH 4.0-7.0; GE Healthcare Life Sciences, Little Chalfont, UK)] containing a protease inhibitor cocktail (Roche Diagnostics, Basel, Switzerland) for 20 min at room temperature. The lysates were cleared by centrifugation at 15,000 x g for 20 min at room temperature. Next, the supernatants were collected and the protein concentration was determined using the Bradford method (Bio-Rad, Inc., Hercules, CA, USA). The protein concentrations in all the samples were equalized to 7.3 mg/ml by dilution with the lysis buffer.

2-DE. Isoelectric focusing was performed with a Bio-Rad Protean IEF cell using 24 cm IPG strips (pH 4.0-7.0; GE Healthcare Life Sciences). Six technical replicates were run for each biological sample (6x CML-T1 and 6x CML-T1/IR). The strips were rehydrated overnight, each in 450 μl of sample, representing 3.3 mg of protein. Isoelectric focusing was performed for 60 kVh, with the maximum voltage not exceeding 5 kV, the current limited to 50 mA/strip and the temperature set to 18˚C. The focused strips were equilibrated and reduced in equilibration buffer A (6 M urea, 50 mM Tris pH 8.8, 30% glycerol, 2% SDS and 450 mg DTT/50 ml of the buffer) for 15 min and then alkylated in equilibration buffer B (6 M urea, 50 mM Tris pH 8.8, 30% glycerol, 2% SDS and 1.125 mg iodacetamide/50 ml). The equilibrated strips were then placed on the top of 10% PAGE gel and secured in place by molten agarose. Electrophoresis was performed in a Tris-glycine-SDS system using a Protean Plus Dodeca Cell apparatus (Bio-Rad, Inc.) with buffer circulation and external cooling (20˚C). The twelve gels were run at a constant voltage of 200 V for 6 h. Following electrophoresis, the gels were washed three times for 15 min in deionized water to remove the SDS. The washed gels were stained in CCB (SimplyBlue SafeStain, Invitrogen Life Technologies, Carlsbad, CA, USA) overnight, and then destained in deionized water.

Gel image analysis. The gels were scanned with a GS 800 calibrated densitometer (Bio-Rad, Inc.). Image analysis was performed with Phoretix 2D software (Nonlinear Dynamics, Newcastle upon Tyne, UK) in semi-manual mode with six gel replicates for one biological sample. Normalization of gel images was based on total spot density, and integrated spot density values (spot volumes) were then calculated after background subtraction. Average spot volume values (averages from all the six gels in the group) for each spot were compared between the groups. Protein spots were considered differentially expressed if they met both of the following criteria: i) the average difference of normalized spot volume was <1.5-fold and ii) the statistical significance of the change determined by the t-test was $P<0.05$.

MALDI MS, protein identification. The spots containing differentially expressed proteins were excised from the gels, cut into small pieces and washed three times with 25 mM ammonium bicarbonate in 50% acetonitrile (ACN). The gels were then dried in a SpeedVac Concentrator (Eppendorf, Hamburg, Germany). Sequencing grade modified trypsin

(6 ng/μl) (Promega) in 25 mM ammonium bicarbonate in 5% ACN was added. Following overnight incubation at 37˚C, the resulting peptides were extracted with 50% ACN. Peptide samples were spotted on a steel target plate (Bruker Daltonics, Bremen, Germany) and allowed to dry at room temperature. Matrix solution (3 mg α-cyano-4-hydroxycinnamic acid in 1 ml of 50% ACN containing 0.1% trifluoroacetic acid) was then added. MS was performed on an Autoflex II MALDI-TOF/TOF mass spectrometer (Bruker Daltonics) using a solid nitrogen laser (337 nm) and FlexControl software in reflectron mode with positive ion mass spectra detection. The mass spectrometer was externally calibrated with Peptide Calibration Standard II (Bruker Daltonics). Spectra were acquired in the mass range of 800-3,000 Da. The peak lists were generated using FlexAnalysis and searched against Swiss-Prot (2014 version) using the Mascot software. The peptide mass tolerance was set to 100 ppm, taxonomy *Homo sapiens* was selected, missed cleavage was set to 1, fixed modification for cysteine carbamidomethylation, and variable modifications for methionine oxidation and protein N-terminal acetylation were further settings selected. Proteins with a Mascot score over the threshold of 56 for $P<0.05$ calculated using the aforementioned settings were considered as identified.

Multidrug resistance (MDR) assay. The Vybrant™ Multidrug Resistance Assay kit (Thermo Fisher Scientific, Inc.) was used to measure drug efflux from the CML-T1 and the CML-T1/IR cells. The cells ($5x10^4$ cells/well) were grown in a 96-well plate for 24 h. Cells were then divided into two groups: the untreated group and the group treated with MDR drug efflux inhibitors cyclosporine A (CsA) and/or verapamil (at a final concentration ranging from 0.4 to 120 μg/ml). After 1 h, calcein AM was added to 100 μl of each examined cell suspension. After another 30 min, the cells in the plate were washed twice with 200 μl of cold RPMI-1640 culture medium, and the fluorescence of the retained calcein in both groups of cells was measured at a wavelength of λ_{ex} = 485 nm and λ_{em} = 538 nm by FluoroMax-3 spectrofluorometer equipped with DataMax software (Jobin Yvon Horriba, Kyoto, Japan).

Cytosolic pH measurement. The assay was conducted as described previously by Kiedrowski (18). Cells were loaded with 1 μM BCECF-AM for 20 min at room temperature. To monitor the BCECF fluorescence, the cells were exposed every 5 sec to 488 and 440 nm excitation and the images of fluorescence emitted at >520 nm (F488 and F440) were measured by a FluoroMax-3 spectrofluorometer equipped with DataMax software (Jobin Yvon Horriba) and saved for offline analysis. In selected experiments, F488/F440 ratios were converted to cytosolic pH values based on *in situ* calibration performed at the end of the experiments as described in Kiedrowski (18).

Measurement of cytosolic Ca^{2+}. Measurements of calcium concentration in the cytosol were performed as previously described (19). Briefly, the cells were washed in a modified HBSS buffer (140 mM NaCl, 5 mM KCl, 2 mM $CaCl_2$, 3 mM $MgCl_2$, 10 mM HEPES, 50 mM glucose pH 7.4) and loaded with 3 μM Fura-2 acetoxymethyl ester (Fura-2/AM) for 30 min at 25˚C in the dark, rinsed, and allowed to rest for 30 min prior to fluorescence measurements using a FluoroMax-3 spectrofluorometer equipped with DataMax software (Jobin Yvon Horriba, France). The fluorescence intensity of Fura-2 (excitation at 340 and 380 nm, and emission at 510 nm) was recorded every 15 sec, with an integration time of 3 sec. The concentration of free intracellular Ca^{2+} was determined as proportional to the ratio of fluorescence at 340/380 nm. The actual Ca^{2+} concentration was calculated with the Grynkiewicz equation (20). The K_d for Ca^{2+} binding to Fura-2 was measured to be 240 nM at the experimental temperature.

Wnt target gene microarray. Total RNA was isolated and purified from the CML-T1 and the CML-T1/IR cells with TRIzol reagent (Thermo Fisher Scientific, Inc.) and an RNeasy Mini kit (Qiagen, Hilden, Germany) according to the manufacturer's instructions. The RNA quality and quantity were determined at a 260/280 nm ratio on a Nanodrop ND-1000 (Thermo Fisher Scientific, Inc.). cDNA was synthesized by M-MLV reverse transcriptase (Promega) using random hexamer primers (Jena Bioscience GmbH).

The expression levels of the 92 genes involved in the Wnt signaling pathway within four control genes was analyzed on a TaqMan® array human Wnt Pathway Fast 96-well plate (Invitrogen Life Technologies) using a StepOnePlus™ Real-Time PCR system (Applied Biosystems, Foster City, CA, USA). Analyses were performed three times for both the CMLT1 and the CMLT1/IR cells. The genes (n=27); genes for which the amplification signals were not observed in one or more replicates simultaneously for the CMLT1 control and the CMLT1/IR, were excluded from the analysis. Relative expression changes of target genes (n=65) were normalized to the expression of the housekeeping gene *GUSB* that is validated for routine molecular monitoring in CML cells (21). Relative expression levels of the genes were evaluated using the $2^{-\Delta\Delta Cq}$ formula according to Livak *et al* (22) showing differential gene expression in the CMLT1/IR cells. For data control checking we re-analyzed differential relative expression using the *GAPDH* control gene, providing highly similar results as with *GUSB*.

BCR-ABL quantification was performed according to the method standardized in the EUTOS for CML project of ELN (www.eutos.org) and data were reported in the International Scale (IS). Primers and probes for BCR-ABL and GUSB were applied according to the European Partnership for Action Against Cancer recommendations and commercial plasmid standards were used to perform calibration curves (Ipsogen, Marseille, France).

Preparation of nuclear and cytoplasmic extracts. Cytoplasmic and nuclear extracts were prepared using a Nuclear and Cytoplasmic Extraction kit (NE-PER; Thermo Fisher Scientific, Inc.) according to the manufacturer's instructions with an additional modification in the final step of the nuclear protein extraction procedure, where the resulting pellets of the nuclear proteins were washed three times in ice cold PBS supplied with a protease inhibitor cocktail (Roche Diagnostics) and re-centrifuged at 16,000 x g to remove cytoplasmic protein contaminations.

Western blotting. Cell pellets were solubilized in lysis buffer (50 mM Tris pH 7.4; 1% Triton X-100, a protease inhibitor cocktail, 1 tablet/10 ml; Roche Diagnostics) on ice for 20 min. The cleared cell lysates (15,000 x g, 20 min) were collected and the protein concentration was determined by the Bradford method (Bio-Rad, Inc.). The samples containing 60 μg of protein were combined with an SDS loading buffer containing DTT, boiled for 5 min and resolved with SDS-PAGE using Novex precast 4-20% gradient gels (Thermo Fisher Scientific, Inc.). The separated proteins were transferred to PVDF membranes using the iBlot system according to manufacturer's instructions (Thermo Fisher Scientific, Inc.). The membranes were then blocked overnight in SuperBlock (PBS) blocking buffer (Thermo Fisher Scientific, Inc.). Then, the membranes were incubated with primary antibodies diluted to 1:1,000 in PBS containing 5% SuperBlock and 0.1% Tween-20. β-actin or Histone H2A (#4970 and #12349) were used as the loading controls; anti-NFAT1 rabbit mAb (#5862), anti-NHERF1 (#8601) and anti-MRP2/ABCC2 rabbit mAb (#12559; all from Cell Signaling Technology, Danvers, MA, USA) diluted 1:1,000 were used to detect the expression of NHERF1, MRP2 and NFAT. After thorough washing in PBS containing 0.1% Tween-20, a secondary anti-rabbit IgG, HRP-linked antibody (#7074; Cell Signaling Technology) was added (1:10,000). The signal was detected using enhanced chemiluminescence (ECL; GE Healthcare Life Sciences) assay, on X-ray film (Kodak, Rochester, NY, USA), developed, scanned and quantified by the Quantity One documentation system (Bio-Rad, Inc.).

Cell viability assays. Cells ($1x10^4$) were grown in a 24-well plate in 1 ml RPMI-1640 media (Thermo Fisher Scientific, Inc.) with increasing concentrations of the tested drugs for 3 days (72 h) at 37˚C and a 5% CO_2 humidified atmosphere. The toxicity of imatinib, amyloride, DCB, thapsigargin, ionomycin, verapamil, carboxyamidotriazole (CAI), FK-506 and CsA was measured using a Vybrant® MTT Cell Proliferation Assay kit (Thermo Fisher Scientific, Inc.) according to the manufacturer's protocol. Absorbance was detected at 570 nm using a microplate reader (Chameleon; Hidex, Turku, Finland).

Results

Development of imatinib-resistant CML-T1/IR subclones. We derived imatinib-resistant cells from an established model of the CML cell line CML-T1 (23). The CML-T1 cells express T-cell surface markers and carry the landmark BCR-ABL1 breakpoint cluster region translocation resulting in production of the p210 Bcr-Abl fusion protein (24). CML-T1 cells are sensitive to imatinib (IC_{50} 0.45±0.015 μM, Fig. 1). The imatinib-resistant CML-T1/IR cells were derived by prolonged cultivation of CML-T1 in increasing concentrations of imatinib. The CML-T1/IR cells tolerated at least a 50-fold higher concentration of imatinib (Fig. 1).

Mutation analysis reveals an imatinib-resistant Y253H mutation in the CML-T1/IR cells. The typical cause of resistance of CML cells to imatinib and other TKI inhibitors is a point mutation in the Abl kinase domain of the BCR-ABL fusion protein (25). We therefore performed mutational analysis of

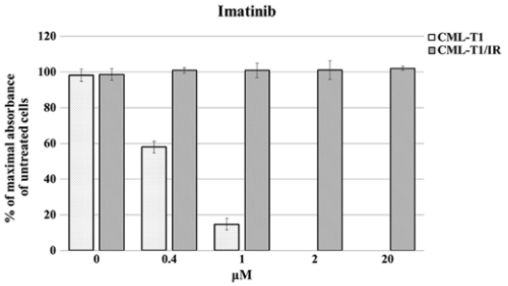

Figure 1. Viability of the CML-T1 and the CML-T1/IR cells in the presence of imatinib. CML-T1 and CML-T1/IR cells were grown in the presence of imatinib for 3 days. The cell viability was determined using an MTT assay on more than six biological replicates of the CML-T1 and CML-T1/IR cells, which were further seeded in three technical replicates onto the 96-well plates. The highest number of viable cells expressed by the maximal absorbance was set as 100%.

BCR-ABL in the CML-T1 and CML-T1/IR cells. We detected a Y253H mutation in the CML-T1/IR cells (69% of BCR-ABL transcripts), which is known to be a frequent causal mutation responsible for resistance to imatinib in human patients (26).

Proteomic analysis reveals upregulation of two NHERF1 variants in the CML-T1/IR cells. We hypothesized that besides the causal mutation in the BCR-ABL kinase domain there are additional, adaptive molecular changes in the CML-T1/IR cells, contributing to or associated with their survival in the presence of imatinib (27,28). These specific features may be exploitable as potential molecular targets for selective growth inhibition of imatinib-resistant cells for future therapies. To identify such alterations, we performed 2-DE proteomic analysis of the CML-T1 and CML-T1/IR cells (Fig. 2A). We identified eight differentially expressed proteins (Fig. 2A and Table I). The most marked change was the increased expression of the Na^+/H^+ exchange regulatory factor 1 (NHERF1 also known as SLC9A3R1). This protein was identified in two markedly upregulated variants of comparable molecular weight but of different isoelectric points (Table I, Fig. 2B). We further confirmed the upregulation of NHERF1 in the CML-T1/IR cells by western blot analysis (Fig. 2C). In addition to NHERF1, we detected upregulation of the endoplasmic reticulum (ER) calcium binding protein calreticulin, microtubule associated proteins and protein chaperones in the CML-T1/IR cells (Table I).

NHERF1: functional analysis. NHERF1 is a multifunctional scaffolding protein containing two PDZ domains (29). Via these domains NHERF1 interacts with various cellular proteins, mostly membrane receptors and transporters, modulating their expression, stability and activity (30). NHERF1 has been implicated in MDR in liver cancer by controlling the expression of MDR exporter MRP2 (31). NHERF1 negatively regulates the activity of sodium hydrogen ion exchanger SLC9A3 (NHE3), thus modulating the pH inside the cell (32). NHERF1 has also been demonstrated to influence cytosolic calcium concentration via transient receptor potential channel 5 protein (TRPC5) (33,34). Recently it was revealed

Table I. Differentially expressed proteins in the CML-T1/IR cells.

Spot no.	Uniprot	Protein name	Fold change	P-value	Sequence coverage (%)	Mascot score	MW (Da)	pI
Upregulated								
1	O14745	Na^+/H^+ exchange regulatory cofactor NHERF1	2.84	<0.009	21	57	39,130	5.55
2	O14745	Na^+/H^+ exchange regulatory cofactor NHERF1	>10	<0.001	32	84	39,130	5.55
3	Q9Y230	RuvB-like 2	6.8	<0.015	29	81	51,296	5.49
4	P27797	Calreticulin	1.8	<0.023	24	71	48,283	4.29
5	P00813	Adenosine deaminase	2.9	<0.009	36	87	41,024	5.63
6	P67936	Tropomyosin α-4 chain	1.56	<0.036	63	198	28,619	4.67
7	P04792	Heat shock protein β-1	>10	<0.001	35	136	22,826	5.98
Downregulated								
8	Q9Y230	RuvB-like 2	-2.17	<0.02	38	149	51,296	5.49
9	Q99536	Synaptic vesicle membrane protein VAT-1 homolog	-3.7	<0.039	34	60	42,122	5.88
10	Q15691	Microtubule-associated protein RP/EB family member 1	-1.86	<0.005	53	89	30,151	5.02
11	P04792	Heat shock protein β-1	-2.2	<0.001	44	75	22,826	5.98

Included in the table are the proteins with an expression difference of at least 1.5-fold and a statistical significance of change P<0.05. MW, molecular weight; pI, isoelectric point.

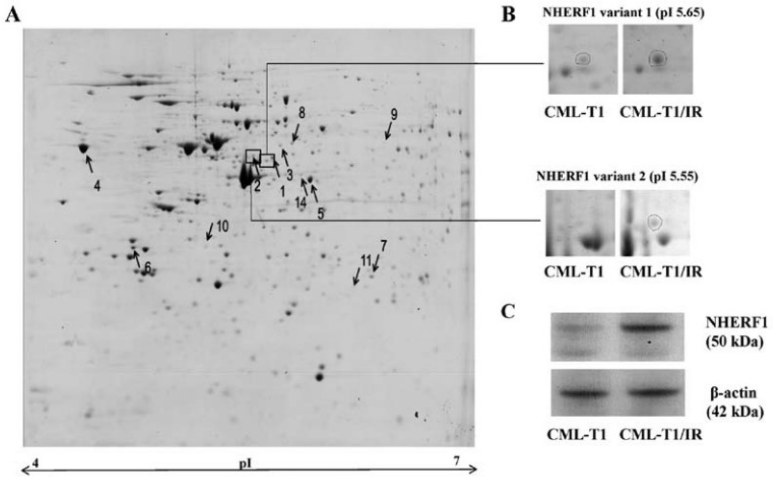

Figure 2. 2-DE analysis of CML-T1/IR and CML-T1 cells. (A) 2-DE gel from the CML-T1/IR cells with differentially expressed proteins indicated by arrows with numbers (↑ upregulated, ↓ downregulated). (B) Two protein variants of NHERF1 were detected as upregulated in the imatinib-resistant CML-T1/IR cells. (C) Verification of altered NHERF1 expression in the total cell lysates of CML-T1 and CML-T1/IR cells by western blot analysis revealed a 2.6-fold increase in the expression of NHERF1 in the CML-T1/IR cells, as quantified by Quantity One software (Bio-Rad, Inc.) based on more than three biological replicates, each performed in three technical replicates.

that NHERF1 negatively regulates the canonical Wnt signaling pathway via direct interaction with a subset of Frizzled (Fzd) receptors (35).

Based on the functions aforementioned, we examined the possible effect of NHERF1 upregulation in the CML-T1/IR cells in order to identify a specific feature of the imatinib-resistant cells which may exhibit a 'molecular weakness' representing a potential therapeutic target. We first evaluated the potential connection of NHERF1 with MDR in the CML-T1/IR cells. Next we tested whether NHERF1 upregulation modulates H^+

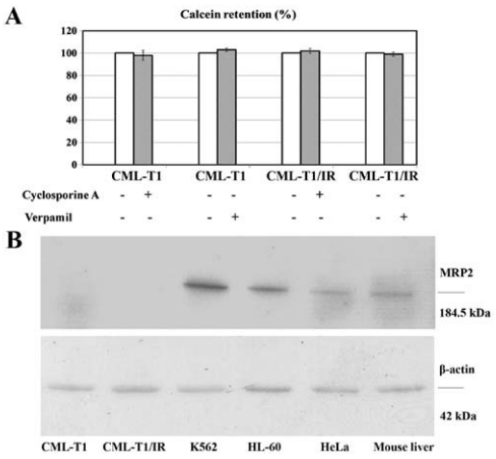

Figure 3. Multidrug resistance (MDR) assay in CML-T1 and CML-T1/IR cells and immunodetection of MRP2 protein by western blot analysis in the CML-T1 and CML-T1/IR cells compared with other cell lysates. (A) Measurement of calcein retention as a surrogate of MDR exporter activity in the CML-T1 and CML-T1/IR cells was performed as described in 'Materials and methods'. Cyclosporine A (CsA) and verapamil were used as inhibitors of MDR. No MDR activity was detected in the CMLT1 and CMLT1/IR cells as reflected by 100% calcein retention in the cells. (B) Cell lysates of CML-T1 and CML-T1/IR were subjected to SDS-PAGE and western blot analysis for immunodetection of MRP2 together with the lysates of K562, HL-60, HeLa cells and mouse liver tissue, which were used as MRP2 positive controls.

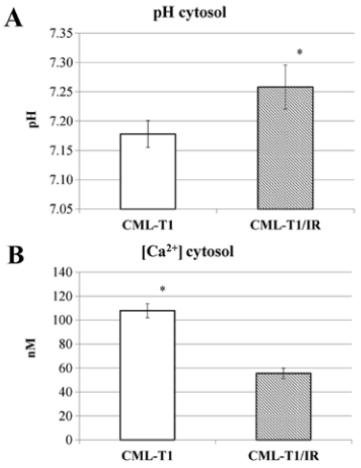

Figure 4. Cellular pH and calcium ion concentration measurements in CML-T1 and CML-T1/IR cells. (A) Intracellular pH was determined using BCECF fluorescence and (B) calcium ion concentration was measured using Fura-2 probe fluorescence measurements. Each graph shows the average values from three repeated measurements performed on three biological replicates.

and Ca^{2+} concentrations in the cytosol of the CML-T1/IR cells and investigated whether NHERF1 upregulation and changes in ion homeostasis affect the activity of the Wnt signaling pathway.

NHERF1 upregulation does not contribute to MDR in the CML-T1/IR cells. We evaluated whether the upregulation of NHERF1 in the CML-T1/IR cells contributes to cell survival in high concentrations of imatinib by increasing the activity of the MDR protein pumps MRP2 as described in liver cancer (36). We performed an *in vitro* MDR assay based on the cellular efflux of the fluorescent probe calcein. This process was shown to be performed by the multidrug exporters MDR1 and MRP2 (37,38). Both the CML-T1 and the CML-T1/IR cells retained 100% of the incorporated calcein (no calcein efflux was detected). The addition of multidrug export inhibitors CsA and verapamil therefore had no effect on efflux. This suggests that these drug exporters are not present/active in CML-T1 and CML-T1/IR cells (Fig. 3A). Furthermore, while we were able to detect MRP2 by western blot in the lysates of several cell types including CML-derived K562 cells, expression of MRP2 in both the CML-T1 and CML-T1/IR cells was under our detection limit (Fig. 3B). We concluded that the activity of multidrug exporters in the CML-T1 and CML-T1/IR cells is negligible and that the increased NHERF1 expression does not affect the activity of MDR1 and MRP2 in the CML-T1/IR cells.

Intracellular concentrations of H^+ and Ca^{2+} ions differ in the CML-T1 and the CML-T1/IR cells. Based on the known interplay between NHERF1 and the Na^+/H^+ exchanger NHE3 with a consequent effect on cellular pH (39) we examined whether the NHERF1 upregulation in the CML-T1/IR cells affects the intracellular pH. We measured the intracellular pH and observed increased cytosolic pH in the CML-T1/IR cells (pH 7.25) compared to the control CML-T1 cells (pH 7.18), as shown in Fig. 4A.

Since NHERF1 was shown to regulate the activity of nonselective calcium permeable cation channels, namely TRPC4 and TRPC5 (34) we examined whether the presence of upregulated NHERF1 (or the increased cytosolic pH) in the CML-T1/IR cells also affects the cytosolic concentration of Ca^{2+} (40). Our measurements revealed a 50% decrease in cytosolic Ca^{2+} concentration in the CML-T1/IR cells (Fig. 4B).

In summary, ion homeostasis in the CML-T1/IR cytosol was altered, with an increased pH and a decreased cytosolic Ca^{2+} concentration compared to the original CMLT1 cells.

Calcium channel blockers and inhibitors of calcium signaling selectively inhibit the viability of CML-T1/IR cells. We hypothesized that the increased pH due to differential Na^+/H^+ exchange (41) and decreased Ca^{2+} concentration in the cytosol (42) contribute to CML-T1/IR survival in the presence of imatinib. To address whether the inhibition of Na^+/H^+ exchange selectively affects the growth of the CML-T1/IR cells, we targeted Na^+/H^+ exchange by amiloride. Since it is well established that a Na^+/Ca^{2+} exchanger (NCX) may also contribute to pH and calcium concentration changes in the cells (43), we further inhibited Na^+/Ca^{2+} exchange by 3',4'-dichlorobenzamil hydrochloride (DCB) (44). We observed that none of the inhibitors had a selective effect on the viability of the CML-T1/IR cells. Both the CML-T1 and the CML-T1/IR cells tolerated comparable concentrations of

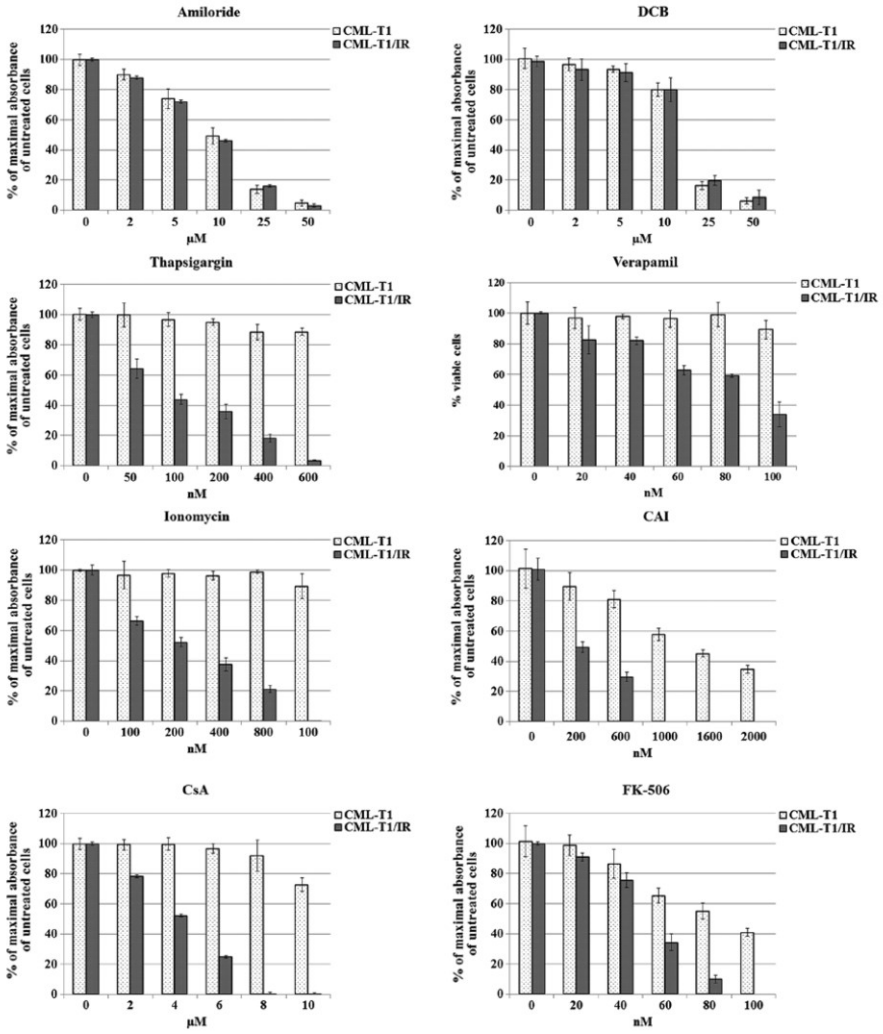

Figure 5. Effects of selected inhibitors on the viability of CML-T1 and CML-T1/IR cells. Cell viability assay was determined using an MTT assay 3 days after addition of inhibitors to the cultivation media. Maximal absorbance (highest number of viable cells) of cells cultivated without imatinib was set as 100%. Each graph represents measurements of at least three biological samples, each further measured in three technical replicates. DCB, 2',4'-dichlorobenzamil hydrochloride; CAI, carboxyamidotriazole.

inhibitors within IC_{50} values of 15 μM for amiloride and 7 μM for DCB (Fig. 5).

To address whether shifted Ca^{2+} homeostasis is crucial for survival of the CML-T1/IR cells, we exposed the CML-T1 and CML-T1/IR cells to increasing concentrations of inhibitors of Ca^{2+} transport and Ca^{2+} signaling, namely thapsigargin, ionomycin, verapamil, and CAI. Thapsigargin inhibits the activity of sarco/ER Ca^{2+} ATPase (SERCA), preventing the uptake of cytosolic Ca^{2+} into the ER, thus increasing the cytosolic Ca^{2+} (45,46). Ionomycin increases intracellular Ca^{2+} by means of its increased entry across the plasma membrane and/or by depletion of intracellular Ca^{2+} stores such as ER (47). The clinically approved drug verapamil blocks voltage-dependent (L-type) Ca^{2+} channels (48). CAI inhibits non-voltage operated calcium channels and blocks both Ca^{2+} influx into the cells and Ca^{2+} release from the intracellular stores (49). Notably, CAI has been previously demonstrated to inhibit the growth of imatinib-resistant CML cell lines *in vitro* (50) and several studies have demonstrated a potential anticancer effect of CAI *in vitro* (51,52).

In a battery of *in vitro* cell viability assays we tested the aforementioned compounds for their toxicity to the CML-T1

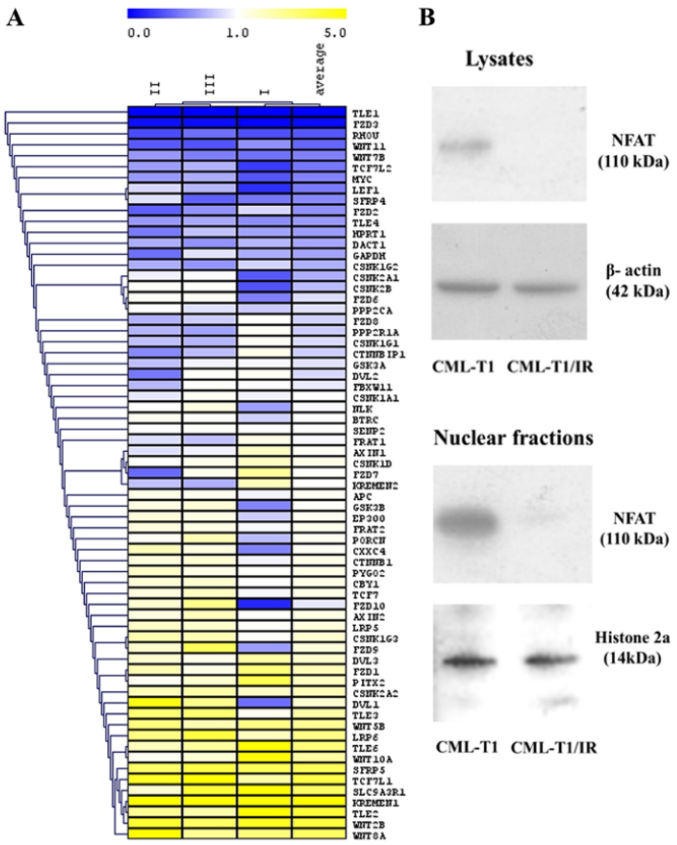

Figure 6. Changes in gene expression of the Wnt signaling pathway and immunodetection of NFAT by western blot analysis in CML-T1 and CML-T1/IR cells. (A) The heatmap shows genes whose mRNA expression was downregulated (blue) or upregulated (yellow) in the CML-T1/IR cells compared to the CML-T1 cells. (B) NFAT protein expression as determined by western blot analysis in the cell lysates and the nuclei of the CML-T1 and CML-T1/IR cells.

and CML-T1/IR cells. All the tested agents were more toxic to the imatinib-resistant CML-T1/IR cells (Fig. 5). Among them, thapsigargin was the most potent in growth inhibition of CML-T1/IR cells, which were at least 16-fold more sensitive to this agent compared to the CML-T1 cells. The IC_{50} for the CML-T/IR cells was 75 nM while the IC_{50} in the CML-T1 cells was not reached at a 1.2 μM concentration of thapsigargin in the media. The CMLT1-IR cells were also 5-fold more sensitive to ionomycin (IC_{50}values 200 nM for the CML-T1/IR cells and >1.6 μM for the CML-T1 cells). Verapamil was ~3-fold more toxic to the CML-T1/IR cells (IC_{50} 30 nM for the CML-T1/IR cells and 90 nM for the CML-T1 cells) and CAI was 2.5-fold more toxic to the CML-T1/IR cells (IC_{50} 200 nM for the CML-T1/IR cells and 1.6 μM for the CML-T1 cells).

Altered calcium homeostasis influences numerous intracellular processes including Wnt signaling. CsA and tacrolimus (FK-506) were shown to modulate calcium homeostasis (53,54) and inhibit Wnt-regulated pro-survival processes in imatinib-resistant cells (56). We, therefore, evaluated the effect of CsA and FK-506 on the proliferation of the CML-T1 and CML-T1/IR cells. In our assays both CsA and FK506 inhibited proliferation of the CML-T1/IR cells at significantly lower concentrations (3- and 1.8-fold, respectively) compared to the CML-T1 cells. The IC_{50} of CsA was 4 μM for the CML-T1/IR cells and 12 μM for the CML-T1 cells; the IC_{50} of FK-506 was 50 nM for the CML-T1/IR cells and 90 nM for the CML-T1 cells (Fig. 5).

In summary, we observed that a disruption of calcium homeostasis (and to a lesser extent also inhibition of Wnt signaling), but not the inhibition of Na^+/H^+ or Na^+/Ca^{2+} exchange was selectively toxic to CML-T1/IR cells. The most effective growth inhibition of CML-T1/IR was achieved by using the agents causing depletion of the intracellular Ca^{2+} stores with an increase in the Ca^{2+} concentration in the cytosol (ionomycin, thapsigargin), but also calcium channel blockers (verapamil) and calcium signaling antagonist CAI. Low molecular weight antagonists of calcium homeostasis, calcium transport blockers and calcium signaling inhibitors may be used to selectively impair the growth of imatinib-resistant

CML-T1/IR cells, thus suggesting their clinical potential in TKI-resistant CML.

The Wnt pathway is dysregulated in the CML-T1/IR cells. NHERF1 has been proven to negatively regulate Wnt signaling via its direct interaction with Fzd receptors (35). The potential of Wnt signaling serving as a therapeutic target is recently a subject of intensive studies in the field of cancer therapy and novel drug discovery (55). We therefore examined whether NHERF1 upregulation (accompanied with altered cytosolic ion concentration) in the CML-T1/IR cells is associated with altered Wnt signaling. We analyzed the activity of the Wnt pathway using RT-PCR Wnt microarray to determine the relative expression of Wnt target genes and regulatory molecules (Fig. 6A). In the CML-T1/IR cells, we observed a decreased expression of genes of the canonical β-catenin-dependent Wnt pathway, namely TLE1, TLE4, TCF7L2, LEF1, MYC and RHOU. Conversely, the expression of negative regulators of this pathway, KREMEN1 and SFRP5 was increased in the CML-T1/IR cells, indicating that the canonical β-catenin-dependent Wnt signaling was decreased in the CML-T1/IR cells.

We also evaluated the expression of genes critical for the non-canonical CaMKII/Ca^{2+}/NFAT Wnt pathway where the expression of mRNA encoding FZD8 receptor, essential for this pathway was decreased in the CML-T1/IR cells. This is contradictory to the results of Gregory *et al* (56), which showed that Wnt signaling contributed (via FZD8) to the pro-surviving effect of the CaMKII/Ca^{2+}/NFAT Wnt pathway in imatinib-resistant cells. To obtain more information on the status of CaMKII/Ca^{2+}/NFAT Wnt signaling in our cells, we determined the presence of transcription factor NFAT, the final effector of this pathway in the cytoplasm and the nuclei of the CML-T1 and CML-T1/IR cells. NFAT was not detected in the CML-T1/IR cells (Fig. 6B), while it was clearly detectable in the CML-T1 cells. The diminished expression of NFAT protein in the CML-T1/IR cells suggests that CaMKII/Ca^{2+}/NFAT Wnt signaling is decreased in these cells and does not contribute to the survival against imatinib in our cell model.

All in all, our data suggest that imatinib resistance is accompanied by significant downregulation of both canonical and noncanonical CaMKII/Ca^{2+}/NFAT Wnt signaling pathways in CML-T1/IR cells.

Discussion

The imatinib-resistant CML-T1/IR cells carry the causal mutation of Y253H in the kinase domain of the BCR-ABL gene. This mutation is undoubtedly the main driving force of resistance to imatinib. However, any resistant phenotype is a result of multiple molecular events including causative, contributing and adaptive cellular processes, enabling survival of the resistant cells. Detailed molecular analysis of therapy-resistant cells potentially opens the path to personalized therapies of drug-resistant malignancies. Using 2-DE analysis we revealed a strong upregulation of a multifunctional protein NHERF1. We demonstrated altered cytosolic pH and decreased calcium levels in the CML-T1/IR cells. While inhibition of Na^+/H^+ and Na^+/Ca^+ exchangers has no specific toxic effect in the resistant CML-T1/IR cells, modulators of cytosolic calcium concentration, calcium channels blockers and calcium signaling inhibitors were significantly more toxic to the CML-T1/IR cells compared to the CML-T1/IR cells. The most prominent toxic effect we observed using ionomycin and thapsigargin was presumably caused by toxic elevation of cytosolic Ca^{2+} and/or by the depletion of Ca^{2+} from ER, leading to ER stress, unfolded protein response and finally to apoptosis (57).

Altered Ca^{2+} concentration in the cytosol may affect the expression of many proteins and modulate signaling pathways such as CaMKII/Ca^{2+}/NFAT Wnt. This was of particular interest to us since this calcium-dependent pathway was previously demonstrated to be critical for the survival of imatinib-resistant CML cells; NFAT inhibitor CsA effectively inhibited proliferation of the imatinib-resistant cells (56). Correspondingly, when we applied NFAT inhibitors, such as CsA or FK-506, in our experiments, we also observed their selective toxicity to CML-T1/IR. However, this growth inhibitory effect appeared to be NFAT-independent in our CML-T1/IR cells, because NFAT was markedly downregulated (if not absent) in the nuclei of the CML-T1/IR cells.

We, therefore, proposed that the selective toxicity of CsA and FK-506 in CML-T1/IR cells is due to their direct effect on calcium homeostasis. The established mechanism of ionomycin and thapsigargin toxicity (the inhibitors with the most pronounced toxic effect to the CML-T1/IR cells) is elevation of cytosolic Ca^{2+} and depletion of Ca^{2+} from the ER (47,45). This suggests that calcium levels in both the cytoplasm and the ER should be considered as critical for the survival of CML-T1/IR cells. Our hypothesis of altered calcium homeostasis was further supported by the results of our 2-DE analysis, where calreticulin was detected as upregulated in the CML-T1/IR cells (Table I). Calreticulin is an ER resident protein, which contributes to proper folding of nascent proteins and serves as a calcium binding buffer in the ER. If CML-T1/IR cells require increased expression of calreticulin to maintain ER Ca^{2+} homeostasis, blocking Ca^{2+} entry to the ER by thapsigargin or depleting Ca^{2+} from the ER by ionomycin can substantially reduce their viability. There is evidence that CsA and FK-506, in addition to their effect on Wnt signaling, may affect calcium homeostasis directly. CsA inhibits the activity of SERCA, an ER ATPase pump responsible for Ca^{2+} influx into the ER from the cytosol (58). FK-506 stimulates the activity of the ryanodine receptor (Ryr) which acts in opposition to SERCA and releases Ca^{2+} from the ER to the cytosol (59). Such a direct toxic effect of these clinically used immunosuppressants on calcium homeostasis may explain their selective cytotoxic effect on the CMLT1/IR cells in the absence of NFAT.

In addition to the selective toxicity of the experimental inhibitors, thapsigargin and ionomycin, three drugs already clinically established, CsA, tacrolimus (FK-506) and verapamil displayed similar selective toxicity to the imatinib-resistant CML-T1/IR cells. Verapamil and tacrolimus are known to inhibit multi-drug export in cancer cells (60,61). However, since there was no detectable multidrug-export activity in the CML-T1/IR cells, we propose that the observed cytotoxic effect of verapamil and tacrolimus was based on direct disruption of calcium homeostasis.

Our proteomic and functional analysis of imatinib resistance in CML cells provides a proof-of-concept and a vision for a future model of personalized TKI-resistant CML therapy, where the isolation of TKI-resistant cells can be combined

with proteomic and functional analysis in order to identify potential therapeutic targets, which may be exploited for selective elimination of the drug-resistant population of cells.

Acknowledgements

This study was supported by the Czech Ministry of Health via the Project for Conceptual Development of Research Organizations grant no. 00023736, and via the 15-32961A grant, by the European Regional Development Fund via grants CZ.1.05/1.1.00/02.0109-BIOCEV, ERDF OPPK CZ.2.16/3.1.00/24001 and ERDF OPPK CZ.2.16/3.1.00/28007, by the Czech Science Foundation (www.gacr.cz) grant 15-14200S, and by the Ministry of Education, Youth and Sports of the Czech Republic (www.msmt.cz) via grants PRVOUK P24/LF1/3 and SVV 260 265/2016.

References

1. Nowell PC and Hungerford DA: Chromosome studies on normal and leukemic human leukocytes. J Natl Cancer Inst 25: 85-109, 1960.
2. Lugo TG, Pendergast AM, Muller AJ and Witte ON: Tyrosine kinase activity and transformation potency of bcr-abl oncogene products. Science 247: 1079-1082, 1990.
3. Deininger MW, Vieira S, Mendiola R, Schultheis B, Goldman JM and Melo JV: *BCR-ABL* tyrosine kinase activity regulates the expression of multiple genes implicated in the pathogenesis of chronic myeloid leukemia. Cancer Res 60: 2049-2055, 2000.
4. Hazlehurst LA, Bewry NN, Nair RR and Pinilla-Ibarz J: Signaling networks associated with BCR-ABL-dependent transformation. Cancer Control 16: 100-107, 2009.
5. Waller CF: Imatinib mesylate. Recent Results Cancer Res 201: 1-25, 2014.
6. Roche-Lestienne C, Soenen-Cornu V, Grardel-Duflos N, Laï JL, Philippe N, Facon T, Fenaux P and Preudhomme C: Several types of mutations of the *Abl* gene can be found in chronic myeloid leukemia patients resistant to STI571, and they can pre-exist to the onset of treatment. Blood 100: 1014-1018, 2002.
7. Kantarjian HM, Talpaz M, O'Brien S, Giles F, Garcia-Manero G, Faderl S, Thomas D, Shan J, Rios MB and Cortes J: Dose escalation of imatinib mesylate can overcome resistance to standard-dose therapy in patients with chronic myelogenous leukemia. Blood 101: 473-475, 2003.
8. Ursan ID, Jiang R, Pickard EM, Lee TA, Ng D and Pickard AS: Emergence of BCR-ABL kinase domain mutations associated with newly diagnosed chronic myeloid leukemia: A meta-analysis of clinical trials of tyrosine kinase inhibitors. J Manag Care Spec Pharm 21: 114-122, 2015.
9. Campbell LJ, Patsouris C, Rayeroux KC, Somana K, Januszewicz EH and Szer J: *BCR/ABL* amplification in chronic myelocytic leukemia blast crisis following imatinib mesylate administration. Cancer Genet Cytogenet 139: 30-33, 2002.
10. Phan CL, Megat Baharuddin PJNB, Chin LP, Zakaria Z, Yegappan S, Sathar J, Tan S-M, Purushothaman V and Chang KM: Amplification of *BCR-ABL* and t(3;21) in a patient with blast crisis of chronic myelogenous leukemia. Cancer Genet Cytogenet 180: 60-64, 2008.
11. Roginskaya V, Zuo S, Caudell E, Nambudiri G, Kraker AJ and Corey SJ: Therapeutic targeting of Src-kinase Lyn in myeloid leukemic cell growth. Leukemia 13: 855-861, 1999.
12. Quentmeier H, Eberth S, Romani J, Zaborski M and Drexler HG: BCR-ABL1-independent PI3Kinase activation causing imatinib-resistance. J Hematol Oncol 4: 6, 2011.
13. Petrak J, Toman O, Simonova T, Halada P, Cmejla R, Klener P and Zivny J: Identification of molecular targets for selective elimination of TRAIL-resistant leukemia cells. From spots to in vitro assays using TOP15 charts. Proteomics 9: 5006-5015, 2009.
14. Lorkova L, Scigelova M, Arrey TN, Vit O, Pospisilova J, Doktorova E, Klanova M, Alam M, Vockova P, Maswabi B, *et al*: Detailed functional and proteomic characterization of fludarabine resistance in mantle cell lymphoma cells. PLoS One 10: e0135314, 2015.
15. Klanova M, Soukup T, Jaksa R, Molinsky J, Lateckova L, Maswabi BCL, Prukova D, Brezinova J, Michalova K, Vockova P, *et al*: Mouse models of mantle cell lymphoma, complex changes in gene expression and phenotype of engrafted MCL cells: Implications for preclinical research. Lab Invest 94: 806-817, 2014.
16. Poláková KM, Polívková V, Rulcová J, Klamová H, Jurcek T, Dvoráková D, Zácková D, Pospísil Z, Mayer J and Moravcová J: Constant BCR-ABL transcript level ≥0.1% (IS) in patients with CML responding to imatinib with complete cytogenetic remission may indicate mutation analysis. Exp Hematol 38: 20-26, 2010.
17. Machova Polakova K, Kulvait V, Benesova A, Linhartova J, Klamova H, Jaruskova M, de Benedittis C, Haferlach T, Baccarani M, Martinelli G, *et al*: Next-generation deep sequencing improves detection of *BCR-ABL1* kinase domain mutations emerging under tyrosine kinase inhibitor treatment of chronic myeloid leukemia patients in chronic phase. J Cancer Res Clin Oncol 141: 887-899, 2015.
18. Kiedrowski L: Cytosolic zinc release and clearance in hippocampal neurons exposed to glutamate - the role of pH and sodium. J Neurochem 117: 231-243, 2011.
19. Kinsella BT, O'Mahony DJ and Fitzgerald GA: The human thromboxane A_2 receptor α isoform (TP_α) functionally couples to the G proteins G_q and G_{11} in vivo and is activated by the isoprostane 8-epi prostaglandin $F_{2\alpha}$. J Pharmacol Exp Ther 281: 957-964, 1997.
20. Grynkiewicz G, Poenie M and Tsien RY: A new generation of Ca^{2+} indicators with greatly improved fluorescence properties. J Biol Chem 260: 3440-3450, 1985.
21. White H, Deprez L, Corbisier P, Hall V, Lin F, Mazoua S, Trapmann S, Aggerholm A, Andrikovics H, Akiki S, *et al*: A certified plasmid reference material for the standardisation of *BCR-ABL1* mRNA quantification by real-time quantitative PCR. Leukemia 29: 369-376, 2015.
22. Livak KJ and Schmittgen TD: Analysis of relative gene expression data using real-time quantitative PCR and the $2^{-\Delta\Delta Ct}$ method. Methods 25: 402-408, 2001.
23. Kuriyama K, Gale RP, Tomonaga M, Ikeda S, Yao E, Klisak I, Whelan K, Yakir H, Ichimaru M, Sparkes RS, *et al*: CML-T1: A cell line derived from T-lymphocyte acute phase of chronic myelogenous leukemia. Blood 74: 1381-1387, 1989.
24. Drexler HG: Leukemia cell lines: In vitro models for the study of chronic myeloid leukemia. Leuk Res 18: 919-927, 1994.
25. Hochhaus A, Kreil S, Corbin AS, La Rosée P, Müller MC, Lahaye T, Hanfstein B, Schoch C, Cross NCP, Berger U, *et al*: Molecular and chromosomal mechanisms of resistance to imatinib (STI571) therapy. Leukemia 16: 2190-2196, 2002.
26. Branford S, Rudzki Z, Walsh S, Grigg A, Arthur C, Taylor K, Herrmann R, Lynch KP and Hughes TP: High frequency of point mutations clustered within the adenosine triphosphate-binding region of BCR/ABL in patients with chronic myeloid leukemia or Ph-positive acute lymphoblastic leukemia who develop imatinib (STI571) resistance. Blood 99: 3472-3475, 2002.
27. Kominsky DJ, Klawitter J, Brown JL, Boros LG, Melo JV, Eckhardt SG and Serkova NJ: Abnormalities in glucose uptake and metabolism in imatinib-resistant human BCR-ABL-positive cells. Clin Cancer Res 15: 3442-3450, 2009.
28. Adamia S, Pilarski PM, Bar-Natan M, Stone RM and Griffin JD: Alternative splicing in chronic myeloid leukemia (CML): A novel therapeutic target? Curr Cancer Drug Targets 13: 735-748, 2013.
29. Reczek D, Berryman M and Bretscher A: Identification of EBP50: A PDZ-containing phosphoprotein that associates with members of the ezrin-radixin-moesin family. J Cell Biol 139: 169-179, 1997.
30. Ardura JA and Friedman PA: Regulation of G protein-coupled receptor function by Na^+/H^+ exchange regulatory factors. Pharmacol Rev 63: 882-900, 2011.
31. Li M, Wang W, Soroka CJ, Mennone A, Harry K, Weinman EJ and Boyer JL: NHERF-1 binds to Mrp2 and regulates hepatic Mrp2 expression and function. J Biol Chem 285: 19299-19307, 2010.
32. He P and Yun CC: Mechanisms of the regulation of the intestinal Na^+/H^+ exchanger NHE3. J Biomed Biotechnol 2010: 238080, 2010.
33. Obukhov AG and Nowycky MC: TRPC5 activation kinetics are modulated by the scaffolding protein ezrin/radixin/moesin-binding phosphoprotein-50 (EBP50). J Cell Physiol 201: 227-235, 2004.
34. Tang Y, Tang J, Chen Z, Trost C, Flockerzi V, Li M, Ramesh V and Zhu MX: Association of mammalian Trp4 and phospholipase C isozymes with a PDZ domain-containing protein, NHERF. J Biol Chem 275: 37559-37564, 2000.

35. Wheeler DS, Barrick SR, Grubisha MJ, Brufsky AM, Friedman PA and Romero G: Direct interaction between NHERF1 and Frizzled regulates β-catenin signaling. Oncogene 30: 32-42, 2011.
36. Karvar S, Suda J, Zhu L and Rockey DC: Distribution dynamics and functional importance of NHERF1 in regulation of Mrp-2 trafficking in hepatocytes. Am J Physiol Cell Physiol 307: C727-C737, 2014.
37. Bosch I and Croop J: P-glycoprotein multidrug resistance and cancer. Biochim Biophys Acta 1288: F37-F54, 1996.
38. Canitrot Y, Lahmy S, Buquen JJ, Canitrot D and Lautier D: Functional study of multidrug resistance with fluorescent dyes. Limits of the assay for low levels of resistance and application in clinical samples. Cancer Lett 106: 59-68, 1996.
39. Donowitz M, Cha B, Zachos NC, Brett CL, Sharma A, Tse CM and Li X: NHERF family and NHE3 regulation. J Physiol 567: 3-11, 2005.
40. Garciarena CD, Youm JB, Swietach P and Vaughan-Jones RD: H^+-activated Na^+ influx in the ventricular myocyte couples Ca^{2+}-signalling to intracellular pH. J Mol Cell Cardiol 61: 51-59, 2013.
41. Rich IN, Worthington-White D, Garden OA and Musk P: Apoptosis of leukemic cells accompanies reduction in intracellular pH after targeted inhibition of the Na^+/H^+ exchanger. Blood 95: 1427-1434, 2000.
42. Pinton P, Ferrari D, Magalhães P, Schulze-Osthoff K, Di Virgilio F, Pozzan T and Rizzuto R: Reduced loading of intracellular Ca^{2+} stores and downregulation of capacitative Ca^{2+} influx in Bcl-2-overexpressing cells. J Cell Biol 148: 857-862, 2000.
43. Condrescu M, Opuni K, Hantash BM and Reeves JP: Cellular regulation of sodium-calcium exchange. Ann NY Acad Sci 976: 214-223, 2002.
44. Iwamoto T, Watanabe Y, Kita S and Blaustein MP: Na^+/Ca^{2+} exchange inhibitors: A new class of calcium regulators. Cardiovasc Hematol Disord Drug Targets 7: 188-198, 2007.
45. Thastrup O, Cullen PJ, Drøbak BK, Hanley MR and Dawson AP: Thapsigargin, a tumor promoter, discharges intracellular Ca^{2+} stores by specific inhibition of the endoplasmic reticulum Ca^{2+}-ATPase. Proc Natl Acad Sci USA 87: 2466-2470, 1990.
46. Inesi G, Hua S, Xu C, Ma H, Seth M, Prasad AM and Sumbilla C: Studies of Ca^{2+} ATPase (SERCA) inhibition. J Bioenerg Biomembr 37: 365-368, 2005.
47. Beeler TJ, Jona I and Martonosi A: The effect of ionomycin on calcium fluxes in sarcoplasmic reticulum vesicles and liposomes. J Biol Chem 254: 6229-6231, 1979.
48. Triggle DJ: L-type calcium channels. Curr Pharm Des 12: 443-457, 2006.
49. Hupe DJ, Boltz R, Cohen CJ, Felix J, Ham E, Miller D, Soderman D and Van Skiver D: The inhibition of receptor-mediated and voltage-dependent calcium entry by the antiproliferative L-651,582. J Biol Chem 266: 10136-10142, 1991.
50. Alessandro R, Fontana S, Giordano M, Corrado C, Colomba P, Flugy AM, Santoro A, Kohn EC and De Leo G: Effects of carboxyamidotriazole on in vitro models of imatinib-resistant chronic myeloid leukemia. J Cell Physiol 215: 111-121, 2008.
51. Perabo FG, Wirger A, Kamp S, Lindner H, Schmidt DH, Müller SC and Kohn EC: Carboxyamido-triazole (CAI), a signal transduction inhibitor induces growth inhibition and apoptosis in bladder cancer cells by modulation of Bcl-2. Anticancer Res 24: 2869-2877, 2004.
52. Guo L, Ye C, Chen W, Ye H, Zheng R, Li J, Yang H, Yu X and Zhang D: Anti-inflammatory and analgesic potency of carboxyamidotriazole, a tumorostatic agent. J Pharmacol Exp Ther 325: 10-16, 2008.
53. Rovira P, Mascarell L and Truffa-Bachi P: The impact of immunosuppressive drugs on the analysis of T cell activation. Curr Med Chem 7: 673-692, 2000.
54. Maguire O, Tornatore KM, O'Loughlin KL, Venuto RC and Minderman H: Nuclear translocation of nuclear factor of activated T cells (NFAT) as a quantitative pharmacodynamic parameter for tacrolimus. Cytometry A 83: 1096-1104, 2013.
55. An SM, Ding QP and Li LS: Stem cell signaling as a target for novel drug discovery: Recent progress in the WNT and Hedgehog pathways. Acta Pharmacol Sin 34: 777-783, 2013.
56. Gregory MA, Phang TL, Neviani P, Alvarez-Calderon F, Eide CA, O'Hare T, Zaberezhnyy V, Williams RT, Druker BJ, Perrotti D, *et al*: Wnt/Ca^{2+}/NFAT signaling maintains survival of Ph^+ leukemia cells upon inhibition of Bcr-Abl. Cancer Cell 18: 74-87, 2010.
57. Krebs J, Agellon LB and Michalak M: Ca^{2+} homeostasis and endoplasmic reticulum (ER) stress: An integrated view of calcium signaling. Biochem Biophys Res Commun 460: 114-121, 2015.
58. Bilmen JG, Wootton LL and Michelangeli F: The inhibition of the sarcoplasmic/endoplasmic reticulum Ca^{2+}-ATPase by macrocyclic lactones and cyclosporin A. Biochem J 366: 255-263, 2002.
59. Chelu MG, Danila CI, Gilman CP and Hamilton SL: Regulation of ryanodine receptors by FK506 binding proteins. Trends Cardiovasc Med 14: 227-234, 2004.
60. Mahon FX, Belloc F, Lagarde V, Chollet C, Moreau-Gaudry F, Reiffers J, Goldman JM and Melo JV: *MDR1* gene overexpression confers resistance to imatinib mesylate in leukemia cell line models. Blood 101: 2368-2373, 2003.
61. Nobili S, Landini I, Giglioni B and Mini E: Pharmacological strategies for overcoming multidrug resistance. Curr Drug Targets 7: 861-879, 2006.

Exosomes released by imatinib-resistant K562 cells contain specific membrane markers, IFITM3, CD146 and CD36 and increase the survival of imatinib-sensitive cells in the presence of imatinib

TEREZA HRDINOVA[1,2], ONDREJ TOMAN[1], JIRI DRESLER[3], JANA KLIMENTOVA[4], BARBORA SALOVSKA[5], PETR PAJER[3], OLDRICH BARTOS[6], VACLAVA POLIVKOVA[1], JANA LINHARTOVA[1], KATERINA MACHOVA POLAKOVA[1,7], HANA KABICKOVA[3], BARBORA BRODSKA[1], MATYAS KRIJT[1], JAN ZIVNY[7], DANIEL VYORAL[1,7] and JIRI PETRAK[1,8]

[1]Institute of Hematology and Blood Transfusion; [2]Department of Cell Biology, Faculty of Science, Charles University, 128 20 Prague 2; [3]Military Health Institute, Military Medical Agency, 160 01 Prague 6; [4]Faculty of Military Health Sciences, University of Defense in Brno, 500 02 Hradec Kralove; [5]Department of Genome Integrity, Institute of Molecular Genetics of The Czech Academy of Sciences, 142 20 Prague 4; [6]Department of Infectious Diseases, First Faculty of Medicine, Charles University and Military University Hospital Prague, 169 02 Prague 6; [7]Institute of Pathological Physiology, First Faculty of Medicine, Charles University, 128 20 Prague 2; [8]Biotechnology and Biomedicine Centre of The Academy of Sciences and Charles University (BIOCEV), First Faculty of Medicine, Charles University, 252 50 Vestec, Czech Republic

Received May 27, 2020; Accepted October 8, 2020

DOI: 10.3892/ijo.2020.5163

Abstract. Chronic myeloid leukemia (CML) is a malignant hematopoietic disorder distinguished by the presence of a BCR-ABL1 fused oncogene with constitutive kinase activity. Targeted CML therapy by specific tyrosine kinase inhibitors (TKIs) leads to a marked improvement in the survival of the patients and their quality of life. However, the development of resistance to TKIs remains a critical issue for a subset of patients. The most common cause of resistance are numerous point mutations in the BCR-ABL1 gene, followed by less common mutations and multiple mutation-independent mechanisms. Recently, exosomes, which are extracellular vesicles excreted from normal and tumor cells, have been associated with drug resistance and cancer progression. The aim of the present study was to characterize the exosomes released by imatinib-resistant K562 ($K562^{IR}$) cells. The $K562^{IR}$-derived exosomes were internalized by imatinib-sensitive K562 cells, which thereby increased their survival in the presence of 2 μM imatinib. The exosomal cargo was subsequently analyzed to identify resistance-associated markers using a deep label-free quantification proteomic analysis. There were >3,000 exosomal proteins identified of which, 35 were found to be differentially expressed. From this, a total of 3, namely the membrane proteins, interferon-induced transmembrane protein 3, CD146 and CD36, were markedly upregulated in the exosomes derived from the $K562^{IR}$ cells, and exhibited surface localization. The upregulation of these proteins was verified in the $K562^{IR}$ exosomes, and also in the $K562^{IR}$ cells. Using flow cytometric analysis, it was possible to further demonstrate the potential of CD146 as a cell surface marker associated with imatinib resistance in K562 cells. Taken together, these results suggested that exosomes and their respective candidate surface proteins could be potential diagnostic markers of TKI drug resistance in CML therapy.

Correspondence to: Mrs. Tereza Hrdinova, Institute of Hematology and Blood Transfusion, U Nemocnice 1, 128 20 Prague 2, Czech Republic
E-mail: tereza.kabickova@uhkt.cz

Dr Jiri Petrak, Biotechnology and Biomedicine Centre of The Academy of Sciences and Charles University (BIOVEC), First Faculty of Medicine, Charles University, Prumyslova 595, 252 50 Vestec, Czech Republic
E-mail: jpetr@lf1.cuni.cz

Abbreviations: CML, chronic myeloid leukemia; TKI, tyrosine kinase inhibitor; $K562^{IR}$, K562 imatinib-resistant; NGS, next-generation sequencing; ddPCR, droplet digital PCR; LFQ, label-free quantification; CFSE, carboxyfluorescein succinimidyl ester; FACS, fluorescent-activated cell sorting; TRPS, tunable-resistive pulse sensing; LC-MS/MS, liquid chromatography coupled with tandem mass spectrometry; AGC, automatic gain control; FDR, false discovery rate; MFI, mean fluorescence intensity

Key words: chronic myeloid leukemia, imatinib mesylate, drug resistance, proteomics, exosome, tyrosine kinase inhibitor, surface marker

Introduction

Chronic myeloid leukemia (CML) is a clonal myeloproliferative disease characterized by reciprocal translocation between

chromosomes 9 and 22, t(9;22). This translocation results in the formation of the Philadelphia (Ph) chromosome, which encodes the fusion BCR-ABL1 oncogene coding a constitutively active Bcr-Abl tyrosine kinase (1-3). The approval of the Bcr-Abl inhibitor, imatinib (Glivec®) for clinical use in 2001 led to a significant improvement in the survival rate and prognosis of patients with CML (4). However, 10-15% of patients develop resistance to imatinib or to new-generation Bcr-Abl inhibitors (5). The resistance to TKIs is primarily caused by point mutations in the Bcr-Abl kinase domain, although other mechanisms that have been proposed include amplification of the BCR-ABL1 gene, overexpression of the Bcr-Abl protein or the presence of additional chromosomal aberrations and mutations (5-8).

An increasing number of studies have suggested that drug resistance in cancer, including leukemia, could be mediated by exosomes (9,10). Exosomes are small (30-150 nm) extracellular membrane vesicles, that are released by cells into the microenvironment upon fusion of multivesicular bodies with the plasma membrane (11). Exosomes contain proteins, lipids, mRNA, microRNAs (miRNAs) and DNA (12,13) and may fuse with other cells (14). They affect numerous physiological and pathological processes, including cancer (15). Exosomes derived from CML cells have been shown to modulate leukemia progression either directly via stimulation of leukemia cells (16), or indirectly through stimulation of other cells involved in leukemia biology, such as macrophages, bone marrow stromal cells and endothelial cells (17-21). Notably, exosomes derived from imatinib-resistant CML cells have recently been shown to fuse with imatinib-sensitive CML cells, thereby increasing their survival in the presence of imatinib (22).

The aims of the present study were: i) To confirm the previously observed pro-survival effect of exosomes derived from imatinib-resistant K562 cells ($K562^{IR}$); ii) to characterize the protein cargo of the exosomes; and iii) to identify potential specific cell surface markers of imatinib resistance in CML cells.

Materials and methods

Materials. All chemicals, unless otherwise stated, were purchased from Merck KGaA.

Cell lines. The human K562 chronic myeloid leukemia cell line was purchased from the German Collection of Microorganisms and Cell Cultures, GmbH and cultured in RPMI medium (Thermo Fisher Scientific, Inc.) supplemented with 10% fetal bovine serum (FBS; Gibco; Thermo Fisher Scientific, Inc.), 100 U/ml penicillin G, 100 μg/ml streptomycin and 7.5% sodium bicarbonate at 37˚C in an humidified incubator with 5% CO_2. The $K562^{IR}$ cells were derived from original imatinib-sensitive K562 cells, that had been cultured in gradually increasing concentrations of imatinib in the culture medium (from 0.1 to 2 μM) for 9 months, as previously described (23). The concentration of imatinib was increased by 0.1 μM at each step and was maintained for 15-30 days, depending on the proportion of surviving cells. The resulting $K562^{IR}$ cell line was resistant to 2 μM imatinib.

Cell viability assay. The K562 and $K562^{IR}$ cell lines were cultured in the presence of different concentrations (0 to 2 μM) of imatinib for 3 days. Imatinib toxicity was determined by measuring cell viability using a Vybrant™ MTT cell proliferation assay kit (Thermo Fisher Scientific, Inc.), following the manufacturer's instructions. Proprietary solvent B containing SDS (from the kit) diluted with 0.01 M HCl was used to solubilize the purple formazan. Absorbance was detected at 570 nm using a microplate reader (Chameleon; Hidex Oy). Data was analyzed using MikroWin 2000 software, v4.0 (Mikrotek Laborsysteme GmbH).

Mutational analysis. The K562 and $K562^{IR}$ cell lines were analyzed using a next-generation sequencing (NGS) method, as previously described (24). Briefly, the amplicon library was prepared using a two-step selective amplification of cDNA, including the BCR-ABL1 kinase domain. At the first step, BCR-ABL1 cDNA was amplified, then primers, from the IRON II study (25), were used to prepare four 350 bp amplicons of the kinase domain. Sequencing was subsequently performed on a GS Junior 454 System, and the data was analyzed using the Amplicon Variant Analyzer software (both from Roche Diagnostics). The raw NGS data are freely available via NCBI Sequence Read Archive (https://www.ncbi.nlm.nih.gov/sra) under the project accession number, PRJNA664680, while the imatinib sensitive K562 and the imatinib resistant K562 cells have the accession numbers, SRX9210642 and SRX9210641, respectively.

BCR-ABL1 gene copy number analysis. The number of BCR-ABL1 gene copies was determined using the quantitative droplet digital PCR (ddPCR) method and a K562 specific assay based on the break-point sequence of the BCR-ABL1 gene (26). ddPCR was performed using a QX200 Droplet Digital PCR system and an Auto Droplet Generator (Bio-Rad Laboratories, Inc.) according to the manufacturer's instructions. The albumin gene was used as a control for the DNA reaction load. QuantaSoft™ v1.7.4.0917 software (Bio-Rad Laboratories, Inc.) was used for data analysis, and samples were analyzed in quadruplicate.

Measurement of BCR-ABL1 transcript levels. Total RNA was isolated from cells using TRIzol® (Thermo Fisher Scientific, Inc.) according to the manufacturer's instructions. cDNA was synthesized using 200 U M-MLV reverse transcriptase (Promega Corporation) and random hexamer primers (Jena Bioscience GmbH) according to the manufacturer's instructions, with incubation at 37˚C for 1 h and denaturation at 95˚C for 5 min. β-Glucuronidase (GUSB) was used as the control gene (27,28). The primers and probes for BCR-ABL1 and GUSB were designed, and the measurement of the expression levels were performed, according to the Europe Against Cancer protocol (29). The method has been standardized in the project of European Leukemia Net (30). The following primers and probes were used: GUSB forward, 5'-GAAAAT ATGTGGTTGGAGAGCTCATT-3, reverse 5-CCGAGT GAAGATCCCCTTTTTA-3 and fluorescein-containing probe, 5'-FAM-CCAGCACTCTCGTCGGTGACTGTT CA-BHQ1-3'; BCR-ABL1 forward, 5'-TCCGCTGACCAT CAATAAGGA-3', reverse 5'-CACTCAGACCCTGAGGCT CAA-3' fluorescein-containing probe, 5'-FAM-CCCTTC AGCGGCCAGTAGCATCTGA-BHQ1-3' (Integrated DNA

Technologies, Inc.). The following thermocycling conditions were used: Initial denaturation at 95˚C for 10 min and 45 cycles of 95˚C for 15 sec and 60˚C for 1 min. For RT-qPCR gene expression analysis, the ERM-AD623 reference material (Join Research Centre, Belgium) (31,32) was used to create the calibration curve for the determination of the number of copies of BCR-ABL1 and GUS gene.

Exosome isolation. The K562 and K562^{IR} cell lines were cultured for 5 days in RPMI medium with 10% exosome-depleted FBS. Exosomes were isolated from 200 ml cell culture media, as previously described (33). Briefly, conditioned medium was obtained as the supernatant from the centrifugation of live cells (300 x g for 10 min at 4˚C). Subsequently, dead cells were removed using a further round of centrifugation (2,000 x g for 10 min at 4˚C). The supernatant was filtered [using a Filtropur S syringe filter (0.22-μm membrane); Sarstedt AG & Co. KG] to remove larger vesicles and cell debris. The resultant suspension was then ultracentrifuged (100,000 x g for 70 min at 4˚C) using a Sorvall™ WX+ ultracentrifuge and a T647.5 fixed angle rotor (Thermo Fischer Scientific, Inc.). Exosome pellets were resuspended in PBS, and sedimented again (100,000 x g for 70 min at 4˚C).

Exosome visualization using transmission electron microscopy/negative staining. Isolated exosomes were resuspended in Trump's 4F:1G fixative, comprising 86 ml distilled water, 10 ml 40% formaldehyde (Merck KGaA), 4 ml 25% glutaraldehyde (Polysciences, Inc.), 1.16 g monosodium phosphate and 0.27 g sodium hydroxide (34), and adsorbed on Formvar/carbon coated grids conditioned with 1% Alcian blue in 1% acetic acid. The adsorbed particles were embedded in a layer of 2% phosphotungstic acid. Grids were viewed at 100 kV using a JEM 2000 CX microscope (JEOL, Ltd.) equipped with an Olympus MegaviewTM II digital camera (Olympus Corporation).

Particle size and concentration measurement using tunable-resistive pulse sensing (TRPS). An aliquot of exosomes resuspended in PBS was placed in the nanopore NP150 (qNano; Izon Science). All samples were measured at defined membrane stretch and with the same applied voltage at two different pressure levels (5 and 11 mbar). Calibration particles were measured directly after the sample measurement, and under identical conditions.

Exosome preparation for tandem mass spectrometry (MS/MS) analysis. A total of 5 independent isolations of exosomes, from both the K562 and K562^{IR} cell lines, were subjected to MS/MS analysis. The filter-aided sample preparation method was used, with some modifications (35). Exosomes in PBS were resuspended in 100 mM ammonium bicarbonate, transferred to spin columns (Amicon Ultra 0.5 ml 10 kDa MWCO centrifugal filters; Merck KGaA) and centrifuged at 26,000 x g for 20 min at 4˚C. The samples were then washed twice with 400 μl 100 mM ammonium bicarbonate and centrifuged again (26,000 x g for 20 min at 4˚C). RapiGest™ (0.1%; Waters Corporation) dissolved in 100 μl 50 mM Tris/HCl, (pH 7.5) was subsequently added to the samples in the spin columns, then the samples were incubated at 95˚C 10 min. After allowing the samples to cool down, 200 μl 0.1% RapiGest™ in 50 mM Tris/HCl, (pH 7.5) with 8 M guanidinium chloride was added, and the samples were subsequently incubated for 20 min at room temperature. The samples were then centrifuged at 18,000 x g for 25 min at 25˚C. Aliquots of the samples (10 μl) were taken, and the protein concentration was quantified using a QuantiPro™ BCA Assay kit (Sigma-Aldrich; Merck KGaA). Subsequently, the samples were reduced with 100 μl 100 mM (Tris)2-carboxyethyl phosphine hydrochloride for 30 min at 55˚C in a thermoshaker (Biosan, Ltd.) set at 600 rpm, alkylated with 100 μl 300 mM iodoacetamide at 37˚C for 30 min in the dark, then centrifuged at 12,000 x g for 35 min at 25˚C. Next, the samples were digested overnight at 37˚C using 2 μg sequencing-grade trypsin (Promega Corporation). The digested samples were then transferred into a new microtube for subsequent centrifugation (12,000 x g for 35 min at room temperature). Empore™ Solid Phase Extraction cartridges (C18; standard density, bed I.D., 4 mm) (3M Company) were used to desalt the peptide mixtures. Peptides were eluted in 60% acetonitrile (ACN)/0.1% trifluoroacetic acid (TFA), then dried in a SpeedVac. Prior to MS analysis, the samples were resuspended in 30 μl 2% ACN/0.1% TFA.

Liquid chromatography (LC) MS/MS (LC-MS/MS)

LC-MS/MS analysis. An UltiMate™ 3000 RSLCnano system controlled by Chromeleon software (Dionex; Thermo Fisher Scientific, Inc.) was used for LC separation. Aliquots (1 μl) of each sample (10X diluted) were loaded onto a PepMap100 C18, 3 μm, 100 Å, 0.075x20 mm trap column (Dionex; Thermo Fisher Scientific, Inc.) at 5 μl/min for 5 min. Peptides were then separated on a PepMap RSLC C18, 2 μm, 100 Å, 0.075x150 mm analytical column (Dionex; Thermo Fisher Scientific, Inc.) using a gradient formed by the mobile phase A [0.1% formic acid (FA)] and mobile phase B (80% ACN/0.1% FA), running from 4-34% in 68 min, and from 34-55% of mobile phase B in 21 min, at a flow rate of 0.3 μl/min at 40˚C. Eluted peptides were on-line electrosprayed into a Q-Exactive™ mass spectrometer using a Nanospray Flex ion source (Thermo Fisher Scientific, Inc.). Positive ion full-scan MS spectra (350-1,650 m/z) were acquired using a $1x10^6$ automatic gain control (AGC) target in the Orbitrap at 70,000 resolution. The top 12 precursors with charge state ≥2 and threshold intensity of $5x10^4$ counts were selected for higher-energy collisional dissociation fragmentation, with a dynamic exclusion window of 30 sec. The isolation window of 1.6 Da and normalized collision energy 27% was used. Each MS/MS spectrum was acquired at a resolution of 17,500, with a $1x10^5$ AGC target and a maximum 100 msec injection time.

Label-free quantification (LFQ): Raw data processing. The raw files were further analyzed using MaxQuant software, v1.5.3.30 (36) [with Andromeda as the search engine (37)] against the *Homo sapiens* subset of the SwissProt database (downloaded on 4th July 2019; 26,468 sequences). Only tryptic peptides, that were at least 7 amino acids in length, with up to two missed cleavages were considered. Mass tolerance was set to 4.5 ppm at the MS level, and 0.5 Da at the MS/MS level. The oxidation of methionine was set as a variable modification, and the carbamidomethylation of cysteine was set as a fixed modification. A false discovery rate (FDR) of 1% was used for peptide spectrum matches and protein identification using a

target decoy approach. Relative quantification was performed using the default parameters of the MaxLFQ algorithm (38), with the minimum ratio count set to 2.

LFQ: Data analysis. The 'proteinGroups.txt' MaxQuant output file was uploaded into Perseus (39) v1.5.2.6. Decoy hits, proteins only identified by site, and potential contaminants were removed. Protein groups quantified in at least four replicates out of five were considered for further $\log_2$ transformation of the LFQ intensities. Missing values were imputed from a normal distribution [Gaussian distribution width, 0.3 standard deviation (SD) and downshift 1.8 SD of the original data]. Data was normalized using the open source tool, Normalyzer (http://quantitativeproteomics.org/normalyzerde) and the variance stabilization normalization method (40). A Student's t-test (permutation based FDR 0.05, S0=0.1) was used for statistical analysis. Finally, proteins from this group with a fold change at least 1.5 were considered as being significantly different ($P<0.05$). Pearson's correlation test was performed to evaluate the inter-run reproducibility of individual LC-MS analyses. Proteins with known or expected cell-surface localization were selected using GenieScore, an algorithm for the prediction of surface localization (41). The Exocarta database (www.exocarta.org) was used to compare the proteins identified with those already found in exosomes.

Western blot analysis. The exosome pellets were lysed in 150 μl lysis buffer containing 140 mM sodium chloride, 10 mM HEPES, 0.15% Triton X100 and a protease inhibitor cocktail (1 tablet/10 ml; Roche Diagnostics), and subsequently incubated on ice for 20 min. The exosome samples were pooled and concentrated in an Amicon Ultra 0.5 ml 3 kDa MWCO centrifugal filter (Amicon Ultra; Merck KGaA) from 3 or 4 individual isolations. The protein concentration was determined using a Micro BCA™ protein assay kit (Pierce; Thermo Fisher Scientific, Inc.) according to the manufacturer's instructions, and protein samples were immediately frozen and stored at -80˚C.

The cell pellets were lysed in CelLytic™ M lysis buffer containing protease inhibitor cocktail (1 tablet/10 ml; Roche Diagnostics) on ice for 20 min. The cleared cell lysates were collected by centrifugation at 15,000 x g for 20 min at 4˚C, and the protein concentration was then determined using the Bradford method (Bio-Rad Laboratories, Inc.).

The lysate samples (30-60 μg) were mixed with Laemmli sample buffer (Bio-Rad Laboratories, Inc.) containing 2-mercaptoethanol and separated on 4-15% or 7.5% (in the case of Bcr-Abl separation) precast gels (Mini PROTEAN® TGX™; Bio-Rad Laboratories, Inc.). The separated proteins were transferred onto polyvinylidene fluoride membranes using the iBlot system, according to manufacturer's instructions (Thermo Fisher Scientific, Inc.). The membranes were blocked for 1 h in SuperBlock™ blocking buffer (Thermo Fisher Scientific, Inc.) and incubated overnight at 4˚C with primary antibodies diluted to 1:1,000 in PBST (PBS, 0.1% Tween-20). The following primary antibodies were used: Anti-c-Abl rabbit polyclonal antibody (cat. no. 2862S; Cell Signaling Technology, Inc.), anti-Bcr-Abl mouse monoclonal antibody (7C6) (cat. no. ab187831; Abcam), anti-GAPDH rabbit monoclonal antibody (cat. no. SAB5600208; Merck KGaA), anti-IFITM3 (cat. no. 59212; Cell Signaling Technology, Inc.), anti-CD146 mouse monoclonal antibody (cat. no. 563619; BD Biosciences), anti-CD36 rabbit monoclonal antibody (cat no. 14347S; Cell Signaling Technology, Inc.) and EXOAB antibody kit 1 (Systems Biosciences, LLC) containing rabbit polyclonal antibodies against CD63, CD81, anti-CD9 and HSP70. After extensive washing in PBST, the membranes were incubated with secondary horseradish peroxidase-conjugated anti-rabbit antibody (cat. no. 7074P2) or anti-mouse antibody (cat. no. 7076P2) (both at 1:20,000 and from Cell Signaling Technology, Inc.) for 90 min at room temperature. Protein bands were detected with an enhanced chemiluminescence detection reagent (Cytiva) using a G:BOX imager (Syngene Europe), and quantified using ImageJ software, v1.8.0 (National Institutes of Health).

Exosome fluorescent labeling and uptake monitoring. Fresh exosomes were washed and resuspended in PBS at room temperature. A 10 mM stock solution of carboxyfluorescein succinimidyl ester (CFSE) (Invitrogen; Thermo Fisher Scientific, Inc.) was diluted to a final concentration of 20 μM and added to the exosomes. The suspension was subsequently mixed and incubated for 25-30 min at room temperature in the dark. The labeling process was stopped by adding 4 ml of cold complete media, containing 10% FBS on ice for 5 min. CFSE-labeled exosomes were diluted in 60 ml PBS, collected by ultracentrifugation (100,000 x g for 70 min at 4˚C) and resuspended in 1.5 ml cell culture media with K562 cells (500,000 cells/ml). CFSE-positive cells were observed under a FluoView FV1000 confocal laser scanning microscope (Olympus Corporation) using an UPlanSAPO 60x NA1.35 oil immersion objective (magnification, x60). A 488 nm laser was used for CFSE excitation, and fluorescence emission was detected with a high sensitivity GaAsP detector at 500-600 nm. Fluorescent images were processed using the FluoView softwarel(FV10 ASW v3.1; Olympus Corporation).

Exosomes and cell co-cultivation. The K562 cells were co-cultured with either $K562^{IR}$-derived or K562-derived exosomes for 4 h, and then treated with 2 μM imatinib for 48 h. Cell viability was measured using a Vybrant® Cell Proliferation Assay kit (Thermo Fisher Scientific, Inc.); proprietary solvent B containing SDS was mixed with 0.01 M HCl and used to solubilize the purple formazan. The absorbance was measured at 570 nm using a microplate reader (Chameleon; Hidex Oy).

FACS analysis. The K562 and $K562^{IR}$ cells ($1.5x10^6$ cells) were washed in washing buffer (PBS supplemented with 0.1% BSA and 2 mM EDTA), centrifuged at 300 x g for 10 min at room temperature, then resuspended in washing buffer. Aliquots (50 μl) of the cell suspension (100,000 cells/tube) were transferred to FACS tubes and 1 μl anti-IFITM3 AF405 (cat. no. ITA8095; 1:50; G-Biosciences; Geno Technology, Inc.), 1 μl anti-CD146 (cat. no. 563619; 1:50; BD Biosciences) and 2 μl anti-Hu CD36 FITC (cat. no. 1F-451-T100; 1:25; EXBIO Praha, a.s.) were added. The samples were incubated in the dark for 30 min at room temperature, then washed again with 1 ml of washing buffer, prior to centrifugation (300 x g for 5 min at 25˚C). Washing buffer (250 μl) was added to the cell pellet, and the samples were analyzed using

flow cytometry, in triplicate, using BD FACSCanto™ II Cell Analyzer (BD Biosciences). The data was analyzed using BD FACSDiva software (v6.1.3; BD Biosciences). MFI was determined for the whole sample, and the fraction of positively stained cells (P2) was determined as the percentage of the parent population.

Statistical analysis. The data are expressed as the mean ± SD, from at least three replicates. Statistical analysis was performed using GraphPad Prism v8.0 software (GraphPad Software, Inc.). Relative resistance of K562 and K562^{IR} cells to imatinib was evaluated using an unpaired Student's t-test. For the investigation of cell survival following exosome exposure, one-way ANOVA with Tukey's post hoc test was used to determine the statistical significance. $P<0.05$ was considered to indicate a statistically significant difference.

Results

Development of imatinib resistant K562 cells. Imatinib-resistant K562^{IR} cells were derived from the originally imatinib-sensitive K562 cells [half-maximal inhibitory concentration (IC_{50}), 0.25-0.35 μM]. The K562^{IR} cells proliferated in imatinib concentrations exceeding 2 μM (Fig. 1).

Characterization of the K562^{IR} cells: Mutation analysis and BCR-ABL1 gene expression. A mutation in the kinase domain of BCR-ABL1 is the most common mechanism by which imatinib (and other TKIs) resistance develops in patients with CML (7). To investigate the mutational status of the BCR-ABL1 kinase domain in the K562^{IR} cells, NGS sequencing was performed; however, no mutations in the kinase domain, with variant allele frequency >1% were found. In patients with TKI resistance but without a kinase domain mutation, an amplification of the BCR-ABL1 gene is typically found (7). Therefore, ddPCR was used to identify the number of BCR-ABL1 gene copies, and it was revealed that the K562^{IR} cells harbored a 2-fold higher number of BCR-ABL1 gene copies compared with that in imatinib sensitive K562 cells (data not shown).

As the BCR-ABL1 gene amplification may result in overexpression of the BCR-ABL1 gene and increase the levels of the Bcr-Abl protein, the mRNA and protein expression levels were compared between the K562 and K562^{IR} cell lines. The results revealed increased expression levels of BCR-ABL1 mRNA (Fig. 2A) and of the Bcr-Abl protein (Fig. 2B).

Exosome characterization. The exosomes were isolated from the K562 and K562^{IR} cell culture supernatants using ultracentrifugation. The exosome purity was verified using transmission electron microscopy, revealing round or cup-shaped vesicles, ranging between 50-150 nm in diameter (Fig. 3). The qNano/TRPS analysis of the exosomes confirmed comparable size distributions of the vesicles, with the highest peak occurring at 100-110 nm. The number of exosomes isolated from the cell media of the K562^{IR} cells ($1.67x10^{11}$ particles/ml) was ~2 times higher compared with that in the K562 cells ($8.14x10^{10}$ particles/ml) (Fig. S1).

To further confirm that the pelleted material represented exosomes, the presence of 'exosomal markers' i.e. proteins commonly found in exosomes (CD63, CD9, CD81, HSP70 and GAPDH) (42), was confirmed using western blot analysis (Fig. 4). As the CML landmark fusion protein, Bcr-Abl was overexpressed in the K562^{IR} cells, it was also possible to show the presence of the Bcr-Abl protein in the corresponding exosomes.

Uptake of K562^{IR}-derived exosomes by the K562 cells. K562-derived exosomes have been previously shown to be taken up by various cell types, such as bone marrow stromal cells, macrophages, endothelial cells and leukemic cells (16,17,19-21,43). Notably, exosomes derived from

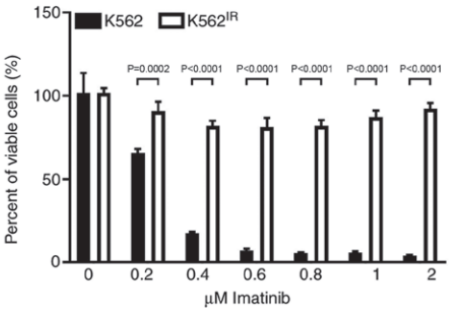

Figure 1. Relative viability of the K562 and K562^{IR} cells cultured in the presence of imatinib for 3 days. The viability was assessed using a MTT assay. Error bars indicate ± SD of three independent measurements. IR, imatinib-resistant.

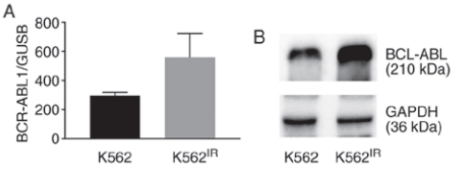

Figure 2. BCR-ABL1 mRNA and Bcr-Abl protein expression levels in the K562 and K562^{IR} cells. BCR-ABL1 (A) mRNA and (B) protein expression levels in the K562 and K562^{IR} cells were determined using reverse transcription-quantitative PCR and western blot analysis, respectively. IR, imatinib-resistant.

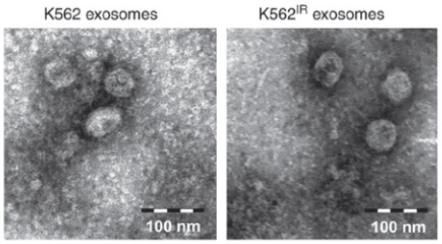

Figure 3. Exosomes from the K562 and K562^{IR} cells were visualized using transmission electron microscopy. Exosomes were defined as round or cup-shaped vesicles, at sizes between 50-150 nm. Scale bar, 100 nm. IR, imatinib-resistant.

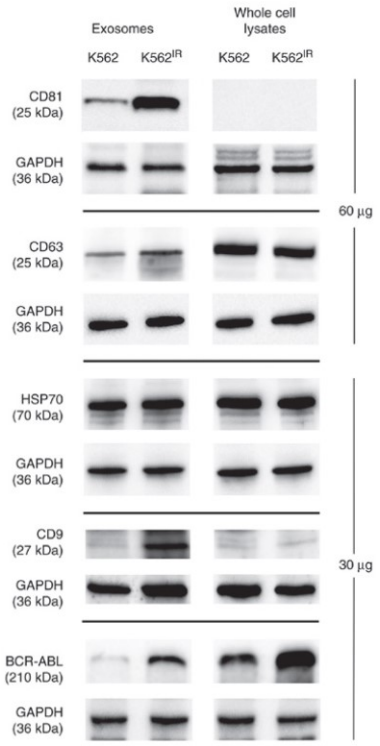

Figure 4. Presence of exosomal markers in the exosomes and cell lysates. Western blot analysis was used to detect the expression levels of known exosomal markers and the Bcr-Abl protein in exosomes isolated from the K562 and K562^{IR} cells, and in corresponding cells. For Bcr-Abl, CD9 and HSP70, 30 μg total protein was loaded for both exosomes and lysates, while 60 μg protein was loaded for CD63 and CD81. Exosomes and cell lysates that were to be probed by the same antibody were always loaded together on a single gel/membrane; the signals obtained are therefore comparable between exosomes and cell lysates. Irrelevant lanes have been cropped from the figure.

imatinib-resistant CML cells have been recently shown to fuse with, and confer drug resistance traits to, imatinib-sensitive CML cells (22). In the present study, the fusion of K562^{IR}-derived exosomes (labelled with fluorescent CFSE) with K562 cells, and the fusion of K562-derived exosomes with K562 cells, was confirmed following a 4-h incubation (Fig. 5). CFSE-positive K562 cells were detected using confocal microscopy, as soon as 1 h after the addition of the labelled exosomes, with the maximum uptake occurring after 4 h, as determined in a pilot time-course experiment (data not shown).

Exosomes from K562^{IR} cells increase survival of K562 cells in the presence of imatinib. Min *et al* (22) demonstrated that exosomes released from imatinib-resistant K562 cells were able to transfer drug-resistant traits to imatinib-sensitive K562 cells. To confirm this observation, K562^{IR}- or K562-derived exosomes were isolated and incubated with K562 cells for 4 h, prior to the addition of imatinib (2 μM) for 2 days. As shown

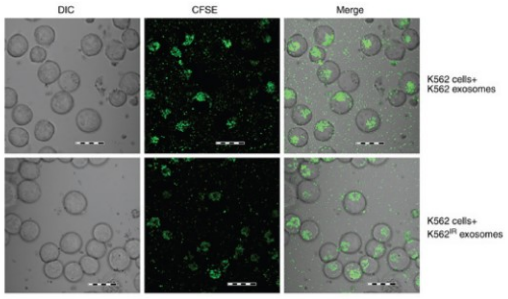

Figure 5. Internalization of the exosomes by the K562 cells visualized using confocal microscopy. The K562^{IR} exosomes loaded with CFSE (green) were internalized into the K562 cells and visualized in the cytoplasm after a 4-h incubation. Similarly, exosomes released from the imatinib-sensitive K562 cells were internalized into the K562 cells. Scale bar, 20 μm. CFSE, carboxyfluorescein succinimidyl ester; IR, imatinib-resistant.

in Fig. 6, exosomes derived from the K562^{IR} cells significantly increased the survival rate of imatinib-sensitive K562 cells in the presence of imatinib, compared with the K562 cells incubated with exosomes derived from K562 cells, and also compared with the K562 cells treated with no exosomes. The control exosomes derived from the K562 cells; however, had no measurable effect on cell viability (Fig. 6).

Therefore, it could be hypothesized that the specific composition of the K562^{IR}-derived exosomes was responsible for the enhanced survival of the K562 cells. To characterize the unique protein content of the exosomes and to identify their specific (preferably surface) markers, a detailed proteomic analysis was subsequently performed.

LFQ proteomic analysis of the exosomes. Exosomes derived from the K562 and K562^{IR} cells were subjected to LFQ proteomic analysis. A total of 10 samples of the respective exosomes, obtained from five independent isolations of both the K562^{IR} and K562 cells, were analyzed using LC-MS/MS (Q-Exactive). With the FDR set to 0.01, between 1,072 and 1,751 exosomal proteins were identified in each sample; in total, 3,218 unique exosomal proteins were identified. Of those, 2,693 proteins were listed in the Exocarta database of exosomal proteomes (www.exocarta.org); therefore, the present study identified 525 novel exosomal proteins.

To determine the quantitative robustness of the label-free analysis, the quantitative similarity of all the LC-MS/MS runs was examined. Correlation analysis revealed good inter-sample reproducibility, with Pearson's correlation coefficients in the range of 0.723-0.971 (Fig. S2). The LFQ analysis provided semi-quantitative data for 1,241 proteins (Table SI).

Differentially abundant proteins. A total of 35 proteins with significantly different quantities were identified in the K562^{IR}-derived exosomes compared with the K562-derived exosomes (fold change >1.5) (Fig. 7 and Table I). Of these 35 proteins, 28 were found to be upregulated, while 7 were downregulated, in the K562^{IR} exosomes. The most upregulated proteins in the K562^{IR} exosomes included interferon-induced transmembrane protein 3 (IFITM3), desmoglein-2 (DSG2),

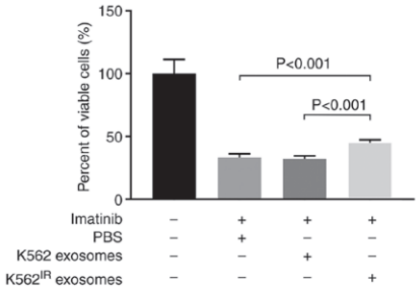

Figure 6. Incubation of the K562^{IR} exosomes with imatinib-sensitive K562 cells increases the cell viability of the K562 cells in the presence of 2 μM imatinib. One-way ANOVA with Tukey's post-hoc test was used. The mean values ± SD were calculated from three independent experiments. IR, imatinib-resistant.

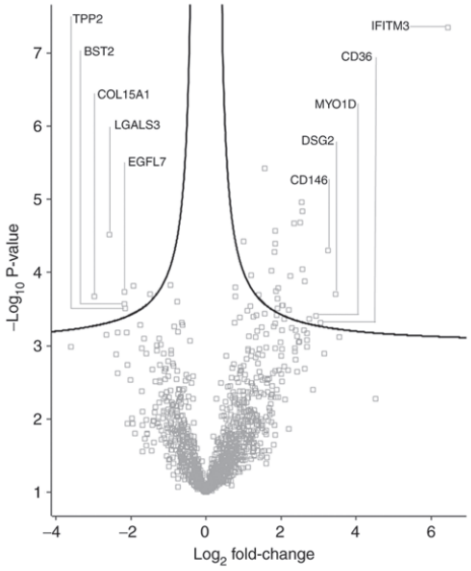

Figure 7. Differentially abundant exosomal proteins were identified using label-free quantification proteomic analysis of the K562 and K562^{IR} exosomes. Proteins with positive log2 fold change were upregulated in the K562^{IR} exosomes, while negative fold-change indicated proteins were down-regulated in the K562^{IR} exosomes. Only the proteins above the black line indicating statistical significance (false discovery rate <0.05, S0=0.1) were considered.

cell-surface glycoprotein MUC18 (CD146) and platelet glycoprotein 4 (CD36). Among the most downregulated were collagen α-1 (XV) chain, galectin-3-binding protein (LGALS3BP), laminin subunit β-1 (LAMB1), bone marrow stromal antigen 2 (BST2) and epidermal growth factor-like protein 7 (EGFL7).

The most highly upregulated proteins (at least 5-fold) were further investigated with special focus on proteins localized on the cell or exosomal membrane. Among the

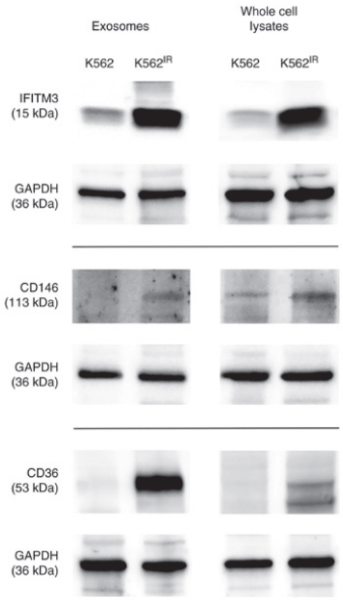

Figure 8. Confirmation of the differential abundance of IFITM3, CD146 and CD36 in the exosomes and cells using western blot analysis with specific antibodies. Protein samples (60 mg) were separated on precast 4-15% SDS PAGE gels. Irrelevant lanes have been cropped from the figure. IFITM3, interferon-induced transmembrane protein 3; IR, imatinib-resistant.

candidates selected by the LFQ proteomic analysis, three such proteins were identified using GenieScore, an algorithm for the prediction of surface localization (41): IFITM3, CD146 (MUC18) and CD36. The presence of these proteins was confirmed in the exosomes and also in the cells of their origin using western blot analysis with specific antibodies (Fig. 8).

The western blot data confirmed the upregulation of all three proteins in the K562^{IR}-derived exosomes, as well as in the 'source' K562^{IR} cells. Therefore, the upregulated surface membrane proteins could potentially serve, not only as exosomal markers, but also as cell-surface markers specific for a resistant population of the K562 cells.

IFITM3 and CD146 as specific surface markers of imatinib-resistant K562 cells. To determine the potential of the identified proteins as cell-surface markers of imatinib resistance, flow cytometric analysis of the K562 and K562^{IR} cells was performed using antibodies against IFITM3, CD146 and CD36. Live cells were used to determine the cell-surface expression of the putative markers.

Flow cytometry revealed markedly increased surface expression levels of IFITM3 and CD146, and to a lesser extent also of CD36, in K562^{IR} cells compared with the K562 cells (Fig. 9). CD146 was detected in 96.2% of the K562^{IR} cells compared with 0.7% of the K562 cells, while IFITM3 was detected in 51.6% of the K562^{IR} cells compared with 4% of the K562 cells. Anti-CD36 antibody stained 10.5% of the

Table I. Differentially abundant proteins in the $K562^{IR}$-derived exosomes, as compared with that in the K562-derived exosomes.

A, Upregulated protein in $K562^{IR}$ exosomes

Protein names	Protein IDs	Gene names	Fold change	Unique peptides	MS/MS	Permutation-based FDR
Interferon-induced transmembrane protein 3	Q01628	IFITM3	87.5	1	24	<0.001
Desmoglein-2	Q14126	DSG2	10.9	10	33	0.002
Cell surface glycoprotein MUC18	P43121	MCAM	9.6	11	28	<0.001
Platelet glycoprotein 4	P16671	CD36	8.4	7	18	0.005
Unconventional myosin-Id	O94832	MYO1D	7.6	21	41	0.004
CD2-associated protein	Q9Y5K6	CD2AP	6.7	29	105	0.004
Multivesicular body subunit 12A	Q96EY5	MVB12A	6.2	2	19	0.001
Golgi integral membrane protein 4	O00461	GOLIM4	6.0	18	37	<0.001
Protein TFG	Q92734	TFG	5.9	3	9	<0.001
Melanoma-associated antigen 4	P43358	MAGEA4	5.8	9	20	<0.001
Spastin	Q9UBP0	SPAST	5.7	9	19	<0.001
Melanotransferrin	P08582	MFI2	5.1	10	19	<0.001
Charged multivesicular body protein 4a	Q9BY43	CHMP4A	4.8	9	35	0.001
Tetraspanin-18	Q96SJ8	TSPAN18	4.6	3	13	0.003
Rab11 family-interacting protein 1	Q6WKZ4	RAB11FIP1	4.1	16	37	0.003
STAM-binding protein	O95630	STAMBP	4.1	9	16	0.003
Rac GTPase-activating protein 1	Q9H0H5	RACGAP1	3.8	10	18	0.002
Hepatocyte growth factor-regulated tyrosine kinase substrate	O14964	HGS	3.8	15	45	0.003
Protein tweety homolog 2	Q9BSA4	TTYH2	3.7	3	13	0.002
Toll-interacting protein	Q9H0E2	TOLLIP	3.7	4	24	0.002
Vacuolar protein sorting-associated protein 4A	Q9UN37	VPS4A	3.5	11	76	<0.001
Syntenin-1	O00560	SDCBP	3.6	22	207	<0.001
Hemoglobin subunit ε	P02100	HBE1	3.6	11	56	<0.001
Charged multivesicular body protein 4b	Q9H444	CHMP4B	3.3	15	86	<0.001
Crk-like protein	P46109	CRKL	3.0	12	56	<0.001
L-aminoadipate-semialdehyde dehydrogenase-phosphopantetheinyl transferase	Q9NRN7	AASDHPPT	2.6	6	10	0.002
Hemoglobin subunit ζ	P02008	HBZ	2.3	13	217	0.001
Heat shock protein 105 kDa	Q92598	HSPH1	2.0	19	79	<0.001

B, Downregulated proteins in $K562^{IR}$ exosomes

Protein names	Protein IDs	Gene names	Fold change	Unique peptides	MS/MS	Permutation-based FDR
DNA topoisomerase 2-β	Q02880	TOP2B	-2.8	7	23	0.002
Tyrosine-protein kinase receptor UFO	P30530	AXL	-3.8	7	21	0.002
Tripeptidyl-peptidase 2	P29144	TPP2	-4.4	57	211	0.003
Epidermal growth factor-like protein 7	Q9UHF1	EGFL7	-4.5	4	10	0.002
Bone marrow stromal antigen 2	Q10589	BST2	-4.5	6	17	0.003
Galectin-3-binding protein	Q08380	LGALS3BP	-5.9	6	17	0.001
Collagen α-1(XV) chain	P39059	COL15A1	-7.9	15	102	0.002

Positive fold change indicates upregulation, while negative fold changes indicates downregulation in $K562^{IR}$-derived exosomes. FDR, false discovery rate; MS, mass spectrometry.

$K562^{IR}$ compared with 3% of the K562 cells. The analysis demonstrated that CD146 expression, in particular, clearly distinguishes K562 from $K562^{IR}$ cells, and therefore it may be used as a reliable cell-surface marker of imatinib resistance in

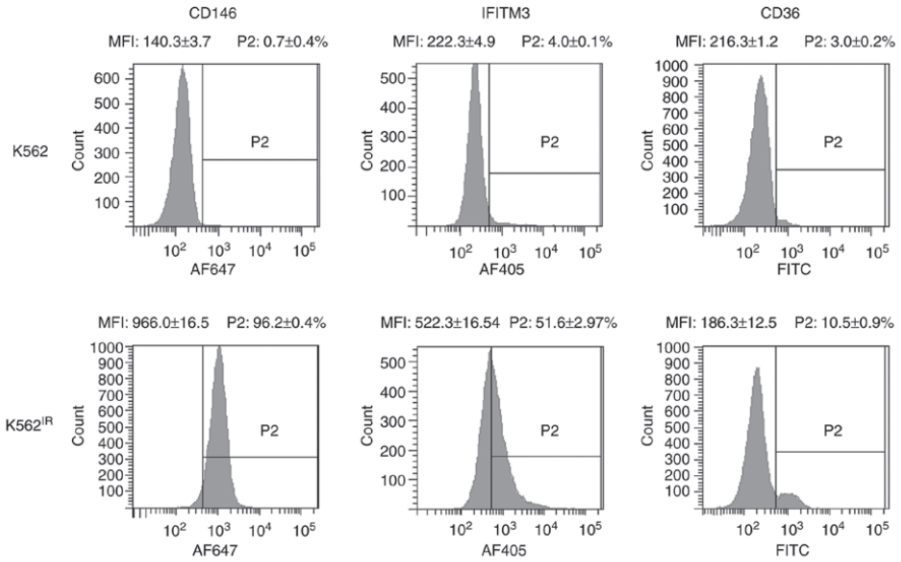

Figure 9. Surface-marker analysis of the K562 and K562^{IR} cells. Flow cytometry was used to confirm the increased expression of CD146, IFITM3 and CD36 on the surface of the K562^{IR} cells. The mean MFI and P2 values ± SD were calculated from three independent experiments. Representative graphs from repeated experiments are shown. IFITM3, interferon-induced transmembrane protein 3; MFI, mean fluorescence intensity; IR, imatinib-resistant.

these cells. In addition, promising results were also obtained with IFITM3.

Discussion

Incubation of isolated and carefully characterized K562^{IR}-derived exosomes with K562 cells, prior to exposure to imatinib, slightly, but significantly, increased the survival of the K562 cells in toxic doses of imatinib (2 μM). Thus, the results confirmed the observation Min *et al* (22) made in the same cell line, providing further evidence for the role of exosomes in the horizontal transfer of information among cancer cells, including pro-survival signals or a drug-resistance trait.

To what extent an exosome-mediated survival plays in the development of resistance to imatinib in patients with CML remains to be determined. A complex interaction between the resistant cells, exosomes and target cells can be hypothesized. The whole process can be spatially separated between the bone marrow and peripheral blood, and may include other than leukemic cells, for example, stromal cells in bone marrow, macrophages or endothelial cells (17,19-21). In addition, it could also be hypothesized that time may also play its role, namely with respect to potentially continuous production of exosomes *in vivo*. Furthermore, considering that several distinct molecular mechanisms of resistance to imatinib have been described (7,8), the role of exosome-mediated survival may differ among patients with CML. We propose that each individual mechanism of imatinib resistance may manifest with a different phenotype of the resistant cell population, affecting protein expression, cellular proliferation rate and other cellular properties, including exosomal content and the rate of exosome shedding. Mutations in the BCR-ABL1 kinase domain, which prevent interaction of imatinib with the Bcr-Abl protein, are the most common cause of resistance to imatinib in patients with CML (7). However, the K562^{IR} cells in the present study did not possess any mutations in the kinase domain; instead, BCR-ABL1 amplification resulted in overexpression at the mRNA and protein levels, which is another mechanism of resistance that has previously been described in specific patients with CML (6,44). This may suggest that the observations in the present study may be specific for the underlying mechanism of resistance in the model used, i.e. the overexpression of BCR-ABL1.

The role of exosomes in cancer progression and drug resistance establishes their potential as a source of biomarkers for monitoring the progression of the disease, the emergence of drug resistance, or the effects of a therapeutic intervention (9,15). A detailed characterization of the specific protein cargo of the exosomes and identification of resistance-associated markers on the surface of K562^{IR} exosomes and K562^{IR} cells was, therefore, performed. The LFQ proteome analysis identified over 3,000 exosomal proteins and provided relative quantitation for 1,241 of them. These datasets represent, to the best of our knowledge, the largest set of exosomal proteins derived from leukemic cells. Among the proteins with significantly different abundance in the K562^{IR} exosomes, the focus was directed to molecules known (or expected) to be localized on the surface of the cells and exosomes. Surface localization ensures proteins are easily accessible as markers or drug targets. A total of 3 significantly upregulated (i.e., >7-fold according the LFQ data) membrane proteins with predicted surface localization were identified in the K562^{IR} exosomes:

IFITM3, CD146 and CD36. Notably, all three putative marker proteins have been previously associated with cancer progression (45-57).

IFITM3 is a member of the interferon-induced transmembrane protein family (58), that is known for its antiviral activity, and has been associated with multiple viruses, including Middle East respiratory syndrome coronavirus (MERS-CoV) and severe acute respiratory syndrome coronavirus (SARS-CoV) (59). IFITM3 has also been found to be overexpressed in patients with AML and in human cell lines derived from gastric, lung, oral and breast tumors (45-49) and has been implicated in cancer progression (45,46), with either pro-proliferative and/or pro-migratory roles (47,48). High expression levels of IFITM3 protein have been associated with poor prognosis in acute myeloid leukemia (49).

CD146 is a transmembrane glycoprotein, that was first identified in malignant melanoma, where it contributed to metastasis (50). CD146 protein overexpression in various types of malignancies, such as melanoma, ovarian and breast cancer, and lung tumors, has been associated with tumor progression, angiogenesis and metastasis (51-53), and its expression has also been associated with drug resistance (54,55).

CD36 is a hematopoietic marker of a subpopulation of primitive (i.e., less differentiated) and blast crisis CML cells (56). Notably, these cell types are known to be less sensitive to imatinib (57). An increase in the protein expression level of CD36 could, therefore, potentially mark a sub-population of $K562^{IR}$ cells with a less differentiated myeloid phenotype.

Using specific antibodies, it was possible to confirm the increase of all three putative marker proteins in both the $K562^{IR}$ exosomes and the $K562^{IR}$ cells. Finally, to confirm the differential expression of IFITM3, CD146 and CD36 proteins on the surface of the $K562^{IR}$ cells and to validate their utility as potential marker of imatinib resistance, flow cytometric analysis of live K562 and $K562^{IR}$ cells was performed using specific antibodies. The results confirmed that CD146 could be a reliable positive marker of imatinib resistance in the K562 cells, which could be used to distinguish and separate populations of $K562^{IR}$ cells using flow cytometry. IFITM3 and CD36 displayed lower differences in expression levels, comparing between the K562 and $K562^{IR}$ cells, and, therefore, have a lower level of accuracy in terms of distinguishing between the resistant and the sensitive cell populations.

Due to their resistance-specific overexpression on the cell surface, CD146 and IFITM3 could be, at least theoretically, exploited as drug targets for molecular therapy in imatinib-resistant CML. In agreement with this, CD146 has been considered to be a promising therapeutic target in CD146-positive cancers, such as melanoma (60). The therapeutic potential of anti-CD146 antibodies for cancer therapy is already being evaluated (61). Similarly, IFITM3 inactivation (knockdown) studies (49,50) have also provided strong support for its future anti-cancer pharmacological potential.

The present study did not address the mechanism of exosome-mediated survival. However, several possible mechanisms may be proposed or envisioned. For example, we hypothesize that exosomes carrying the molecular target of the drug could shift the drug/target ratio in the recipient cells upon fusion. In the present study, BCR-ABL1 fusion gene amplification and overexpression were identified in the $K562^{IR}$ cells, which resulted in upregulation of the fusion kinase in the $K562^{IR}$ exosomes. The process of the causative kinase being delivered by $K562^{IR}$ exosomes to the recipient K562 cells may, thus, hypothetically shift the imatinib/Bcr-Abl ratio and increase the survival rate of the K562 cells.

Alternatively, and additionally, exosomes may transfer other pro-survival molecules or their precursors, namely proteins, RNAs or DNAs. In their original study, Min *et al* (22) identified miR-365 as a molecule partly responsible for the pro-survival effect of exosomes derived from imatinib-resistant K562 cells. However, the beneficial effect of miR-365 alone was lower compared with the administration of the whole exosomes (22), suggesting that other molecules are involved in the process. It is, therefore, possible to hypothesize that IFITM3 could be a potential pro-survival candidate molecule, as it regulates STAT3 phosphorylation (62) and signaling, leading to cell proliferation, angiogenesis and drug resistance (63). Similarly, CD146 could theoretically contribute to survival of the target cells, as it mediates chemoresistance in small-cell lung cancer and in breast cancer through the activation of AKT kinase (54,55). However, whether the CD146 and/or IFITM3 molecules contained within the 'resistant' exosomes are able to actually exert their signaling function in the recipient cells, thereby stimulating their survival in the presence of imatinib, remains to be determined.

It is well-known that the K562 cells represent a single cellular model of CML, which may differ significantly from the complex and heterogeneous situation in CML *in vivo*. Whether the markers identified in the $K562^{IR}$ model are also overexpressed in the leukemic cells of patients with imatinib resistant CML remains to be verified. Unfortunately, such a confirmatory study will be complicated by several factors. The therapy of patients with limited response to imatinib is promptly changed to a newer TKI (64), typically without bone marrow sampling. Therefore, leukemia cells from patients with CML that are truly resistant to imatinib are very rare. The future study would be required to include a large number of bone marrow samples obtained from patients with different degrees of response to imatinib. Secondly, the mechanisms of imatinib resistance may differ between patients, with and without mutations in the Bcr-Abl kinase domain, and the study must include both types of patients. Thirdly, the necessary isolation of Ph-positive leukemia cells from the complex bone marrow samples may severely limit the cellular material available for the verification of the candidate protein expression. Nevertheless, performing the verification study would be essential before proposing CD146 and IFITM3 as novel and clinically relevant markers of imatinib resistance, or potential drug targets for imatinib resistant CML.

Acknowledgements

Not applicable.

Funding

This study was supported by the Ministry of Education, Youth and Sports of the Czech Republic (grant nos. Progress Q26, SVV 260 521, UNCE/MED/016), the Ministry of

Health of the Czech Republic (grant nos. NC19-01-00083 and NC19-02-00130) and by the Project for Conceptual Development of Research Organizations (grant no. 00023736) of the Ministry of Health of the Czech Republic. The authors also acknowledge support from the projects CZ.1.05/2.1.00/19.0400 and CZ.1.05/1.1.00/02.0109 from the Research and Development for Innovations Operational Program co-financed by the European Regional Development Fund and the state budget of the Czech Republic. The LFQ MS work was supported by the Ministry of Interior, Czech Republic (grant no. VH20172020012) and by the Ministry of Defense of the Czech Republic through a long-term organization development plan (grant no. 907930101413). A grant was also provided from the Czech Academy of Sciences (grant no. L200521953).

Availability of data and materials

The datasets generated and analyzed during the current study have been deposited to the ProteomeXchange Consortium via the PRIDE (65) partner repository with the dataset identifier PXD019283.

Authors' contributions

TH, OT, DV and JP conceived the study and designed the experiments. TH, OT, JD, JK and PP were responsible for the LC-MS/MS data acquisition and interpretation. JL derived the resistant K562^{IR} cells. VP performed BCR-ABL1 mutational, amplification and transcript analysis. KMP supervised the establishment of the resistant K562^{IR}, BCR-ABL1 NGS and ddPCR analyses and interpreted the data. HK performed the electron microscopy experiments. BB performed confocal microscopy. TH, BS and OB performed statistical analyses of the LFQ proteomic data. TH, MK and JZ performed the FACS analysis. JP and TK wrote the manuscript. All authors critically evaluated and approved the final version of the manuscript.

Ethics approval and consent to participate

Not applicable.

Patient consent for publication

Not applicable.

Competing interests

The authors declare that they have no competing interests.

References

1. Nowell PC and Hungerford DA: A minute chromosome in human chronic granulocytic leukemia. Science 132: 1497, 1960.
2. Rowley JD: Letter: A new consistent chromosomal abnormality in chronic myelogenous leukemia identified by quinacrine fluorescence and Giemsa staining. Nature 243: 290-293, 1973.
3. Heisterkamp N, Stephenson JR, Groffen J, Hansen PF, de Klein A, Bartram CR and Grosveld G: Localization of the c-abl oncogene adjacent to a translocation break point in chronic myelocytic leukaemia. Nature 306: 239-242, 1983.
4. Druker BJ, Talpaz M, Resta DJ, Peng B, Buchdunger E, Ford JM, Lydon NB, Kantarjian H, Capdeville R, Ohno-Jones S and Sawyers CL: Efficacy and safety of a specific inhibitor of the BCR-ABL tyrosine kinase in chronic myeloid leukemia. N Engl J Med 344: 1031-1037, 2001.
5. Lahaye T, Riehm B, Berger U, Paschka P, Müller MC, Kreil S, Merx K, Schwindel U, Schoch C, Hehlmann R and Hochhaus A: Response and resistance in 300 patients with BCR-ABL-positive leukemias treated with imatinib in a single center: A 4.5-year follow-up. Cancer 103: 1659-1669, 2005.
6. Gadzicki D, von Neuhoff N, Steinemann D, Just M, Büsche G, Kreipe H, Wilkens L and Schlegelberger B: BCR-ABL gene amplification and overexpression in a patient with chronic myeloid leukemia treated with imatinib. Cancer Genet Cytogenet 159: 164-167, 2005.
7. Gorre ME, Mohammed M, Ellwood K, Hsu N, Paquette R, Rao PN and Sawyers CL: Clinical resistance to STI-571 cancer therapy caused by BCR-ABL gene mutation or amplification. Science 293: 876-880, 2001.
8. Mahon FX, Deininger MW, Schultheis B, Chabrol J, Reiffers J, Goldman JM and Melo JV: Selection and characterization of BCR-ABL positive cell lines with differential sensitivity to the tyrosine kinase inhibitor STI571: Diverse mechanisms of resistance. Blood 96: 1070-1079, 2000.
9. Steinbichler TB, Dudas J, Skvortsov S, Ganswindt U, Riechelmann H and Skvortsova II: Therapy resistance mediated by exosomes. Mol Cancer 18: 58, 2019.
10. Nehrbas J, Butler JT, Chen DW and Kurre P: Extracellular vesicles and chemotherapy resistance in the AML microenvironment. Front Oncol 10: 90, 2020.
11. Johnstone RM, Adam M, Hammond JR, Orr L and Turbide C: Vesicle formation during reticulocyte maturation. Association of plasma membrane activities with released vesicles (exosomes). J Biol Chem 262: 9412-9420, 1987.
12. Valadi H, Ekstrom K, Bossios A, Sjostrand M, Lee JJ and Lotvall JO: Exosome-mediated transfer of mRNAs and microRNAs is a novel mechanism of genetic exchange between cells. Nat Cell Biol 9: 654-659, 2007.
13. Thakur BK, Zhang H, Becker A, Matei I, Huang Y, Costa-Silva B, Zheng Y, Hoshino A, Brazier H, Xiang J, *et al*: Double-stranded DNA in exosomes: A novel biomarker in cancer detection. Cell Res 24: 766-769, 2014.
14. Prada I and Meldolesi J: Binding and Fusion of Extracellular vesicles to the plasma membrane of their cell targets. Int J Mol Sci 17: 1296, 2016.
15. Maacha S, Bhat AA, Jimenez L, Raza A, Haris M, Uddin S and Grivel JC: Extracellular vesicles-mediated intercellular communication: Roles in the tumor microenvironment and anti-cancer drug resistance. Mol Cancer 18: 55, 2019.
16. Raimondo S, Saieva L, Corrado C, Fontana S, Flugy A, Rizzo A, De Leo G and Alessandro R: Chronic myeloid leukemia-derived exosomes promote tumor growth through an autocrine mechanism. Cell Commun Signal 13: 8, 2015.
17. Corrado C, Raimondo S, Saieva L, Flugy AM, De Leo G and Alessandro R: Exosome-mediated crosstalk between chronic myelogenous leukemia cells and human bone marrow stromal cells triggers an interleukin 8-dependent survival of leukemia cells. Cancer Lett 348: 71-76, 2014.
18. Cai J, Wu G, Tan X, Han Y, Chen C, Li C, Wang N, Zou X, Chen X, Zhou F, *et al*: Transferred BCR/ABL DNA from K562 extracellular vesicles causes chronic myeloid leukemia in immunodeficient mice. PLoS One 9: e105200, 2014.
19. Jafarzadeh N, Safari Z, Pornour M, Amirizadeh N, Forouzandeh Moghadam M and Sadeghizadeh M: Alteration of cellular and immune-related properties of bone marrow mesenchymal stem cells and macrophages by K562 chronic myeloid leukemia cell derived exosomes. J Cell Physiol 234: 3697-3710, 2019.
20. Taverna S, Flugy A, Saieva L, Kohn EC, Santoro A, Meraviglia S, De Leo G and Alessandro R: Role of exosomes released by chronic myelogenous leukemia cells in angiogenesis. Int J cancer 130: 2033-2043, 2012.
21. Mineo M, Garfield SH, Taverna S, Flugy A, De Leo G, Alessandro R and Kohn EC: Exosomes released by K562 chronic myeloid leukemia cells promote angiogenesis in a Src-dependent fashion. Angiogenesis 15: 33-45, 2012.
22. Min QH, Wang XZ, Zhang J, Chen QG, Li SQ, Liu XQ, Li J, Liu J, Yang WM, Jiang YH, *et al*: Exosomes derived from imatinib-resistant chronic myeloid leukemia cells mediate a horizontal transfer of drug-resistant trait by delivering miR365. Exp Cell Res 362: 386-393, 2018.

23. Toman O, Kabickova T, Vit O, Fiser R, Polakova KM, Zach J, Linhartova J, Vyoral D and Petrak J: Proteomic analysis of imatinib-resistant CML-T1 cells reveals calcium homeostasis as a potential therapeutic target. Oncol Rep 36: 1258-1268, 2016.
24. Machova Polakova K, Kulvait V, Benesova A, Linhartova J, Klamova H, Jaruskova M, de Benedittis C, Haferlach T, Baccarani M, Martinelli G, *et al*: Next-generation deep sequencing improves detection of BCR-ABL1 kinase domain mutations emerging under tyrosine kinase inhibitor treatment of chronic myeloid leukemia patients in chronic phase. J Cancer Res Clin Oncol 141: 887-899, 2015.
25. Kohlmann A, Grossmann V, Nadarajah N and Haferlach T: Next-generation sequencing-feasibility and practicality in haematology. Br J Haematol 160: 736-753, 2013.
26. Linhartova J, Hovorkova L, Soverini S, Benesova A, Jaruskova M, Klamova H, Zuna J and Machova Polakova K: Characterization of 46 patient-specific BCR-ABL1 fusions and detection of SNPs upstream and downstream the breakpoints in chronic myeloid leukemia using next generation sequencing. Mol Cancer 14: 89, 2015.
27. Moravcova J, Rulcova J, Polaková KM and Klamova H: Control genes in international standardization of real-time RT-PCR for BCR-ABL. Leuk Res 33: 582-584, 2009.
28. Rulcova J, Zmekova V, Zemanova Z, Klamova H and Moravcova J: The effect of total-ABL, GUS and B2M control genes on BCR-ABL monitoring by real-time RT-PCR. Leuk Res 31: 483-491, 2007.
29. Gabert J, Beillard E, van der Velden VH, Bi W, Grimwade D, Pallisgaard N, Barbany G, Cazzaniga G, Cayuela JM, Cavé H, *et al*: Standardization and quality control studies of 'real-time' quantitative reverse transcriptase polymerase chain reaction of fusion gene transcripts for residual disease detection in leukemia-a Europe Against Cancer program. Leukemia 17: 2318-2357, 2003.
30. Müller MC, Cross NCP, Erben P, Schenk P, Hanfstein B, Ernst T, Hehlmann R, Branford S, Saglio G and Hochhaus A: Harmonization of molecular monitoring of CML therapy in Europe. Leukemia 23:1957-1963, 2009.
31. Deprez L, Mazoua S, Corbisier P, Trapmann S, Schimmel H, White H, Cross N and Emons H: The certification of the copy number concentration of solutions of plasmid DNA containing a BCR-ABL b3a2 transcript fragment. Certified reference material: ERM-AD623a, ERM-AD623b, ERM-AD623c, ERM-AD623d, ERM-AD623e ERM-AD623f Luxembourg: Publications Office of the European Union; 2012. Report number EUR 25248; ISBN 978-92-79-23343-2, 2012.
32. White H, Deprez L, Corbisier P, Hall V, Lin F, Mazoua S, Trapmann S, Aggerholm A, Andrikovics H, Akiki S, *et al*: A certified plasmid reference material for the standardisation of BCR-ABL1 mRNA quantification by real-time quantitative PCR. Leukemia 29: 369-376, 2015.
33. Thery C, Amigorena S, Raposo G and Clayton A: Isolation and characterization of exosomes from cell culture supernatants and biological fluids. Curr Protoc Cell Biol Chapter 3: Unit 3.22, 2006.
34. McDowell EM and Trump BF: Histologic fixatives suitable for diagnostic light and electron microscopy. Arch Pathol Lab Med 100: 405-414, 1976.
35. Wisniewski JR, Zougman A and Mann M: Combination of FASP and StageTip-based fractionation allows in-depth analysis of the hippocampal membrane proteome. J Proteome Res 8: 5674-5678, 2009.
36. Cox J and Mann M: MaxQuant enables high peptide identification rates, individualized p.p.b.-range mass accuracies and proteome-wide protein quantification. Nat Biotechnol 26: 1367-1372, 2008.
37. Cox J, Neuhauser N, Michalski A, Scheltema RA, Olsen JV and Mann M: Andromeda: A peptide search engine integrated into the MaxQuant environment. J Proteome Res 10: 1794-1805, 2011.
38. Cox J, Hein MY, Luber CA, Paron I, Nagaraj N and Mann M: Accurate proteome-wide label-free quantification by delayed normalization and maximal peptide ratio extraction, termed MaxLFQ. Mol Cell Proteomics 13: 2513-2526, 2014.
39. Tyanova S, Temu T, Sinitcyn P, Carlson A, Hein MY, Geiger T, Mann M and Cox J: The Perseus computational platform for comprehensive analysis of (prote)omics data. Nat Methods 13: 731-740, 2016.
40. Chawade A, Alexandersson E and Levander F. Normalyzer: A tool for rapid evaluation of normalization methods for omics data sets. J Proteome Res 13: 3114-3120, 2014.
41. Waas M, Snarrenberg ST, Littrell J, Jones Lipinski RA, Hansen PA, Corbett JA and Gundry RL: SurfaceGenie: A web-based application for prioritizing cell-type specific marker candidates. Bioinformatics 36: 3447-3456, 2020.
42. Kowal J, Arras G, Colombo M, Jouve M, Morath JP, Primdal-Bengtson B, Dingli F, Loew D, Tkach M and Théry C: Proteomic comparison defines novel markers to characterize heterogeneous populations of extracellular vesicle subtypes. Proc Natl Acad Sci USA 113: E968-E977, 2016.
43. Tadokoro H, Umezu T, Ohyashiki K, Hirano T and Ohyashiki JH: Exosomes derived from hypoxic leukemia cells enhance tube formation in endothelial cells. J Biol Chem 288: 34343-34351, 2013.
44. Chandran RK, Geetha N, Sakthivel KM, Aswathy CG, Gopinath P, Raj TVA, Priya G, Nair JKKM and Sreedharan H: Genomic amplification of BCR-ABL1 fusion gene and its impact on the disease progression mechanism in patients with chronic myelogenous leukemia. Gene 686: 85-91, 2019.
45. Hu J, Wang S, Zhao Y, Guo Q, Zhang D, Chen J, Li J, Fei Q and Sun Y: Mechanism and biological significance of the overexpression of IFITM3 in gastric cancer. Oncol Rep 32: 2648-2656, 2014.
46. Zhang D, Wang H, He H, Niu H and Li Y: Interferon induced transmembrane protein 3 regulates the growth and invasion of human lung adenocarcinoma. Thorac Cancer 8: 337-343, 2017.
47. Yang M, Gao H, Chen P, Jia J and Wu S: Knockdown of interferon-induced transmembrane protein 3 expression suppresses breast cancer cell growth and colony formation and affects the cell cycle. Oncol Rep 30: 171-178, 2013.
48. Gan CP, Sam KK, Yee PS, Zainal NS, Lee BKB, Abdul Rahman ZA, Patel V, Tan AC, Zain RB and Cheong SC: IFITM3 knockdown reduces the expression of CCND1 and CDK4 and suppresses the growth of oral squamous cell carcinoma cells. Cell Oncol (Dordr) 42: 477-490, 2019.
49. Liu Y, Lu R, Cui W, Pang Y, Liu C, Cui L, Qian T, Quan L, Dai Y, Jiao Y, *et al*: High IFITM3 expression predicts adverse prognosis in acute myeloid leukemia. Cancer Gene Ther 27: 38-44, 2019.
50. Lehmann JM, Riethmuller G and Johnson JP: MUC18, a marker of tumor progression in human melanoma, shows sequence similarity to the neural cell adhesion molecules of the immunoglobulin superfamily. Proc Natl Acad Sci USA 86: 9891-9895, 1989.
51. Lei X, Guan CW, Song Y and Wang H: The multifaceted role of CD146/MCAM in the promotion of melanoma progression. Cancer Cell Int 15: 3, 2015.
52. Wu GJ and Dickerson EB: Frequent and increased expression of human METCAM/MUC18 in cancer tissues and metastatic lesions is associated with the clinical progression of human ovarian carcinoma. Taiwan J Obstet Gynecol 53: 509-517, 2014.
53. Watson-Hurst K and Becker D: The role of N-cadherin, MCAM and beta3 integrin in melanoma progression, proliferation, migration and invasion. Cancer Biol Ther 5: 1375-1382, 2006.
54. Tripathi SC, Fahrmann JF, Celiktas M, Aguilar M, Marini KD, Jolly MK, Katayama H, Wang H, Murage EN, Dennison JB, *et al*: MCAM Mediates Chemoresistance in Small-Cell Lung Cancer via the PI3K/AKT/SOX2 signaling pathway. Cancer Res 77: 4414-4425, 2017.
55. Liang YK, Zeng D, Xiao YS, Wu Y, Ouyang YX, Chen M, Li YC, Lin HY, Wei XL, Zhang YQ, *et al*: MCAM/CD146 promotes tamoxifen resistance in breast cancer cells through induction of epithelial-mesenchymal transition, decreased ERα expression and AKT activation. Cancer Lett 386: 65-76, 2017.
56. Ye H, Adane B, Khan N, Sullivan T, Minhajuddin M, Gasparetto M, Stevens B, Pei S, Balys M, Ashton JM, *et al*: Leukemic stem cells evade chemotherapy by metabolic adaptation to an adipose tissue niche. Cell Stem Cell 19: 23-37, 2016.
57. Landberg N, von Palffy S, Askmyr M, Lilljebjörn H, Sandén C, Rissler M, Mustjoki S, Hjorth-Hansen H, Richter J, Ågerstam H, *et al*: CD36 defines primitive chronic myeloid leukemia cells less responsive to imatinib but vulnerable to antibody-based therapeutic targeting. Haematologica 103: 447-455, 2018.
58. Bailey CC, Zhong G, Huang IC and Farzan M: IFITM-Family Proteins: The Cell's First Line of Antiviral Defense. Annu Rev Virol 1: 261-283, 2014.
59. Wrensch F, Winkler M and Pöhlmann S: IFITM proteins inhibit entry driven by the MERS-coronavirus spike protein: Evidence for cholesterol-independent mechanisms. Viruses 6: 3683-3698, 2014.

60. Nollet M, Stalin J, Moyon A, Traboulsi W, Essaadi A, Robert S, Malissen N, Bachelier R, Daniel L, Foucault-Bertaud A, *et al*: A novel anti-CD146 antibody specifically targets cancer cells by internalizing the molecule. Oncotarget 8: 112283-112296, 2017.
61. Stalin J, Nollet M, Dignat-George F, Bardin N and Blot-Chabaud M: Therapeutic and Diagnostic Antibodies to CD146: Thirty Years of Research on Its Potential for Detection and Treatment of Tumors. Antibodies (Basel) 6: 17, 2017.
62. Wang H, Tang F, Bian E, Zhang Y, Ji X, Yang Z and Zhao B: IFITM3/STAT3 axis promotes glioma cells invasion and is modulated by TGF-β. Mol Biol Rep 47: 433-441, 2020.
63. Johnston PA and Grandis JR: STAT3 signaling: Anticancer strategies and challenges. Mol Interv 11: 18-26, 2011.
64. Hochhaus A, Baccarani M, Silver RT, Schiffer C, Apperley JF, Cervantes F, Clark RE, Cortes JE, Deininger MW, Guilhot F, *et al*: European LeukemiaNet 2020 recommendations for treating chronic myeloid leukemia. Leukemia 34: 966-984, 2020.
65. Perez-Riverol Y, Csordas A, Bai J, Bernal-Llinares M, Hewapathirana S, Kundu DJ, Inuganti A, Griss J, Mayer G, Eisenacher M, *et al*: The PRIDE database and related tools and resources in 2019: Improving support for quantification data. Nucleic Acids Res 47: D442-D450, 2019.